

AD-A087 795

ARMY ENGINEER WATERWAYS EXPERIMENT STATION VICKSBURG MS

F/G 8/6

THE GEOMETRY OF SELECTED U.S. TIDAL INLETS.(U)

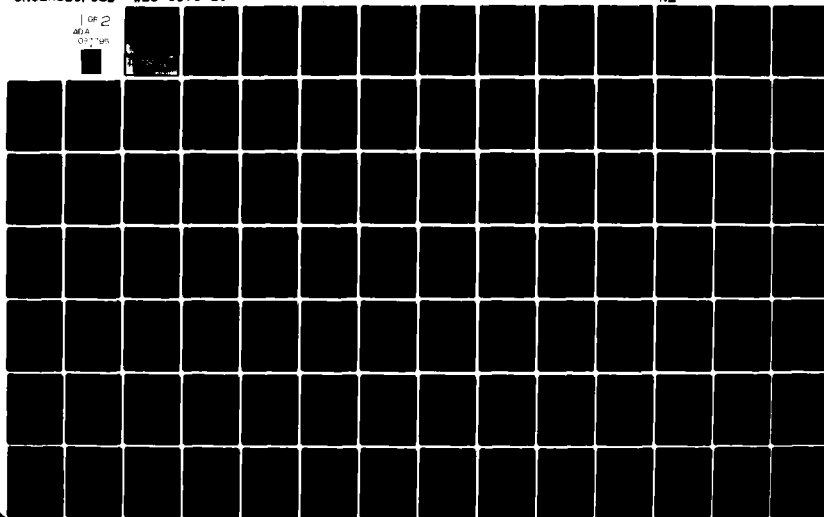
MAY 80 C L VINCENT, W D CORSON

UNCLASSIFIED

WES-011-20

NL

1 OF 2
ADA
01-11-80



The Geometry of Selected U.S. Tidal Inlets

LEVEL

12
R.S.

by

Charles L. Vincent and William D. Corson

ADA087795

GITI REPORT 20



May 1980

DTIC
SELECTED
AUG 12 1980
C



Reprint or republication of any of this material shall give appropriate credit to the U.S. Army Coastal Engineering Research Center.

Limited free distribution within the United States of single copies of this publication has been made by this Center. Additional copies are available from:

*National Technical Information Service
ATTN: Operations Division
5285 Port Royal Road
Springfield, Virginia 22161*

Contents of this report are not to be used for advertising, publication, or promotional purposes. Citation of trade names does not constitute an official endorsement or approval of the use of such commercial products.

The findings in this report are not to be construed as an official Department of the Army position unless so designated by other authorized documents.

Cover Photo: Drum Inlet, North Carolina, 13 March 1962
Courtesy of the U.S. Geological Survey

UNCLASSIFIED

SECURITY CLASSIFICATION OF THIS PAGE (When Data Entered)

REPORT DOCUMENTATION PAGE		READ INSTRUCTIONS BEFORE COMPLETING FORM
1. REPORT NUMBER GITI Report 20 ✓	2. GOVT ACCESSION NO. AD-A087795	3. RECIPIENT'S CATALOG NUMBER
4. TITLE (and Subtitle) THE GEOMETRY OF SELECTED U.S. TIDAL INLETS.		5. TYPE OF REPORT & PERIOD COVERED (9) Final Report
		6. PERFORMING ORG. REPORT NUMBER
7. AUTHOR(s) Charles L. Vincent William D. Corson		8. CONTRACT OR GRANT NUMBER(s) (11) M02 12 1
9. PERFORMING ORGANIZATION NAME AND ADDRESS U.S. Army Engineer Waterways Experiment Station Hydraulics Laboratory ✓ P.O. Box 631, Vicksburg, Mississippi 39180		10. PROGRAM ELEMENT, PROJECT, TASK AREA & WORK UNIT NUMBERS B31647
11. CONTROLLING OFFICE NAME AND ADDRESS Department of the Army Coastal Engineering Research Center Kingman Building, Fort Belvoir, Virginia 22060 (12)		12. REPORT DATE May 1980
14. MONITORING AGENCY NAME & ADDRESS (if different from Controlling Office) (14) ITI-27		13. NUMBER OF PAGES 163
		15. SECURITY CLASS. (of this report) Unclassified
		15a. DECLASSIFICATION/DOWNGRADING SCHEDULE
16. DISTRIBUTION STATEMENT (of this Report) Approved for public release; distribution unlimited.		
17. DISTRIBUTION STATEMENT (of the abstract entered in Block 20, if different from Report)		
18. SUPPLEMENTARY NOTES		
19. KEY WORDS (Continue on reverse side if necessary and identify by block number) Inlet classification Tidal inlet geometry Tidal inlets		
20. ABSTRACT (Continue on reverse side if necessary and identify by block number) The geometry of the throat and ebb delta of 67 U.S. tidal inlets is investigated. Thirteen parameters indicative of the tidal inlet geometry are defined and measured with correlations developed. The correlation study indicated a number of strong statistical relationships with minimum inlet width cross-sectional area being particularly important. Cluster analysis and discriminant analysis are applied to the data and an objective classification of the inlets into six groups achieved.		

DD FORM 1473 1 JAN 73 EDITION OF 1 NOV 65 IS OBSOLETE

UNCLASSIFIED

SECURITY CLASSIFICATION OF THIS PAGE (When Data Entered)

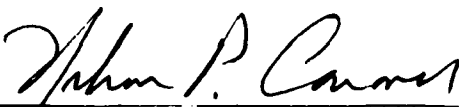
FOREWORD


This report was prepared by the Wave Dynamics Division of the Hydraulics Laboratory at the U.S. Army Engineer Waterways Experiment Station (WES) as one of a series of reports on the General Investigation of Tidal Inlets (GITI). The GITI research program is under the technical surveillance of the U.S. Army Coastal Engineering Research Center (CERC) and is conducted by CERC, WES, other government agencies, and by private organizations. This report contains detailed results of a project on the classification of inlets on the basis of their geometry.

The report was prepared by C.L. Vincent, formerly with WES, now Chief, Oceanography Branch, CERC, and W.D. Corson, under the supervision of R.W. Whalin, Chief of the Wave Dynamics Division, and H.B. Simmons, Chief of the Hydraulics Laboratory. CERC technical direction was provided by C. Mason under the general supervision of R.M. Sorensen. Technical Directors of CERC and WES were T. Saville, Jr., and F.R. Brown, respectively.

Comments on this publication are invited.

Approved for publication in accordance with Public Law 166, 79th Congress, approved 31 July 1945, as supplemented by Public Law 172, 88th Congress, approved 7 November 1963.


NELSON P. CONOVER
Colonel, Corps of Engineers
Commander and Director
Waterways Experiment Station


TED E. BISHOP
Colonel, Corps of Engineers
Commander and Director
Coastal Engineering Research Center

Accession For	
NTIS GRA&I	<input checked="checked" type="checkbox"/>
DDC TAB	<input type="checkbox"/>
Unannounced	<input type="checkbox"/>
Justification	
For	
Distribution	
All other copies	
For	
Distribution	
For	
Distribution	

A

PREFACE

1. The Corps of Engineers, through its Civil Works program, has sponsored, over the past 23 years, research into the behavior and characteristics of tidal inlets. The Corps' interest in tidal inlet research stems from its responsibilities for navigation, beach erosion prevention and control, and flood control. Tasked with the creation and maintenance of navigable U.S. waterways, the Corps dredges millions of cubic yards of material each year from tidal inlets that connect the ocean with bays, estuaries, and lagoons. Design and construction of navigation improvements to existing tidal inlets are an important part of the work of many Corps offices. In some cases, design and construction of new inlets are required. Development of information concerning the hydraulic characteristics of inlets is important not only for navigation and inlet stability, but also because inlets, by allowing for the ingress of storm surges and egress of flood waters, play an important role in the flushing of bays and lagoons.

2. A research program, the General Investigation of Tidal Inlets (GITI), was developed to provide quantitative data for use in design of inlets and inlet improvements. It is designed to meet the following objectives:

To determine the effects of wave action, tidal flow, and related phenomena on inlet stability and on the hydraulic, geometric, and sedimentary characteristics of tidal inlets; to develop the knowledge necessary to design effective navigation improvements, new inlets, and sand transfer systems at existing tidal inlets; to evaluate the water transfer and flushing capability of tidal inlets; and to define the processes controlling inlet stability.

3. The GITI is divided into three major study areas: (a) inlet classification, (b) inlet hydraulics, and (c) inlet dynamics.

a. *Inlet Classification.* The objectives of the inlet classification study are to classify inlets according to their geometry, hydraulics, and stability, and to determine the relationships that exist among the geometric and dynamic characteristics and the environmental factors that control these characteristics. The classification study keeps the general investigation closely related to real inlets and produces an important inlet data base useful in documenting the characteristics of inlets.

b. *Inlet Hydraulics.* The objectives of the inlet hydraulics study are to define tide-generated flow regime and water level fluctuations in the vicinity of coastal inlets and to develop techniques for predicting these phenomena. The inlet hydraulics study is divided into three areas: (1) idealized inlet model study, (2) evaluation of state-of-the-art physical and numerical models, and (3) prototype inlet hydraulics.

(1) *The Idealized Inlet Model.* The objectives of this model study are to determine the effect of inlet configurations and structures on discharge, head loss, and velocity distribution for a number of realistic inlet shapes and tide conditions. An initial set of tests in a trapezoidal inlet was conducted between 1967 and 1970. However, in order that subsequent inlet models are more representative of real inlets, a number of "idealized" models representing various inlet morphological classes are being developed and tested. The effects of jetties and wave action on the hydraulics are included in the study.

(2) **Evaluation of State-of-the-Art Modeling Techniques.** The objectives of this part of the inlet hydraulics study are to determine the usefulness and reliability of existing physical and numerical modeling techniques in predicting the hydraulic characteristics of inlet-bay systems, and to determine whether simple tests, performed rapidly and economically, are useful in the evaluation of proposed inlet improvements. Masonboro Inlet, North Carolina, was selected as the prototype inlet which would be used along with hydraulic and numerical models in the evaluation of existing techniques. In September 1969 a complete set of hydraulic and bathymetric data was collected at Masonboro Inlet. Construction of the fixed-bed physical model was initiated in 1969, and extensive tests have been performed since then. In addition, three existing numerical models were applied to predict the inlet's hydraulics. Extensive field data were collected at Masonboro Inlet in August 1974 for use in evaluating the capabilities of the physical and numerical models.

(3) **Prototype Inlet Hydraulics.** Field studies at a number of inlets are providing information on prototype inlet-bay tidal hydraulic relationships and the effects of friction, waves, tides, and inlet morphology on these relationships.

c. Inlet Dynamics. The basic objective of the inlet dynamics study is to investigate the interactions of tidal flow, inlet configuration, and wave action at tidal inlets as a guide to improvement of inlet channels and nearby shore protection works. The study is subdivided into four specific areas: (1) model materials evaluation, (2) movable-bed modeling evaluation, (3) reanalysis of a previous inlet model study, and (4) prototype inlet studies.

(1) **Model Materials Evaluation.** This evaluation was initiated in 1969 to provide data on the response of movable-bed model materials to waves and flow to allow selection of the optimum bed materials for inlet models.

(2) **Movable-Bed Model Evaluation.** The objective of this study is to evaluate the state-of-the-art of modeling techniques, in this case movable-bed inlet modeling. Since, in many cases, movable-bed modeling is the only tool available for predicting the response of an inlet to improvements, the capabilities and limitations of these models must be established.

(3) **Reanalysis of an Earlier Inlet Model Study.** In 1957, a report entitled, "Preliminary Report: Laboratory Study of the Effect of an Uncontrolled Inlet on the Adjacent Beaches," was published by the Beach Erosion Board (now CERC). A reanalysis of the original data is being performed to aid in planning of additional GITI efforts.

(4) **Prototype Dynamics.** Field and office studies of a number of inlets are providing information on the effects of physical forces and artificial improvements on inlet morphology. Of particular importance are studies to define the mechanisms of natural sand bypassing at inlets, the response of inlet navigation channels to dredging and natural forces, and the effects of inlets on adjacent beaches.

4. This report presents a classification of inlets based on objective analysis of similarities between inlet geometric characteristics. The report contains substantial amounts of inlet geometric data obtained from aerial photos and boat sheets which may be applicable to site-specific studies.

CONTENTS

	Page
CONVERSION FACTORS, U.S. CUSTOMARY TO METRIC (SI).	10
SYMBOLS AND DEFINITIONS.	11
I INTRODUCTION	15
1. Historical Perspective.	15
2. Inlet Classification.	15
3. Study Objectives.	16
4. Previous Classifications.	17
II SELECTION OF INLETS AND PARAMETERS	17
1. Inlets Selected for Study	17
2. Orientation	19
3. Definition of Inlet Geometric Parameters.	19
4. Representation of Channel Cross Section, Channel Profile and Ebb Delta Shapes: Mathematical Considerations	22
5. Distribution of Inlet Parameters.	36
III RELATIONSHIPS AMONG THE GEOMETRIC PARAMETERS	36
1. Procedures.	36
2. Direct Relationships Between Various Parameters	37
3. Relationships to the Cross-Sectional Area of the MIWC	43
4. Relationships to W/L.	47
5. Discussion.	52
IV CLASSIFICATION OF INLETS	53
1. Mathematical Considerations	53
2. Cluster Analysis.	54
3. Inlet Clusters Derived.	55
4. Discussion.	67
V MATHEMATICAL DEFINITION OF INLET CLASSIFICATION.	68
1. Objectives.	68
2. Mathematical Considerations	69
3. Discriminant Analysis of Inlet Data	72
4. Discussion.	76
VI EVALUATION OF THE PROBABILITY THAT AN INLET NOT IN THE ANALYSIS BELONGS TO A CLUSTER.	77
1. Data Preparation.	77
2. Probability Calculations.	78
3. A Simple Example.	79
VII INLET GEOMETRY: A SUMMARY DISCUSSION.	79
VIII SUMMARY.	83
LITERATURE CITED	84

CONTENTS--Continued

	Page
APPENDIX	
A PLOTS OF MINIMUM INLET WIDTH CROSS SECTION CHANNEL PROFILE, AND EBB DELTA GEOMETRY FOR SELECTED INLETS	87
B VALUES OF THE 13 INLET GEOMETRIC PARAMETERS BY INLET	155
C HISTOGRAMS OF THE B VALUES	157
D MEAN AND STANDARD DEVIATION VECTORS REQUIRED IN EIGENVECTOR ANALYSIS	160
E EIGENVECTORS FOR THE MINIMUM INLET CROSS SECTION, CHANNEL PROFILE, AND EBB DELTA GEOMETRY ANALYSES	161
F COMPUTER PROGRAM FOR THE CALCULATION OF THE PROBABILITY THAT AN INLET BELONGS TO AN INLET GROUP.	162

TABLES

1 Geographic order of inlets with survey dates, inlet conditions, and source of data.	18
2 Mean and standard deviation of parameters.	36
3 Inlets by cluster group.	57
4 Significance of differences among clusters, based on a student's t test for differences between means.	58
5 Mean (\bar{x}) and standard deviations (S_x) of geometric parameters by cluster groups.	59
6 Discriminant analysis results for three variables.	73
7 Discriminant analysis results for 13 variables	74
8 Posterior probabilities (P) that inlets belong to specified clusters .	75
9 Discriminant analysis results for six variables.	76
10 A simple example of the calculation of the probability that an inlet belongs to a given group	79

FIGURES

1 Measurement of inlet minimum width (W)	21
2 Measurement of alternate inlet width	21
3 Measurement of channel parameters DCC and L.	22
4 Measurement of ebb delta area (AED).	23

CONTENTS

FIGURES--Continued

	Page
5 Minimum inlet width cross-section parameters	25
6 Channel profile parameters	26
7 Examples of inlet cross sections showing the major variations in EM1, EM2, and EM3.	29
8 Examples of inlet profiles showing the major variations in EC1 and EC2	30
9 Grid mesh for describing ebb delta geometry.	31
10 Measurement of ebb delta radius, r, and alinement of ebb delta grid. .	31
11 Contour maps of mean ebb delta geometry and the first three eigenvectors of ebb delta geometry.	34
12 Examples of inlets showing the major variations in ED1 and ED2	35
13 DMX versus DMA	37
14 DMX versus DCC	38
15 DMX versus L	39
16 DMX versus EC1	39
17 DMA versus EC1	41
18 DCC versus EC1	41
19 L versus EC1	42
20 L versus AED	42
21 DMX versus ED2	44
22 DMA versus ED2	44
23 DCC versus ED2	45
24 L versus ED2	45
25 EM1 versus ED1	46
26 EC1 versus AED	46

CONTENTS

FIGURES--Continued

	Page
27 A_c versus DMX.	48
28 A_c versus DCC.	48
29 A_c versus L.	49
30 A_c versus AED.	49
31 ED2 versus A_c	50
32 W/L versus DMA/DCC	50
33 W/L versus ED1	51
34 Normalized channel profile for different values of W/L	51
35 Dendrogram of the cluster analysis	56
36 Mean and standard deviations of the 13 variables by cluster group. . .	60
37 Variational range of variables by inlet group.	63
38 Schematic relationship between two clusters (A,B), the line defined by the discriminant analysis for two variables (x_1, x_2). . . .	69

CONVERSION FACTORS, U.S. CUSTOMARY TO METRIC (SI) UNITS OF MEASUREMENT

U.S. customary units of measurement used in this report can be converted to metric (SI) units as follows:

Multiply	by	To obtain
inches	25.4	millimeters
	2.54	centimeters
square inches	6.452	square centimeters
cubic inches	16.39	cubic centimeters
feet	30.48	centimeters
	0.3048	meters
square feet	0.0929	square meters
cubic feet	0.0283	cubic meters
yards	0.9144	meters
square yards	0.836	square meters
cubic yards	0.7646	cubic meters
miles	1.6093	kilometers
square miles	259.0	hectares
knots	1.852	kilometers per hour
acres	0.4047	hectares
foot-pounds	1.3558	newton meters
millibars	1.0197×10^{-3}	kilograms per square centimeter
ounces	28.35	grams
pounds	453.6	grams
	0.4536	kilograms
ton, long	1.0160	metric tons
ton, short	0.9072	metric tons
degrees (angle)	0.01745	radians
Fahrenheit degrees	5/9	Celsius degrees or Kelvins ¹

¹To obtain Celsius (C) temperature readings from Fahrenheit (F) readings, use formula: $C = (5/9) (F - 32)$.

To obtain Kelvin (K) readings, use formula: $K = (5/9) (F - 32) + 273.15$.

SYMBOLS AND DEFINITIONS

Symbol	Restriction ¹	Definition
A	3	exponent in general regression equation
A, a_{ij}	5	matrix used in formation of discriminant functions containing within-cluster variance products
A_c		area of the minimum width cross section
AED		area of the ebb delta
a_i	1	generalized eigenvector weighting coefficient
B	3	exponent in general regression equation
B, b_{ij}	5	matrix used in formation of discriminant function containing population variance products
C, c_{ij}	4	matrix containing distance coefficients
C_i	3	coefficients in a generalized regression equation
C_{ij}	5	coefficients in discriminate functions
DCC		depth at crest of outer bar in channel
D_{ij}^2		mahalanobis squared distance
DMA		average depth of minimum inlet width cross section
DMX		maximum depth of minimum inlet width cross section
d_i		depth at a mesh point on a grid system
d_i^*		normalized depth at a mesh point
EC1		weighting coefficient on first eigenvector of channel profile
EC2		weighting coefficient on second eigenvector of channel profile
ED1		weighting coefficient on first eigenvector of ebb delta shape
ED2		weighting coefficient on second eigenvector of ebb delta shape
EM1		weighting coefficient on first eigenvector of MIWC shape
EM2		weighting coefficient on second eigenvector of MIWC shape
EM3		weighting coefficient on third eigenvector of MIWC shape

¹Restriction of a definition to a given section.

SYMBOLS AND DEFINITIONS--Continued

Symbol	Restriction	Definition
e_i		arbitrary eigenvector
F, F_{ij}	3,5	F ratio either univariate or multivariate
F, F_{ij}	4	statistical matrix of inlet data
F_i	3	coefficient in generalized regression coefficient
F^0, f_{ij}^0		matrix of observations normalized to 0 mean and unit standard deviation
f		arbitrary function
\bar{f}_j		mean value of j^{th} parameter
G_i		coefficient in a generalized regression equation
g		number of clusters
h_i		normalized depth
i		subscripts, individual use varies
J		exponent in a general regression equation
j		subscripts, individual use varies
j^{S_i}, s_{mi}	3,5	standard deviation for variable computed within a cluster
K, k		subscripts, individual use varies
L		channel length
l_{ij}		components of an eigenvector
M, m		number of inlets or variables
N, n, n_j		number of inlets or variables
P	5	number of inlets in an analysis
\underline{P}		profile vector
P_{ijk}, P_i^*	5,6	probability that a given inlet from a given cluster belongs in another cluster; posterior probability that an inlet belongs to a cluster
P_q	5,6	prior probability that an inlet belongs to a cluster
q		general subscript
R		coefficient of discrimination

SYMBOLS AND DEFINITIONS--Continued

Symbol	Restriction	Definition
r		number of inlets in a given analysis
S_{ijk}, S_i	5,6	discriminant function
T, t_{ij}		total variance matrix (population wide)
u		ratio of pooled to total variance
V_{ij}		correlation matrix
W	2,3,4,6,7	minimum inlet width
W, w_{ij}	5	pooled variance matrix
X_i, X_{ij}		generalized coordinate or parameter in eigenvector, cluster, and discriminant analyses
Z^*, Z		general variables in eigenvector analyses
Γ		covariance matrix
γ		dependent variable in a general regression equation
λ		eigenvalue
ν		degrees of freedom
ξ		vector of normalized depths in an eigenvector analysis of the ebb delta shape
σ_j		standard deviation
ϕ		variance included in an eigenvector analysis

THE GEOMETRY OF SELECTED U.S. TIDAL INLETS

by
Charles L. Vincent and William D. Corson

I. INTRODUCTION

1. Historical Perspective.

Along the coasts of the United States, numerous inlets exist through which water, sediment, nutrients, and pollutants are exchanged between the oceans and estuaries by flows that are largely forced by tides. Among the approximately 300 major inlets, a wide diversity in hydraulic conditions and morphology is found. Inlet widths vary from a few hundred to more than 20,000 feet and average depths vary from a few feet to more than 50 feet. Historically, the economic importance of inlets has primarily been in their role as waterways for commercial navigation, but their potential for recreational interests has also been recognized. More recently, the effects upon the ecology of estuarine areas caused by changes in inlet configuration due either to nature or man have received attention. The combination of the large size of the inlet-estuarine systems and the complexity of the physical processes makes the study of inlets difficult; as a result, planning and management of inlets often rely on a less than desirable information base.

2. Inlet Classification.

Both fixed-bed and movable-bed physical models of tidal inlets have been used extensively since 1930 to examine possible effects of proposed modification of inlets through construction of jetties and dredging. More recently, numerical models have been formulated to simulate inlet hydrodynamics. Both types of models provide valuable insight into the hydrodynamics of the inlet system but neither provide accurate quantitative estimates of sediment transport or shoal and scour patterns. These models provide qualitative indications of the effect of proposed modifications which are then extrapolated through knowledge of the behavior of the prototype or other inlets to reach final conclusions concerning the probable success of the proposed modifications. In the future, advanced models and additional knowledge of the physical processes should improve the ability to project the effect of modifications to inlets, but it is still likely that empirical knowledge of inlet systems and their response to change will continue to be an important part of the information base for inlet planning and management decisions.

The inlet classification tasks of the General Investigation of Tidal Inlets (GITI) program were formulated to improve the empirical data base on inlets and inlet processes. It was recognized that although a wide diversity of inlets exists, the same basic physical processes occur at all inlets though in differing magnitudes and settings. Because of these common processes, inlets which appear to be similar should be studied to explain reasons for the similarities. The study has several values. First, an extensive and consistent empirical data base would be collected for a large number of inlets. Second, similar inlets would be classed together to provide Corps personnel performing specific site studies a guide to inlets with similar characteristics. Third, the study should better define the relationships among many inlets, which should provoke better explanations for the similarities and differences found.

Early in the planning phase of the inlet classification task, three aspects of inlets were selected for examination: hydraulics, geometry (or morphology), and stability. The efforts were designed to produce three independent classifications. In a later phase of research, efforts will be designed to interrelate the three separate classifications and investigate the reasons for correspondence between well-defined classifications. This report details efforts on the geometric classification. Results from the hydraulic classification studies are given in Jarrett (1976). Results from the stability analyses are given in Vincent and Corson (in preparation, 1980).

It should be noted that all inlets are complex enough to be considered dissimilar. Yet as this report shows, when the larger scale geometric properties of inlet systems are analyzed, striking similarities are found and inlet characteristics are shown to vary in consistent ways.

3. Study Objectives.

An analysis of the morphology of inlets requires the study of inlet topography and bathymetry. Of particular interest are the lengths, depths, cross sections and orientation of channels, and the area, height, and location of shoals. Inlet morphology results from tide- and wave-generated sediment transport over a wide range of space and time scales. The features adjust to the present hydrodynamic environment, but often relate to past conditions. A further complication is the geology of a particular inlet which may deform the processes in a unique way. Modifications by man can alter the morphology as well. The primary objectives of this study were (a) to isolate a set of parameters that can be used to quantify inlet geometry, (b) to analyze relationships between the basic parameters selected, and (c) to analyze the relationships between inlets based upon the parameters selected.

The first step in the research is the selection of parameters that satisfactorily describe inlet geometry. These parameters should be representative of the response of the sediment mass to the hydraulic processes. Additionally, for the parameters to be useful in any classification process, all must be readily and consistently definable.

After consistent geometric information has been collected for a large number of inlets containing as diverse geometries as possible, the data are examined for relationships among the geometric parameters. The tidal deltas and channels develop as a result of interaction between tide- and wave-generated flow fields. In the long term, the magnitudes of these processes vary within rather narrow limits excluding the effects of unusually severe storms. Intuitively, it is expected that, undisturbed, the geometry of the inlet adjusts to the processes. Likewise, even given the varying influences of wave- and tide-generated phenomena, consistent variations in the geometric parameters are expected to occur representing the time-space integration of their effect. Few such relationships have been found previously. The best known empirical relationship for inlet characteristics is that of O'Brien (1931), between inlet throat cross-sectional area and tidal prism.

The final task will be classification of the inlets according to their geometry. As discussed in greater detail later in this report, classification is the process of ordering inlets on the basis of the relationships among them. Based on the parameters chosen, the similarities between inlets will be examined

and the inlets organized accordingly. The classification process is difficult because the inlet geometry is mathematically multidimensional; however, recent advances in numerical taxonomy have provided objective means for examining structural organizations. Thus, the differences among inlets can be objectively measured and the significance of the differences tested. The result will be a statistical basis on which inlet characteristics can be examined. Hydraulic or geologic factors must eventually explain the reasons for the organization.

It should be noted that some of the analyses in this report rely heavily on the statistical methods of eigenvector analysis, cluster analysis, and discriminant analysis. The motivation for use of these methods, which have rarely been used in engineering (but are widely applied in the fields of geology, biology, psychology, and process control), can be realized if the futility of examining manually the covariant properties of a moderate to large number of variables among 50 or more inlets is recognized. The statistical methods are required to examine objectively the relationships among the variables and the inlets.

The scope of this report is only to analyze the geometry of the inlet systems, not their hydraulics and stability. However, relationships which appear to have relevance to these other aspects of inlet systems are so noted.

4. Previous Classifications.

A review of the literature indicates that few efforts have been made to classify inlets according to geometry. Foremost in this effort has been the work by Galvin, et al. (1971a, 1971b) and Galvin (1971) to collect dimensional information on inlet geometry and relate inlet characteristics to longshore transport distributions. This work resulted in the definition of four types of inlets based on shape and offset of the inlet flanks: overlapping offset, updrift offset, downdrift offset, and negligible offset.

The other major inlet classification research has been that of Caldwell (1955) in defining three classes of inlets based on hydraulic characteristics. Class I inlets have peak floodflows occurring before high tide by less than 1 hour with the tidal range of the inlet and the ocean approximately equal. In Class II inlets the peak floodflow precedes high tide by 2 to 3 hours and tidal ranges in the ocean and inside the inlet are about equal. The Class III inlets have peak floodflows less than 1 hour before high tide but have tidal ranges inside the inlet substantially less than outside.

Bruun (1967) and Bruun and Gerritsen (1957, 1959) related the stability of inlets to the ratio of the net longshore drift to the maximum inlet discharge. They further suggested classing inlets according to their natural bypassing capabilities.

The present report is related to the efforts of Galvin, et al. (1971a, 1971b) and Galvin (1971). Emphasis is placed on the morphologic characteristics of the inlets and a quantitative investigation of their covariant properties.

II. SELECTION OF INLETS AND PARAMETERS

1. Inlets Selected for Study.

The 67 inlets studied in this report are listed by number and geographic location in Table 1. The date of the survey used, the condition of the inlet

Table 1. Geographic order of inlets with survey dates, inlet conditions, and source of data.

Inlet No.	Name and Location	Survey Date ¹	Inlet condition ²	Source ³
Atlantic coast				
1	Moriches Inlet, N.Y.	1933	D	C&GS 5322
2	Fire Island Inlet, N.Y.	1950	J, D	C&GS 7800
3	Beach Haven-Little Egg Inlet, N.J.	1954	NI	C&GS 8220
4	Brigantine Inlet, N.J.	1954	NI	C&GS 8221
5	Great Egg Inlet, N.J.	1962, 1974	NI	C&GS 8676; NOS 12316
6	Corson Inlet, N.J.	1975	NI	USAE
7	Townsend Inlet, N.J.	1937	NI	C&GS 6231
8	Hereford Inlet, N.J.	1937	NI	C&GS 6236
9	Chincoteague Inlet, Va.	1962	NI	C&GS 8764
10	Metomkin Inlet, Va.	1862	NI	C&GS 794
11	Wachapreague Inlet, Va.	1911	NI	C&GS 3304
12	Oregon Inlet, N.C.	1937	NI	C&GS 6228
13	Hatteras Inlet, N.C.	1916, 1935	NI	C&GS 3922 and 5814
14	Beaufort Inlet, N.C.	1952	D	C&GS 7963
15	Carolina Beach Inlet, N.C.	1967	NI	USAE CB1 67-7
16	Lockwoods Folly Inlet, N.C.	1924	NI	C&GS 4450
17	Shallotte Inlet, N.C.	1934	NI	C&GS 5657
18	Tubbs Inlet, N.C.	1924	NI	C&GS 4450
19	Little River Inlet, S.C.	1934	NI	C&GS 5656
20	Murrells Inlet, S.C.	1926, 1974	NI	C&GS; USAE
21	North Inlet, S.C.	1925	NI	C&GS 4521
22	South Santee River Inlet, S.C.	1925	NI	C&GS 4522
23	Price Inlet, S.C.	1963	NI	C&GS 8779
24	Capers Inlet, S.C.	1963	NI	C&GS 8779
25	Dewees Inlet, S.C.	1963	NI	C&GS 8779
26	Lighthouse Inlet, S.C.	1921	NI	C&GS 4181
27	Stono Inlet, S.C.	1965	NI	C&GS 8870
28	Fripps Inlet, S.C.	1934, 1972	NI	C&GS 5717; NOS 793
29	Doboy Inlet, Ga.	1919, 1972	NI	C&GS 4099; NOS 574
30	Nassau Inlet, Fla.	1934, 1971	NI	C&GS 5798 and 1110
31	Fort George Inlet, Fla.	1924	J	C&GS 4376
32	St. Augustine Inlet, Fla.	1924	NI	C&GS 4453
33	Ponce de Leon Inlet, Fla.	1925	NI	C&GS 4478
34	Sebastian Inlet, Fla.	1930	J	C&GS 5028
35	Boca Raton Inlet, Fla.	1929	NI	C&GS 5015
36	Hillsboro Inlet, Fla.	1929	NI	C&GS 5015
Gulf coast				
37	Big Marco Pass, Fla.	1891, 1970	NI	C&GS 2038; NOS 1254
38	Gordon Pass, Fla.	1975, 1970	J	NOS 11430 and 1254
39	Redfish Pass, Fla.	1960	NI	C&GS 8598
40	Captiva Pass, Fla.	1960	NI	C&GS 8555 and 8362
41	Boca Grande Pass, Fla.	1956, 1970	D	C&GS 8358; NOS 1255
42	Gasparilla Pass, Fla.	1956	NI	C&GS 8193 and 8196
43	Stump Pass, Fla.	1955	NI	C&GS 8192
44	Midnight Pass, Fla.	1955	NI	C&GS 8154
45	Big Sarasota Pass, Fla.	1954	NI	C&GS 8098
46	Longboat Pass, Fla.	1953	NI	C&GS 8035
47	Pass A Grille, Fla.	1926	NI	C&GS 4569
48	Clearwater Pass, Fla.	1949	NI	C&GS 7875
49	Pensacola Pass, Fla.	1919	D	C&GS 4103
50	San Luis Pass, Tex.	1933	NI	C&GS 5488
51	Pass Cavallo, Tex.	1934	NI	C&GS 5864
Pacific coast				
52	Morro Bay Inlet, Calif.	1938	NI	USAE A-2585
53	Bolinas Inlet, Calif.	1929	NI	C&GS 4975
54	Drakes Inlet, Calif.	1860	NI	C&GS 720
55	Bodega Bay Inlet, Calif.	1931	NI	C&GS 5162
56	Humboldt Bay Inlet, Calif.	1859	NI	C&GS 5710
57	Coos Bay Inlet, Oreg.	1885	NI	USAE CB-1-18
58	Umpqua River Inlet, Oreg.	1903	NI	USAE UM-1-11
59	Siuslaw River Inlet, Oreg.	1891	NI	USAE SL-1-8
60	Alsea Bay Inlet, Oreg.	1914	NI	USAE AL-1-7
61	Yaquina Bay Inlet, Oreg.	1920	J	USAE YB-1-63
62	Siletz River Inlet, Oreg.	1931	NI	USAE SE-1-7/1
63	Netarts Bay Inlet, Oreg.	1957	NI	C&GS 8372
64	Tillamook Bay Inlet, Oreg.	1910	NI	USAE TM-1-20
65	Nehalem Inlet, Oreg.	1957	J	C&GS 8368
66	Willapa Bay Inlet, Wash.	1935	NI	USAE E-4-2-91
67	Grays Harbor Inlet, Wash.	1894	NI	USAE Sheet 524 13 Dec. Report

¹When two dates are shown, the second date refers to the survey used in ebb delta analysis.

²NI indicates inlet was not jettied at survey date and dredging information was unknown at survey date; D indicates inlet may have been dredged before survey date; J indicates inlet has jetties in survey date shown.

³USAE charts were obtained from the area USAE Districts.

(jettied or dredged), and the source of the data are given. About 50 percent of the inlets are on the Atlantic coast, 25 percent on the Pacific, and 25 percent on the Gulf of Mexico.

The primary constraints used in selection of the inlets and particularly surveys used were (a) potential Corps involvement, (b) natural condition or only minor modification by man, (c) excellent survey coverage of the ebb tidal delta, and (d) correspondence to inlets under study in the stability analyses. As a result, a wide range of survey dates was used. *Care should be used in applying specific data from this report in other analyses because later survey data may be available.* It must be emphasized that when an inlet is specifically discussed in this report the reference is related to the condition of the inlet at the survey date which may be very different than the present condition.

More than 500 boat sheets for more than 100 inlets were analyzed in preliminary studies. The inlets chosen are expected to typify the wide range and diversity of inlet conditions without bias toward any of the parameters. In this way an appropriate sample of the statistical population of inlets was chosen. Because a wide range in dates and sources of surveys has been used, it is important to recognize that the accuracy of the data does vary. It is expected that the errors are random and not biased.

2. Orientation.

Throughout this report the orientation of features and graphs of the features will be specified using the convention that LEFT signifies left of an observer standing on the mainland looking seaward. Depths are negative below mean low water (MLW).

3. Definition of Inlet Geometric Parameters.

To examine the variation of inlet geometry and to derive an inlet classification, it is essential to select a consistently definable set of parameters that describes the basic characteristics of inlet geometry. More than 50 parameters have been measured and examined at various inlets to select parameters for final study. Some parameters were readily discarded because of definitional difficulties. Others were discarded because they proved insignificant in preliminary cluster analyses. The parameters selected for final analysis appear readily definable at most inlets and in previous tests proved to be important descriptors of inlets.

As noted later in the examination of the parameters used, there are no descriptors of the flood tidal delta or the bay system. Approximately 20 variables examined produced no consistent set of meaningful parameters. This is a result of the extreme complexity of the bay areas, the slow adjustment of these areas to changes at the inlet, and the great influence of geologic factors. The bay channels result not only from current inlet conditions but may be remnants of older tidal deltas or may result from the influence of estuarine processes not directly related to the inlets. It is recommended that the characteristics of these systems as related to the inlets be considered as a separate estuarine classification system.

The sections of the inlet system considered in this report are those parts located beyond what is defined as the minimum inlet width cross section (MIWC)

and includes all of the ebb tidal delta. Characteristics included are the dimensions and shape of the following:

- (a) The MIWC profile.
- (b) The main channel from the MIWC to a point beyond the crest of the ebb tidal delta.
- (c) The ebb tidal delta.

These are the areas that are highly influenced by a combination of waves, wave-generated longshore currents, and tidal currents. They also include the areas of the inlet that frequently pose the most difficulty in maintenance of navigation channels.

a. Channel Cross Section at Minimum Inlet Width (MIWC). The characteristics of the narrow parts of the inlet gorge are to a great degree determined by the exchange of waters between bay and ocean. The shape and size of the channel result from a balance between tidal current transport of sediment through the channel and wave-generated transport into the inlet from adjacent beaches. Here attention is focused on the channel cross section located at the minimum inlet width (measured at MLW). For hydraulic considerations, the cross section with minimum area has generally been used; it is frequently located close to the MIWC. Another consideration in the choice of the MIWC is that the minimum inlet width can be defined on photos which are a major source of inlet stability data. The use of MIWC allows for correspondence between the two data sets.

The minimum width, W , of an inlet will be defined as the minimum distance between the shorelines bounding the inlet. This definition can easily be applied to cases similar to the situation in Figure 1. Fortunately, this is the dominant case encountered. However, two inlets similar to the one in Figure 2 occurred in the set of inlets studied. Figure 2 shows that a minimum width near the inlet throat may not allow the parameters defined for this study to be measured in a manner consistent with the other inlets. An alternate inlet width (Fig. 2) was used. This width was determined to be given by a line with minimum length parallel to the shoreline bend and seaward of any channel bifurcation. W is given in feet.

After the minimum inlet width was established and measured at M_L , a detailed cross section was plotted. The depths were recorded as a function of distance from the left. The average depth, DMA , was calculated and the maximum depth, DMX , noted. Both DMA and DMX are negative quantities. The cross-sectional area, A_C , was determined and found, as expected, to be very close to $DMA \times W$. Hence, it is a redundant parameter. The analysis of the cross-sectional shapes is defined later in this report. DMA and DMX are given in feet.

b. Channel Profile. From the MIWC, the deepest channel was noted and traced seaward (Fig. 3). The depths were recorded as a function of distance along the length of the channel from the MIWC. The channel was stopped at that point where minimum depth across the outer bar, DCC , was located. The channel length, L , was defined as the distance measured along the channel from the MIWC to the crest of the bar in the channel. The analysis of the shape of this profile is discussed later. A definitional sketch for DCC and L is given in Figure 3. Profiles of the 67 inlets selected are plotted in Appendix A. L and DCC are given in feet; DCC is a negative quantity.

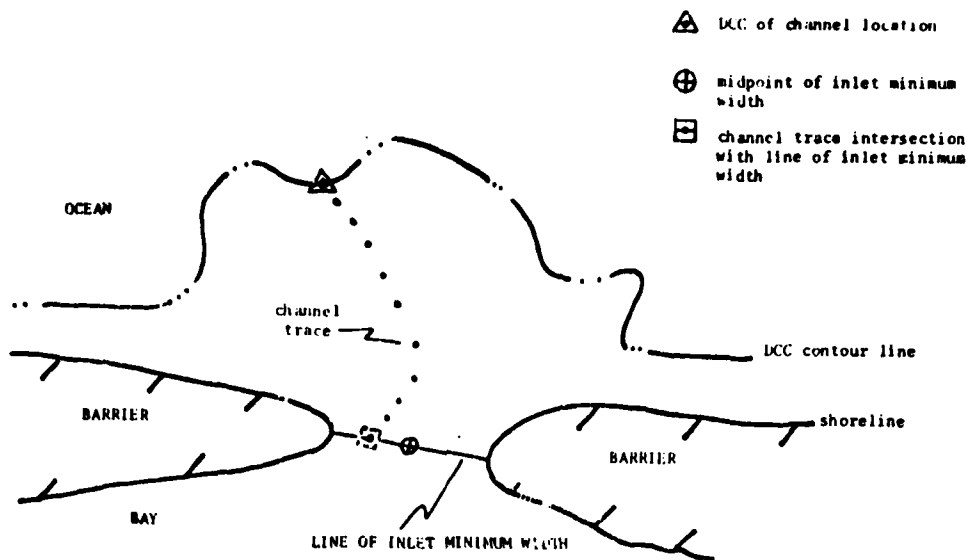


Figure 1. Measurement of inlet minimum width (W).

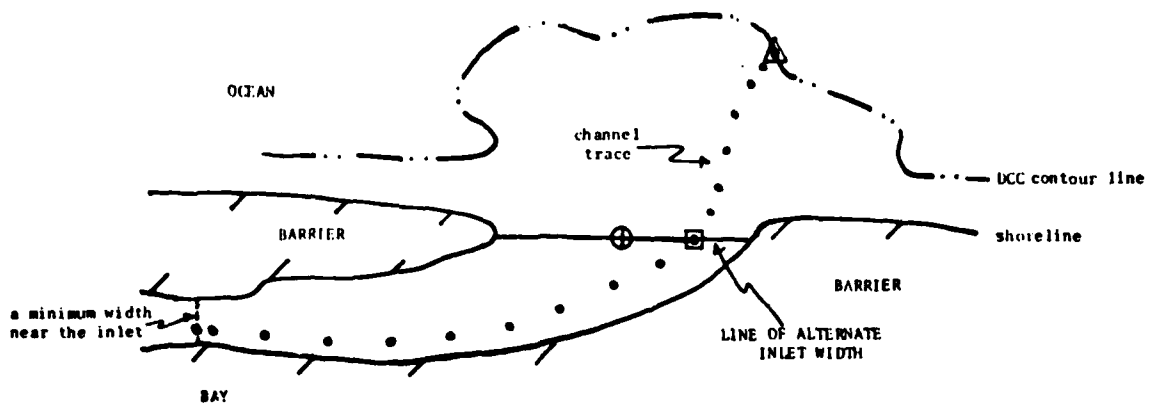


Figure 2. Measurement of alternate inlet width.

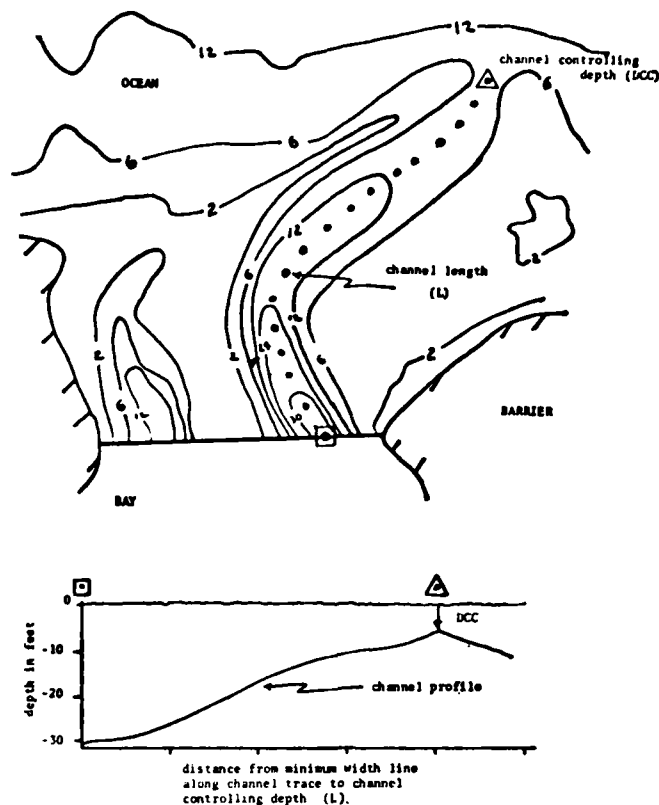


Figure 3. Measurement of channel parameters DCC and L.

c. Measurement of Ebb Tidal Delta Area. Ebb tidal delta area (AED) is defined as the area seaward of the inlet bounded by the shoreline, the contour depth at the crest of the outer bar in the channel, DCC, to a point where it parallels the shoreline and the line of inlet minimum width (Fig. 4). Using a Bruning Areagraph chart No. 4849 and hydrographic charts, the area of the ebb delta was first calculated in square inches and then, using the scale of the hydrographic chart, was recorded in square miles.

4. Representation of Channel Cross Section, Channel Profile, and Ebb Delta Shapes: Mathematical Considerations.

An important characteristic of a channel cross section, profile, or shoal is its shape. Unless the shape is simple, it is difficult to express succinctly in mathematical terms. Previous techniques have relied upon the definition of some simple, but arbitrary parameters that can be demonstrated by the case of a channel cross section. A typical parameter selected to describe the shape would be the distance from one side of the inlet to the point of maximum depth. However, if the cross section had two major channels, two such parameters would be defined. As can be seen, the solution is to define N in such parameters. If a cross section has less than N channels, the values for the nonexistent channels would be set zero. Herein lies a mathematical ambiguity: a zero value implies a channel at the base point for measurement. It is possible to define additional parameters to relieve the ambiguity, but the problems tend to be

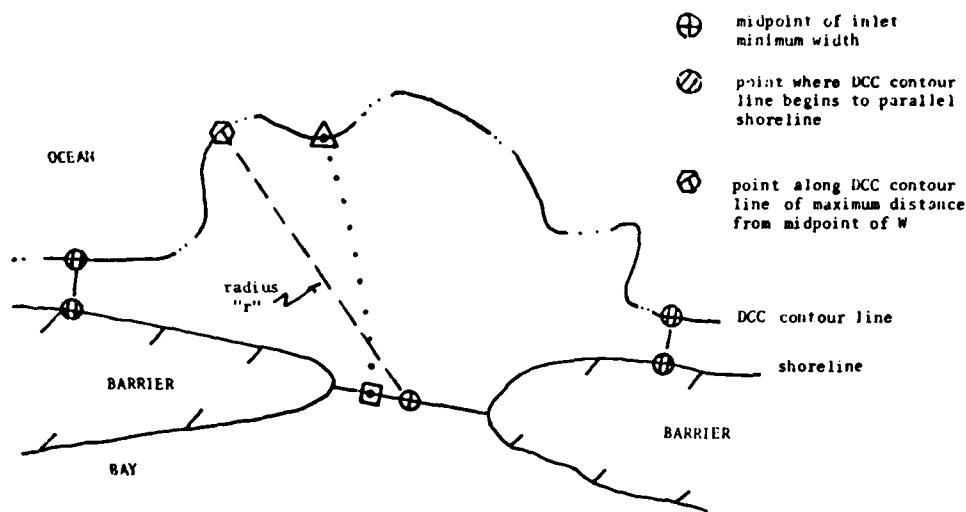


Figure 4. Measurement of ebb delta area (AED).

compounded. Another approach used is to fit the curve or surface with a mathematical function such as a Fourier series or orthogonal polynomials. This is satisfactory only if a few functions are required.

Recent research has resulted in a simple method for representing shapes. The analysis results in a succinct parameterization based on rigorously derived mathematical functions that, in the sense of least squares optimization, are those functions that best fit the shapes under consideration. The method is termed an eigenvector analysis and is directly related to an R-mode principal component analysis (Kendall and Stuart, 1968). It has been used to examine shape variations in meteorologic parameters such as spatial pressure, temperature, and rainfall fields (Kutzbach, 1967); in Inner Continental Shelf bathymetry (Resio, et al., 1977); in profiles across barrier islands (Vincent, et al., 1976); in beach profiles (Winant, Inman, and Nordshrom, 1975; Vincent and Resio, 1976); and in channel cross sections (Vincent, 1976). An heuristic explanation of the technique is given in the present report for a channel cross section. More rigorous explanations of the mathematics can be found in Kendall and Stuart (1968), Resio, et al. (1977), and Vincent (1976).

A channel cross section can be represented as an M component vector, \underline{z}^* ,

$$\underline{z}^* = (d_1, d_2, \dots, d_M) \quad (1)$$

where d_i is the depth at the i^{th} location along a traverse. What is sought through an eigenvector analysis is a series of M geometric shapes, represented as M vectors, $\underline{e}_1, \underline{e}_2, \underline{e}_3, \dots, \underline{e}_M$ each with M components such that

$$\underline{z}^* = \underline{\mu} + a_1 \underline{e}_1 + a_2 \underline{e}_2 + \dots + a_M \underline{e}_M \quad (2)$$

where a_1, a_2, \dots, a_M are a series of coefficients that weight the individual shape vectors in reconstructing the original cross-section shape \underline{z}^* ; $\underline{\mu}$ is a constant vector representing the mean shape.

To apply an eigenvector analysis it is necessary to have a set of N cross sections, $\underline{Z}_1^*, \underline{Z}_2^*, \dots, \underline{Z}_N^*$, which are typical of the variation expected in the shape under study and with $N \gg M$. Typically, these vectors are given as deviations with respect to the mean shape, $\underline{\mu}$

$$\underline{\mu} = \frac{1}{N} \sum_{i=1}^N \underline{Z}_i^* \quad (3)$$

that is,

$$\underline{Z}_i = \underline{Z}_i^* - \underline{\mu} \quad (4)$$

The $M \times M$ covariance matrix, Γ , for the M components of \underline{Z} is constructed from the N observations of \underline{Z} . The shapes desired are solutions \underline{e} to the matrix equation

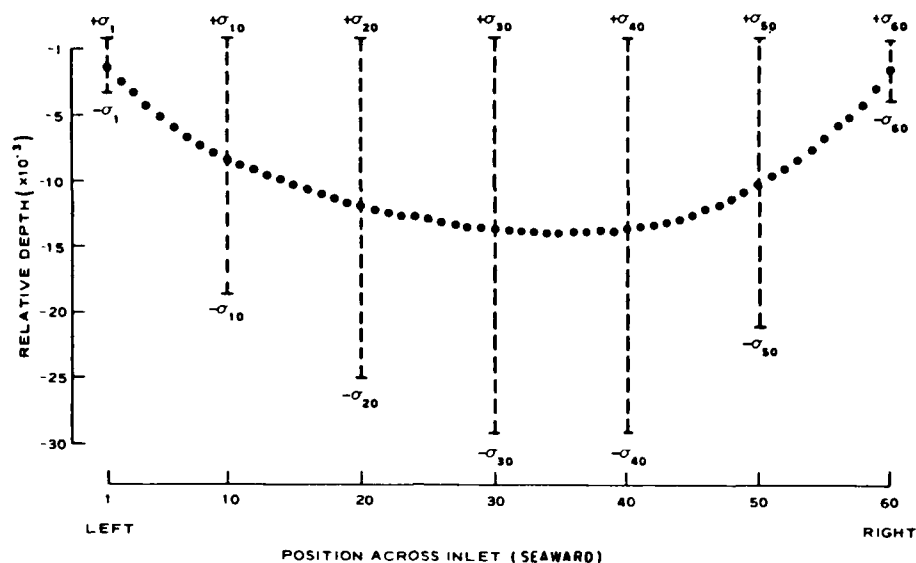
$$\Gamma \underline{e} = \lambda \underline{e} \quad (5)$$

where λ is an eigenvalue. There are M eigenvectors \underline{e} and M eigenvalues λ if Γ is of rank M . The shapes derived in this manner have several important properties:

- (a) For $i \neq j$, $\underline{e}_i \cdot \underline{e}_j = 0$; the shapes are orthogonal.
- (b) For $i = j$, $\underline{e}_i \cdot \underline{e}_j = 1$; the shapes are unit vectors.
- (c) The magnitude of the eigenvalue λ_i associated with shape \underline{e}_i is expressly the variance in the set of original profiles explained by shape \underline{e}_1 .
- (d) It can be mathematically demonstrated that by ordering the shapes by descending value of the associated eigenvalue, \underline{e}_1 must be that shape component that explains the most variance in the set of cross sections; \underline{e}_2 must be that shape that explains the next most variance given that is orthogonal (or independent) of \underline{e}_1 ; and so forth for all others.
- (e) Given an individual eigenvector, \underline{e}_1 , with $\underline{e}_1 = (1_{i1}, 1_{i2}, \dots, 1_{im})$, the components 1_{ij} represent the contribution of the eigenvectors \underline{e}_i to variation at transect location j . The effect that \underline{e}_i has in contributing to reconstruction of the individual profiles can be seen by plotting $1_{i1}, 1_{i2}, \dots, 1_{im}$ as in Figures 5 and 6. (An analogy can be drawn to a harmonic expansion where

$$f(x) = \sum_{i=1}^n \sigma_i \sin(ix) :$$

the σ_i corresponds to a_i and $\sin(ix)$ corresponds to \underline{e}_i . The values 1_{ij} correspond to the individual value of $\sin(ix)$ for some given x-ordinate x_j .)



NOTE: σ_i = STANDARD DEVIATION AT LOCATION i

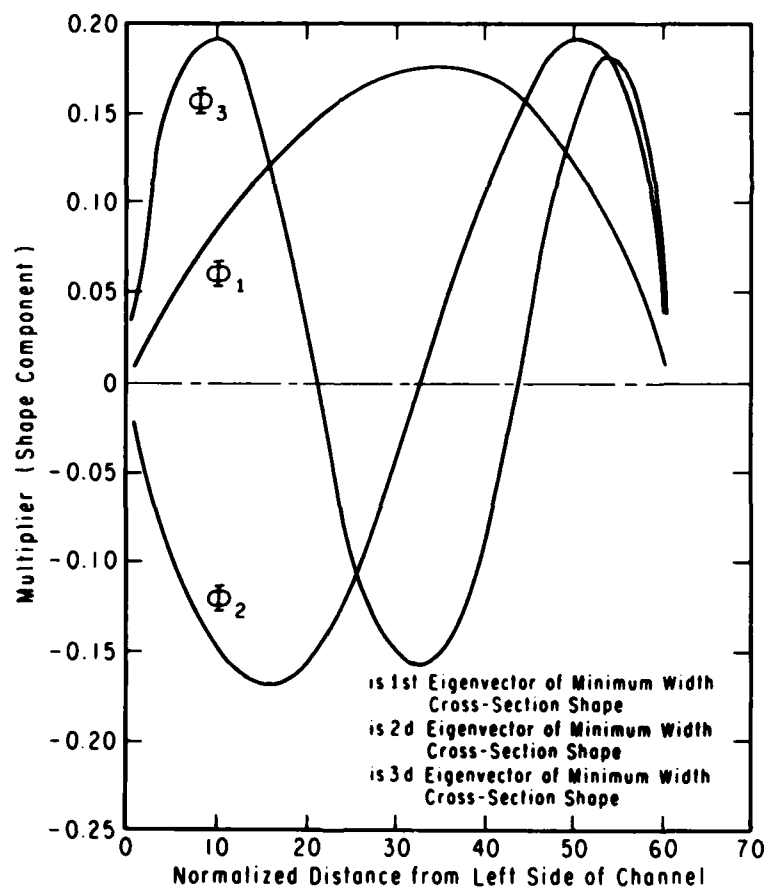


Figure 5. Minimum inlet width cross-section parameters. Mean cross section and pointwise standard deviation are shown along with the shapes of the first three eigenvectors.

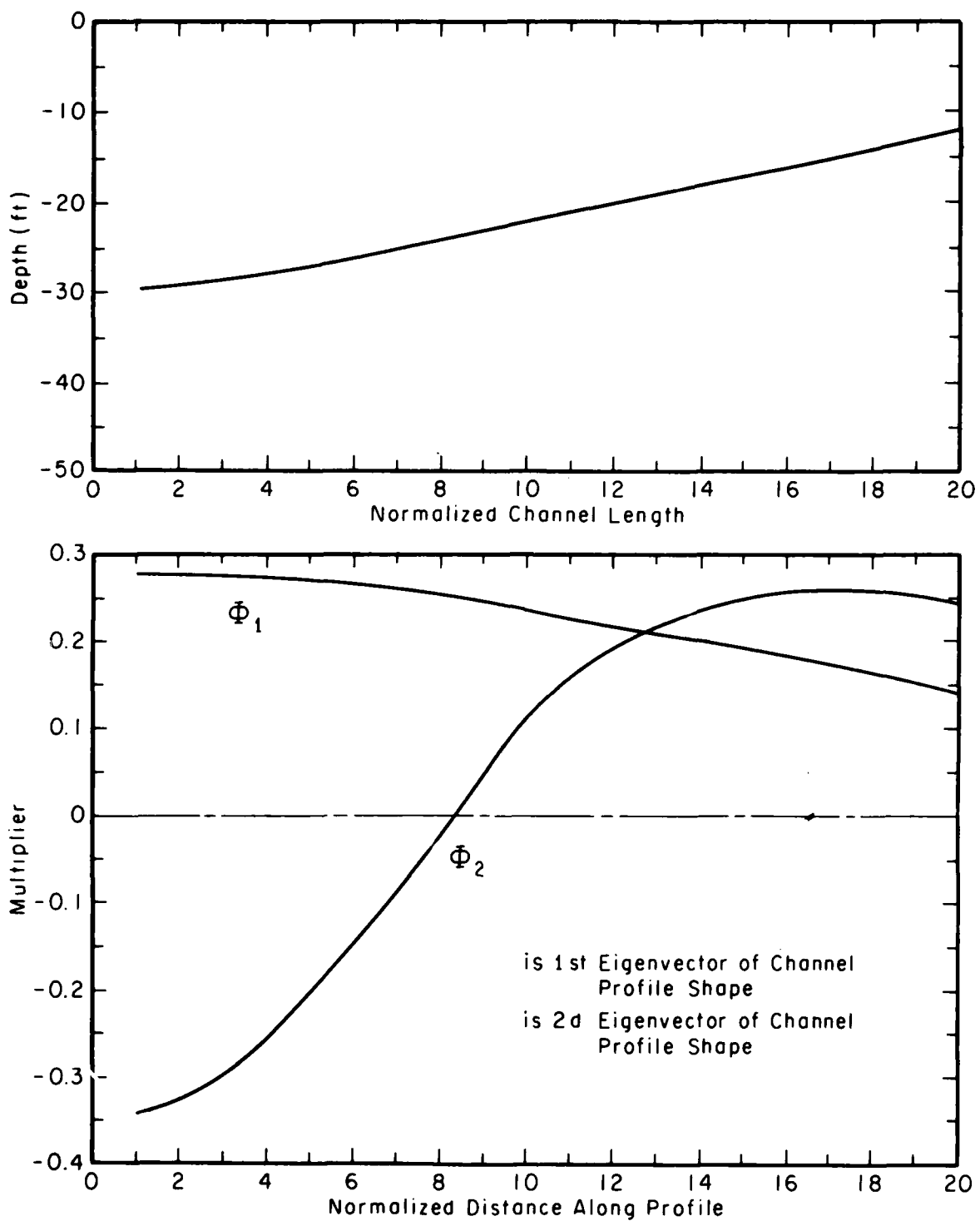


Figure 6. Channel profile parameters. The mean profile and the first two eigenvectors of profile shape are shown.

Thus, through an eigenvector analysis shape functions are derived that are an optimal decomposition of shape variations. Further, there is a new representation of the profile in the M dimensional eigenvector space; i.e., \underline{Z}_i is transformed to a vector

$$\underline{a}_i = (a_{i1}, a_{i2}, \dots, a_{iM}) \quad (6)$$

where a_{ij} are the weighting coefficients displaying the part of the decomposition of cross-sectional shape \underline{Z}_i explained by \underline{e}_j .

The primary advantage of the eigenvector analysis is now apparent. Having ranked $\lambda_1, \lambda_2, \dots, \lambda_M$ in descending order, it is convenient to find if there is an index K such that $\lambda_{K+1} + \dots + \lambda_M$ is sufficiently small to be neglected. If so, an estimate of the original shapes \underline{Z}_i is

$$\hat{\underline{Z}}_i = \underline{\mu} + a_{i1}\underline{e}_1 + a_{i2}\underline{e}_2 + \dots + a_{iK}\underline{e}_K \quad (7)$$

where $K < M$, thereby reducing the number of components in eigenvector space to estimate \underline{Z}_i by $M - K$. Values of K and of 2 and 3 can produce extremely good reproductions of \underline{Z}_i , while greatly reducing the number of parameters needed to describe the shape. Further, the method used to derive the parameters is objective and rigorous.

The parameters now used to describe the shape are the coefficients a_1, a_2, \dots, a_K , which indicate the importance of the shape functions $\underline{e}_1, \underline{e}_2, \dots, \underline{e}_K$ in the given inlet cross section. For the following analysis, M varied from 20 to 60 and N varied from 67 to more than 420. In the cases of channel cross sections at minimum inlet width and for the profiles along the channel thalweg, extra profiles were analyzed to provide a wider variety of inlet conditions.

It should be noted that the method was described by an example using a cross section or profile. It is evident that for any single-valued function in two- or three-dimensional space, a component vector

$$\underline{Z} = [f(x_1, y_1), f(x_2, y_2), \dots, f(x_M, y_M)] \quad (8)$$

can be defined if an intrinsic grid system (x_i, y_i) can be established for every observation of f . Hence, as is the case for the ebb tidal delta geometry studied here, spatial fields of data can be analyzed.

a. Shape of the Cross Section at Minimum Inlet Width. For every inlet examined, the depth as a function of distance from the left side of the minimum width cross section was recorded. The depth d_i was interpolated linearly at 60 evenly spaced points across the inlet, resulting in a 60-component vector

$$\underline{W} = (d_1, d_2, \dots, d_{60}) \quad (9)$$

Plots of the cross sections are provided in Appendix A. The depths were normalized by the minimum width W of the inlet to give a dimensionless geometry

$$\underline{W}^* = \left(\frac{d_1}{W}, \frac{d_2}{W}, \dots, \frac{d_{60}}{W} \right) \quad (10)$$

An eigenvector analysis was performed and the first three shapes plotted in Figure 5 along with the mean shape. The variance associated with \underline{e}_1 is 86 percent of the total, 8 percent with \underline{e}_2 , and 3 percent with \underline{e}_3 . Thus, three vectors explained 97 percent of the variance and the remaining 57 shapes were ignored.

The parameters (a_1 , a_2 , and a_3) describing the shape of the cross section will be noted as EM1, EM2, and EM3 and are the weighting, dimensionless coefficients for shapes \underline{e}_1 , \underline{e}_2 , and \underline{e}_3 , respectively. As a guide to the interpretations of the values of EM1, EM2, and EM3, the following generalizations are made:

- (a) Positive EM1—cross section shallower than the mean.
- (b) Negative EM1—cross section deeper than the mean.
- (c) Positive EM2—left asymmetric.
- (d) Negative EM2—right asymmetric.
- (e) Positive EM3—single channel.
- (f) Negative EM3—center shoal with two side channels.

Examples of four inlets that represent these six variations are provided in Figure 7. It should be noted that in Figure 7 the profiles are plotted in real depth not in normalized depth. Hence, although Port Royal Sound and Dewees have depths of about 40 to 50 feet, their relative depths are vastly different because Port Royal Sound is 10 times the width of Dewees. Thus, EM1 is 0.0590 for Port Royal and -0.0810 for Dewees.

The eigenvector representations appear to be realistic expressions of cross-sectional shape variability. The first eigenvector scales the shape according to its shallowness or deepness with regard to the mean. The second eigenvector displays the asymmetry of the inlet channels. The third eigenvector displays a tendency toward a single or a multiple channel system. The eigenvector analyses not only provide a succinct mathematical representation of cross-section shape, but the shapes derived closely resemble major shape variations generally recognized as important.

It should be noted that the sign of EM2 is a directional quantity. For the analyses later in this report the magnitude of EM2 is used without the sign. This is done because the direction of asymmetry is unimportant unless correlation is made to another directional quantity.

b. Shape of the Main Channel Depth Profile. The method for determining the centerline of the main channel was discussed previously. As with the MIWC, depths were recorded as a function of arc length along the channel centerline from the minimum width cross section to the crest of the ebb tidal delta. At 20 evenly spaced points the depth was linearly interpolated and a profile vector constructed

$$\underline{P} = (d_1, d_2, \dots, d_{20}) \quad (11)$$

The first two calculated eigenvectors are plotted with the mean in Figure 6. The first eigenvector explained 87 percent of the total variance, the second 8 percent, and the third 3 percent. Only the first two eigenvectors are used to

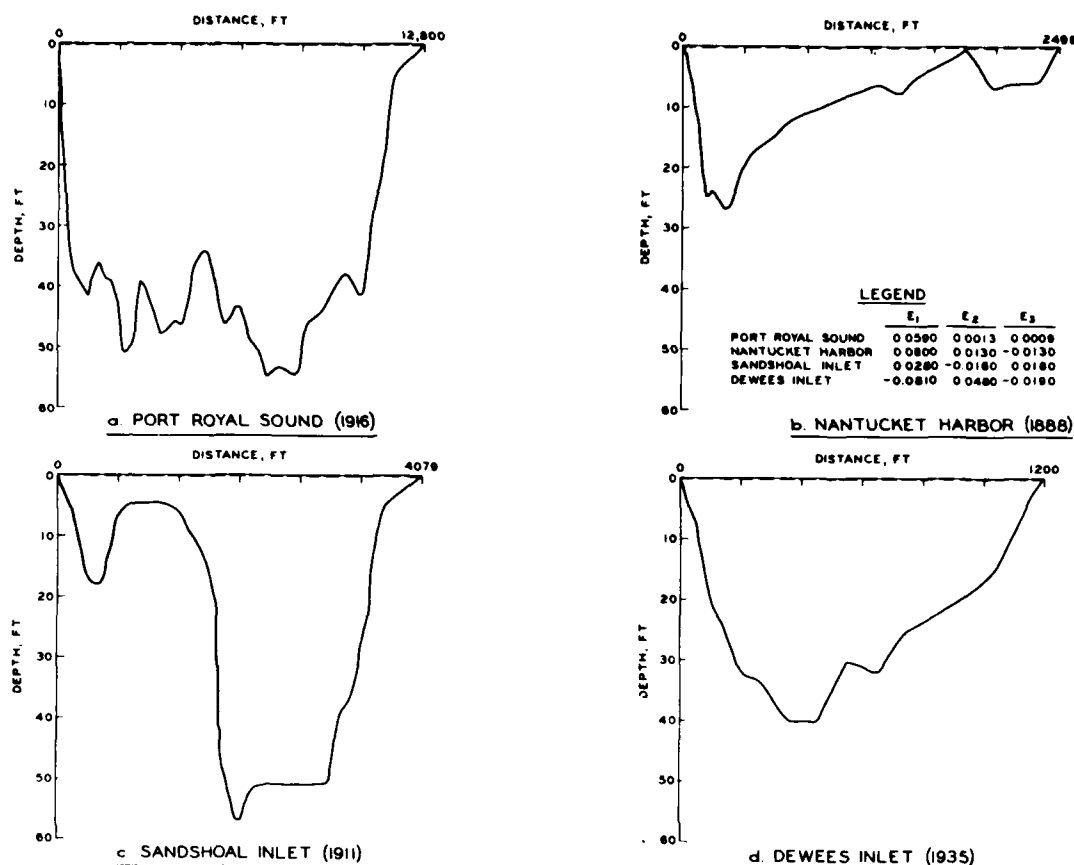


Figure 7. Examples of inlet cross sections showing the major variations in EM1, EM2, and EM3. Note that the eigenvectors were computed for the normalized depth.

parameterize channel shape, and the other 18 are ignored. Four examples of natural profiles for different eigenvector weightings are given in Figure 8.

The parameters used are denoted as EC1 and EC2 and the respective weighting coefficients for e_1 and e_2 . When EC1 is a positive number the result is a channel which is in general shallower than the mean of all channels; when it is a negative value, the result is the opposite. When EC2 is a positive value, the inner part of the channel (closer to the MIWC) is relatively deep and the outer part is shallow. For EC2 negative, the inner part of the channel is shallow and the outer part deep.

Again, the patterns represented in the eigenvectors are variations typical of inlet channel profiles. The first eigenvector is very much related to the total depth of the channel. The second eigenvector indicates the presence of a bar near one end of the channel and scour near the other end.

c. Shape of the Ebb Delta. A primary difficulty in parameterization of inlet morphology is representation of the offset of the inlet and the shape of the ebb tidal delta. Several approaches were tried unsuccessfully. In all cases definitional ambiguities occurred, particularly in the definition of

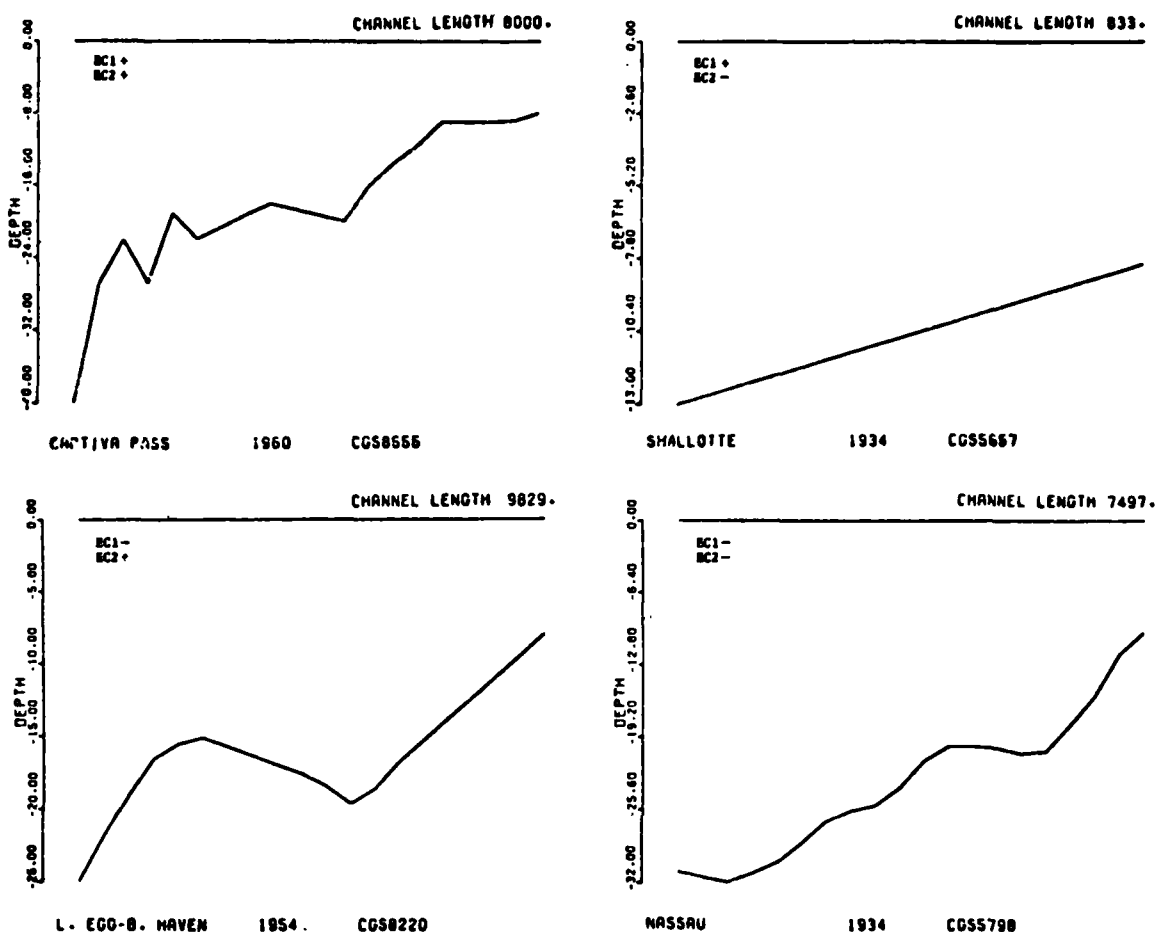


Figure 8. Examples of inlet profiles showing the major variations in EC1 and EC2.

offset. The set of parameters tended to be unwieldy to analyze and very difficult to interpret. An eigenvector analysis of the spatial pattern of depths over the ebb delta was attempted and the results afforded a simpler set of parameters.

(1) Construction and Alinement of Ebb Tidal Delta Grid. A semicircular grid (Fig. 9) was constructed to compare the morphology of the 67 ebb tidal deltas at the same size, i.e., to normalize the delta geometry. A radius of 5 inches was chosen as a working size to represent the prototype distance, r , as shown in Figure 10. The radii were spaced at 10° intervals, and the concentric semicircles were separated by one-half inch.

The alinement of the grid was determined by the trend of the local shoreline and the location of the inlet minimum width midpoint. The midpoint of the base line of the grid was positioned on the midpoint of the inlet minimum width line, and the base line of the grid was set parallel to the general trend of the local shoreline. The radii were directed seaward, and the recording points were located over parts of the ebb tidal delta. The left side of the grid viewed from the base line facing seaward remains left for all coastlines; i.e.,

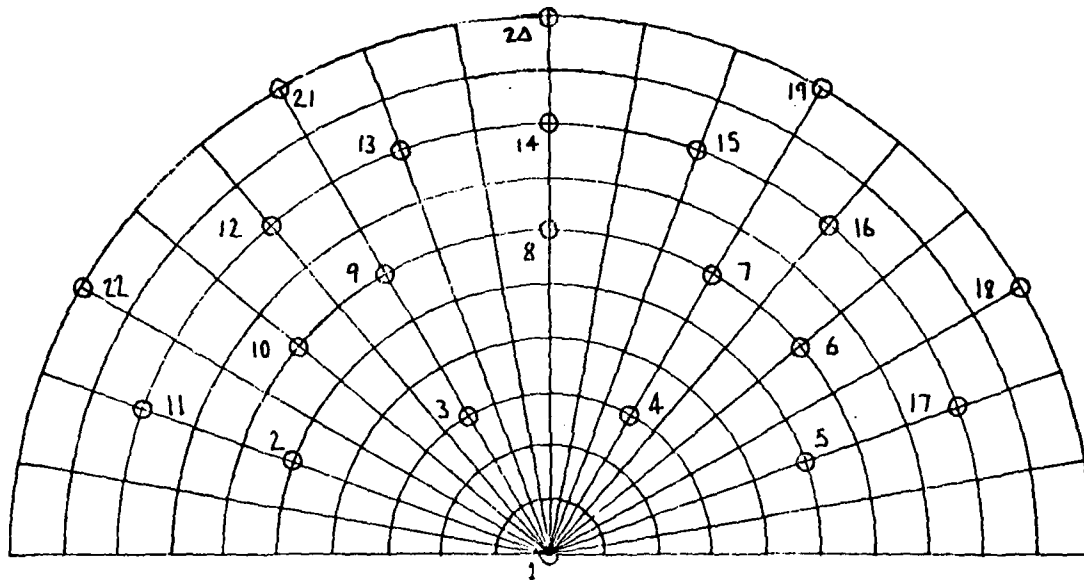


Figure 9. Grid mesh for describing ebb delta geometry. Sampling points are numbered.

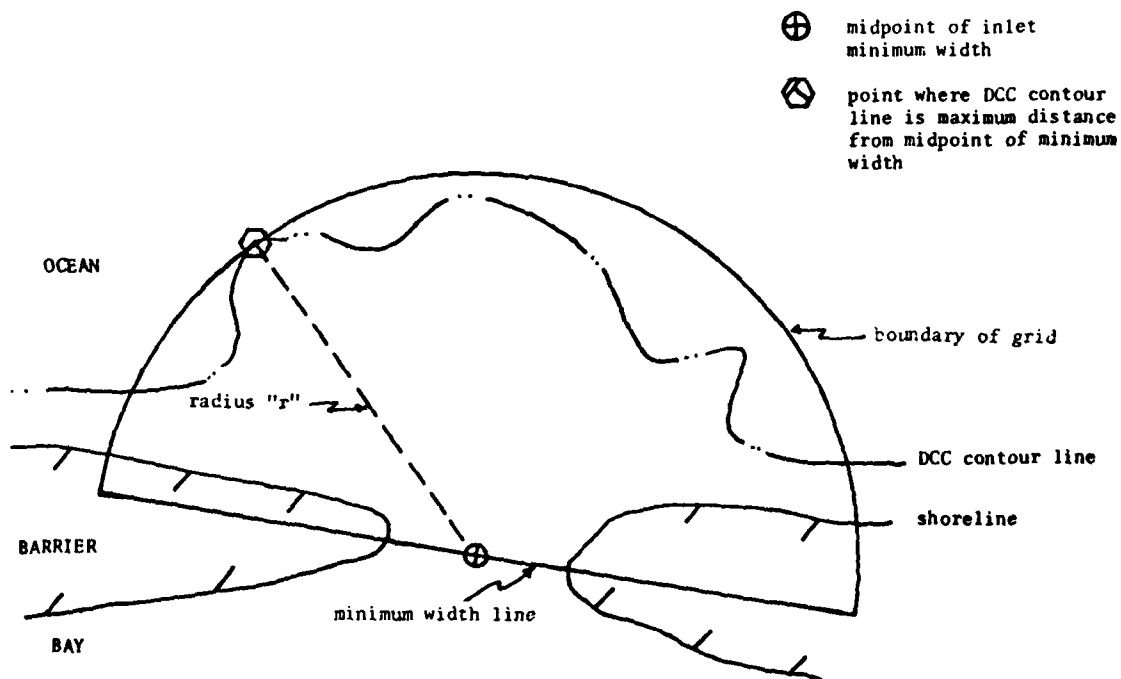


Figure 10. Measurement of ebb delta radius, r , and alignment of ebb delta grid.

for the U.S. Atlantic coast, left will be directed generally northward and for the U.S. Pacific coast, left will be trending southward. After the depths were recorded the grid was "flipped," as necessary, so that the shallower side of the inlet was always on the right side of the grid. This was done because the objective of the analysis in which the data are used is to define the geometry of the delta, which is by definition nondirectional. If a grid point fell outside of the delta, the depth was recorded as well. Plots of the ebb deltas used are given in normalized distance format in Appendix A.

Because of the differing ebb delta sizes it was necessary to normalize the ebb deltas so that they were geometrically similar; i.e., the ebb delta sizes on the map were reduced or expanded to have approximately the same area. This was achieved by reducing (or expanding) the scale of the chart until all of the ebb deltas, defined as all points interior of the depth contour equivalent to the controlling depth (DCC), were just contained within the semicircle defined previously. This was, in general, straightforward but there were a few instances such as Moss Bay, California, where the shoreline is not linear but makes a 90° bend near the inlet. In such cases the alinement of the grid was adjusted to be as consistent as possible to the other charts.

For a number of inlets, the basic charts did not contain sufficient data. Depths from charts closest in time to the basic chart used were substituted. The inherent assumption in this substitution is that the rate of change of ebb delta shape is small with time. This should be recognized as a possible source of random error in comparison to the other variates.

(2) Selection of Grid Recording Points. Within the grid constructed for normalizing the ebb tidal deltas, there are 191 radii semicircle intersections. Twenty-two were selected to represent the topography of the ebb tidal delta. The location of those points is shown in the sample grid (Fig. 9). The amount and location of the recording points were not intended to give a precise description of the delta but to give a consistent recording of data for similar locations on various deltas that have been normalized by size. The number of points is in part limited by the number of deltas available for eigenvector analysis which requires that the number of grid points be substantially less than the number of inlets (22 versus 67).

(3) Eigenvectors of the Ebb Tidal Delta Geometry. To reiterate, the geometry analyzed represents a reorientation so that the primary mass of the delta is to the right side of the grid. Further, the depths over the delta have been normalized by the average depth of the MIWC. Thus, the ebb delta vector is given by

$$\xi = (h_1, h_2, \dots, h_{22}) \quad (12)$$

where

$$h_i = \frac{d_i}{DMA} \quad (13)$$

with d_i the depth at the i^{th} intersection on the grid. The eigenvector analysis was performed on the correlation matrix rather than the covariance matrix to prevent the depths around the perimeter of the grid from dominating the analysis.

The correlation matrix contains the correlation V_{ij}

$$V_{ij} = \frac{1}{N} \sum_{k=1}^N \frac{(d_{ki} - \bar{d}_i)(d_{kj} - \bar{d}_j)}{\sigma_i \sigma_j}$$

with N the number of samples, σ_i , σ_j the standard deviations and \bar{d}_i and \bar{d}_j the mean depths at locations i and j respectively, and d_{ki} and d_{kj} the depths at locations i and j for inlet k . The mean geometry and the first three eigenvectors are presented in Figure 11. Examples of inlets corresponding to different weighting are provided in Figure 12.

The mean geometry exhibits a central channel and a shoal mass on the right that is distinctly shallower than the left as is expected by definition. The first eigenvector explains 36 percent of the total variance and represents a deep delta (depths deeper than the mean delta) when the weighting coefficient, ED1, is positively valued; when negatively weighted the depths are shallow indicating a relatively well-developed delta. The second eigenvector explains 15 percent of the variation. When its weighting function, ED2, is positive, the right-hand shoal area is made even shallower, the central channel is deepened, and the left-hand shoal is shallower (but not to the same degree as the right-hand shoal). When ED2 is negative the shoals are deeper and the channel shallower. The third eigenvector explains 10 percent of the variance, is somewhat more complex, and appears to represent a finer representation of the channel location. Only ED1 and ED2 are used in the analyses because the third eigenvector appears to be a smaller scale variation that is less likely to be related to the other descriptors used here. ED1 and ED2 are dimensionless.

To further discuss the geometry represented by the parameters ED1 and ED2, it should be noted that the values analyzed are relative depths (depth divided by DMA). Thus, ED1 represents variation in ebb delta thickness relative to the average channel depth. For ED1 positive, the delta is relatively deep; i.e., the differences between channel depth and shoal depths are less than when ED1 is negative. For ED1 < 0, the shoals are higher relative to the channel depth, thus to a large degree ED1 indicates how incised into the shoal the channel is. ED2 to a certain degree as well indicates not only an increased (or decreased) asymmetry of the shoal mass, but how incised the channel is. When ED2 is positive the shoals are more asymmetric and the channels deeper. When negative, the reverse is true.

A comparison of the variance explained by the first three eigenvectors in the ebb tidal delta analysis to that for the channel (first two eigenvectors) and MIWC (first three eigenvectors) analyses indicates that only 61 percent as opposed to 95- to 97-percent variance is explained. This is due to two major reasons. The ebb delta analysis is over a two-dimensional grid compared to one-dimensional traverse; thus, there is an additional degree of variation possible. Secondly, the results tend to indicate that the channel and minimum inlet width cross-sectional shapes are highly organized but that the ebb delta shape is less so. In the first two cases, the shape factors are likely to be strongly related to tidal currents which are perhaps an order of magnitude larger than the wave-induced forces. Over the ebb tidal delta, however, the difference is less; thus, the shape must strongly represent the interplay of two driving forces.

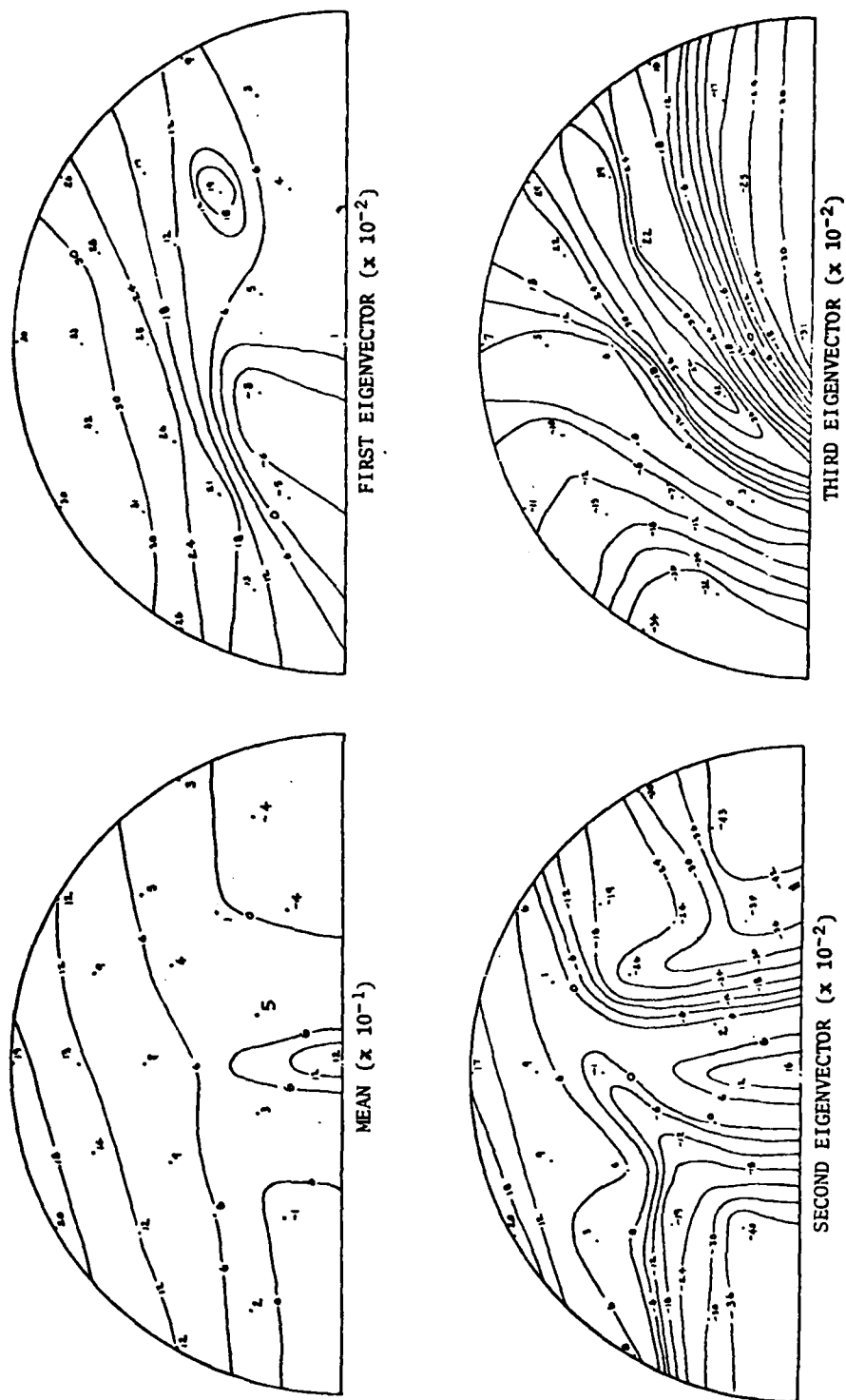


Figure 11. Contour maps of mean ebb delta geometry and the first three eigenvectors of ebb delta geometry.

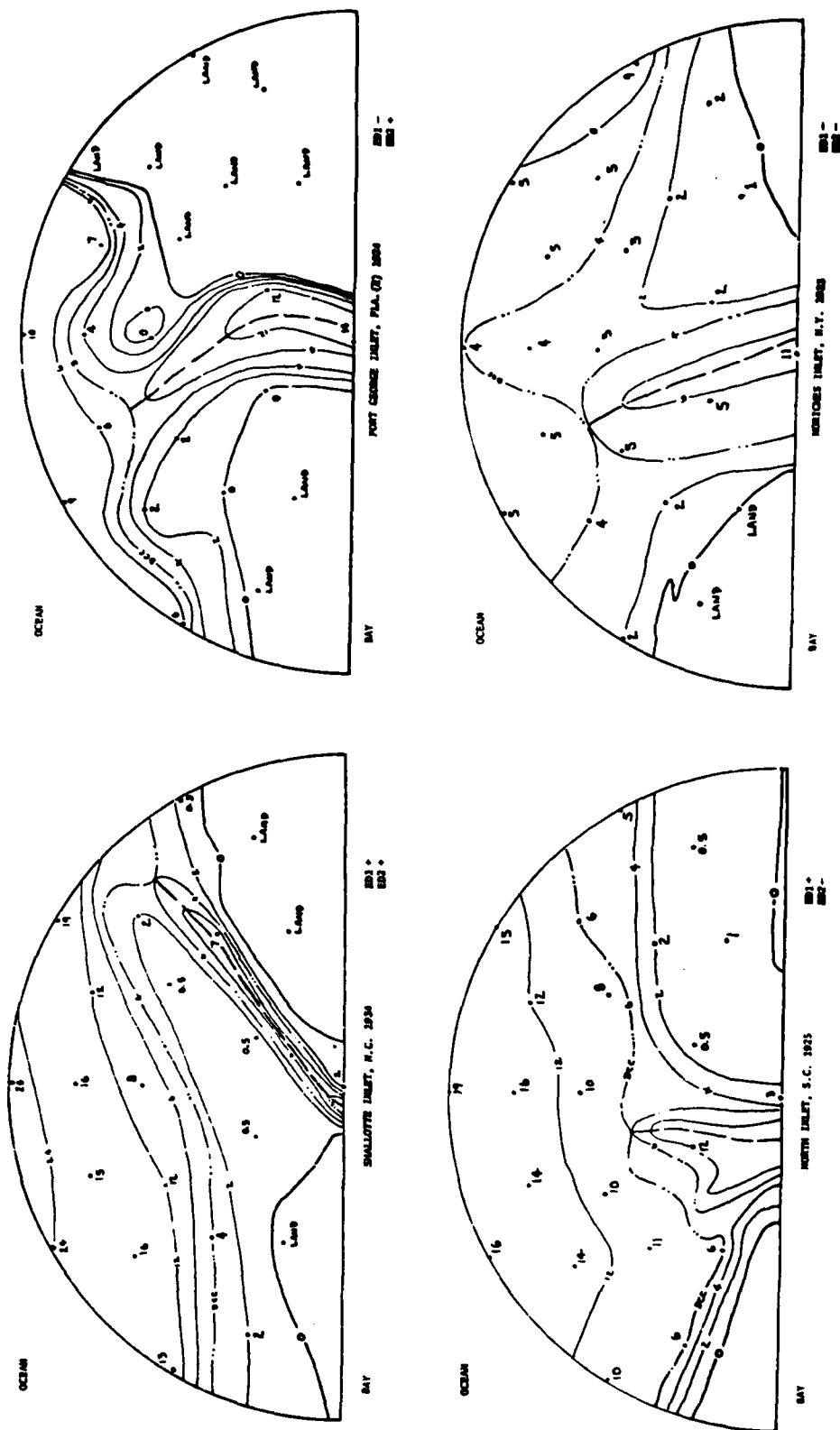


Figure 12. Examples of inlets showing the major variations in ED1 and ED2.

5. Distribution of Inlet Parameters.

The arithmetic mean and standard deviation of each of the 13 variables are given in Table 2. These variables include both the direct geometric parameters (W, L, DMX, DMA, DDC, and AED) and the eigenvector parameters for the cross-section shape (EM1, EM2, and EM3), channel profile (EC1 and EC2), and ebb delta (ED1 and ED2). A listing of the data by inlet is provided in Appendix B. Histograms of the values are provided in Appendix C.

Table 2. Mean and standard deviation of parameters.

Variable and No.	Mean	Standard deviation
DMX 1	-28.9851	17.4230
DMA 2	-11.4851	6.90464
W 3	3332.04	4036.59
DCC 4	-8.51493	6.65547
L 5	7111.99	5692.89
EM1 6	0.0085268	0.074429
EM2 7	0.0032447	0.032041
EM3 8	-0.000441	0.023791
EC1 9	14.7692	49.3612
EC2 10	5.75760	12.9366
ED1 11	0.000002985	2.89729
ED2 12	0.000001492	1.58685
AED 13	2.52133	4.40776

III. RELATIONSHIPS AMONG THE GEOMETRIC PARAMETERS

1. Procedures.

The number of possible combinations of 13 variables, as well as dimensionless and bifunctional relationships that can be formed from these variables, is large. Three guidelines were used to reduce the task. First, all combinations of pairs of the 13 parameters were examined. Then, relationships to the area of the MIWC were investigated. Finally, various but not all dimensionless combinations were considered. The combinations selected were those that appeared both logical and fruitful on the basis of relationships seen on other plots.

The procedure used to evaluate possible relationships was to first plot the variables concerned in nontransformed coordinates. If a functional relationship appeared, the coordinates were transformed by appropriate combination of logarithm transforms if the relationships appeared nonlinear. In the appropriate coordinate system a linear regression was performed to statistically fit the curve, estimate the degree of fit through the coefficient of determination (R^2), and produce 95-percent confidence bands. The methods used are common statistical techniques and are discussed in a number of textbooks (Kendall and Stuart, 1961; Krumbein and Graybill, 1965; Dixon and Massey, 1969). Based on this regression analysis, an F ratio (the ratio between the mean squares due to the regression and the mean sum of the squared deviations not explained by the regression) was computed. Because there are 67 inlets in the study this ratio must be greater than a 7.08 value for the F distribution with $v_1 = 1$ and $v_2 = 65$ degrees of freedom for the regression, or curve fit, to be significant at a 5-percent level.

The analyses are discussed first for direct relationships between individual variables. Next, relationships to the cross-sectional area of the MIWC are discussed. Finally, relationships to a dimensionless parameter W/L are discussed.

2. Direct Relationships Between Various Parameters.

a. Strong Relationships.

(1) DMX versus DMA. Figure 13 provides a linear plot of DMX versus DMA. The parameters appear strongly related as is confirmed in the curve fit analysis. The statistically derived relationship is

$$DMA = -1.42 + 0.347 DMX \quad (14)$$

noting both DMA and DMX are negatively defined (i.e., a depth of 17 feet is recorded as -17). The F ratio of the curve fitting regression is 215 and R^2 is 76.8 percent; both are extremely significant.

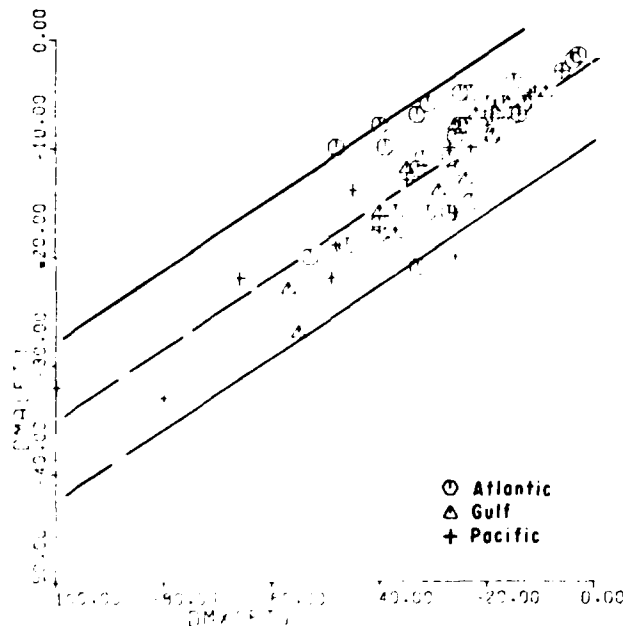


Figure 13. DMX versus DMA.

It was not unexpected to find a relationship between the average depth of the MIWC and the maximum depth therein. However, the strength of the relationship is greater than initially expected. It would appear that there is a higher degree of coherence in the form of the cross section than generally assumed.

(2) DMX versus DCC. Figure 14 provides a log plot of these variates (signs deleted). The relationship found is

$$DCC = 0.5662 DMX^{0.78} \quad (15)$$

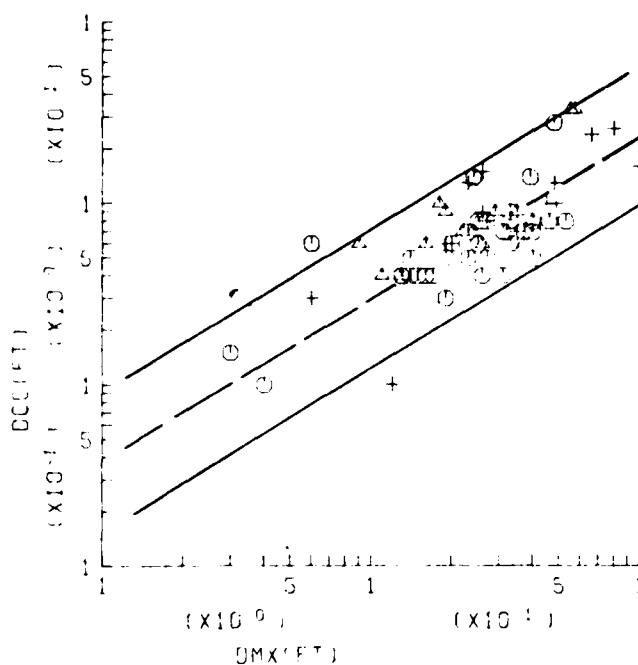


Figure 14. DMX versus DCC.

The relationship has an F ratio of 89 which is significant. The coefficient of determination is 57.9 percent.

The relationship between the maximum depth in the MIWC and the depth at the crest of the outer bar again is highly significant and implies a consistent adjustment of the channel depth profile to the crest of the outer bar. It should be noted however that considerable variability still remains.

(3) DMX versus L. Figure 15 provides a linear plot of L as a function of DMX. The relationship between DMX and L is less significant than those previously discussed but is still highly significant with an F ratio of 60 and R^2 of 48 percent. The curve fit is (with DMX negatively defined)

$$L = 539 - 226.7 \text{ DMX} \quad (16)$$

As expected, a relatively long channel is associated with a relatively deep inlet throat.

(4) DMX versus EC1. Figure 16 is a linear plot of these parameters. If EC1 can be consistently predicted, the channel profile can be predicted reasonably well because EC1 represents 87 percent of the shape variation in the profile. The F ratio of 346 is the highest achieved in this study, as is the coefficient of determination value of 84 percent. The linear relationship is (with DMX negatively defined)

$$\text{EC1} = 90.1 + 2.6 \text{ DMX} \quad (17)$$

where DMX is again negative valued. It can be seen that a relatively deep channel corresponds to a relatively deep inlet, remembering that a channel deeper than the mean has a negative EC1.

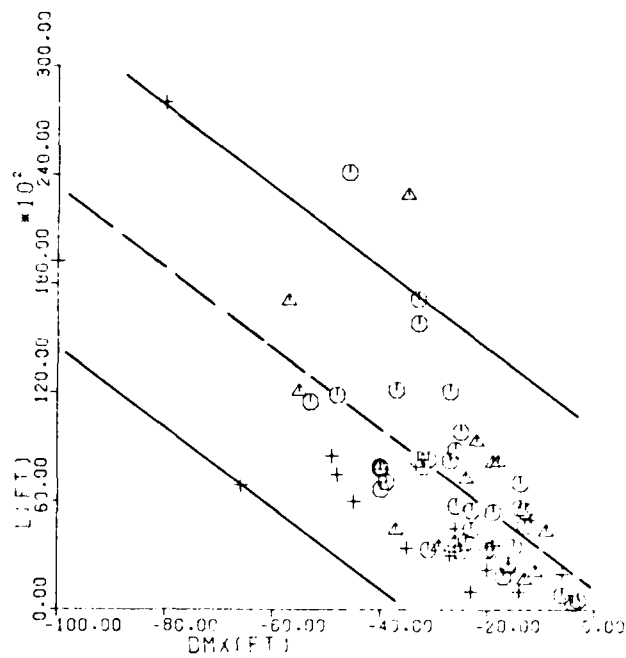


Figure 15. DMX versus L.

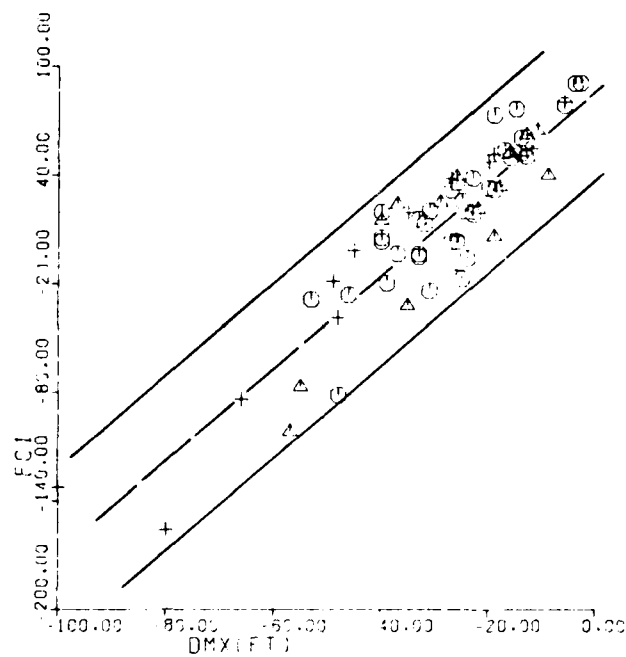


Figure 16. DMX versus EC1.

(5) EC1 versus DMA, DCC. Given the relationships between DMA, DCC, and DMX, good relationships to EC1 are expected. The equations, F ratios, and R^2 values are

$$EC1 = 81.9 + 5.8 \text{ DMA} \quad (18)$$

with $F = 131$ and $R^2 = 66.9$ percent, and

$$EC1 = 66.7 + 6.1 \text{ DCC} \quad (19)$$

with $F = 136$ and $R^2 = 67.6$ percent. DMA and DCC are negative valued. Thus, a relatively deep channel corresponds to both a relatively deep inlet and a relatively deep bar channel. The corresponding plots are Figures 17 and 18.

(6) EC1 versus L. Figure 19 provides a linear plot of EC1 versus L. The relationship is strong with F at 89 and R^2 at 58 percent. The equation is

$$EC1 = 61.7 - 0.0067L \quad (20)$$

In this case, lengthening the channel increases the channel depth and the controlling depth at the ebb tidal delta.

(7) AED versus L. As Figure 20 shows, the area of the ebb delta (AED) is strongly related to channel length and in statistical significance is second only to that between DMX and EC1. The F ratio is 327 and R^2 is 83.4 percent. The relationship is nonlinear and given by

$$AED = 3.9245 \times 10^{-7} L^{1.71} \quad (21)$$

AED is measured in square miles, L in feet. Since the ebb delta is bounded on the offshore side by the DCC contour and the channel extends to this same contour, it was expected that increasing L would also increase AED.

The strong relationship between L and AED is unexpected. A small partial correlation was initially supposed but not to the degree found. The limits of the delta are defined in this study by the contour equivalent to DCC, the depth of the crest of the outer bar in the channel. Given the relationships described previously in combination with this relationship, it is evident that there is a strong covariance among many of the major components of the inlet geometry. It is interesting to note that W and to a lesser degree DMA are not related to the other parameters.

b. Weak Relationships. The relationships discussed above are all highly significant. There are a number of other relationships involving DMX, DMA, DCC, and ED1, ED2, EM1 and ED2, EC1 and ED2, and AED and EC1, which appear potentially promising. In all cases, however, additional data are needed to further define the curve and confirm a functional relationship. For this reason curve fitting was not performed.

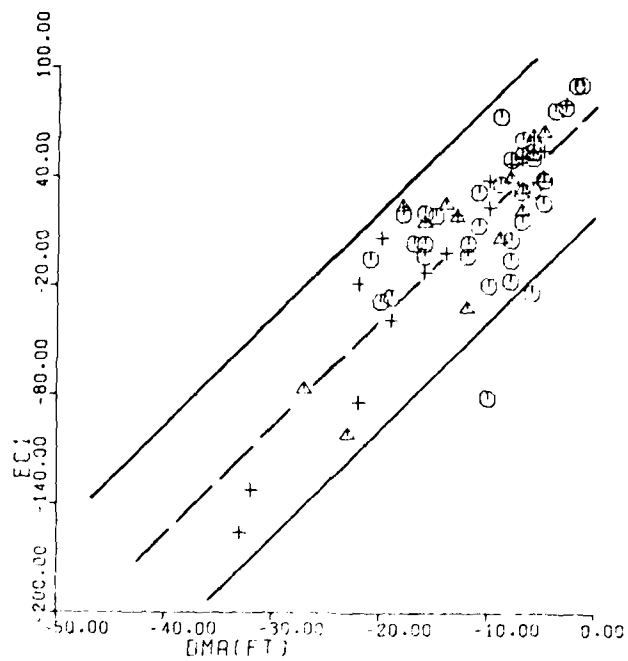


Figure 17. DMA versus EC1.

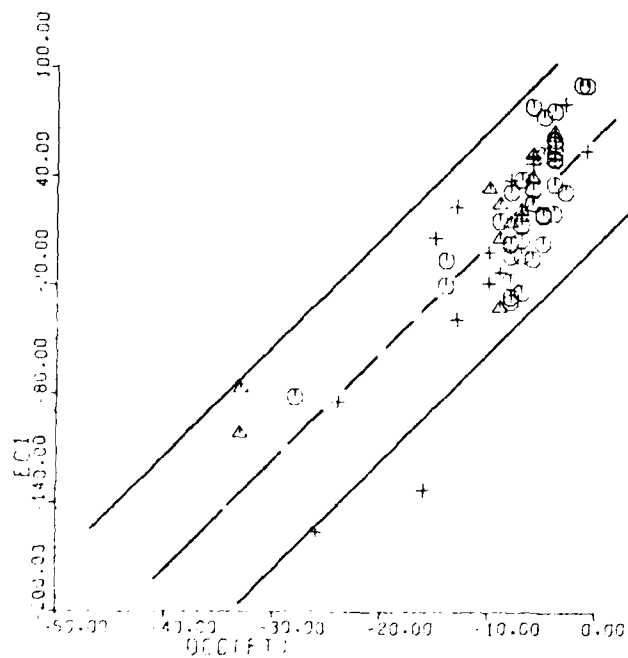


Figure 18. DCC versus EC1.

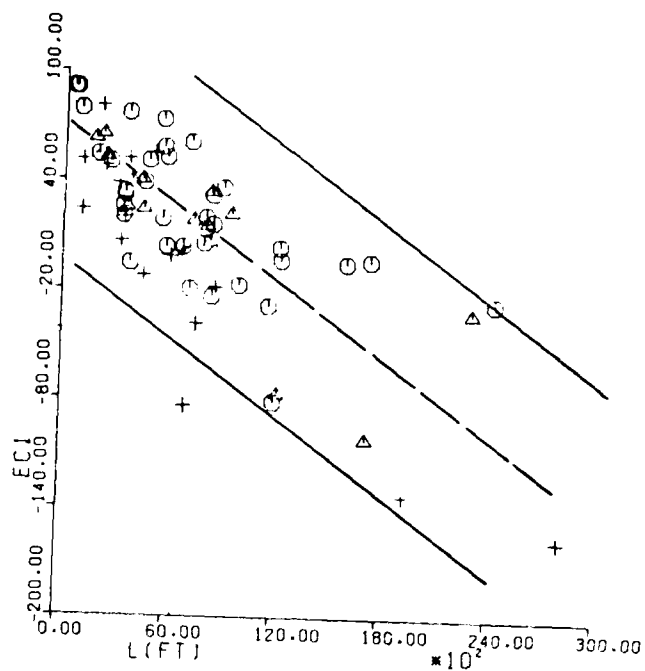


Figure 19. L versus EC1.

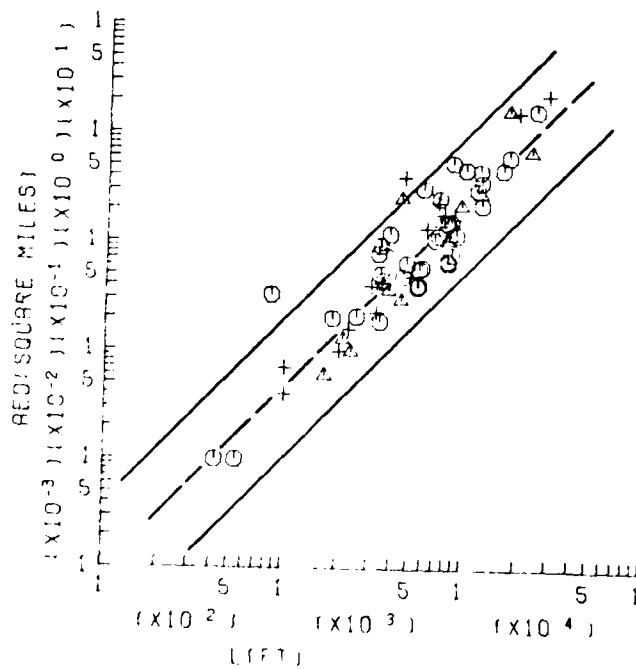


Figure 20. L versus AED.

From Figures 21, 22, and 23 it can be seen that the ebb tidal delta function ED2 (which describes the degree of delta asymmetry) appears related to DMX, DMA, and DCC in the following manner

$$ED2 = \frac{C_0}{\gamma^B} - C_1, B > 0 \quad (22)$$

where γ is either DMX, DMA, or DCC (positively defined) and C_0, C_1 , and B are positive constants that must be determined in a regression analysis. Thus, for decreasing depths in the channels, shoal asymmetry appears to become somewhat more prevalent. Channel length L follows a relationship with ED2 equivalent, in form, to those followed by DMX, DMA, and DCC (see Fig. 24).

Figure 25 indicates a relationship between the shape of the MIWC given by EM1 and the relative depth of the outer bar given by ED1. The form of the relationship (with F_0, F_1, F_2 and A positive constants) is

$$ED1 = F_0 + F_1(EM1 - F_2)^A, A > 0 \quad (23)$$

This indicates that for relatively shallow inlets (widths greater compared to depths; positive EM1), the ebb tidal delta is relatively flat (depths large compared to DMA; positive ED1). A less well-developed ebb tidal delta is related to a shallow channel, with the channel not as well incised into the shoal. With increasingly negative EM1, the channel is more incised into the shoal.

A final relationship is shown in Figure 26 between AED and EC1. The form of the relationship with G_0, G_1, G_2 , and J positive constants

$$EC1 = \frac{G_0}{(G_1 - AED)^J} - G_2, J > 0 \quad (24)$$

Given the correlation between L and AED and L and EC1, this is not unexpected.

3. Relationships to the Cross-Sectional Area of the MIWC.

a. Strong Relationships. The geometric parameter previously shown to be most important to inlet hydraulics is the minimum cross-sectional area. Its relationship to the tidal prism of the inlet has been defined by O'Brien (1931) and Jarrett (1976). As mentioned previously, the MIWC is, in most instances, located close to the minimum area cross section. Thus, the areas should be approximately equivalent. Since W and DMA did not appear as dominant factors in the previous analyses, it was decided to consider their bifunctional relationship to the area of the MIWC, A_c

$$A_c = W \times DMA \quad (25)$$

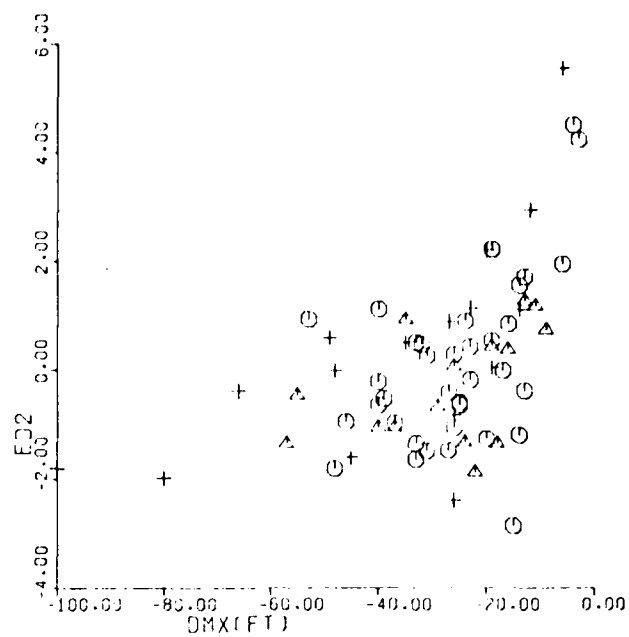


Figure 21. DMX versus ED2.

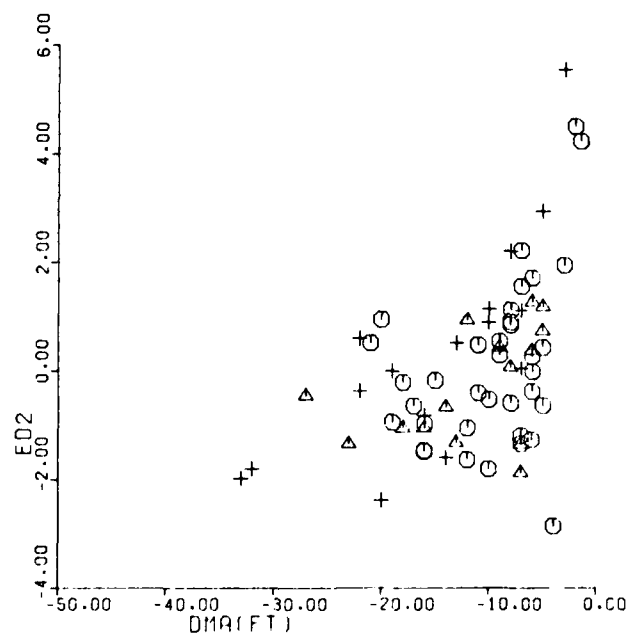


Figure 22. DMA versus ED2.

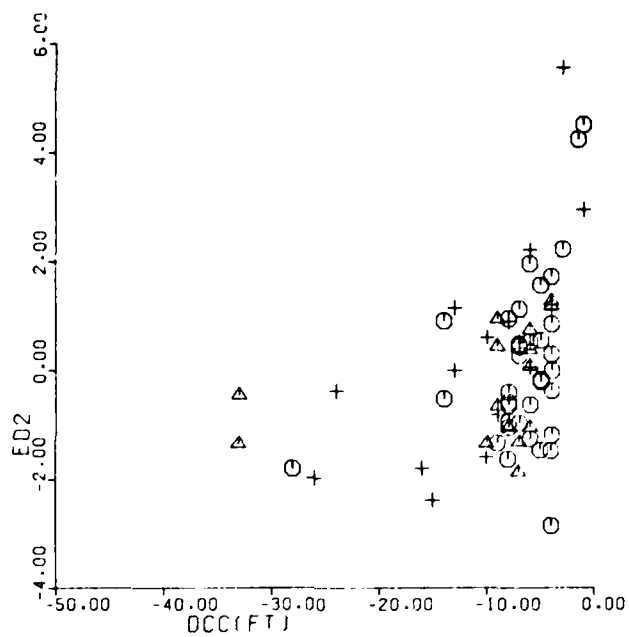


Figure 23. DCC versus ED2.

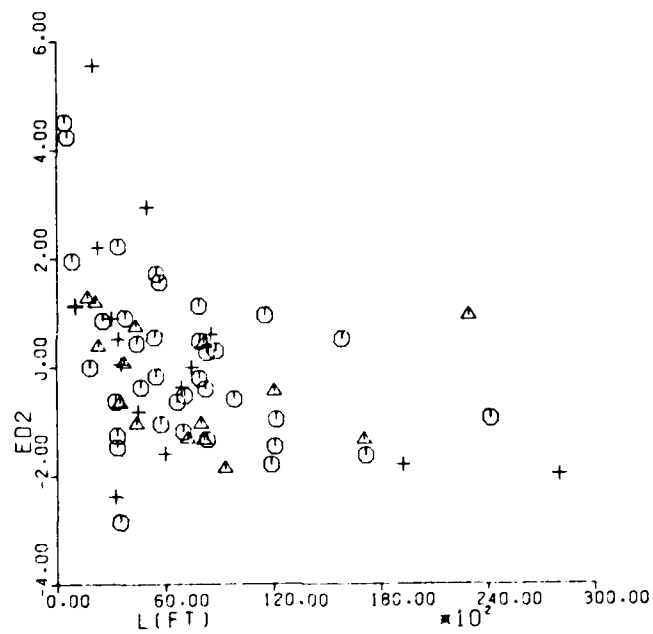


Figure 24. L versus ED2.

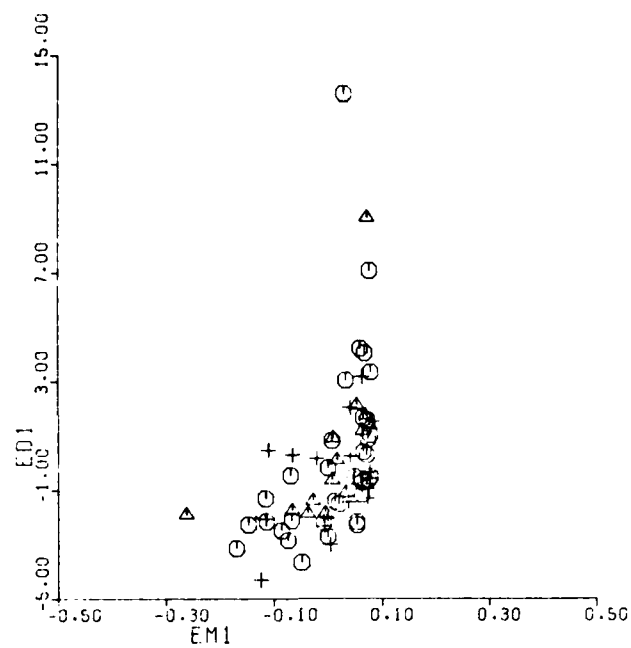


Figure 25. EM1 versus ED1.

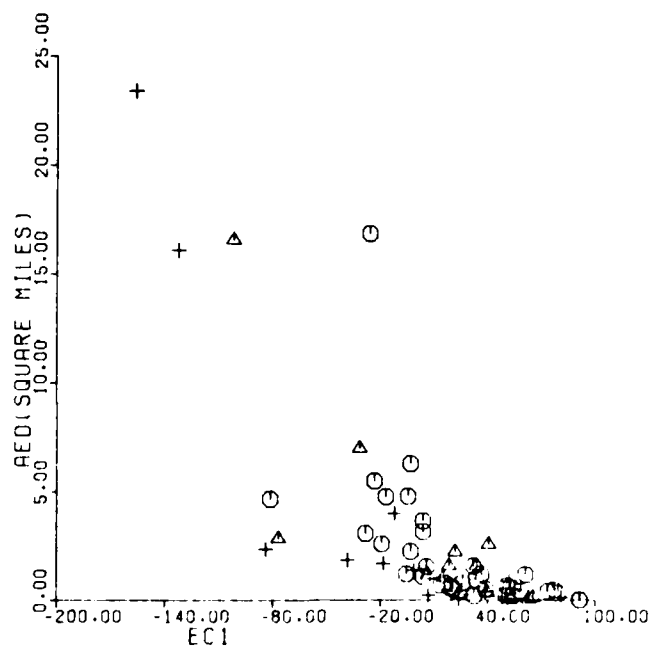


Figure 26. EC1 versus AED.

Log plots of A_c versus DMX, DCC, L, and AED appeared highly significant. The functional relationships, associated F ratios and R^2 values are

$$(1) \text{ DMX} = 0.5479A_c^{0.38}, F = 133, R^2 = 67.6 \text{ percent.}$$

$$(2) \text{ DCC} = 0.2367A_c^{0.34}, F = 66, R^2 = 50.2 \text{ percent.}$$

$$(3) \text{ L} = 23.92A_c^{0.55}, F = 238, R^2 = 77.5 \text{ percent.}$$

$$(4) \text{ AED} = 3.1480 \times 10^{-5}A_c^{1.04}, F = 260, R^2 = 80.0 \text{ percent.}$$

The plots are provided in Figures 27 to 30. These relationships are unquestionably significant statistically and provide valuable insight to the excellent covariance relationships noted previously. The relations have significant design implications and provide an indication of the great degree of the co-adjustment of the inlet geometry. A broader discussion is given at the end of this section.

b. Weak Relationships. Figure 31 indicates a relationship between ED2 and A_c . It is approximated by

$$\text{ED2} = \frac{C_0}{A_c^B} - C_1, B > 0 \quad (26)$$

with C_0 , C_1 , and B positive constants unrelated to any other constants previously defined.

4. Relationships to W/L.

Of the numerous dimensionless relationships tried, the parameter W/L was most successful. The primary relationship found is to the dimensionless parameter DMA/DCC shown in Figure 32. The relationship is described by

$$\frac{\text{DMA}}{\text{DCC}} = 0.9289(W/L)^{-0.42} \quad (27)$$

The F ratio is 30.8, R^2 is 32.1 percent. The regression is significant above 5 percent. There is appreciable scatter, but the low R^2 value is likely due to three to five points. Additional points would possibly increase the R^2 value.

There is a weak relationship (Fig. 33) of W/L to ED1 (which is dimensionless). It is given by

$$\text{ED1} = -1.36 + 2.85(W/L) \quad (28)$$

The F ratio is 8.4 and just barely significant.

Both relationships tend to indicate the following adjustment. As W/L decreases from a value of 1.5 or so, the ebb tidal delta tends to become more developed (ED1, smaller) and a strong bar crest develops (DMA/DCC increases). This is shown graphically in Figure 34, which provides average channel profiles with the depths normalized by DMA, grouped by classes of W/L values.

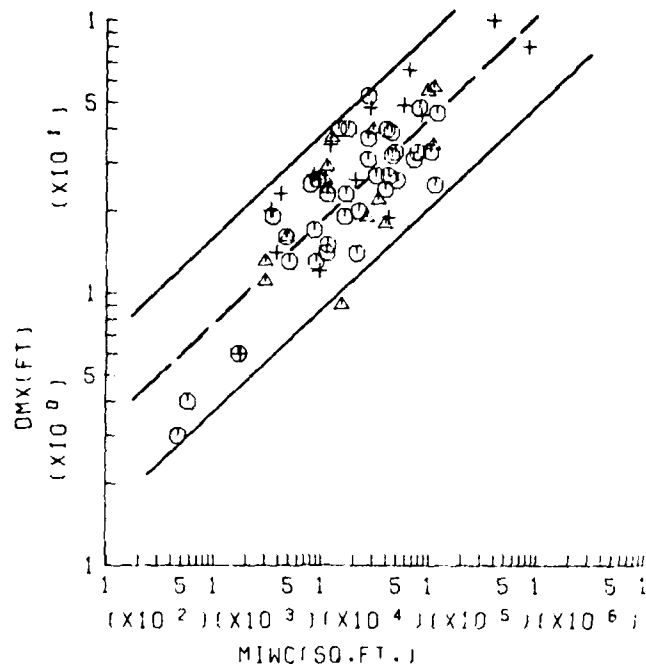


Figure 27. A_c versus DMX.

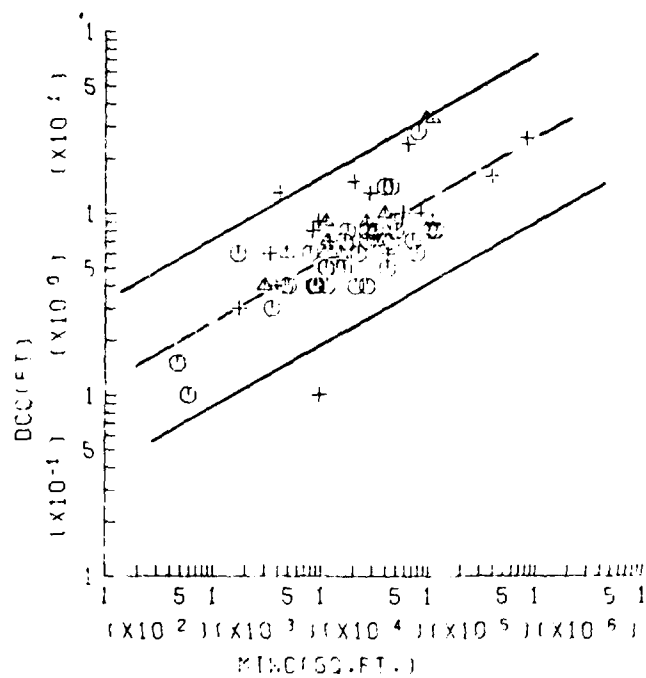


Figure 28. A_c versus DCC.

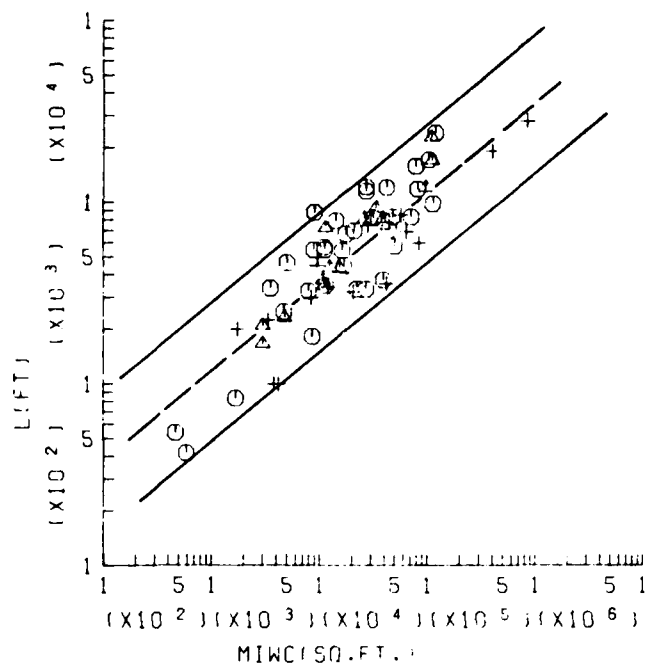


Figure 29. A_c versus L .

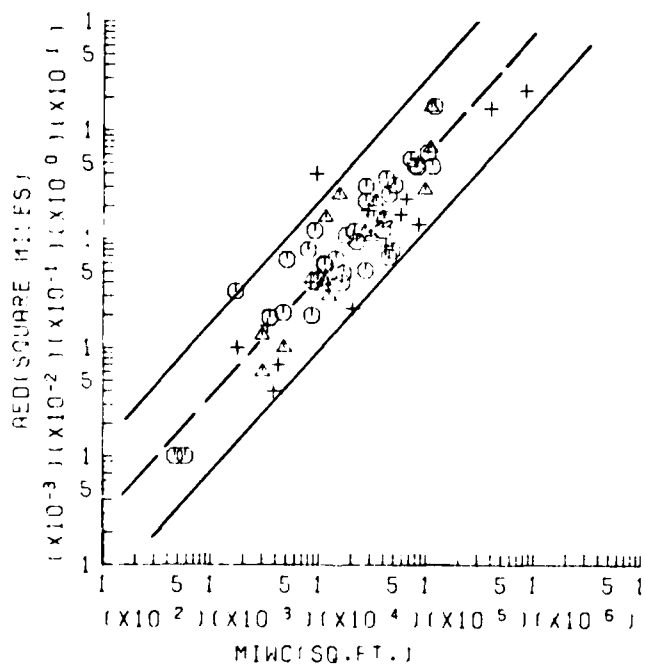


Figure 30. A_c versus AED .

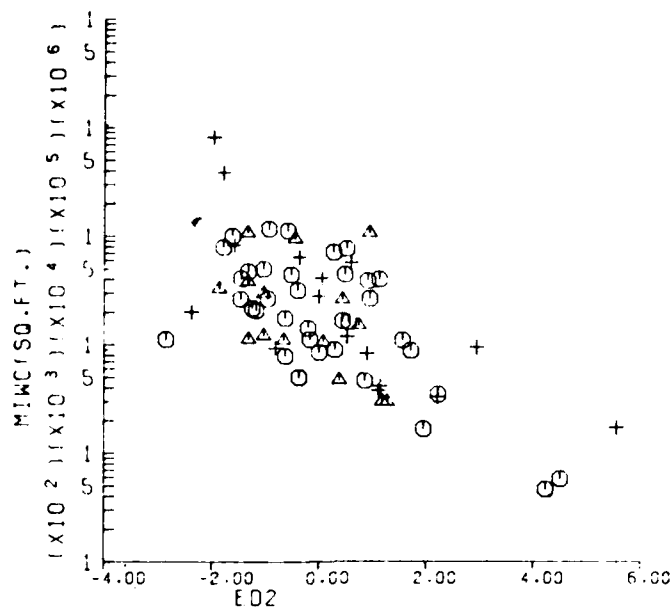


Figure 31. ED2 versus A_G .

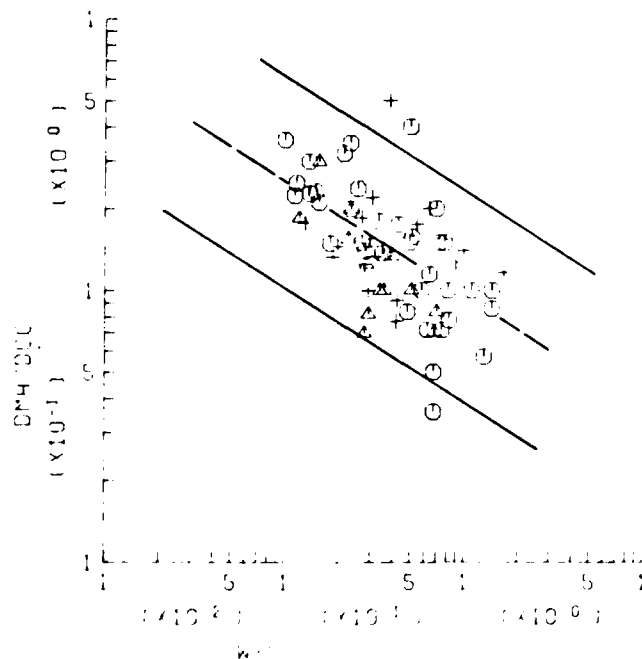


Figure 32. W/L versus DMA/DCC.

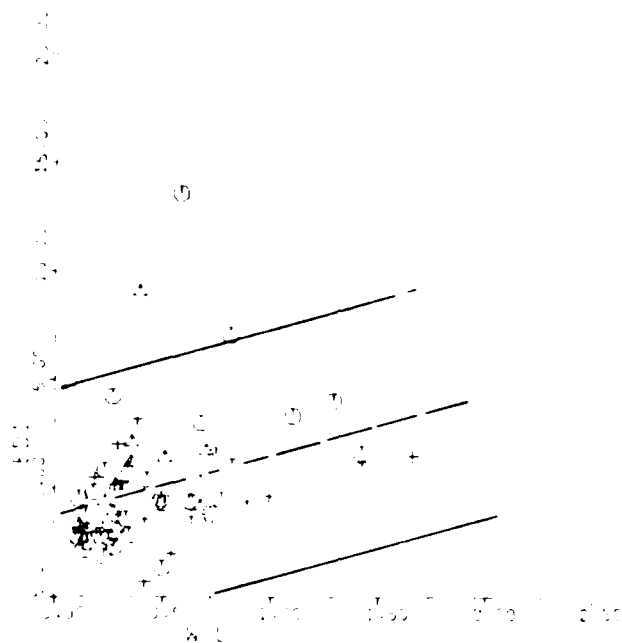


Figure 33. W/L versus $ED1$.

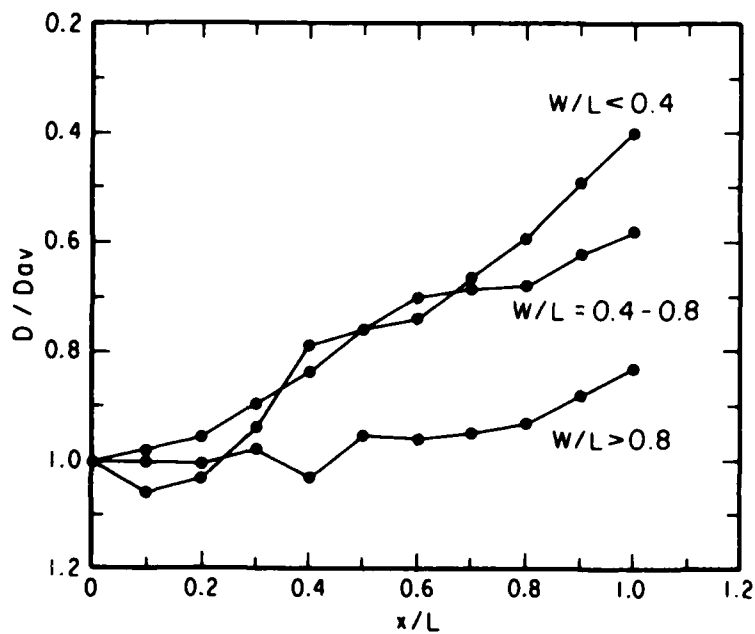


Figure 34. Normalized channel profile for different values of W/L .

5. Discussion.

The analyses presented show strong relationships among many of the parameters selected to describe inlet geometry. Weak-to-moderate partial correlations had been expected, but the strength of the relationships implies a more highly organized covariance or coadjustment of many elements of inlet geometry than has been recognized previously. The implications of the results have impact upon the understanding of the adjustment of inlets to wave and tide processes and may indicate relationships useful for the design of inlet improvements.

The relationships among DMX, DMA, DCC, L, and EC1 and AED are placed into perspective by the relationship of these variables to the area of the MIWC, A_o . To reiterate, the cross-sectional area is directly related to the channel length, depth at the crest of the outer bar in the channel, and the ebb tidal delta area. The relationship of all these variables suggests that, as in the case of the tidal prism, the cross-sectional area of the inlet appears to be a controlling variable. Thus, for a given tidal prism, the area is to a certain degree determined for fixed tidal range. With increasing discharge, A_o increases, and as long as velocities remain above the critical velocity for sediment transport, the flow in the channel tends on the average to be large enough to control the length of the channel, and, therefore, the location of the crest of the outer bar. The strength of the relationship between DCC and A_o would indicate that even at this point where wave and tidal transport would conceptually be of the same order, the tidal forces (represented by A_o) are still predominant in influencing certain geometric parameters. Using the 87-percent explanation of channel profile variance by EC1, the control of the channel depth profile (represented by EC1, EC2) is primarily related to A_o (given the strong relationship between A_o and EC1). EC2 is not related to A_o and it is suspected, given the shape of EC2 (Fig. 6), this variable represents an adjustment of the channel for varying wave climates. However, since there is no parameter distinctly representing wave conditions in this study (which would correspond to A_o for tides), it is impossible to further evaluate a wind-wave dependence.

The strength of relationship between A_o and AED is surprising even though partial correlation is expected. However, given the adjustment of channel length to A_o , and the tendency for the principal ebb flow to remain as a jet, simple constraints of geometry, wave refraction, and diffraction appeared to dictate the eventual size of the bar, as discussed by Bates (1953). Deviations from this gross-scale geometry would appear to result from major geologic differences such as deviation away from a fairly straight coastline.

The correlation between the second eigenvector of ebb tidal delta geometry (ED2) and the cross-sectional area shows that for smaller cross-sectional areas the right side (in normalized geometry space) of ebb tidal delta is relatively more highly developed than for larger A_o . This would agree with the scaling of the tide and wave processes discussed before. For the smaller A_o , the discharges are lower, and velocities over the inlet delta flanks are probably less. Thus, for even moderate wave conditions, sediment transported onto the shoals is not moved as easily offshore or to edge of the delta.

The analysis shows that the maximum depth in the cross section is highly related to A_o . This would seem to imply that in the principal flow area of

the channel the geometry of the channel is largely determined by the magnitude of the flow, since A_c has been shown to be related to tidal prism. Although considerable variability in the shape is expected, the gross-scale geometry of the channel represented mainly by DMX appears determined.

It is interesting to note again that W and (to a lesser degree) DMA did not exhibit strong covariance or relate as well to the other parameters as some of the other parameters did. This suggests that W and DMA are free parameters with respect to the tide; i.e., given a particular cross section, W and DMA are much freer to adjust themselves and may widely vary according to wave climates. It is unclear, however, how DMA, DMX, A_c , or W coadjusts to the wave-tide regime as it is unclear how A_c and the tidal prism coadjust.

The preceding comments must also consider that the cross-sectional area A_c is an adjustment to capacity of the tidal current and wave transport of sediment although it is likely that for an A_c of any appreciable size the tidal capacity must dominate. The results presented here suggest that to the first order the tidal flows, scaled by A_c , determine the gross-scale geometry of the inlet delta and channels (within geologic limitations). The wave-related changes appear as a modification to this geometry until A_c becomes so small that ebb flows are weak relative to the wave forces.

The relationships developed here appear to have potential use in engineering planning and design. They represent geometric adjustments to natural conditions, and at present, care must be taken in their use until the implications suggested by the relationships have been thoroughly analyzed.

IV. CLASSIFICATION OF INLETS

1. Mathematical Considerations.

Classification is essentially a statistical process whether done numerically or manually. If the set of all possible inlet morphologies (of which this study has a small sample of individuals) is considered, the hypothesis arises that there are K subpopulations of inlets which have different morphologic characteristics due to some basic physical difference in the inlets themselves. Two problems need consideration:

(a) Can the characteristics of the subpopulations be estimated through proper parameter selection and sampling?

(b) Can each individual in the sample be assigned to the correct subpopulation?

The size of K is not known, nor is a sufficient set of parameters, X_1, X_2, \dots, X_n , known which is necessary for solution of the problem. Compounding these basic difficulties are random, hopefully unbiased, errors in estimates of X_1, X_2, \dots, X_n for each individual in this sample which may cause misassignment of the individual. Finally, it must be assumed that the sample used contains enough examples from the K subpopulations to allow resolution of the problem.

Because of these difficulties, objective statistical techniques for classification analyses were only recently developed, with the biologic scientific

community in the forefront of its development. The analysis of the structure of populations through objective methods is termed *numerical taxonomy*. Classification analyses denote derivation of taxonomic structure. Discrimination analyses denote assignment of individuals to the classes derived. Sneath and Sokal (1973) provide an excellent introduction to the subject; a simple introduction is given in Davis (1973).

Numerical taxonomists have developed their own terminology which in general will not be applied here. The objective of this part of the report is to present as simply as possible the application of cluster analysis to the inlet classification project. The reason for use of this technique to help unravel the taxonomic structure of inlet morphologies lies in the sheer mass of information that must be analyzed and in a desire to be objective in the final stratification of inlets.

2. Cluster Analysis.

The method employed here is a weighted pair group average (WPGA) clustering technique (Sneath and Sokal, 1973; Davis, 1973). If N parameters are measured for M inlets the data can be represented as an $N \times M$ matrix F in which the element f_{ij} is the measurement of the j th parameter for the i th inlet. The mean value of each parameter can be calculated

$$\bar{f}_j = \frac{1}{M} \sum_{k=1}^M f_{kj} \quad (29)$$

and the associated standard deviation estimated

$$\sigma_j = \frac{1}{M} \left(\sum_{k=1}^M (f_{kj} - \bar{f}_j)^2 \right)^{1/2} \quad (30)$$

A matrix F^0 (with elements f_{ij}^0) can be formed by transforming each element of F in the following way

$$f_{ij}^0 = \frac{f_{ij} - \bar{f}_j}{\sigma_j} \quad (31)$$

F^0 represents transformation of parameters to have mean 0 and standard deviation 1. Finally, a matrix C can be computed with elements C_{ij} defined as

$$C_{ij} = \frac{1}{N} \left(\sum_{k=1}^N (f_{ik}^0 - f_{jk}^0)^2 \right)^{1/2} \quad (32)$$

C_{ij} represents an Euclidean distance between inlets i and j in the M -dimensional space defined by the M parameters standardized to have mean 0 and standard deviation 1. Other distance measures such as correlation coefficients can be used. Here the distance function is chosen because its interpretation is simple and geometrically appealing. In most cases taxonomic structures derived using the distance and correlation functions are equivalent (Sneath and Sokal, 1973; Davis, 1973).

Cluster analysis is so termed because the technique orders the individual inlets into groups or clusters based upon certain fixed methodologies. As indicated in Sneath and Sokal (1973) there is a wealth of possibilities from which to choose. In the WPGA method, the matrix C is surveyed to find the element C_{ij} which is minimum. The other elements of C involving either i or j (such as C_{ik} or C_{jk}), are replaced with $1/2(C_{ik} + C_{jk})$. In essence the individual inlets i and j are replaced by a composite, synthetic inlet equal to their average. The inlets joined together are those "closest" or most similar in terms of the distance function. Thus, the inlets i and j form a cluster. This process is continued with new clusters being formed or with inlets added to old clusters. Eventually, these groups of inlets are likewise joined together until the distance relationship among all inlets, as arranged in hierarchical order of similarity, has been determined. The pattern in which the inlets cluster, and the values of the function C_{ij} at which the clustering occurs, can be shown by a dendrogram (Fig. 35).

The value C_{ij} at which the clustering occurs is indicative of the similarity of the two elements under consideration. For C_{ij} near zero, the inlets are quite similar because the distance in the normalized parameter space is small. The unresolved problem of many cluster analyses is to determine at what values of C_{ij} distinct cluster discrimination occurs. In general, the question cannot be answered. In the case of M normally distributed random variables with mean 0 and standard deviation 1, a mean value of the Euclidean distance measure C_{ij} can be calculated for which the hypothesis that individual clusters are significantly different is acceptable. In the case of this study (for $M = 13$ variables), this value is approximately 1.3 with a 95-percent confidence band of 0.95 to 1.85 (Sneath and Sokal, 1973). The hypothesis of normal distribution certainly is not true for all of the variables treated here, but the precise effect of this upon the distance function is unknown. Because the variables do not differ radically from the normal, the effect is not expected to be major. However, the cluster analysis should be considered only as a guide to possible subpopulations.

The dendrogram (or graphical presentations of the taxonomic structure) of the inlet relationships was examined. Dendrograms are constructed so that it is possible to determine how the individual inlets are grouped together as clusters, at what values of the distance function the inlets join a cluster and the values of the distance function between clusters. Clusters with distance function values of 1.3 or greater were separated. For each pair of clusters, the hypothesis that the difference in means is zero was tested for each of the 13 variables using a standard student's t test applied for comparison of means (Davis, 1973). Rejection of this hypothesis at a 10-percent level of significance will be termed significant clustering on the basis of the variable tested.

3. Inlet Clusters Derived.

The dendrogram showing the taxonomic structure of the 67 inlets (Fig. 35) is explained as follows: The horizontal axis labeled distance coefficient indicates the value of C_{ij} for which an inlet joins one cluster or two clusters join together. The vertical axis contains the names of the inlets and the values at which the inlet joins the dendrogram. The dotted lines are the branches of the dendrogram displaying how the inlets are linked. In Figure 35, Moriches joins Stump Inlet at a value of 0.27, and Price joins this cluster with a value

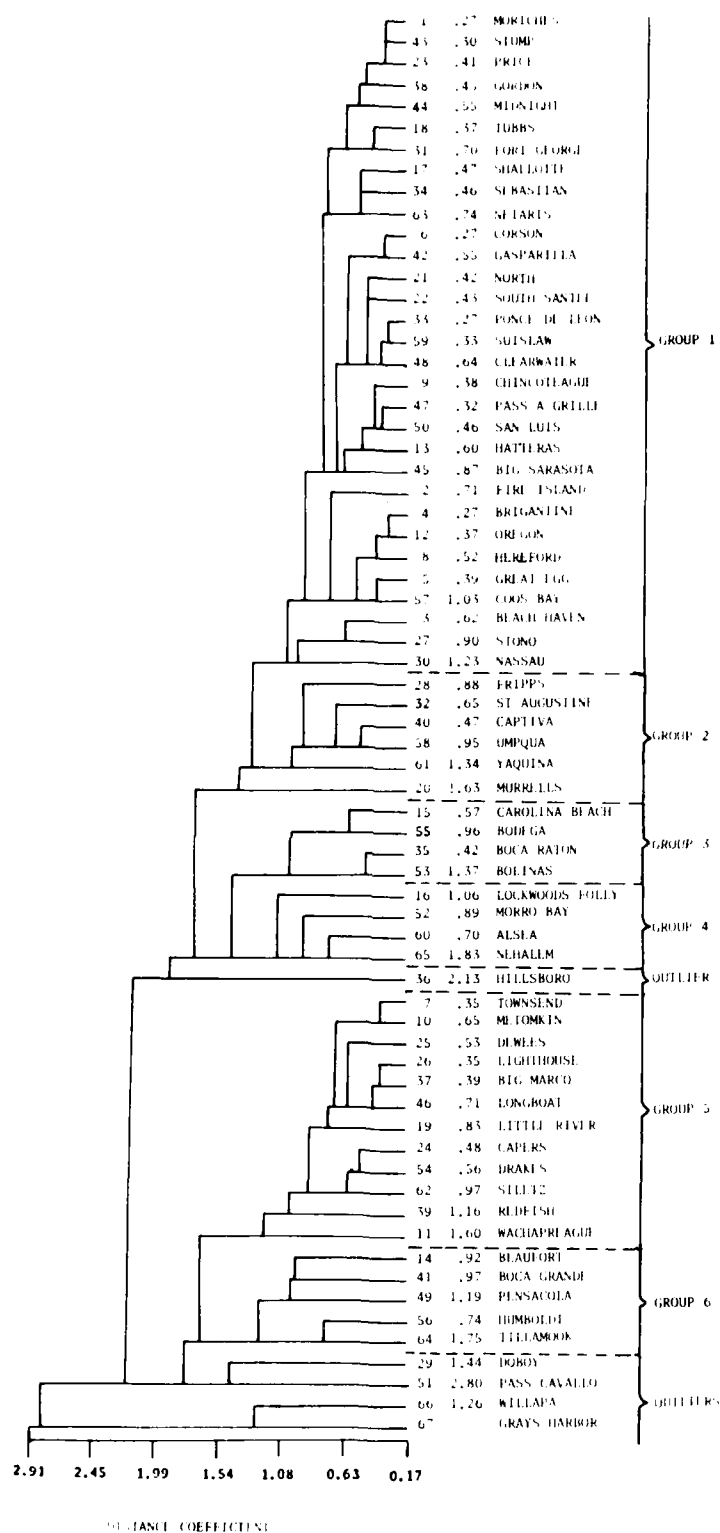


Figure 35. Dendrogram of the cluster analysis.

of 0.41. The cluster containing Moriches, Stump, Price, Gordan, and Midnight is joined with Tubbs and Fort George. The distance values are all below 1.3, which is the criterion selected as the point of inlet cluster definition. The cluster labeled cluster 1 joins cluster 2 with a value of 1.34. Because the distance function is above 1.3, the two clusters are considered far enough apart to be statistically different, thus indicating two subpopulations. For the distance value of 1.3 chosen to indicate significant clustering, six clusters were defined. The inlets in each cluster are listed in Table 3. Of 67 inlets in the analysis, all but five are in well-defined clusters. These five inlets will be termed outliers because they do not fit in the clusters defined. The five inlets will be discussed at the end of the section describing the individual clusters.

Table 3. Inlets by cluster group.

Group 1	Group 2	Group 3	Group 4	Group 5	Group 6	Outliers
Moriches	Fripps	Carolina Beach	Lockwoods Folly	Townsend	Beaufort	Hillsboro
Stump	St. Augustine	Bodega	Morro Bay	Metomkin	Boca Grande	Doboy
Price	Captiva	Boca Raton	Alsea	Dewees	Pensacola	Pass Cavallo
Gordon	Umpqua	Bolinas	Nehalem	Lighthouse	Humboldt	Willapa
Midnight	Yaquina			Big Marco	Tillamook	Grays Harbor
Tubbs	Murrells			Longboat		
Fort George				Little River		
Shallotte				Capers		
Sebastian				Drakes		
Netarts				Redfish		
Corson				Wachapreague		
Gasparilla				Siletz		
North						
South Santee						
Ponce de Leon						
Siuslaw						
Clearwater						
Chincoteague						
Pass A Grille						
San Luis						
Hatteras						
Big Sarasota						
Fire Island						
Brigantine						
Oregon						
Hereford						
Great Egg						
Coos Bay						
Beach Haven						
Stono						
Nassau						

a. Statistical Measures of the Significance of the Cluster Analysis. The clusters were selected on the basis of a Euclidean distance value of 1.3 which was chosen on the basis of the expected difference if the variables conformed to the constraints listed previously.

Given six clusters there are 15 possible pairs of clusters, i.e., clusters 1 and 2, 1 and 3, and so forth. In Table 4, for each of the 15 pairs, the levels of significance based on a student's t test for the hypotheses that the mean cluster value for each of the 13 parameters is different are provided. The number of times that this hypothesis is accepted as true provides a measure of how different the two clusters in a pair are. If only a few of the 13 parameters test out as significant, then statistically there is less confidence that the clusters are distinct. Of the 15 pairs of clusters, clusters 1 and 3 are most

Table 4. Significance of differences among clusters, based on a student's t test for differences between means.

Variable and No.	Cluster pairs ¹														
	1-2	1-3	1-4	1-5	1-6	2-3	2-4	2-5	2-6	3-4	3-5	3-6	4-5	4-6	5-6
DMX 1	5	5	x	1	1	1	x	x	1	5	1	1	10	1	1
DMA 2	1	5	1	1	1	1	x	x	x	1	1	1	x	5	5
W 3	x	5	5	1	x	1	1	1	10	x	5	5	5	5	1
DCC 4	x	1	x	x	1	5	x	x	1	5	1	1	10	1	1
L 5	5	1	5	x	1	5	5	x	x	x	1	1	5	1	1
LM1 6	1	1	1	1	5	x	1	1	x	10	5	x	x	1	1
/LM2/ 7	10	1	1	1	1	5	1	x	10	1	x	x	1	1	x
EM3 8	1	10	1	1	x	10	x	1	5	5	1	10	1	5	1
EC1 9	10	5	x	10	1	x	x	x	1	5	1	1	x	1	1
LC2 10	x	x	x	1	x	x	x	5	x	10	5	x	x	x	x
ED1 11	x	10	1	1	5	5	1	10	10	10	x	x	5	5	x
ED2 12	1	1	x	x	10	1	5	5	x	5	1	1	x	1	x
AED 13	x	5	x	x	1	5	x	10	10	x	5	5	x	10	1
Total	8	12	7	9	10	10	6	7	8	10	11	9	7	12	9
At 10 pct	2	2	0	1	1	1	0	2	4	3	0	1	2	1	0
At 5 pct	2	5	2	0	2	5	2	2	1	5	4	2	3	4	2
At 1 pct	4	5	5	8	7	4	4	3	3	2	7	6	2	7	7

¹ x = no difference
 10 = significant above 10 pct
 5 = significant above 5 pct
 1 = significant above 1 pct

different in that 12 of 13 variables have mean values accepted as different at a 10-percent level of significance; only 5 variables are significant above 1 percent, however. Clusters 1 and 5 have eight variables different above 1 percent. Comparisons of clusters 1 and 6, 3 and 5, 4 and 6, and 5 and 6 have seven variables significantly different above 1 percent. Clusters 2 and 4 appear most similar with only six variables different at significant levels above 10 percent; however, four of the variables are significantly above 1 percent.

The comparisons presented in Table 4 strengthen the conclusion that the clusters selected stratify the inlet sample into apparent distinct groups which have measurable differences. It is an inability of current statistical theory, however, to state with a level of certainty that the groups chosen are truly optimal in a population-wide sense. However, the grouping appears a useful separation of inlets into groups which are distinguishable in terms of geometry.

An interesting observation is apparent in the analysis shown in Table 4. There is no single variate that serves as a distinguishing parameter for all clusters. The differences between clusters result from differing combinations of the 13 variates. This observation agrees in large degree with the observations of Sneath and Sokal (1973), who note that it is a rarity to find one single parameter which serves as the distinguishing character in populations characterized by continuous variates. This condition appears to be a property of natural systems which are in some sense evolutionary.

The primary reasons for performing the cluster analysis were to achieve an objective classification analysis and to have an automated analysis because of the difficulty of trying to analyze manually many variables for a large sample. The problem of the massiveness of the data set and its multivariate nature, though circumvented in the cluster analysis, is still present when the characteristics of the clusters must be presented. Table 5 provides a summary of the mean value and standard deviation of each variable by cluster group. Figure 36 provides plots of these values by group. Figure 37 provides plots of the limits of each cluster in selected bivariate spaces. Table 5 and Figures 36 and 37 are

Table 5. Mean (\bar{x}) and standard deviations (S_x) of geometric parameters by cluster groups.

Variate No.	Group 1		Group 2		Group 3	
	31 in group		6 in group		4 in group	
	\bar{x}	S_x	\bar{x}	S_x	\bar{x}	S_x
1	-22.064	9.452	-31.666	10.826	-10.750	6.057
2	-7.4838	2.460	-16.500	6.0484	-4.7500	2.277
3	3838.48	3126.29	2430.00	821.55	479.250	112.0
4	-6.7741	2.732	-8.0000	3.6968	-2.7500	1.089
5	5824.74	3186.45	8524.50	4465.68	1698.00	1121.57
6	0.053216	0.028212	0.009150	0.043314	-0.01292	0.060804
7	0.007371	0.007350	0.013100	0.008928	0.035700	0.020233
8	0.001842	0.010989	-0.03111	0.023616	-0.00782	0.003525
9	31.0073	28.4379	13.3392	30.3303	63.9250	23.3762
10	3.38039	10.6752	0.591000	12.9217	-2.4000	1.73494
11	0.596639	1.75246	0.935267	2.91009	-0.94270	1.83906
12	0.074729	1.16700	-1.4760	0.874847	3.35075	1.73692
13	1.45384	1.54533	1.98167	1.68433	0.085000	0.068738

Variate No.	Group 4		Group 5		Group 6	
	4 in group		12 in group		5 in group	
	\bar{x}	S_x	\bar{x}	S_x	\bar{x}	S_x
1	-25.000	6.81909	-32.250	9.02889	-54.800	6.67533
2	-11.750	3.03109	-14.500	3.66288	-20.200	5.70614
3	625.000	181.698	986.333	368.541	4149.80	2205.54
4	-8.2500	3.26917	-6.4166	1.60511	-26.200	7.41350
5	2854.00	12833.3	6358.92	609.850	11084.00	3683.57
6	-0.10365	0.059373	-0.09195	0.060985	0.026520	0.028208
7	0.099050	0.013779	0.024325	0.018467	0.027880	0.017421
8	-0.04547	0.029605	0.026141	0.017507	0.000320	0.007656
9	26.4027	14.3285	18.5774	19.5098	-76.303	20.7898
10	8.84250	9.99347	13.6317	12.4815	4.22800	13.7223
11	-2.9542	0.869864	-1.7367	1.16426	-1.2243	0.824321
12	0.165550	0.846309	-0.33561	1.00880	-0.79226	0.668396
13	1.17750	1.63462	1.02000	0.851782	6.26400	5.56253

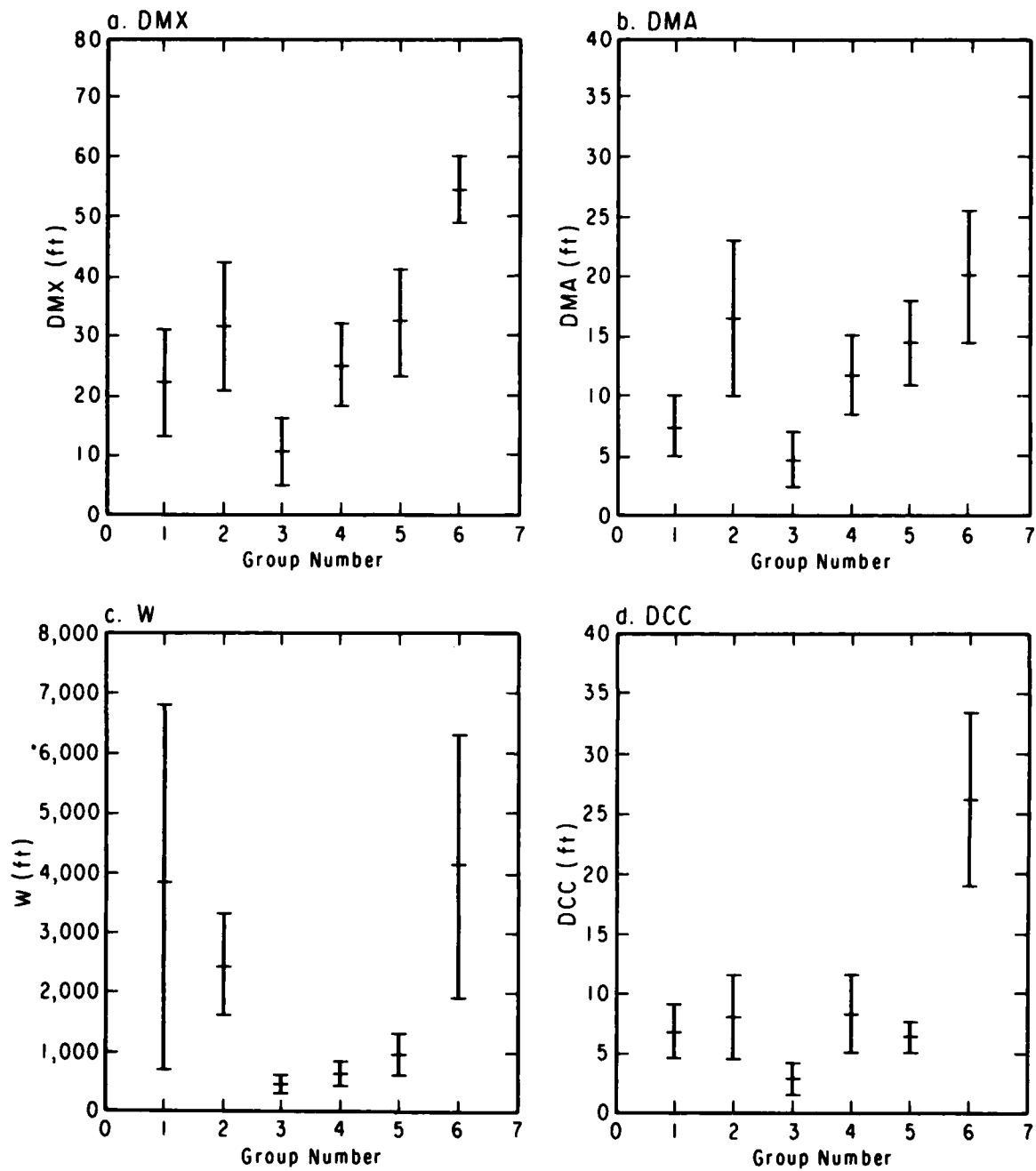


Figure 36. Mean and standard deviations of the 13 variables by clusters.

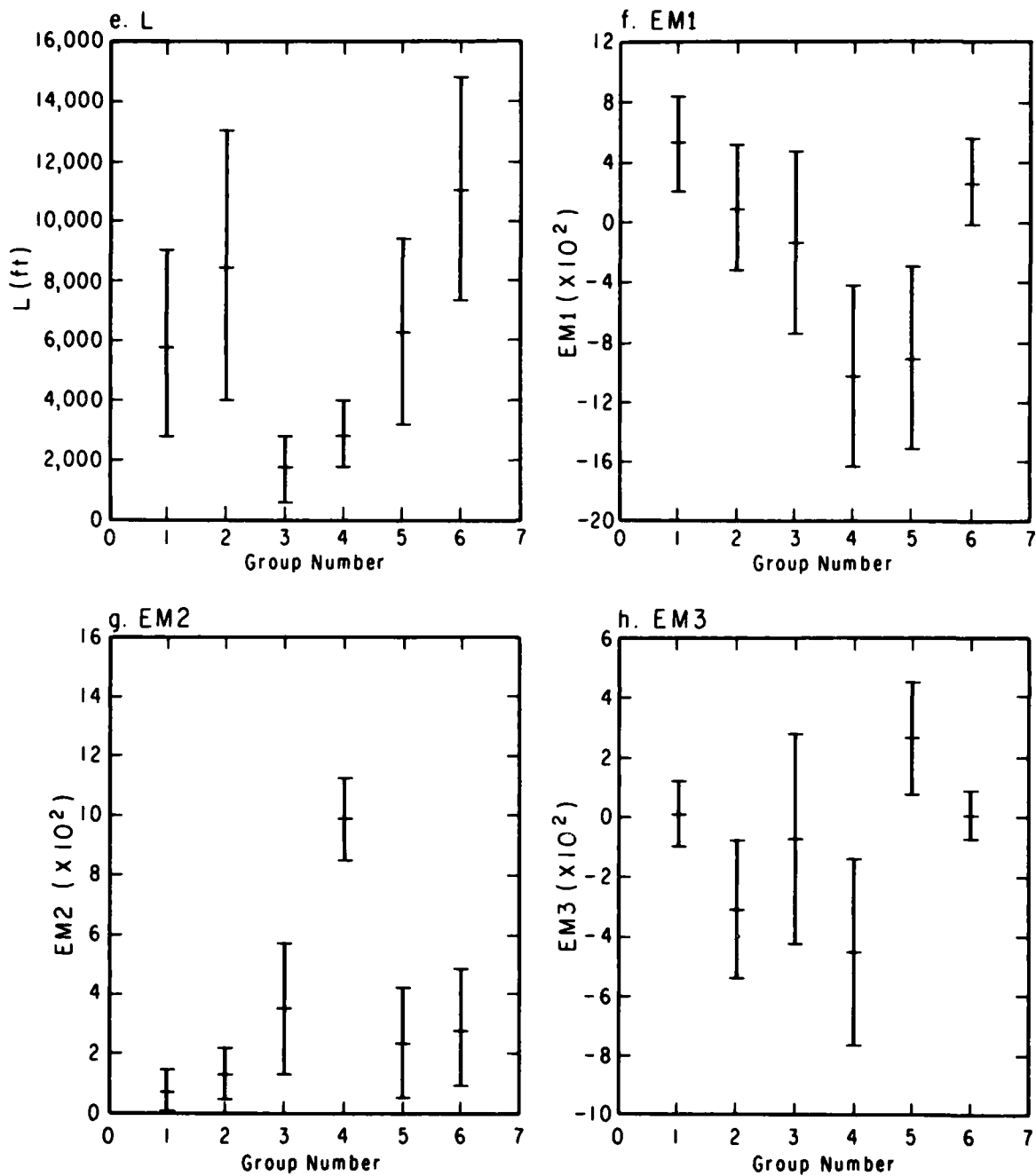


Figure 36. Mean and standard deviations of the 13 variables by clusters.--Continued

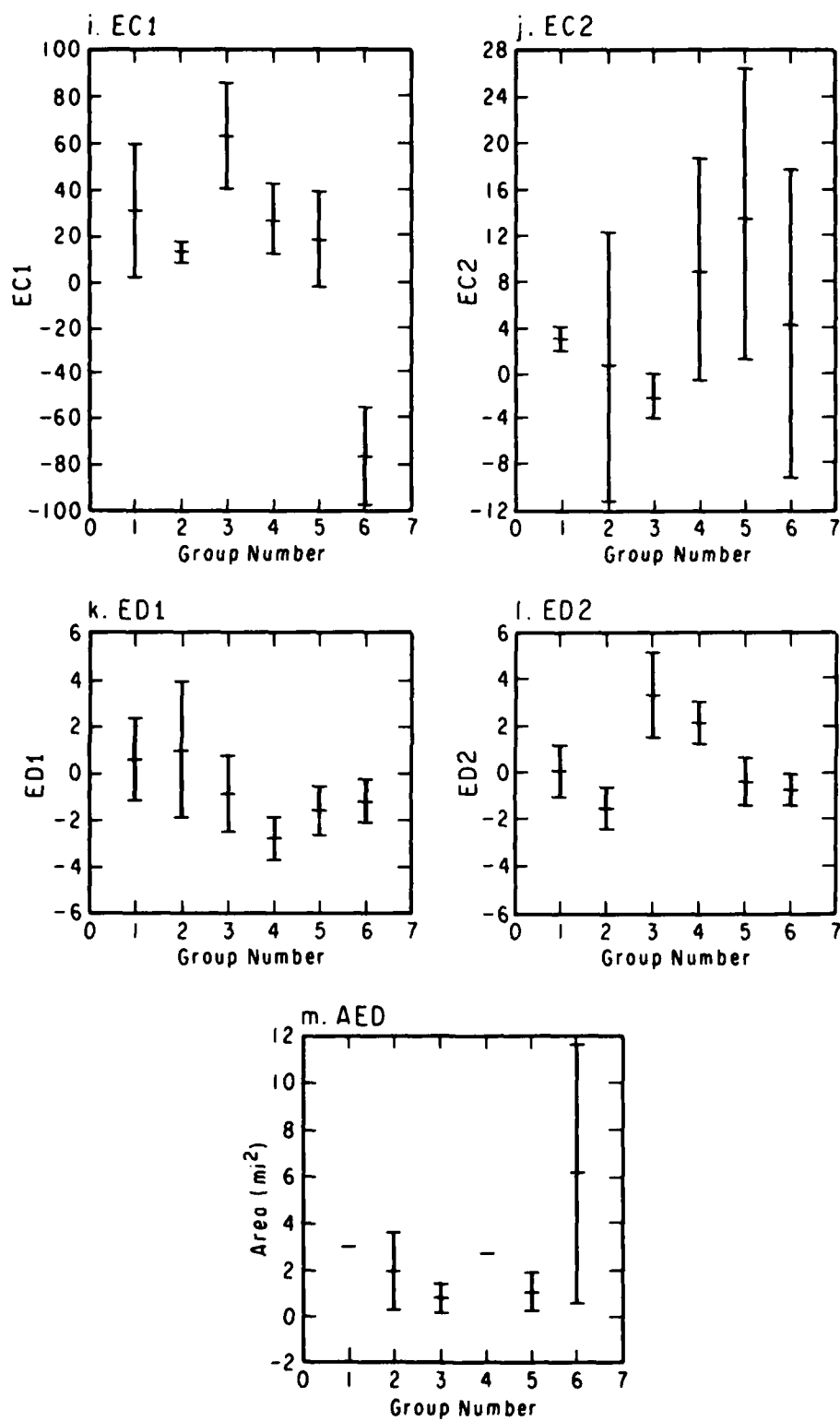


Figure 36. Mean and standard deviations of the 13 variables by clusters.--Continued

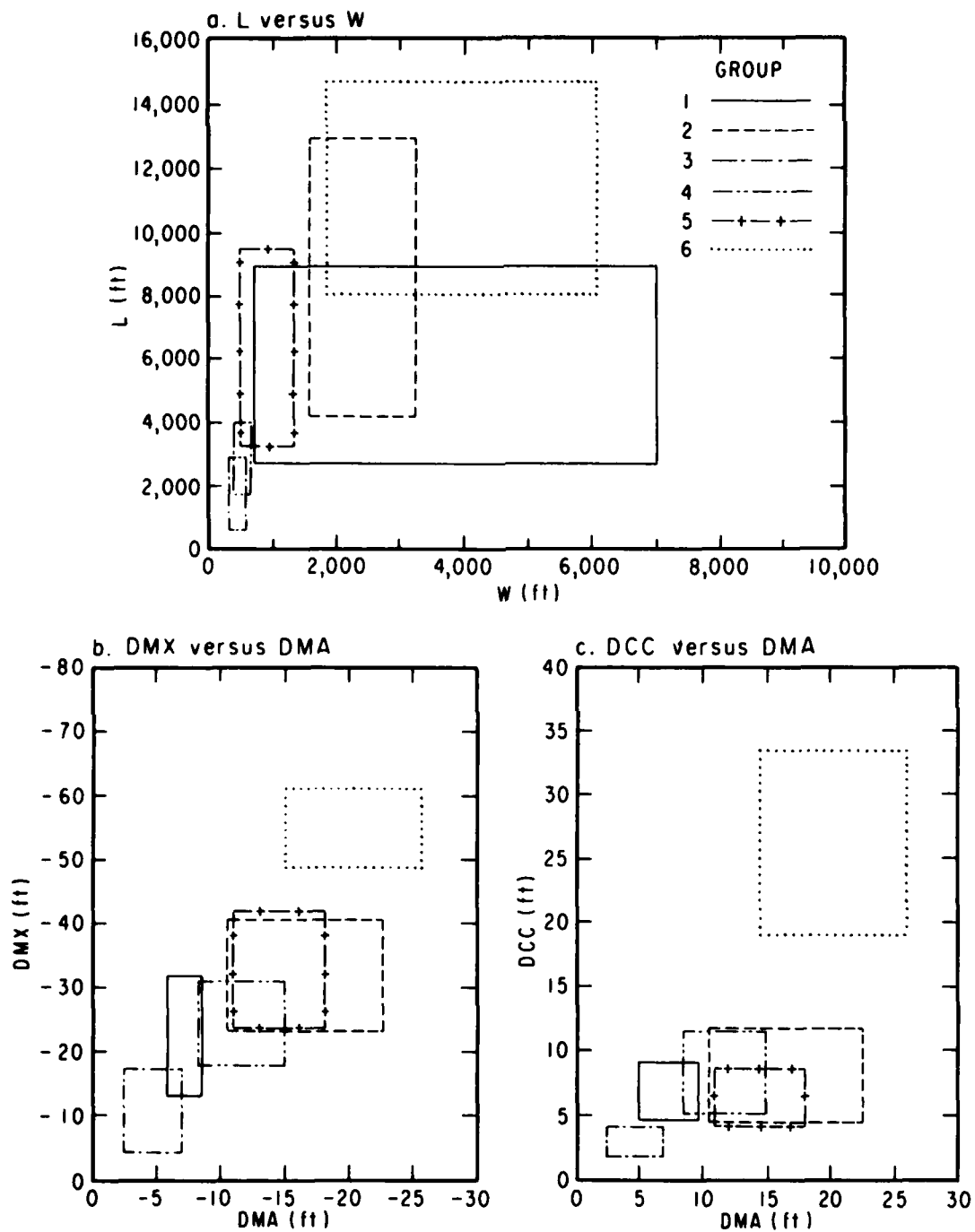


Figure 37. Variational range of variables by inlet group.

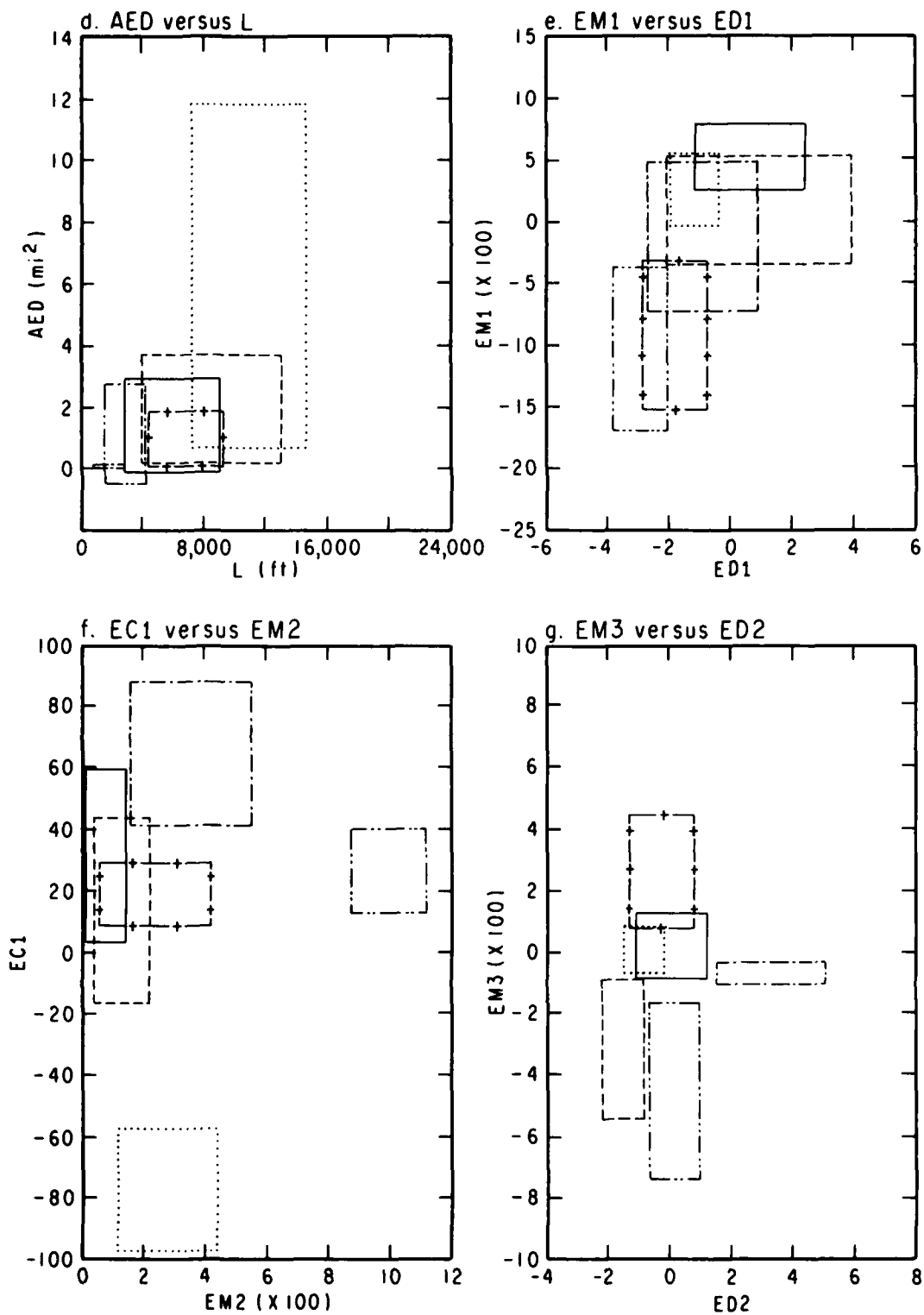


Figure 37. Variational range of variables by inlet group.--Continued

intended to help clarify differences and similarities between clusters. The limits are defined to be those rectangles with centers located at

$$(\bar{x}_i, \bar{x}_j) \quad (33)$$

where \bar{x}_b is the mean value of the b^{th} (of 13) variates for the a^{th} (of 6) clusters. The corners of the rectangles are located at

$$(\bar{x}_i \pm s_i, \bar{x}_j \pm s_j) \quad (34)$$

where s_b is the standard deviation associated with \bar{x}_b . Thus, for Figure 37(a) the six rectangles corresponding to the six clusters are plotted in (W,L) space. Each rectangle can be interpreted as the region in (W,L) space for which no less than 66 percent of the inlets in each cluster lie. Where two rectangles such as for clusters 1 and 3 do not overlap, it is evident that based on W and L the clusters are relatively disjointed, for the same value range for a variable, as shown in Table 4. Conversely, overlapping rectangles usually indicate that there is no significant difference between the two variables (e.g., see N and L for cluster pairs 3 and 4 in Table 4). The degree of overlap determines the degree of similarity between the two clusters. It should be noted that major overlap can occur only in one variable, as in clusters 1 and 6 for channel length, L. Further, even though clusters 2 and 5 do not overlap for W, they do in L.

b. Description of the Inlet Clusters (mean values are given for all variates).

(1) Cluster 1. The first cluster is by far the largest and represents almost half of the inlets. The geographic extent of the 31 inlets includes inlets on all three coasts. The dendrogram (Fig. 35) does not indicate a necessarily homogeneous grouping because of the number of small clusters. However, the low values of the distance coefficients suggest that this internal stratification is possibly due to only a few variates. Since it is a substructure, it will not be further considered here because it occurred at too low a level of significance.

From Table 5, a cluster 1 inlet has moderate width and length ($W \approx 3,800$ feet, $L \approx 5,800$ feet). In (DMX,DMA) space (Fig. 37,b) it has shallow average and maximum depths ($DMA \approx 7.5$ feet, $DMX \approx -22$ feet). Depth at the crest of the bar is moderate ($DCC \approx -7$ feet). The MIWC shape is quite shallow ($EM1 \approx 0.053$), tends not to be overly asymmetric ($EM2 \approx 0.0074$), and is neither consistently deep-centered nor multichanneled ($EM3 \approx 0.0018$). The channel profile (Fig. 37,f) is moderately shallow ($EC1 \approx 31$) and has a slightly steeper slope ($EC2 \approx 3.4$). The ebb delta geometry is moderately deeper ($ED1 \approx 0.60$) and not extremely asymmetric ($ED2 \approx 0.075$). The ebb delta area is small ($AED \approx 1.45$ square miles). The variables by which cluster 1 differs from the other clusters are given in Table 4.

(2) Cluster 2. The second cluster is comprised of six inlets located on the three coasts. Cluster 2 inlets are moderately wide ($W = 2,400$ feet), but not as wide as cluster 1 inlets, and have a fairly long channel ($L = 8,500$ feet). The MIWC is moderately deep ($DMA = 16.5$ feet, $DMX = 32$ feet). The depth of the crest of the ebb tidal delta is moderate ($DCC = 8$ feet). The

MIWC is near the mean shallowness ($EM1 = 0.009$), and is moderately asymmetric ($EM2 = 0.013$, $EM3 = -0.031$). The channel profile is relatively shallow but close to the mean ($EC1 = 13.3$). The channel profile steepness is relatively variable ($EC2 = 0.59$). The ebb tidal delta is moderately deep ($ED1 = 0.93$) and not highly asymmetric ($ED2 = -1.5$). The average ebb tidal delta area is intermediate ($AED = 1.98$ square miles).

(3) Cluster 3. Cluster 3 has only four inlets. Two are on the Atlantic coast and two on the Pacific coast. These inlets have the narrowest width ($W = 480$ feet) and the shortest channel length ($L = 1,700$ feet). The depth values are shallowest ($DMX = 11$ feet, $DMA = 5$ feet, $DCC = 3$ feet); the channel profile is also shallow ($EC1 = 64$, $EC2 = -2.4$). The MIWC shape is slightly deeper than the mean shape ($EM1 = -0.013$) and more asymmetric ($EM2 = 0.036$, $EM3 = -0.008$). The ebb tidal delta is shallow ($ED1 = -0.94$), fairly asymmetric ($ED2 = 3.35$), and small ($AED = 0.09$ square miles).

(4) Cluster 4. Cluster 4 is comprised of four inlets, three of which are on the Pacific coast. The minimum inlet width is relatively small ($W = 625$ feet) and the channel length is short ($L = 2,850$ feet). The principal depths are generally in the shallow-to-intermediate range ($DMX = 25$ feet, $DMA = 11$ feet, $DCC = 8$ feet) and the channel profile is in the intermediate value ranges ($EC1 = 26.4$, $EC2 = 8.8$). The MIWC shape is relatively deep ($EM1 = -0.10$) and very asymmetric ($EM2 = 0.099$, $EM3 = -0.045$). The ebb tidal delta is relatively shallow and slightly asymmetric ($ED1 = -2.95$, $ED2 = 0.17$), and has an area of 1.18 square miles.

(5) Cluster 5. Cluster 5 includes 12 inlets that are geographically distributed on all three coasts. These inlets are relatively narrow but have moderately long channels ($W = 990$ feet, $L = 6,300$ feet). Depths in the channels are relatively deep ($DMX = 32$ feet, $DMA = 15$ feet, $DCC = 6$ feet, $EC1 = 18.5$, $EC2 = 13.6$). The MIWC geometry is deep and moderately asymmetric ($EM1 = -0.09$, $EM2 = 0.024$, $EM3 = 0.026$). The ebb tidal delta is shallow and symmetric ($ED1 = -1.7$, $ED2 = -0.34$), and has an area of 1.02 square miles.

(6) Cluster 6. Cluster 6 consists of five inlets, again geographically distributed on all coasts. These inlets are the widest, longest, and deepest ($W = 4,100$ feet, $L = 11,000$ feet, $DMX = 55$ feet, $DMA = 20$ feet, $DCC = 26$ feet, $EC1 = -76$, $EC2 = 42$). The MIWC is shallow and only moderately asymmetric ($EM1 = 0.027$, $EM2 = 0.028$, $EM3 = 0.0003$). The ebb delta is relatively deep, symmetric and large ($ED1 = -1.2$, $ED2 = -0.79$, $AED = 6.3$ square miles), though not as deep or symmetric as some other inlet clusters.

(7) Outliers. There are five inlets that do not fit any of the clusters defined. Most of these inlets appear relatively large. They do not all, however, cluster together. Hillsboro appears intermediate to a combination of clusters 1, 3, and 4. Doboy and Pass Cavallo are close to each other as are Willapa and Grays Harbors. Unfortunately, for inlets of this size it is often difficult to define the measures such as crest of the bar and length of channel because of either the complexity and size of the inlet or poor data.

c. Differences Among Clusters. In terms of width and length, clusters 3 and 4 are the most similar, with cluster 5 inlets slightly wider and longer. Inlets of clusters 1, 2, and 6 tend to be much wider and longer than clusters 3, 4, and 5. The primary differences between clusters 3, 4, and 5 are in depth

(Fig. 37,b) and relative asymmetry (EM2, Table 5). Cluster 3 tends to be shallower than cluster 4 which is shallower than cluster 5. Clusters 1, 2, and 6 follow a similar ordering; however, cluster 1 inlets tend to be somewhat shallower than cluster 4.

Figure 37(e) provides an interesting summary of the geometric differences. In this figure the first principal components of inlet cross-section geometry (EM1) (which gives relative depth of the cross section to its width) are plotted against the corresponding component of ebb delta geometry (ED1) (which gives relative depth of the delta to channel depth). The arrangement of clusters is nearly hierarchical. Cluster 1 represents the shallowest inlet cross sections ($EM1 > 0$) and has correspondingly a relatively deep outer bar compared to channel depths ($ED1 > 0$). Cluster 6 has almost as shallow an MIWC, but the ebb delta is much shallower compared to channel depths ($ED1 < 0$). Cluster 2 has slightly deeper cross section than cluster 1 or 6, but the ebb delta is relatively more like cluster 1. Cluster 3 has deeper cross sections than clusters 1, 2, or 6, and a shallower bar than clusters 1 and 2. Cluster 5 has a much deeper cross section and shallower delta than those clusters previously mentioned. Cluster 4 has a slightly deeper cross section and shallower bar than cluster 5.

If the clusters are ranked in ascending value of mean cross-sectional areas, the order of clusters is cluster 3 (2,000 square feet), cluster 4 (7,000 square feet), cluster 5 (14,000 square feet), cluster 1 (29,000 square feet), cluster 2 (40,000 square feet), and cluster 6 (84,000 square feet). The ranking here follows that for both width and average depth as should be expected. It again confirms the observation that, to a great degree, inlets are ordered by size.

4. Discussion.

The objective of the analyses just presented was to investigate the possibility that inlets can be stratified into a small set of classes on the basis of inlet geometry and to describe the classes found. The classification analysis was based upon the multivariate statistical method of cluster analysis. The statistical significance of the clusters found was tested in a variety of ways and showed the clustering acceptable.

The analysis determined six clusters of inlets that contained all but five inlets in the original sample. Inlets in the individual clusters normally include examples from two or three coasts which must imply that there is no inherent reason, based on the geometric parameters analyzed, for stratification of inlets solely on a geographic basis. The inlet clusters can be arranged hierarchically on the basis of size. The statistical tests give strong evidence that even for the clusters with a small number of inlets the differences would not be expected by sampling errors and give credence to a hypothesis of a series of inlet subpopulations.

It is instructive to consider further the question of whether the clusters represent a taxonomic substructure. The discussion on the relationships between the geometric parameters provided evidence that inlet geometry was organized or scaled according to size. The clusters are likewise organized. That the clustering is not likely due to a lack of more inlets in the sample to fill in the gaps can be exemplified by comparison of clusters 3 and 4. The differences in mean width between these two clusters is less than 200 feet, yet

the mean DMA for cluster 3 is almost one-third that of cluster 4. This would be unexpected if the differences were due to sampling alone. The clusters represent important differences in inlet geometry other than just a scaling process. The implications of this in relation to scaling of inlet geometry shown previously are considered in more detail in Section VII.

The clusters presented here represent the taxonomic structure of the sample of 67 inlets analyzed. Because it is felt that this sample is fairly representative of the range of inlets on the U.S. coasts, the statistics derived can be considered estimates of the population statistics for all inlets of the types sampled here. As has been indicated by the outliers in the analysis, the very large inlets are not well represented in this analysis. An addition of inlets in this range might provide additional clustering. Addition of inlets in the range already clustered should be expected to redefine the statistics of the clusters presented but should not force combination of clusters already defined.

It should again be stressed that the inlets assigned to each cluster represent the condition of the inlet at a particular time (Table 1), not necessarily today. There is no a priori reason why an inlet in a particular cluster must remain there. A question not considered here is the stability characteristics of each of the cluster types.

The cluster analysis shows that inlet geometry has a strong substructure rather than being a homogeneous but randomly variable population. The analysis is based on a sample of inlets believed typical of a majority of U.S. inlets and clearly implies an adjustment of inlet geometry, in addition to the scaling of inlets, according to size, that requires explanation. The particular clusters presented must be considered a first-order stratification of inlets on the basis of inlet geometry that could be refined by addition of more inlets or more parameters. The small number of clusters provided a reasonable framework for investigating the geometric variability of inlets. It is intuitive that a finer stratification might be forced through addition of more parameters, but it is perhaps judicious to not further refine the classification until the physical reasons for the structure presented have been better explained.

V. MATHEMATICAL DEFINITION OF INLET CLASSIFICATION

1. Objectives.

The cluster analysis indicated that six clusters of inlets can be defined in the sample analyzed. If the view is taken that this sample provides the estimates of the multivariate mean and variance statistics of the 13 variables for 6 clusters of inlets, it is desirable to form a series of equations which mathematically defines the classes. What is sought is a way of assigning each member of the sample to a cluster on the basis of a probability measure and a way to ultimately derive a series of equations which allows assignment of inlets not in the analysis to the clusters.

The method used to produce the equations is a discriminant analysis. The cluster analysis gave an indication of the subpopulation structure of inlet geometry from a sample of inlets. The clusters so defined were used to develop estimates of the subpopulation mean and variance statistics. The discriminant

analysis takes these subpopulation estimates and produces equations defining the subpopulation limits. The original sample is reexamined to see if any misclassification has occurred.

2. Mathematical Considerations.

Discriminant analysis is a widely used statistical technique. Any number of sources are available for reference but Kendall and Stuart (1968), Davis (1973), and Dixon (1974) are particularly helpful. The equations presented here are from Dixon (1974). They are presented briefly so that quantities later presented in tables can be more readily explained.

The basic concept behind a discriminant analysis can be seen in Figure 38 if it is assumed that two clusters (A,B) have been found in analysis on two variables X_1 , X_2 . It is somewhat intuitive to seek a line

$$0 = Q + \lambda_1 X_1 + \lambda_2 X_2 \quad (35)$$

where Q , λ_1 and λ_2 are constants, in (X_1, X_2) space such that cluster A primarily lies to one side, with B on the other. Depending on the cluster means and variances, there may be many or few elements that may be misclassified. The misclassification occurs either because random errors in measurement happen or because of faulty recognition; i.e., an element of A is incorrectly called an element of B. The line defined provides a basis of dividing (X_1, X_2) space into half planes, mathematically defining the clusters A and B. The equation of the line is defined to minimize the ratio of the difference between the pair of multivariate means to the multivariate variance within clusters.

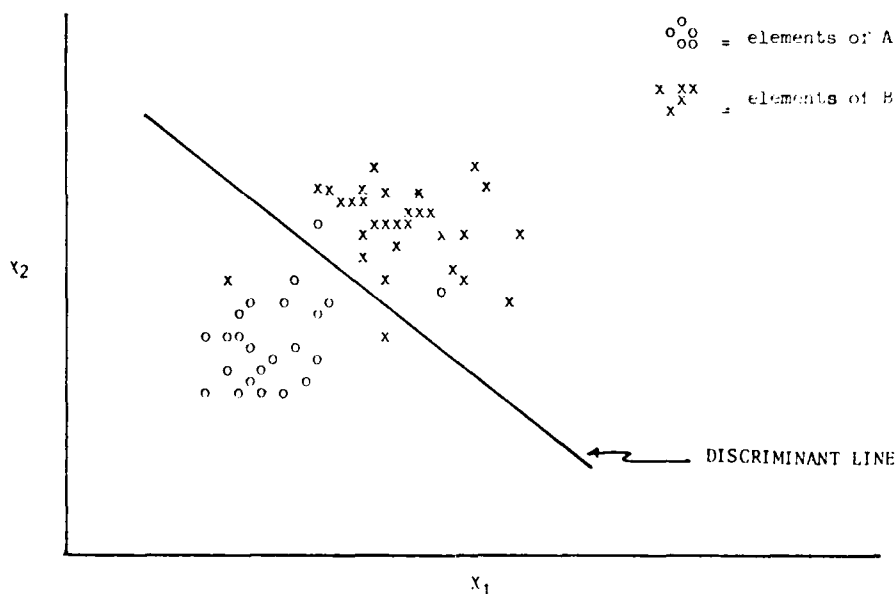


Figure 38. Schematic of the relationship between clusters A and B, the line defined by the discriminant analysis for variables X_1 and X_2 by which A and B are classified.

The problem is somewhat more complex in that there are $g(= 6)$ clusters and $p(= 13)$ variables. The simple explanations above have matrix equation analogs. The equations presented here are defined for a stepwise discriminant analysis where variables are added one by one in order of "best" discrimination. This is to imply that the variable added into the analysis is that variable which maximizes an F ratio which tests the hypothesis that the multivariate mean values for the clusters differ. The process of the addition of variables continues until all are in the analysis. At any step in the analyses consider that $1 \leq r \leq p$ variates are currently in the analysis and that $p - r$ are not. The following parameters are needed. Defining

(a) x_{mki} to be the value of the i^{th} variable of the k^{th} inlet from the m^{th} cluster

(b) N_m number of inlets in cluster m

(c) $n = n_1 + n_2 + \dots + n_g$: total number of inlets (36)

(d) $\bar{x}_i = \frac{1}{n} \sum_{m=1}^g \sum_{k=1}^{n_m} x_{mki}$: the mean value of the variable x_i (37)

(e) ${}_m\bar{x}_i = \frac{1}{n_m} \sum_{k=1}^{n_m} x_{mki}$: the mean of x_i in cluster m (38)

(f) $s_{mi} = \left(\frac{1}{n_m - 1} \sum_{k=1}^{n_m} (x_{mki} - {}_m\bar{x}_i)^2 \right)^{1/2}$: the standard deviation of the i^{th} variable for inlets in cluster m (39)

(g) $(w_{ij}) = \sum_{m=1}^g \sum_{k=1}^{n_m} (x_{mki} - {}_m\bar{x}_i) (x_{mkj} - {}_m\bar{x}_j)$ (40)

(h) $(t_{ij}) = \sum_{m=1}^g \sum_{k=1}^{n_m} (x_{mki} - \bar{x}_i) (x_{mkj} - \bar{x}_j)$ (41)

the matrices

$$W = \begin{pmatrix} w_{11} & w_{12} \\ w_{21} & w_{22} \end{pmatrix} \quad (42)$$

and

$$T = \begin{pmatrix} t_{11} & t_{12} \\ t_{21} & t_{22} \end{pmatrix} \quad (43)$$

are formed where w_{11} and t_{11} are $r \times r$ cross-product matrices (within group and population-wide) with elements w_{ij} and t_{ij} (g and h above) respectively, for the r variables in the analysis

at the given step; W_{12} , W_{21} , W_{22} , T_{12} , T_{21} , and T_{22} involve $p - r$ of the p variates not currently in the analysis. (If all p variables are in the analysis, $W = W_{11}$ and $T = T_{11}$.)

Forming two new matrices

$$A = \begin{pmatrix} W_{11}^{-1} & W_{11}^{-1} W_{12} \\ W_{21} W_{11}^{-1} & W_{22} - W_{21} W_{11}^{-1} W_{12} \end{pmatrix} = (a_{ij}) \quad (44)$$

and

$$B = \begin{pmatrix} T_{11}^{-1} & T_{11}^{-1} T_{12} \\ T_{21} T_{11}^{-1} & T_{22} - T_{21} T_{11}^{-1} T_{12} \end{pmatrix} = (b_{ij}) \quad (45)$$

g discriminant functions can be formed, one for each cluster.

The g discriminant functions are defined by

$$S_{\ell mk} = C_{m0} + \sum_{j=1}^r C_{mj} x_{\ell kj} \quad (46)$$

where $S_{\ell mk}$ is the value for the k^{th} inlet of the ℓ^{th} cluster on the m^{th} (of g) discriminant functions. The coefficients in the equation are defined as

$$C_{mi} = (n - g) \sum_{j=1}^h k \bar{x}_{ij} a_{ij} \quad (47)$$

and

$$C_{m0} = \frac{1}{2} \sum_{j=1}^r C_{mj} m \bar{x}_j \quad (48)$$

where r is the number of variables in the analysis at the given step and the other variables are as previously defined.

Given two arbitrary clusters (m, ℓ) the Mahalanobis squared distance, D^2 is

$$D_{m\ell}^2 = \sum_{i=1}^r (C_{mi} - C_{\ell i}) (m \bar{x}_i - \ell \bar{x}_i) \quad (49)$$

This function measures the statistical difference between the multivariate means for the two clusters. An F value for the difference between clusters for testing purposes is

$$F_{m\ell} = \frac{(n - g - r + 1)}{r(n - g) (n_m + n_\ell)} D_{m\ell}^2 \quad (50)$$

with r and $n - g - r + 1$ degrees of freedom. If the value of F is significant at some level α , then the chance that the multivariable means for the two clusters are equal is no more than α . The values of α normally used are 5 and 1 percent. If the F test is significant at one of these α , the clusters are considered distinct.

It is also possible to test the equality of all group means simultaneously by forming the ratio

$$u = \frac{\det(W_{11})}{\det(T_{11})} \quad (51)$$

and calculating

$$F = \frac{1 - u^{1/2}}{u^{1/2}} \times \frac{yz + 1 - r(g - 1)/2}{r(g - 1)} \quad (52)$$

where $z = r^2(g - 1)^2 - 4/r^2 + (g - 1)^2 - 5$ if $r^2 + (g - 1)^2 \neq 5$, $z = 1$ otherwise, and

$$y = \frac{n - [r + (g - 1) + 3]}{2} \quad (53)$$

This F ratio has $r(g - 1)$ and $yz + 1 - r(g - 1)/2$ degrees of freedom. The F test again tests whether or not the clusters defined are considered distinct among each other on some level of significance.

Finally, it is possible to calculate the posterior probability that inlet k of cluster ℓ actually belonged to cluster m ;

$$P_{\ell mk} = \frac{P_m \exp(S_{\ell mk})}{\sum_{i=1}^g P_i \exp(S_{\ell ik})} \quad (54)$$

with $S_{\ell mk}$ defined previously and

$$P_q = \frac{n_q}{n} \quad (55)$$

the prior probability that the inlet belonged to a given cluster, q . As discussed in the discriminant analysis of the data, equation (54) can be used to calculate the probability that an inlet not in the analysis belongs to a particular cluster.

3. Discriminant Analysis of Inlet Data.

A stepwise discriminant analysis as described was performed incorporating all 13 variables. Then a more restricted analysis was performed involving only the six variables DMX, DMA, W, DCC, L, and AED to see if simpler discriminant functions could be derived.

a. Stepwise Analyses. In the first analysis the objective is to find what minimum set of variables provided adequate cluster discrimination; i.e., what set of variates produces a series of equations that separates the majority of the inlets into the original clusters derived on the basis of equation (49) and listed by equation (50). For this to occur, the F ratio must be significantly above a given level, taken to be 1 percent in this study, for every pair of the original six clusters. The analysis proceeded by selecting one by one from the set of 13 variables the ones that increase discrimination. Using a 1-percent level of significance, the first three variables added were EM2, DCC, EM3, and provided acceptable discrimination at 1 percent. The discriminant functions derived are given in Table 6 as are the F ratios and a classification matrix which indicates how many inlets of each cluster are classified as belonging to another cluster. The coefficients of the discriminant function given in Table 6(a) can be used to calculate the probabilities that inlet belongs to a given cluster using equation (54). The matrix of F ratios (Table 6,b) is used to test the significance that any two clusters are statistically different based on a critical value of the F ratio. In this case, the F ratio must have a value of at least 4.3 in order to accept the hypothesis that the multivariate means for pairs of clusters are not equal. The classification matrix (Table 6,c) indicates the number of inlets in each cluster classified as being in given clusters based on the discriminant functions. The classification matrix indicates that a total of 11 of the 62 inlets analyzed (the other five were neglected) are misclassified; i.e., on the basis of the functions developed, the inlets are in the wrong cluster.

Table 6. Discriminant analysis results for three variables (DCC, EM2, and EM3).

a. Coefficients for discriminant functions based on three variables.						
		Function				
Variable		Type 1	Type 2	Type 3	Type 4	Type 5
DCC	4	-0.63177	-0.86600	-0.10791	-0.46587	-0.39405
EM2	7	9.80824	37.70808	217.03775	596.79672	124.51817
EM3	3	-22.05960	-148.67054	-38.05051	-195.98555	70.51399
		Constant				
		-2.84953	-8.35835	-6.91221	-38.67190	-5.34260
b. F ratios for cluster pairs. ¹						
		Group				
	Group	Type 1	Type 2	Type 3	Type 4	Type 5
	TYPE 2	7.46081				
	TYPE 3	9.26294	0.18310			
	TYPE 4	70.37405	37.51754	20.55116		
	TYPE 5	11.89979	18.34436	5.58241	32.56055	
	TYPE 6	55.66262	27.90051	45.12044	63.35884	60.14134
c. Classification matrix.						
		Number of cases classified into group				
	Group	Type 1	Type 2	Type 3	Type 4	Type 5
	TYPE 1	30	0	0	0	1
	TYPE 2	3	3	0	0	0
	TYPE 3	2	0	2	0	0
	TYPE 4	0	0	0	4	0
	TYPE 5	4	0	0	0	8
	TYPE 6	0	1	0	0	4

¹The F test has 3 and 51 degrees of freedom and an F value of 4.3 is significant at a 1-percent level.

The next step was to continue adding variables in order to determine what minimal group of variables provides adequate cluster discrimination and is closest to the initial clusters determined. After nine variables (EM2, DCC, DM3, DMA, EM1, ED2, ED1, EC2, and W) were added, the cluster discrimination did not differ in classification matrix for an analysis with the full set of

variables. In this instance only one inlet is misclassified. This is Tillamook of cluster 6 which is classified in cluster 2 by the analysis. The discriminant functions for the full case of 13 variables, the F ratios for cluster pairs, and the classification matrix are given in Table 7. Table 8 gives the posterior probabilities for each of the 62 inlets; i.e., the probability based on the analysis that the inlet should be in a given cluster. Again, the statistical tests on the cluster pairs are significantly above 1 percent.

b. Truncated Parameter Analysis. The second discriminant analysis was performed only with the variables DMX, DMA, W, DCC, L, and AED. It was recognized that these variables are more easily measured than the other variables. Thus, if these variables provide a viable cluster discrimination, they would provide a simpler basis for classification.

Table 9 provides the F ratios for cluster pairs and the classification matrix for this analysis. For the F ratios computed with $v_1 = 6$ and $v_2 = 51$ degrees of freedom, a value greater than 3.25 is required to reject the hypothesis of equal multivariate means (or to accept the hypothesis that the clusters are different). Table 9 indicates that numerous cluster pairs (1-3, 1-4, 2-4, 2-5, 3-4, 4-5) do not meet this criteria. Hence, the simplification to these few variables does not reproduce the clusters originally formed on the basis of all 13 variables.

Table 7. Discriminant analysis results for 13 variables.

a. Coefficients for discriminant functions based on 13 variables.						
Function						
Variable	Type 1	Type 2	Type 3	Type 4	Type 5	Type 6
DMX 1	-1.36236	-1.76092	-1.33475	-1.12992	-1.30346	-1.22433
DMA 2	-1.24218	-2.09015	-0.83469	-0.47462	-1.37509	-1.64654
W 3	0.00283	0.00211	0.00329	0.00376	0.00247	0.00154
DCC 4	-2.20527	-2.31469	-1.81093	-2.46253	-1.60977	-4.24291
L 5	0.76051	0.00671	0.00026	0.00014	0.00673	0.00035
MI 6	-7.11257	-21.83881	-34.11697	-101.60954	-73.07272	-34.87820
IS 7	9.94051	-50.70179	288.22370	748.50166	65.99466	-135.51750
IS 8	-195.17353	-330.82570	-246.22120	-443.10246	-70.30244	-369.25660
EC 9	0.86302	0.93846	0.86230	0.96286	0.82931	0.92330
EC 10	-0.19929	-0.41634	-0.16273	-0.00902	-0.15155	-0.57077
DP 11	0.96601	2.51213	0.12991	0.77541	1.14926	1.28759
EC 12	1.65025	0.96279	4.61465	3.16339	1.08608	1.59527
AED 13	1.07074	1.39159	1.87022	2.76669	1.23236	1.67421
Constant						
	-48.95216	-74.75946	-57.24019	-98.36555	-52.02636	-102.44255
b. F ratios for cluster pairs. ¹						
Group						
Group	Type 1	Type 2	Type 3	Type 4	Type 5	Type 6
TYPE 2	5.67719					
TYPE 3	4.90181	7.71520				
TYPE 4	10.64291	14.38265	5.31142			
TYPE 5	8.64286	7.18999	5.91832	14.35312		
TYPE 6	15.38552	6.28558	13.52328	10.39554	15.62871	
c. Classification matrix.						
Number of cases classified into group						
Group	Type 1	Type 2	Type 3	Type 4	Type 5	Type 6
TYPE 1	31	0	0	0	0	0
TYPE 2	0	6	0	0	0	0
TYPE 3	0	0	4	0	0	0
TYPE 4	0	0	0	4	0	0
TYPE 5	0	0	0	0	12	0
TYPE 6	0	1	0	0	0	4

¹The F test has 13 and 44 degrees of freedom and an F value of 2.6 is significant at a 1-percent level.

Table 8. Posterior probabilities (P) that inlets belong to specified clusters (S) is the discriminant function value).

Case	Type	Group					
		Type 1	Type 2	Type 3	Type 4	Type 5	Type 6
1	TYPE 1	4.697 1.000	28.832 0.000	28.135 0.000	104.070 0.000	19.169 0.000	73.909 0.000
2	TYPE 1	4.344 0.907	26.909 0.000	27.624 0.000	97.153 0.000	11.121 0.013	65.814 0.000
3	TYPE 1	5.032 0.993	25.219 0.000	31.251 0.000	101.743 0.000	13.864 0.007	60.943 0.000
4	TYPE 1	7.226 0.920	34.047 0.000	8.473 0.078	98.247 0.000	16.983 0.003	31.467 0.000
5	TYPE 1	10.680 0.863	44.433 0.000	23.444 0.000	98.894 0.000	12.662 0.137	37.799 0.000
6	TYPE 1	15.679 0.984	26.206 0.001	19.970 0.018	60.739 0.000	28.969 0.000	72.168 0.000
7	TYPE 1	9.175 0.996	32.527 0.000	15.453 0.004	84.578 0.000	24.458 0.000	69.694 0.000
8	TYPE 1	10.547 0.983	15.379 0.017	27.606 0.000	91.246 0.000	31.906 0.004	58.017 0.000
9	TYPE 1	7.053 1.000	28.325 0.000	22.420 0.000	90.271 0.000	24.774 0.000	65.431 0.000
10	TYPE 1	12.135 0.999	37.314 0.000	22.047 0.001	104.754 0.000	27.759 0.000	90.386 0.000
11	TYPE 1	10.046 1.000	30.506 0.000	23.193 0.000	72.737 0.000	31.703 0.000	60.107 0.000
12	TYPE 1	5.789 0.998	15.237 0.002	24.441 0.000	75.092 0.000	23.883 0.000	28.329 0.000
13	TYPE 1	7.073 0.999	17.395 0.001	45.113 0.000	113.708 0.000	25.817 0.000	60.611 0.000
14	TYPE 1	6.259 1.000	25.992 0.000	37.062 0.000	101.770 0.000	22.167 0.000	51.461 0.000
15	TYPE 1	1.592 1.000	24.610 0.000	24.841 0.000	90.562 0.000	19.586 0.000	94.694 0.000
16	TYPE 1	7.007 1.000	27.202 0.000	31.932 0.000	98.302 0.000	30.462 0.000	74.123 0.000
17	TYPE 1	5.543 1.000	30.203 0.000	24.806 0.000	95.002 0.000	26.289 0.000	72.866 0.000
18	TYPE 1	8.960 1.000	21.470 0.000	46.146 0.000	102.074 0.000	31.614 0.000	56.071 0.000
19	TYPE 1	7.504 0.998	16.591 0.002	47.075 0.000	113.863 0.000	27.629 0.000	57.614 0.000
20	TYPE 1	0.483 1.000	30.537 0.000	39.259 0.000	98.723 0.000	30.764 0.000	51.034 0.000
21	TYPE 1	10.002 1.000	25.501 0.000	43.529 0.000	120.738 0.000	23.775 0.000	61.036 0.000
22	TYPE 1	16.253 0.992	24.380 0.003	43.964 0.000	119.231 0.000	32.076 0.000	54.315 0.000
23	TYPE 1	18.980 1.000	37.324 0.000	41.653 0.000	91.410 0.000	37.779 0.000	56.418 0.000
24	TYPE 1	9.392 1.000	28.447 0.000	24.819 0.000	91.223 0.000	27.813 0.000	96.049 0.000
25	TYPE 1	3.925 1.000	23.628 0.000	31.795 0.000	108.869 0.000	18.314 0.000	60.100 0.000
26	TYPE 1	7.147 1.000	28.716 0.000	37.339 0.000	106.935 0.000	21.266 0.000	67.744 0.000
27	TYPE 1	9.071 1.000	29.812 0.000	38.427 0.000	92.631 0.000	23.545 0.000	45.270 0.000
28	TYPE 1	13.295 0.900	17.820 0.020	53.790 0.000	115.219 0.000	31.629 0.000	51.542 0.000
29	TYPE 1	31.075 1.000	68.705 0.000	71.293 0.000	109.132 0.000	52.402 0.000	110.261 0.000
30	TYPE 1	15.116 1.000	30.281 0.000	46.197 0.000	99.349 0.000	29.182 0.000	94.616 0.000
31	TYPE 1	39.819 1.000	15.140 0.000	44.625 0.000	108.547 0.000	53.611 0.000	80.258 0.000
1	TYPE 2	33.327 0.000	14.107 1.000	57.457 0.000	100.873 0.000	51.538 0.000	57.269 0.000
2	TYPE 2	33.190 0.000	12.984 1.000	71.471 0.000	130.169 0.000	37.755 0.000	64.610 0.000
3	TYPE 2	15.475 0.017	4.217 0.983	44.083 0.000	91.247 0.000	23.100 0.000	41.003 0.000
4	TYPE 2	24.017 0.000	7.623 1.000	57.963 0.000	104.854 0.000	35.679 0.000	44.077 0.000
5	TYPE 2	47.057 0.000	17.202 0.975	84.070 0.000	109.297 0.000	55.354 0.000	24.171 0.000
6	TYPE 2	36.054 0.012	24.699 0.988	84.130 0.000	131.602 0.000	56.510 0.000	78.477 0.000
1	TYPE 3	37.788 0.000	61.457 0.000	12.290 0.998	35.226 0.000	27.510 0.001	108.450 0.000
2	TYPE 3	34.077 0.000	64.829 0.000	8.868 1.000	28.765 0.000	41.258 0.000	110.270 0.000
3	TYPE 3	29.972 0.000	69.992 0.000	5.099 1.000	70.084 0.000	40.080 0.000	120.311 0.000
4	TYPE 3	27.842 0.001	94.184 0.000	10.652 0.999	79.394 0.000	51.424 0.000	99.227 0.000
1	TYPE 4	112.139 0.000	121.334 0.000	61.262 0.000	13.993 1.000	108.850 0.000	167.164 0.000
2	TYPE 4	110.751 0.000	140.445 0.000	57.635 0.000	12.718 1.000	96.143 0.000	156.603 0.000
3	TYPE 4	65.779 0.000	78.940 0.000	37.483 0.000	9.396 1.000	64.595 0.000	128.561 0.000
4	TYPE 4	104.185 0.000	100.664 0.000	63.978 0.000	7.491 1.000	51.427 0.000	140.492 0.000
1	TYPE 5	38.402 0.000	43.512 0.000	42.871 0.000	73.475 0.000	11.125 1.000	95.813 0.000
2	TYPE 5	40.397 0.000	98.175 0.000	39.091 0.000	55.589 0.000	13.467 1.000	103.801 0.000
3	TYPE 5	20.090 0.002	29.465 0.000	40.550 0.000	82.756 0.000	5.506 0.998	76.086 0.000
4	TYPE 5	13.468 0.095	25.923 0.000	26.852 0.000	79.691 0.000	7.051 0.949	71.642 0.000
5	TYPE 5	13.977 0.113	24.461 0.000	34.951 0.000	73.704 0.000	7.966 0.907	60.994 0.000
6	TYPE 5	11.240 0.213	23.010 0.000	23.908 0.000	56.692 0.000	6.979 0.747	58.094 0.000
7	TYPE 5	27.844 0.019	41.807 0.000	50.325 0.000	134.406 0.000	17.586 0.999	89.391 0.000
8	TYPE 5	15.260 0.044	30.770 0.000	36.061 0.000	98.720 0.000	7.071 0.979	70.243 0.000
9	TYPE 5	9.242 0.329	29.147 0.000	24.171 0.000	61.306 0.000	5.913 0.572	61.577 0.000
10	TYPE 5	24.899 0.001	51.743 0.000	32.973 0.000	97.324 0.000	9.143 0.799	80.262 0.000
11	TYPE 5	61.009 1.000	62.573 0.000	89.140 0.000	131.489 0.000	24.110 1.000	102.562 0.000
12	TYPE 5	50.452 0.000	66.310 0.000	76.643 0.000	114.814 0.000	16.611 1.000	113.846 0.000
1	TYPE 6	59.155 0.000	63.579 0.000	126.641 0.000	154.783 0.000	82.022 0.000	17.896 1.000
2	TYPE 6	130.740 0.000	99.669 0.000	170.217 0.000	197.156 0.000	143.905 0.000	34.799 1.000
3	TYPE 6	111.963 0.000	81.691 0.000	162.437 0.000	206.014 0.000	125.655 0.000	20.719 1.000
4	TYPE 6	57.625 0.000	40.102 0.000	90.342 0.000	127.094 0.000	70.008 0.000	13.404 1.000
5	TYPE 2	47.057 0.000	17.202 0.975	84.070 0.000	109.297 0.000	55.354 0.000	24.171 0.000

Table-9. Discriminant analysis results for six variables (DMX, DMA, W, DCC, L, and AED).

a. Coefficients for discriminant functions based on six variables.						
		Function				
Variable		Type 1	Type 2	Type 3	Type 4	Type 5
DMX	1	-0.01854	0.05781	-0.32853	-0.05528	-0.11917
DMA	2	-0.26602	-1.01319	-0.24483	-0.69066	-0.72908
W	3	0.00047	0.00018	0.00002	-0.00008	-0.00017
DCC	4	-0.44963	-0.35977	-0.14915	-0.47531	-0.17968
L	5	0.00040	0.00046	0.00006	-0.00026	0.00027
AED	13	-0.80547	-0.68665	-0.27004	0.01939	-0.50517
b. F ratios for cluster pairs. ¹						
		Group				
	Group	Type 1	Type 2	Type 3	Type 4	Type 5
	TYPE 2	5.12826				
	TYPE 3	1.78298	3.98680			
	TYPE 4	3.94152	1.79447	1.59160		
	TYPE 5	7.86091	1.00934	3.88856	1.38131	
	TYPE 6	27.33511	14.50145	10.67884	10.78398	21.18214
c. Classification matrix.						
		Number of cases classified into group				
	Group	Type 1	Type 2	Type 3	Type 4	Type 5
	TYPE 1	31	0	0	0	0
	TYPE 2	1	3	0	0	2
	TYPE 3	3	0	1	0	0
	TYPE 4	1	0	0	2	1
	TYPE 5	3	0	0	0	6
	TYPE 6	0	1	0	0	4

¹The F test has 6 and 51 degrees of freedom, and an F value of 3.25 is significant at a 1-percent level.

4. Discussion.

Since it is not possible to discriminate the original clusters with a truncated parameter set, the discriminant functions must be chosen from the stepwise analysis of the complete parameter set. It would be possible to use the three variable-based functions (Table 6). However, these variables are relatively difficult to derive. It is recommended that the functions based on the full set (Table 8) be used. The effort involved is not that much greater than for the three variable cases.

Several implications result from the discriminant analysis. First, the stepwise discriminant analysis again offers strong evidence, based upon multivariate analyses of variance, that the clusters are well defined. The misclassification of only one inlet and the strength of the posterior possibilities (Table 9) provide evidence of this. The discriminant functions derived provide a basis of assignment of the inlets to the original clusters.

The second implication seen is the dependence of the analysis on the shape functions introduced (EM1, EM2, EM3, EC2, ED1, and ED2). The clusters cannot be discriminated without them. This, in conjunction with their appealing geometric interpretation, suggests that they perform an adequate and useful representation of inlet geometry.

Thirdly, it is seen that DMX, AED, EC1, and L are perhaps redundant parameters because in the stepwise discrimination they provide no further refinement. They are maintained for purely descriptive purposes.

Through the discriminant analysis, functions have been derived that mathematically define the clusters. From these functions it is possible to derive

the probability that an inlet belongs to a given cluster. The relationships and cluster discrimination appear statistically significant at a very high level.

VI. EVALUATION OF THE PROBABILITY THAT AN INLET NOT IN THE ANALYSIS BELONGS TO A CLUSTER

The analyses presented in this report represent a classification of 67 inlets at selected times. It is desirable to have a method for placing an inlet not in the analysis into the classification. Such a method would also allow comparison of the later condition of an inlet in the analysis with the condition originally used. In the strictest sense, the appropriate method would be to enter the new inlet into the analysis and redo the entire classification and discriminant analysis. This is a time-consuming and laborious exercise. It should not be considered unless a large number of inlets are to be entered. The following method represents a simplified method for estimating the probability that the new inlet belongs to a given cluster. The principal assumptions required are that (a) the new inlet does belong to one of the clusters and (b) the discriminant functions calculated in Section V are adequate statistical formulas describing the classification.

1. Data Preparation.

To use the discriminant functions, it is necessary to measure and calculate the 13 variables used in the same fashion as they were for this report. For the variables, DMX, DMA, W, DCC, L, and AED, the definitions are straightforward. For the variables EM1, EM2, EM3, EC1, EC2, ED1, and ED2, the definitions are less straightforward. The following discussion describes how the values can be calculated efficiently.

Taking the minimum inlet width cross-section eigenvectors ($\underline{e}_1, \underline{e}_2, \underline{e}_3$) as an example, the following steps from Section II are necessary to find the weightings EM1, EM2, and EM3:

(a) A cross section at the minimum inlet width is drawn.

(b) The 60 evenly spaced points across the profile are located and the depth recorded with the order in which the depths are listed based on the convention of Section II. Each depth is divided by W.

(c) The mean depth and the standard deviation for each depth location (calculated and listed in App. D) are used to normalize each depth

$$d_i^* = \frac{d_i - \bar{d}_i}{S_i} \quad (56)$$

where d_i is the newly measured depth, \bar{d}_i and S_i are the mean and standard deviation respectively, and d_i^* is the normalized value.

(d) A new vector $\underline{D}_* = (d_1^*, d_2^*, \dots, d_{60}^*)$ is formed (57)

(e) For \underline{e}_1 the coefficients are taken from Appendix E to form

$$\underline{e}_1 = (e_{11}, e_{12}, \dots, e_{60}) \quad (58)$$

(f) The value of EM1 is calculated by the vector dot product of \underline{e}_1 (from App. E) and D_* .

$$EM1 = \underline{e}_1 \cdot D_* = \sum_{i=1}^{60} e_{1i} d_i^* \quad (59)$$

(g) EM2 is calculated by forming \underline{e}_2 from Appendix E and taking

$$EM2 = \underline{e}_2 \cdot D_* = \sum_{i=1}^{60} e_{2i} d_i^* \quad (60)$$

(h) EM3 is calculated by forming \underline{e}_3 from Appendix E and taking

$$EM3 = \underline{e}_3 \cdot D_* = \sum_{i=1}^{60} e_{3i} d_i^* \quad (61)$$

The values of EC1, EC2, ED1, and ED2 can likewise be calculated following the procedures of Section II and using values of Appendixes D and E. A final check would be to find an inlet similar in characteristics to one in this report and compare values to see if the ones newly calculated look reasonable.

2. Probability Calculations.

To calculate the desired probability, it is necessary to evaluate the following values, S_i where i will range from 1 to 6.

$$S_i = C_{i0} + \sum_{j=1}^{13} C_{ij} X_j \quad (62)$$

where C_{i0} is the constant on the i^{th} discriminant function (eq. 48), C_{ij} is the coefficient for the j^{th} of 13 variables for the i^{th} discriminant function (eq. 47), and X_j is the value of the j^{th} variable. The subscript i relates the discriminant function to the appropriate inlet group and equation (62) is seen to be analogous to equation (46). In actual computations, the values of C_{i0} and C_{ij} would come from Table 7(a).

The computation of the six values S_i gives only the values of the discriminant functions. The probability that the inlet belongs to inlet group i is p_i^* calculated by

$$p_i^* = \frac{P_i \exp(S_i)}{\sum_{j=1}^6 p_j^* \exp(S_j)} \quad (63)$$

where P_j is the a priori probability of belonging to a given inlet group

$$P_j = \frac{N_j}{62} \quad (64)$$

where N_j is the number of inlets in the j^{th} group ($N_j = 31, 6, 4, 4, 12, 5$ for $j = 1$ to 6, respectively). Equation (63) is analogous to equation (54).

These equations for calculating the discriminant functions and the probabilities have been programed into a simple computer program given in Appendix F. It is written in a time-sharing format with unformatted input and output. With minor modifications, it can be operational on almost any digital computer.

3. A Simple Example.

Table 10 provides a simple example of input to the program—the values of the 13 variables for a hypothetical inlet. The results indicate that the inlet group for which the probability is highest is group 3 with a value of 0.85. The second highest is group 4 with a value of 0.14.

Table 10. A simple example of the calculation of the probability that an inlet belongs to a given group.

Input to computer program (App. F)			
DMX -25.0	DMA -15.0	N 1,000.0	
DCC -4.0	L 1,500.0	EM3 0.0	
EM1 -0.1	¹ EM2 0.08	AED 0.15	
EC1 20.0	EC2 -1.0		
ED1 -3.0	ED2 1.0		
Output from program			
Group	S_i	P_i (a priori probability)	P_i^* (probability from discriminant analysis)
1	34.3	0.500	0.000
2	23.5	0.097	0.000
3	49.0	0.065	0.853
4	46.2	0.065	0.141
5	41.8	0.193	0.001
6	-2.9	0.081	0.000

¹EM2 input as absolute value.

VII. INLET GEOMETRY: A SUMMARY DISCUSSION

The initial objective of the study was the definition of a series of parameters that satisfactorily describes the major components of the inlet throat and outer bar. After preliminary studies 13 variables were selected incorporating its factors that describe both the physical dimensions of the inlet and the shape (or geometry). Many of the parameters have been used previously and have analogous roles in describing the hydraulic character of inlets. Other parameters are new and are a result of recent research into the field of shape analysis.

The results of the statistical analyses performed in the study suggest that the parameters chosen are a set sufficient for resolving a series of principal questions regarding the variability of inlet geometry. Through careful measurement of these variates a series of relationships among the geometric parameters has been defined.

The eigenvector-generated description of geometric components of inlet bar and channel shapes provided a clear, concise indication of the covariability of these factors with the other variates. Although the mathematics of their derivation is not trivial, the resulting parameters can be interpreted in a simple fashion. As the discriminant analysis indicates, they have an important role in defining the clustering found. It is expected that these parameters and others like them will find an increasingly important role in the description and analysis of landforms.

The set of parameters chosen and the particular definitions used are by no means the only ways of representing inlet morphology. It is evident that some of the parameters are redundant, but these have been retained for descriptive purposes. Any future classification analyses should consider their elimination. One major variate not directly used in the study is ebb delta volume defined along the lines suggested in Dean and Walton (1975). It is obvious that some of this information is retained in the ebb delta eigenvectors; the principal difficulty lies in the consistent definition of the base surface above which the volume is taken. In areas with multiple, and possibly overlapping inlet deltas as is the case in a number of coastal areas, the base surface is difficult if not impossible to define.

One principal goal of the classification study was to analyze the relationships among the geometric parameters chosen. It was a reasonable expectation to find moderate partial correlations among the parameters. A major outcome of the study is the series of strong relationships found that is statistically significant at high levels. It is apparent from the study that many of the geometric factors are interrelated in a predictable manner and that the parameters DMX, DMA, DCC, L, and AED in particular can be co-related. Likewise, when inlet width did not appear as a controlling parameter in the variable cross plots, the strength of the relationships of so many parameters to the area of the minimum inlet width cross section, A_c (estimated by $W \times DMA$), was unexpected. These relationships to A_c provided a key to an understanding of the adjustment of inlet geometry.

The major implication of the relationships found is the large scale coadjustment of inlet geometry that appears scaled by the parameter A_c . As A_c increases, the inlet channel becomes less incised into the outer bar, the relative depth of the channel across the bar increases, the channel length is increased, the ebb delta area enlarges, and channel depths deepen. It is apparent that this adjustment occurs as a response to the wave and tide processes and that the relationships found are statistical summaries of complex hydraulic-sediment interactions in widely ranging geologic settings. An important component of future research should be an effort to place the relationships in the perspective of the wave and tide processes at the inlets studied.

The relationships found may have direct design implications for a number of practical engineering problems involving the design of inlet modifications. If the tidal prism-minimum cross-sectional area relationship of O'Brien (1931) is assumed, it is apparent that given one prism, then one A_c , and hence a narrow range of inlet geometries is possible. Whether this is in fact realistic, or whether the geometry predicted is an equilibrium-type form that the condition might produce is unknown. A further implication of the analysis is that the

internal adjustment of DMX, DMA, L, and DCC (among other parameters) suggests that the detail of the geometry is highly coordinated. Even the shape of the channel profile appears to be determined to a large degree. The adjustments established in this report result in inlet channel geometries unlike those currently used in design practice. Examples of this construction of constant depth channels while most of the natural channels have a significant slope and construction of steep-sided or U-shaped channel cross sections while natural channels are more gently sloping. The implication of this upon the success or failure of the proposed modifications to an inlet is unknown.

It is not clear, if the relationships developed here are applied in the design of a jettied or dredged channel, how they are to be applied, or whether they will be a valid prediction of inlet response. As an example, if an inlet is modified to have a highly constricted cross-sectional area, it is not evident that DMX, DCC, or L must respond as predicted because the throat geometry inherently associated with the given cross section is not necessarily preserved in the proposed modification. It is perhaps reasonable to expect that the equations will produce bounds for the response; however, even this is not assured. It is thus recommended that, before these relationships are used in design, more research and experimental effort be given to provide a better understanding of their implications.

The second principal goal of the study was to investigate a possible classification of inlets based upon inlet geometry. The objectives were to see if a subpopulation structure existed and, if it existed, to define it. The resulting classification would produce a better understanding of inlet variability and would aid personnel in design projects to find prototype inlets of similar characteristics. The results of both the cluster analysis and the discriminant analysis indicate the presence of at least six well-defined clusters or types of inlets based on geometry. The cluster analysis provided the taxonomic structure of the set of inlets analyzed and produced a preliminary classification. The discriminant analysis further refined the classification to produce a series of functions that allows assignment of inlets to the six clusters. It was also recognized that the very large inlets were not represented sufficiently in the analysis to provide reliable clustering or discrimination.

Examination of the relationships among the clusters derived indicated that the scaling process evident in the other analyses is preserved. The significant result of the classification analyses, however, is that the clusters systematically organize inlets on the basis of width, depth, and shape in a way that accounts for some of the scatter observed in simple relationships among parameters. Thus, clusters 3 and 4 differ only slightly in width, but greatly in terms of the other variables. Clusters 4 and 5 have similar depths and widths of the cross section but differing depths at the crest of the outer bar, and so forth for other pairs of clusters. In part, the clusters would appear to account for some of the variability in geometry that may be attributable to wave action. Whether this is indeed the case will require future research relating the wave and tide processes to the geometry.

To summarize the implications of both the classification and parameter variation studies, it is essential to realize that they are complementary, together explaining in some detail the systematic organization of tidal inlet geometry. The cross-sectional area, A_c , can be simplistically considered as

a scaling parameter that relates the relative magnitudes of wave- and tide-generated sediment transport. With increasing area, the tide processes appear to dominate the wave processes; inlet geometry varies accordingly. The size of the cross-sectional area scales the bar and channel geometry in a fairly regular pattern. As a result it must be concluded that, except for small inlets, the tide-generated processes to a large degree determine the geometry. Even in the smaller inlets tidal control is still evident.

The classification analyses substantiate the scaling relationship, but indicate that there are systematic deviations of inlet geometry not fully explained by the scaling relationship. The clusters found represent this organization. It is clear also that if the deviations away from the scaling relationships were purely random it would be fortuitous to have the discriminant analysis significant at a high level. The implication must be that the organization is real and forced by some underlying cause.

The absence of width, and less so average depth, as important scaling factors in many relationships shown in Section III and the absence of relationships between EC2 and EM2 and other parameters underscore the lack of a parameter that performs a scaling for wave action in the way that A_o scales the larger scale geometry. EC2, which describes the slope of the channel profile, is probably related to onshore-offshore sediment transport by waves at the edges of the delta and perhaps less so to longshore transport. EM2, which gives cross-section asymmetry, would be more likely related to wave-caused longshore transport. If this is so, there would not be necessarily a good relationship between EM2 and EC2.

In addition to meeting the primary objectives of the study, the parameters chosen and the analyses performed place the variation of inlet geometry into a better perspective of the varying influences of waves and tides. It is important to recognize that the conclusions drawn are based upon an interpretation of the morphology of tidal inlet systems and by design have not involved estimates of the hydrodynamic processes. This approach was, in part, followed to see if a natural organization of inlet variability was evident which would motivate research into the correspondence between process and form. The results of the study justify the need for performance of this work.

As is often the case in studies of this type, more questions are generated than resolved. In particular the results should motivate study into the relationships between the types of inlet geometry found and tidal prisms, ranges and currents, net and gross longshore drift, and onshore and offshore sediment movement by waves. The certainty of whether the inlet types are natural by-passers of sand or not needs to be established. The variation of inlet stability by inlet type requires examination. Finally, the number of inlets analyzed should be increased.

Several of the parameters and a number of analyses used in this report have not been extensively used in either the engineering or geologic literature. When the scientific questions of a study involve multidimensional variation, there is a wealth of statistical procedures that can be used in a rigorous method of investigation. Given the complex multidimensional variation typical of inlet geometry, it is difficult to see how the results obtained here could have been achieved using only one-dimensional methods.

VIII. SUMMARY

Parameters have been devised that measure and describe inlet throat and ebb delta morphology. When these parameters are measured for inlets where sufficient chart data are available, the parameters are shown to vary in a consistent fashion that appears to be scaled according to the relative magnitude of the tidal processes. When the subpopulation structure is examined, inlets can be initially clustered into six classes which can be mathematically discriminated. The classification provides a systematic organization of inlet geometry that is related to deviations from the basic scaling relationship probably due to the influence of wave action. The relationships and classification found are statistically significant at high levels which provides confidence in the results.

In a statement generally attributed to O'Brien, there are said to be two types of inlets: large and small. This study to a large degree confirms this observation, but beyond that shows the adjustment of inlet geometry to be systematic and predictable.

LITERATURE CITED

- BATES, C.C., "Ratond Theory of Delta Formation," *Bulletin of the American Association of Petroleum Geologists*, No. 37, 1953, pp. 2119-2162.
- BRUUN, P., "Tidal Inlets and Littoral Drift," Universit ets forlaget, Oslo, Norway, 1967.
- BRUUN, P., and GERRITSEN, F., "Investigations of Existing Data on Tidal Inlets," Interim Report, Coastal Engineering Laboratory, University of Florida, Gainesville, Fla., 1957.
- BRUUN, P., and GERRITSEN, F., "Natural By-Passing of Sand at Coastal Inlets," *Journal of the Waterways and Harbors Division*, Vol. 85, No. WW4, Part 1, Dec. 1959, pp. 75-107.
- CALDWELL, J.M., "Tidal Currents at Inlets in the United States," *Journal of the Hydraulics Division*, Vol. 81, No. 716, 1955.
- DAVIS, J.C., *Statistics and Data Analysis in Geology*, John Wiley & Sons, Inc., New York, 1973.
- DEAN, R.G., and WALTON, T.L., "Sediment Transport Processes in the Vicinity of Inlets with Special Reference to Sand Trapping," *Estuarine Research*, Vol. 2, Academic Press, San Francisco, Calif., 1975.
- DIXON, W.J., ed., "BMD-Biomedical Computer Programs," University of California Press, Los Angeles, Calif., 1974.
- DIXON, W.J., and MASSEY, F.J., *Introduction to Statistical Analysis*, McGraw-Hill, New York, 1969.
- GALVIN, C.J., "Inlets and Wave Direction; Wave Climate and Coastal Processes," *Proceedings of the Symposium on Water, Environment and Human Needs*, Massachusetts Institute of Technology, 1971, pp. 44-78.
- GALVIN, C.J., et al., "Study of Inlets," *Abstract, Journal of Coastal Shallow Water Research Conference*, Vol. 2, No. 81, 1971a.
- GALVIN, C.J., et al., "Study of Inlets-Geometry Project," Memorandum for Record, U.S. Army, Corps of Engineers, Coastal Engineering Research Center, Washington, D.C., 1971b.
- JARRETT, J.T., "Tidal Prism-Inlet Area Relationships," GITI Report 3, U.S. Army, Corps of Engineers, Coastal Engineering Research Center, Fort Belvoir, Va., and U.S. Army Engineer Waterways Experiment Station, Vicksburg, Miss., Feb. 1976.
- KENDALL, M.G., and STUART, A., "Inference and Relationship," Vol. II, *The Advanced Theory of Statistics*, Hafner Publishing Co., New York, 1961.
- KENDALL, M.G., and STUART, A., "Design and Analysis, and Time Series," Vol. III, *The Advanced Theory of Statistics*, Hafner Publishing Co., New York, 1968.

- KRUMBEIN, W.C., and GRAYBILL, F.A., *An Introduction to Statistical Models in Geology*, McGraw-Hill, New York, 1965.
- KUTZBACH, J., "Empirical Eigenvectors of Sea Level Pressure, Surface Temperature and Precipitation Complexes over North America," *Journal of Applied Meteorology*, Vol. 6, 1967, pp. 791-802.
- O'BRIEN, M.P., "Estuary Tidal Prisms Related to Entrance Areas," *Journal of Civil Engineering*, Vol. I, No. 8, 1931, pp. 738-739.
- RESIO, D.T., et al., "Systematic Variations in Offshore Bathymetry," *Journal of Geology*, Vol. 85, 1977, pp. 105-113.
- SNEATH, P.H.A., and SOKAL, R.R., *Numerical Taxonomy*, W.H. Freeman & Co., San Francisco, Calif., 1973.
- VINCENT, C.L., "A Method for the Mathematical Analysis of the Cross-Sectional Geometry of Tidal Inlet Channels," *Journal of Mathematical Geology*, Vol. 8, No. 6, 1976, pp. 635-647.
- VINCENT, C.L., and CORSON, W.D., "Analysis of the Stability of Selected U.S. Tidal Inlets," GITI Report, U.S. Army, Corps of Engineers, Coastal Engineering Research Center, Fort Belvoir, Va., and U.S. Army Engineer Waterways Experiment Station, Vicksburg, Miss. (in preparation, 1980).
- VINCENT, C.L., and RESIO, D.T., "Analysis of Patterns of Beach Change," *National Meeting of the American Society of Civil Engineers*, San Diego, Calif., Apr. 1976.
- VINCENT, C.L., et al., "Systematic Variations in Barrier Island Topography," *Journal of Geology*, Vol. 84, 1976, pp. 583-594.
- WINANT, C., INMAN, D., and NORDSHROM, C., "Description of Seasonal Beach Changes Using Empirical Eigenfunctions," *Journal of Geophysical Research*, Vol. 80, 1975, p. 1979.

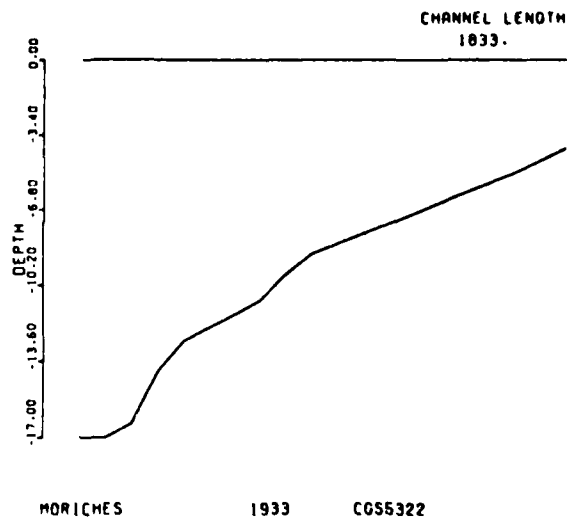
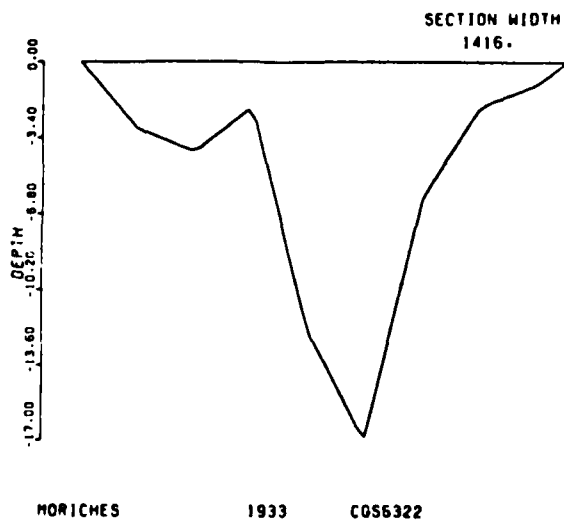
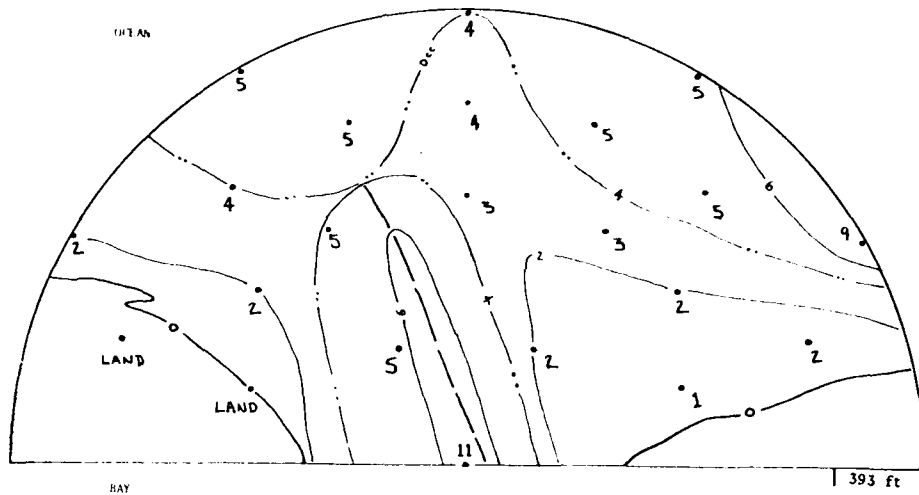
PRECEDING PAGE BLANK-NOT FILMED

APPENDIX A

PLOTS OF MINIMUM INLET WIDTH CROSS SECTION, CHANNEL PROFILE,

AND

EBB DELTA GEOMETRY FOR SELECTED INLETS



MORICHES

1933

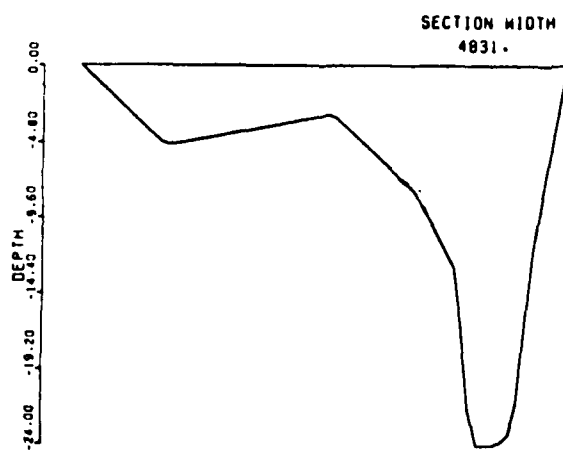
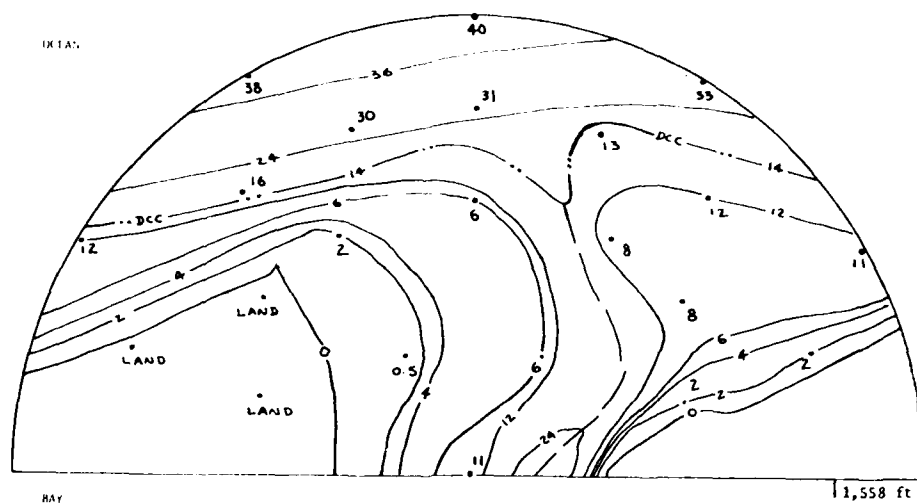
CG55322

MORICHES

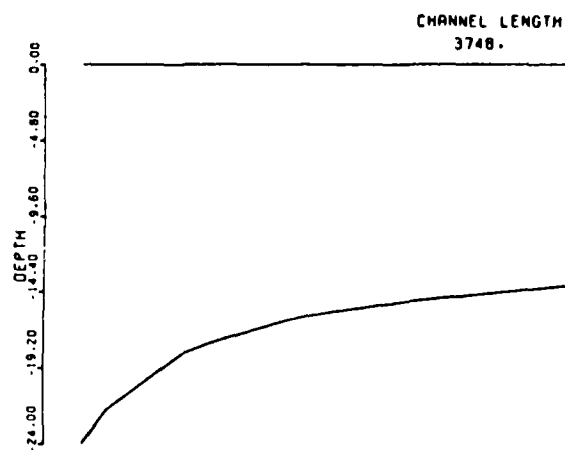
1933

CG55322

Moriches Inlet, N.Y. 1933

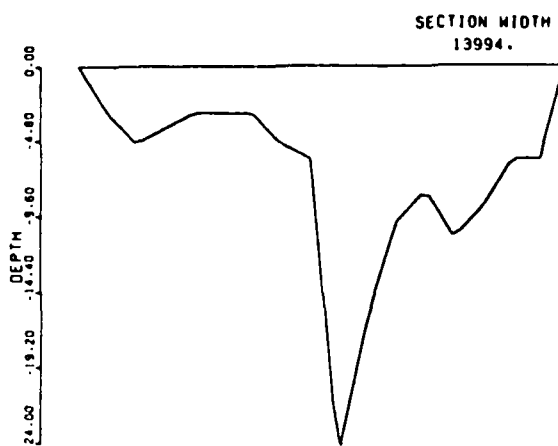
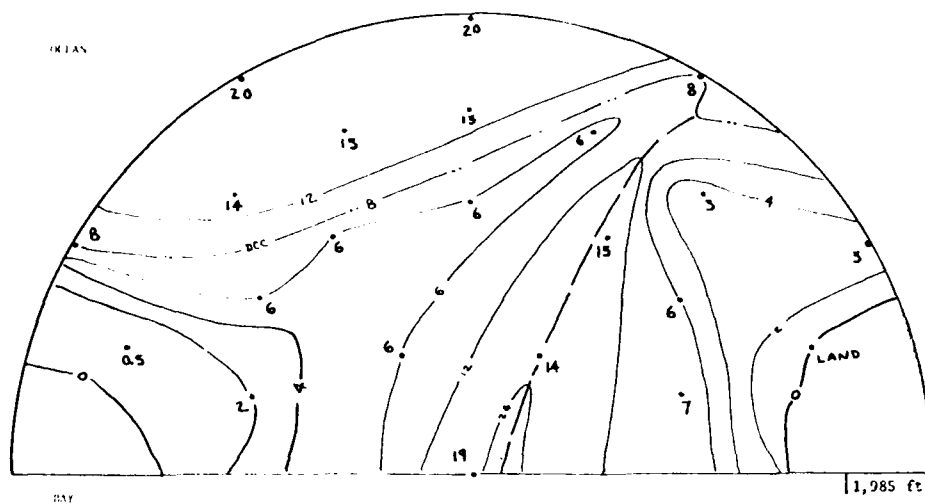


FIRE ISLAND 1950 CGS7800



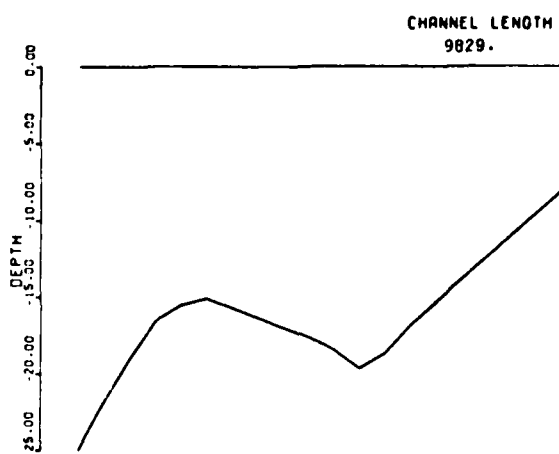
FIRE ISLAND 1950 CGS7800

Fire Island Inlet, N.Y. 1950



BEACH HAVEN-L. EGG 1954

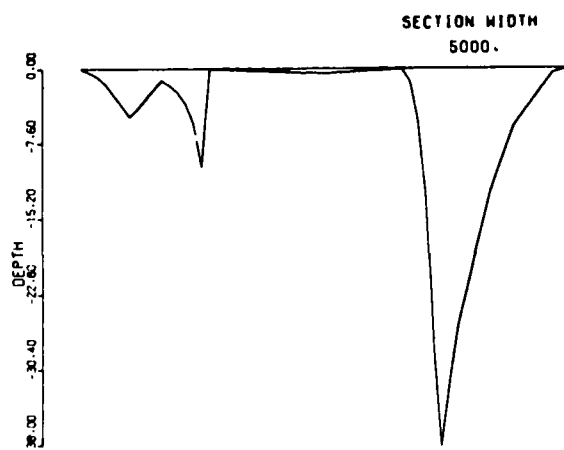
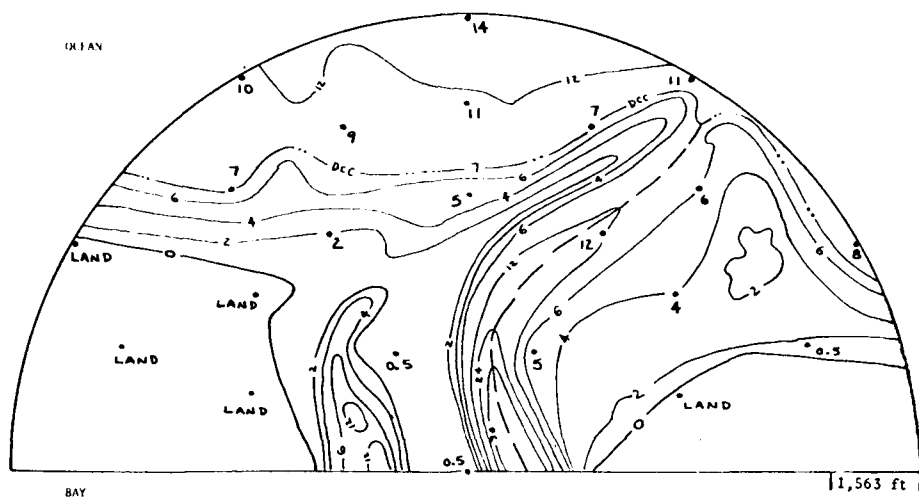
CGS0220



L. EGG-B. HAVEN 1954

CGS0220

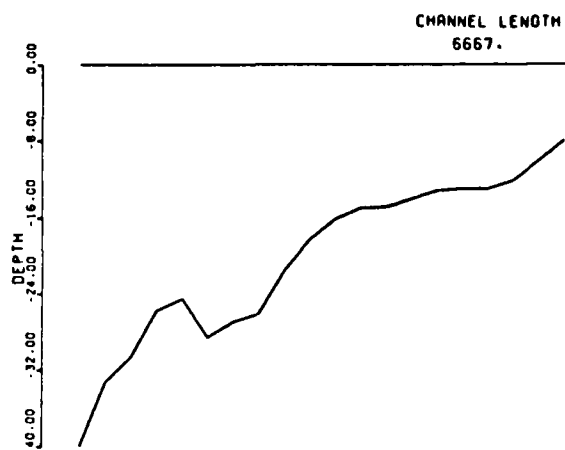
Beach Haven-Little Egg Inlet, N.J. 1954



BRIGANTINE

1954

COS8221

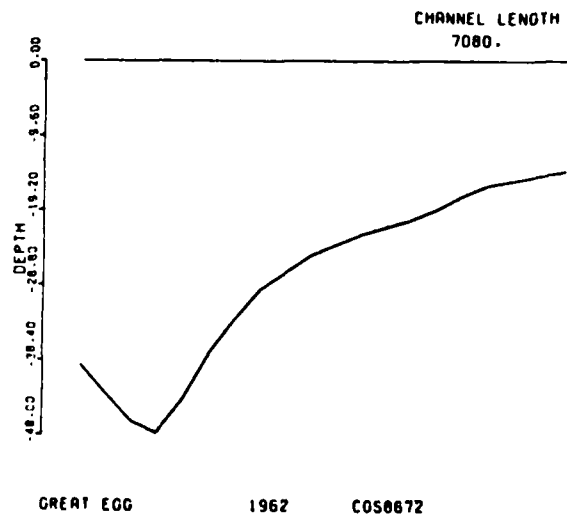
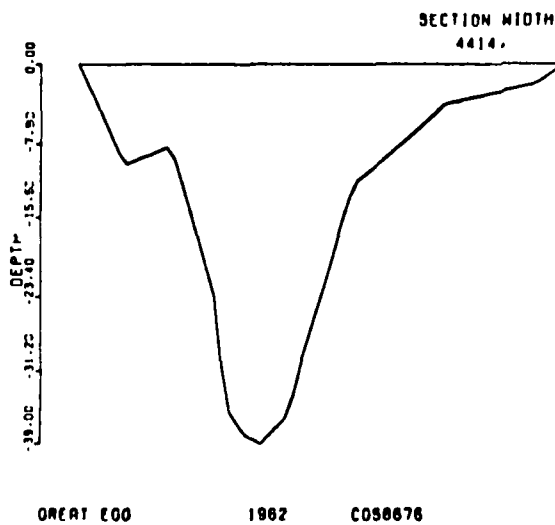
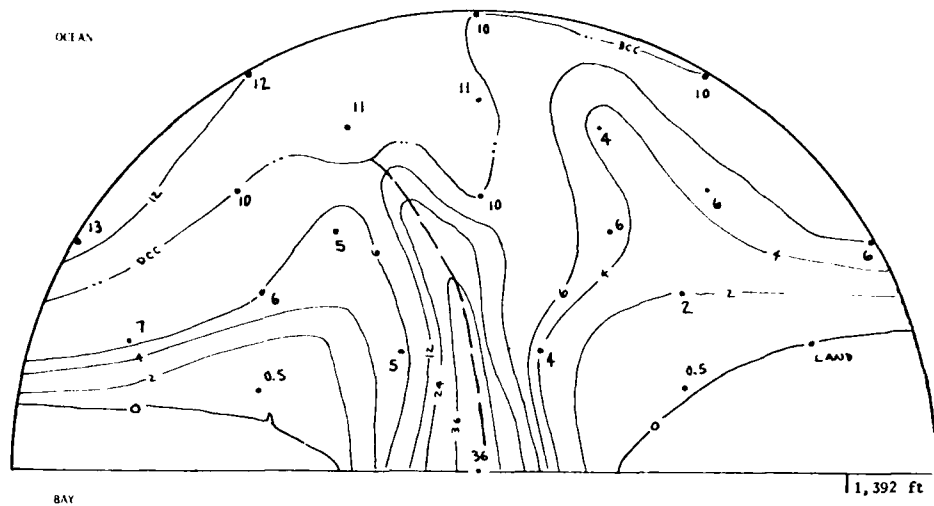


BRIGANTINE

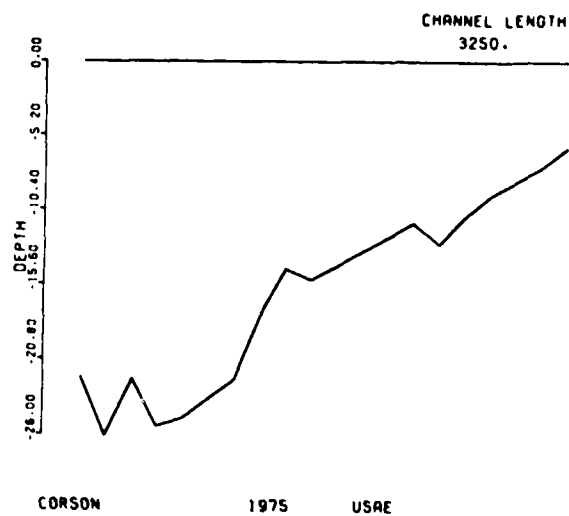
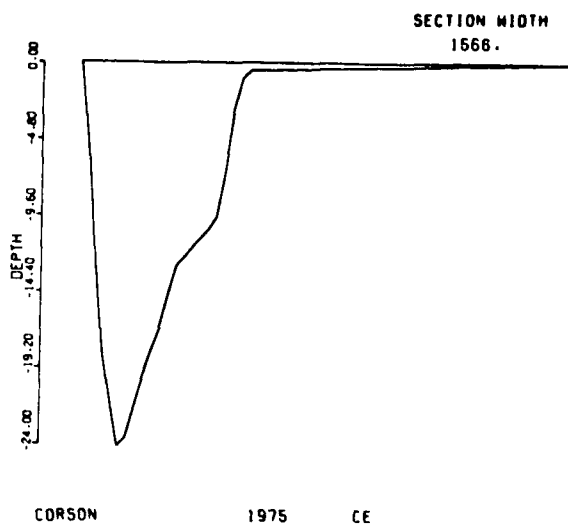
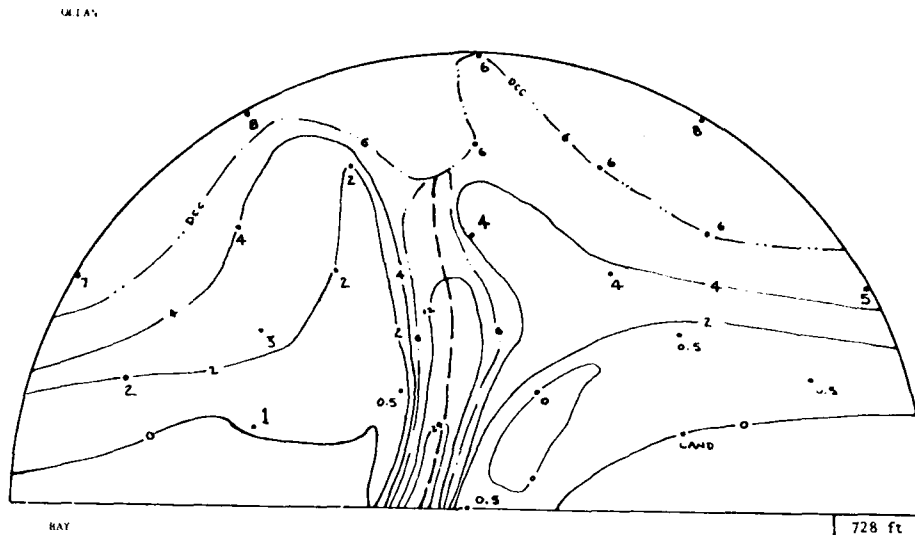
1954

COS8221

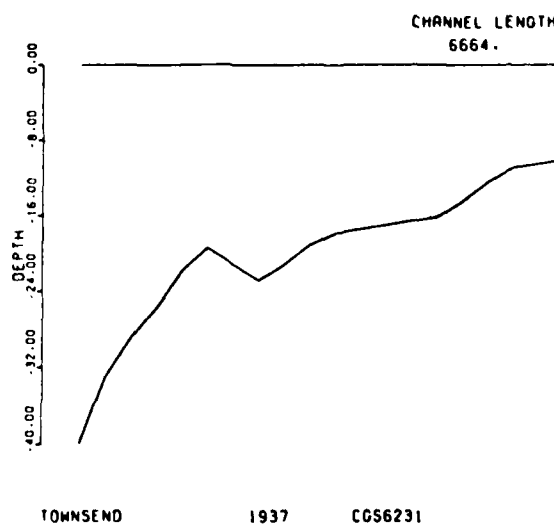
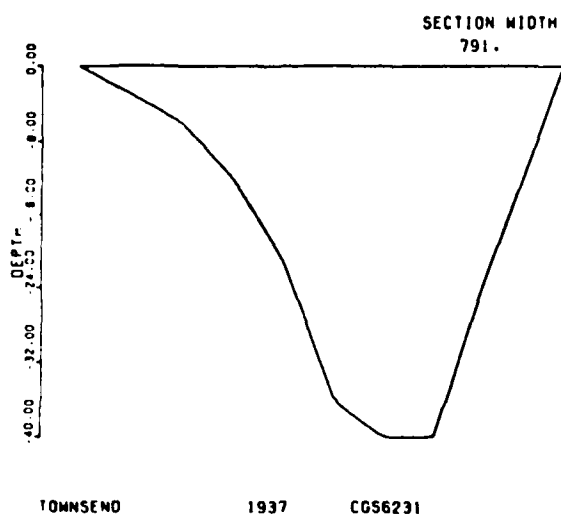
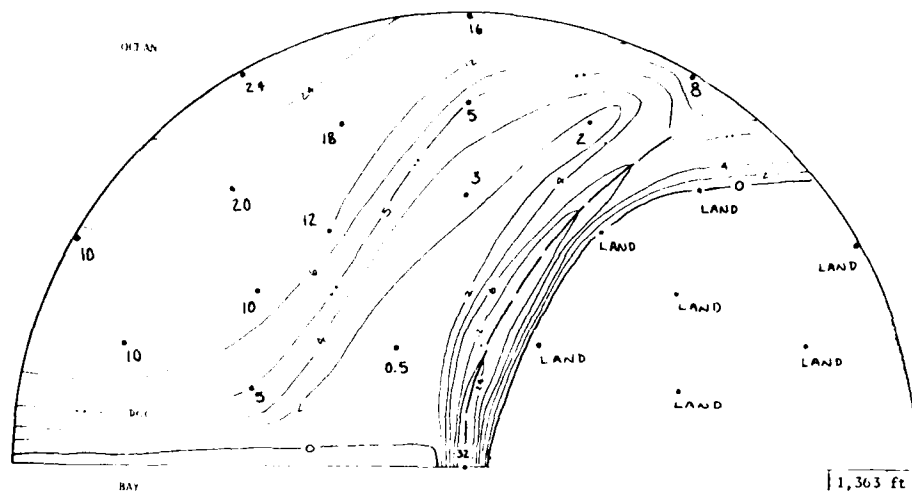
Brigantine Inlet, N.J. 1954



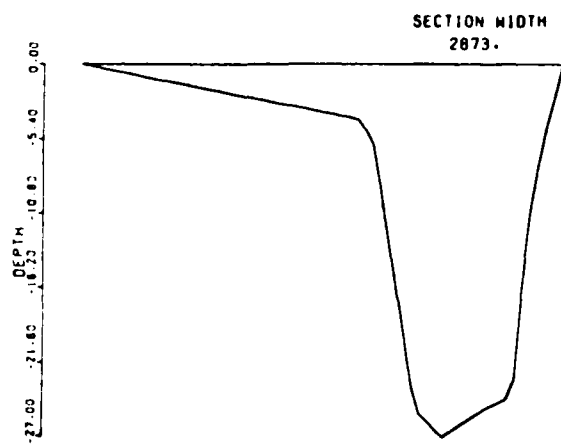
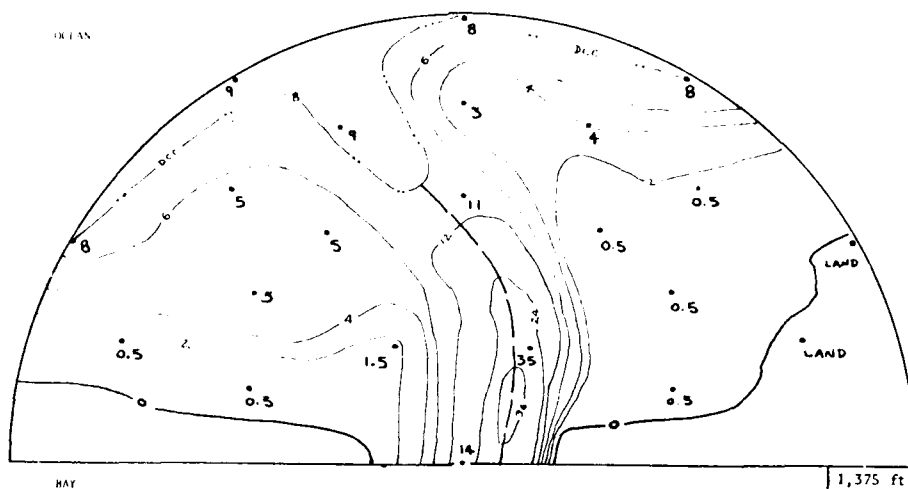
Great Egg Inlet, N.J. 1974



Corson Inlet, N.J. 1975



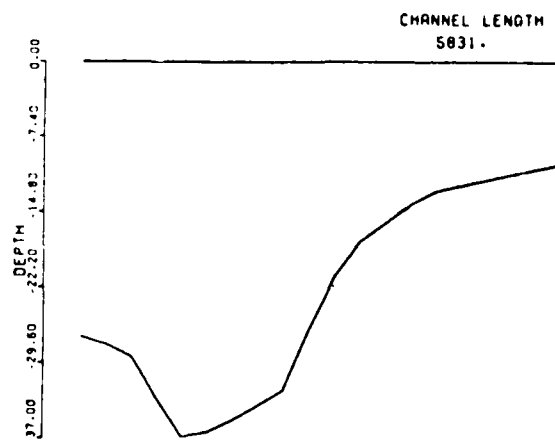
Townsend Inlet, N.J. 1937



HEREFORD

1937

CG56236

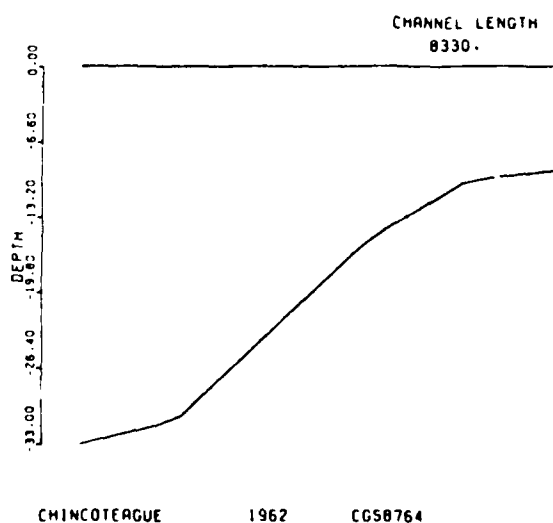
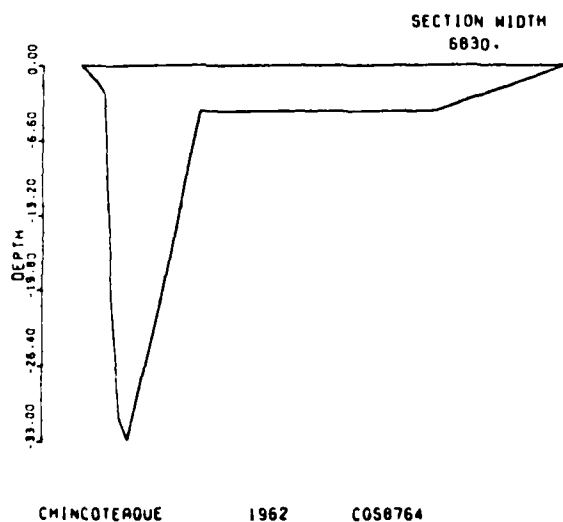
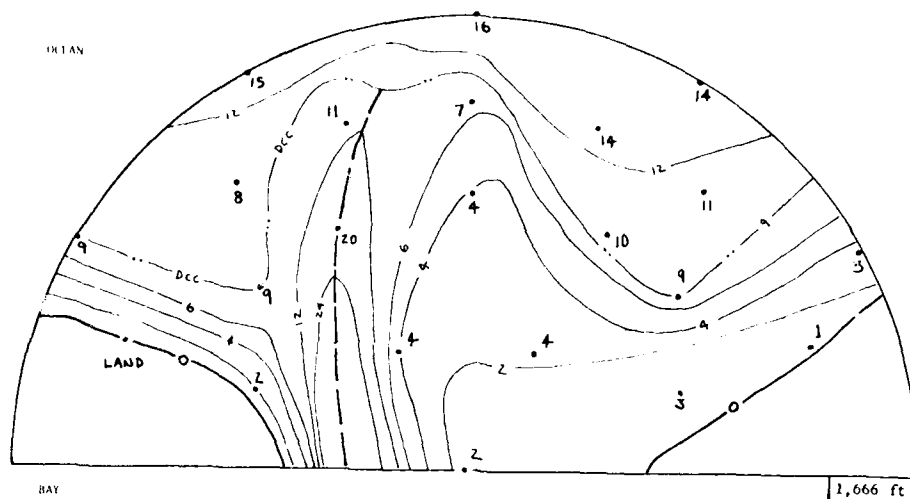


HEREFORD

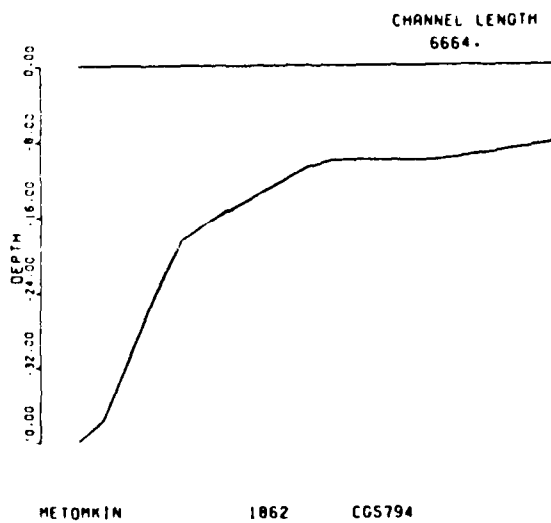
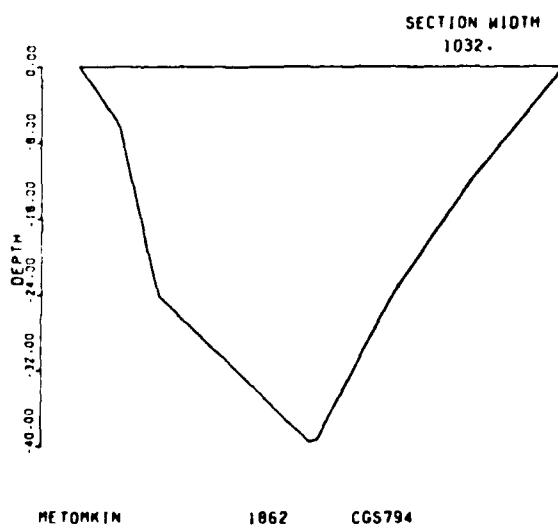
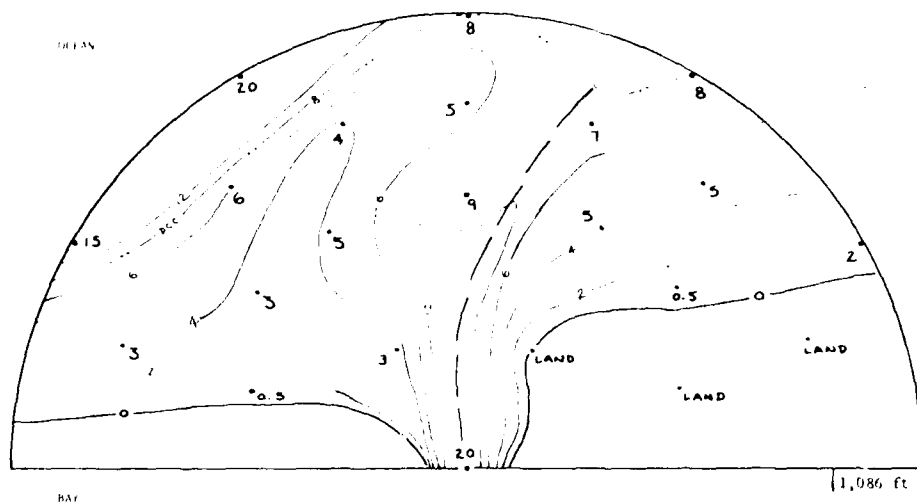
1937

CG56236

Hereford Inlet, N.J. 1937



Chincoteague Inlet, Va. 1962



Metomkin Inlet, Va. 1862

AD-A087 795

ARMY ENGINEER WATERWAYS EXPERIMENT STATION VICKSBURG MS

F/G 8/6

THE GEOMETRY OF SELECTED U.S. TIDAL INLETS.(U)

MAY 80 C L VINCENT, W D CORSON

UNCLASSIFIED

WES-GITI-20

NL

2 OF 2

ALIA

0-1000

0-1000

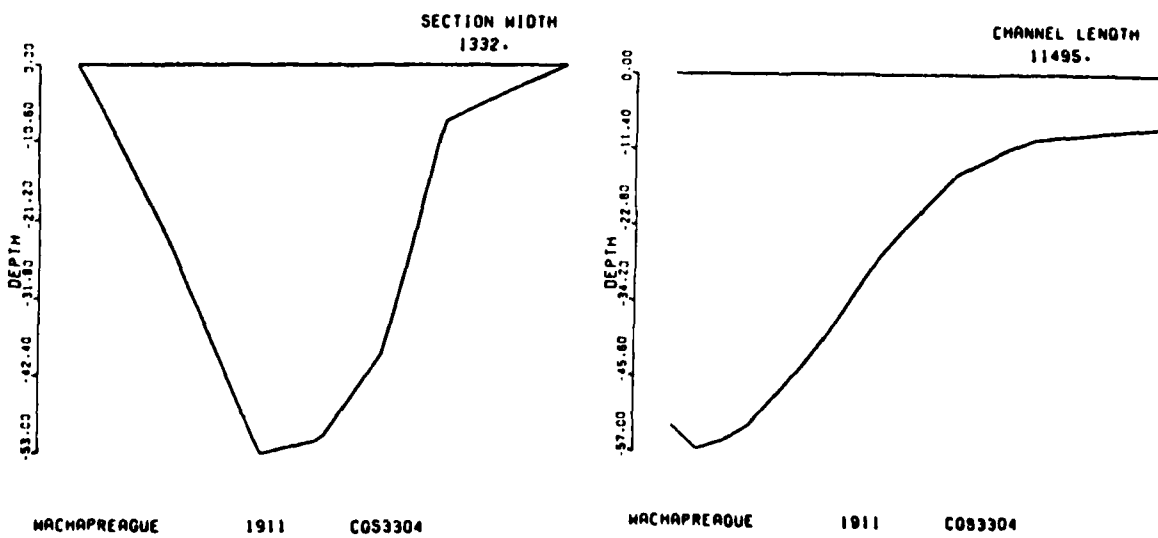
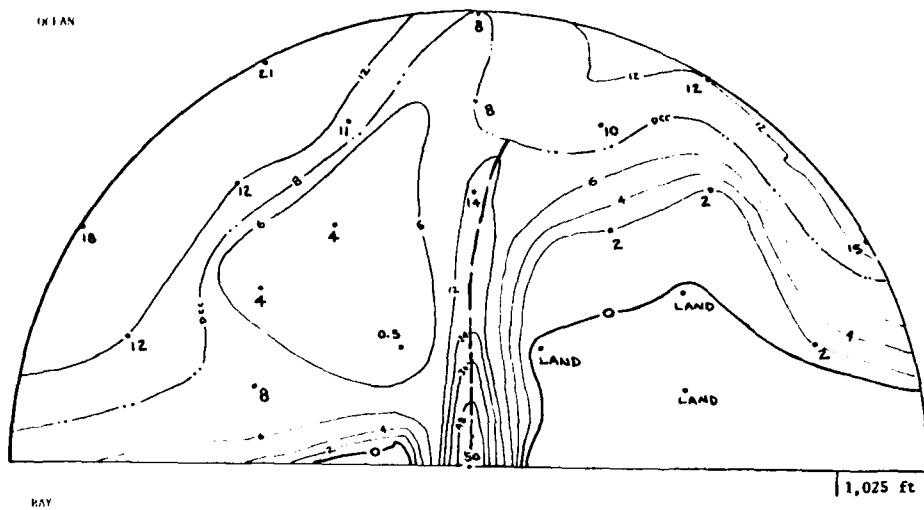
END

DATE

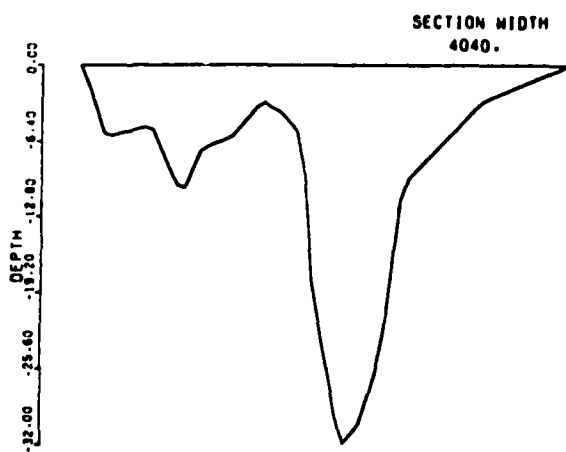
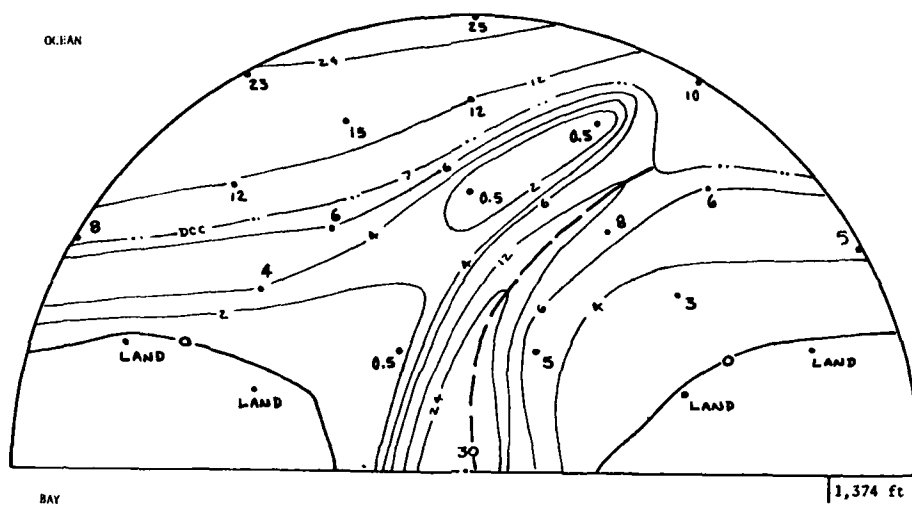
FILMED

8-80

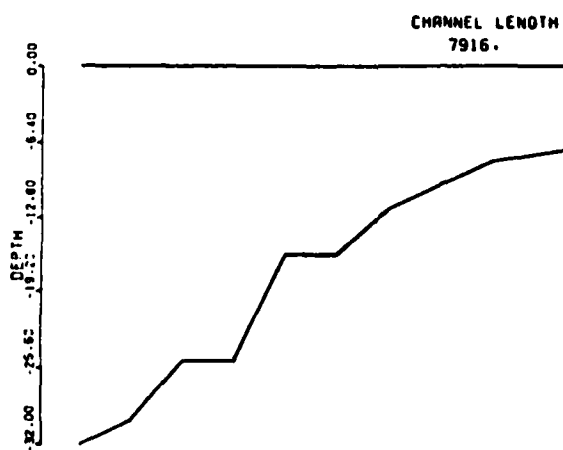
DTIC



Wachapreague Inlet, Va. 1911

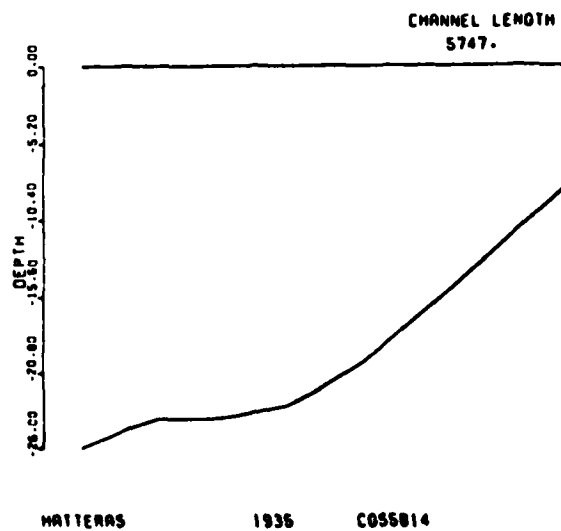
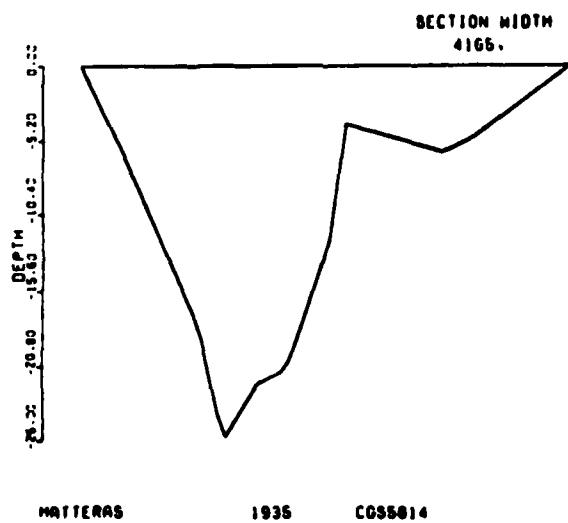
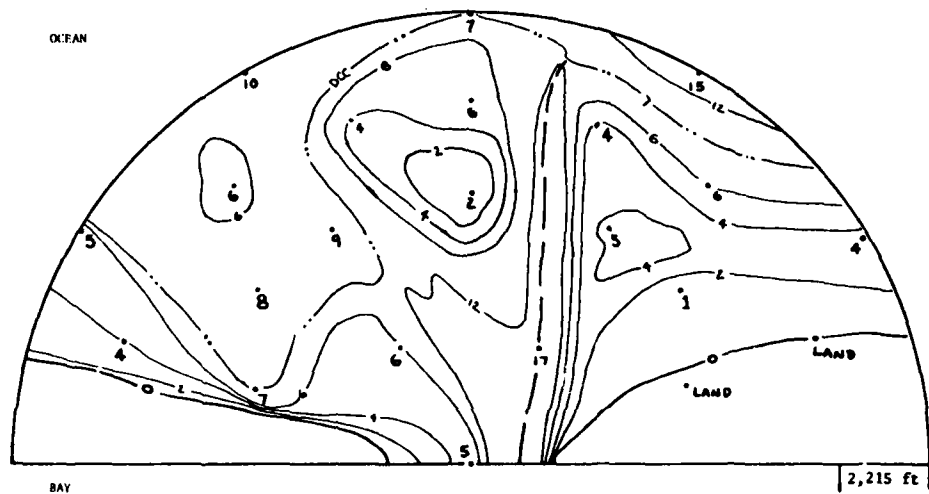


OREGON 1937 CGS6228

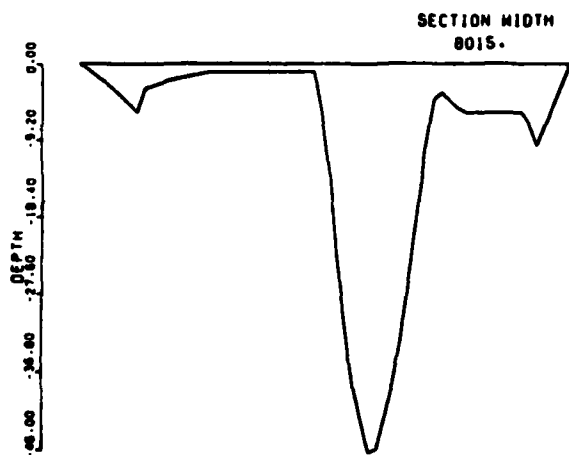
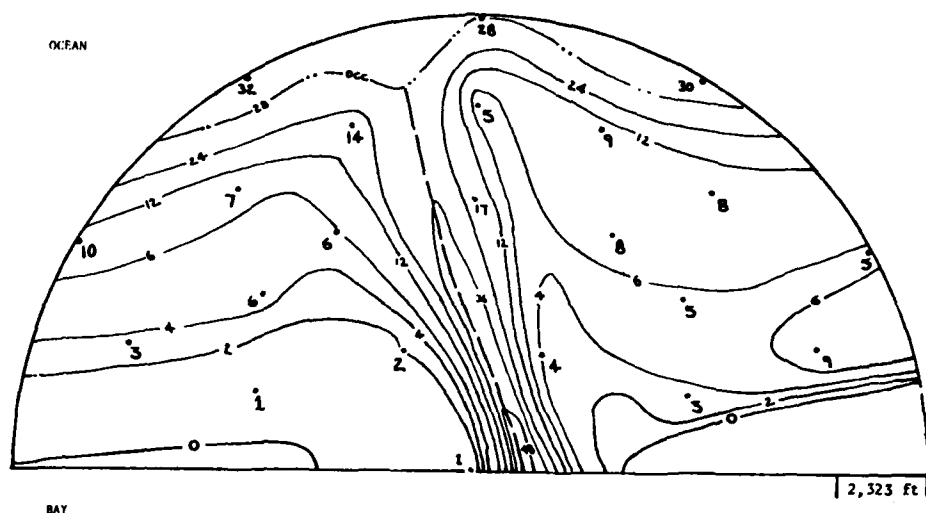


OREGON 1937 CGS6228

Oregon Inlet, N.C. 1937

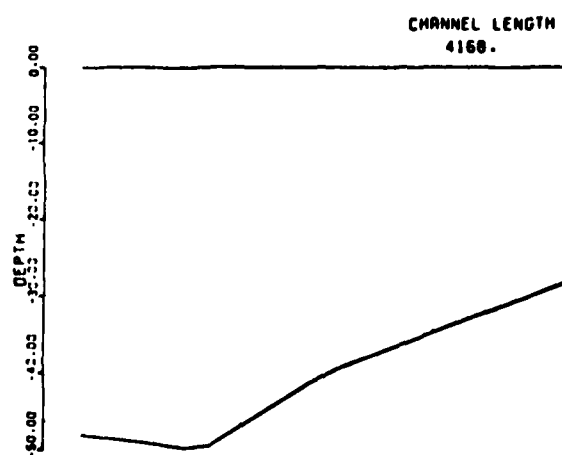


Hatteras Inlet, N.C. 1916



BEAUFORT

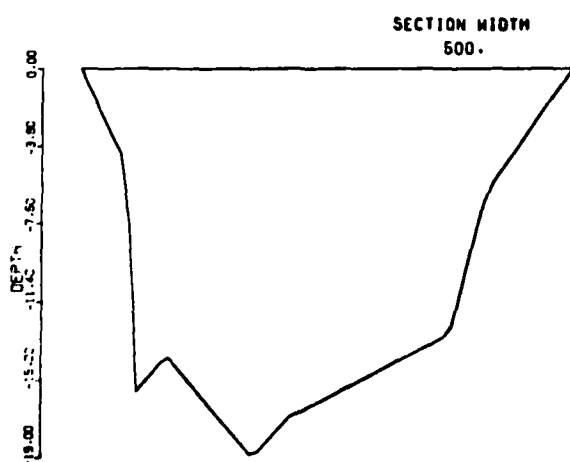
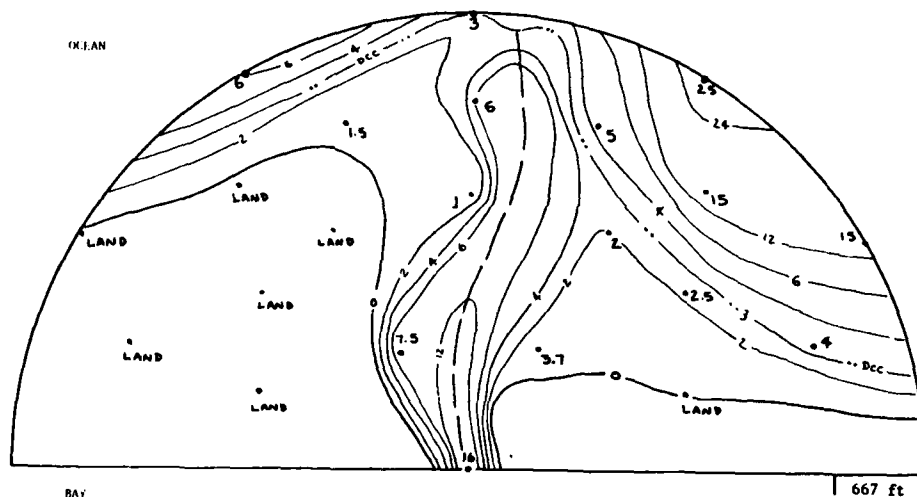
1952-53 COS7963



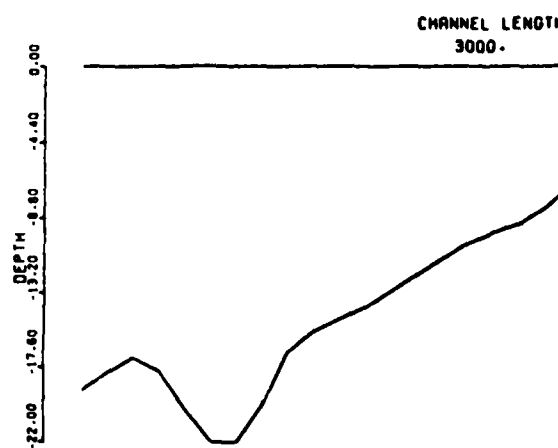
BEAUFORT

1952-1953 COS7963

Beaufort Inlet, N.C. 1952-53

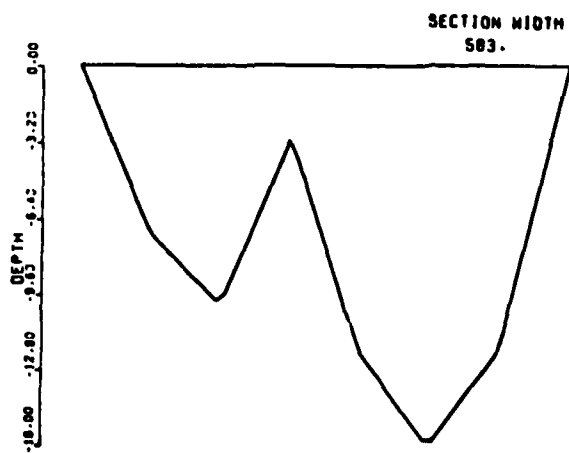
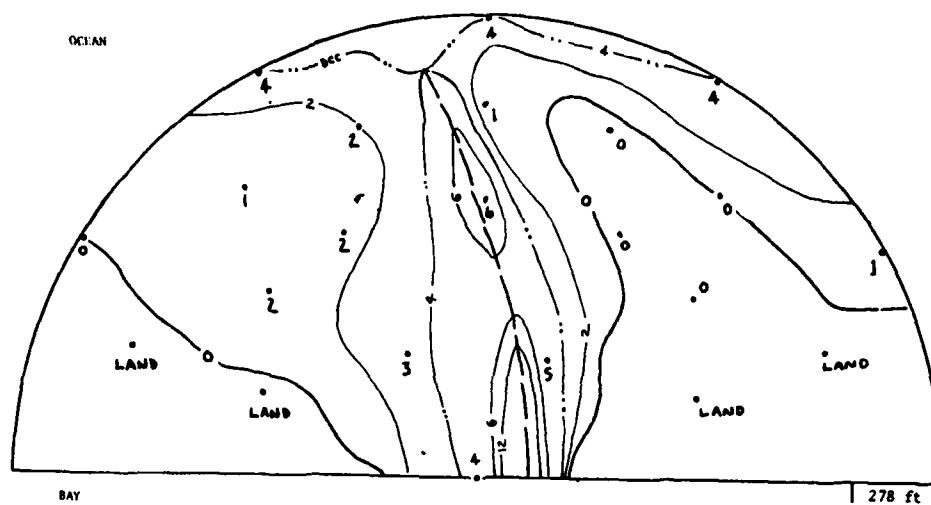


CAROLINA BEACH 1967 CBI 67-7

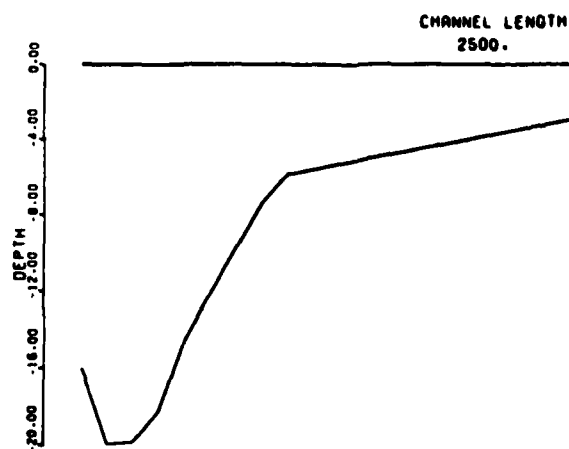


CAROLINA BEACH 1967 USRE CBI 67-7

Carolina Beach Inlet, N.C. 1967

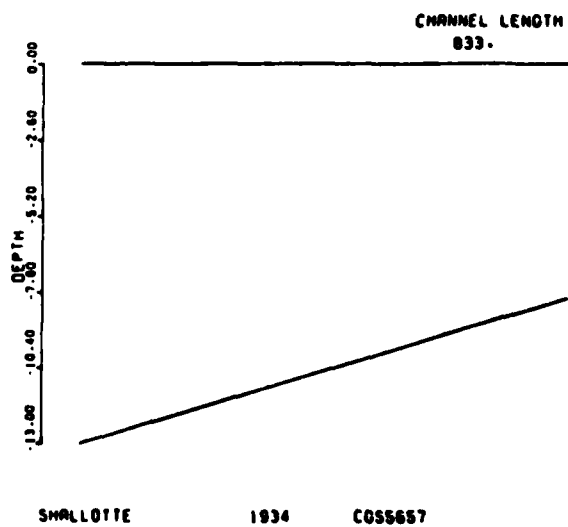
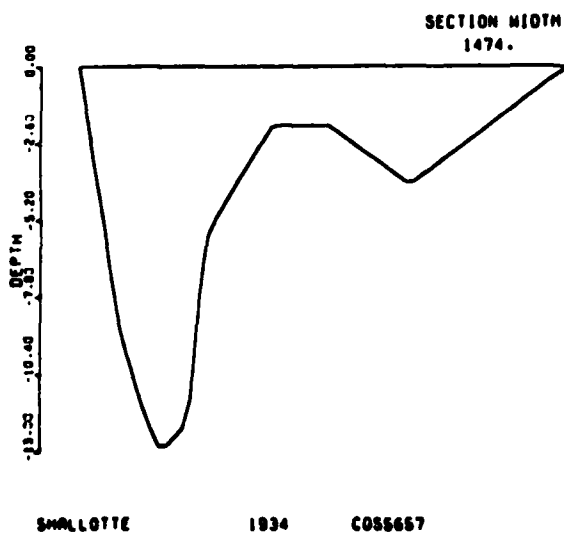
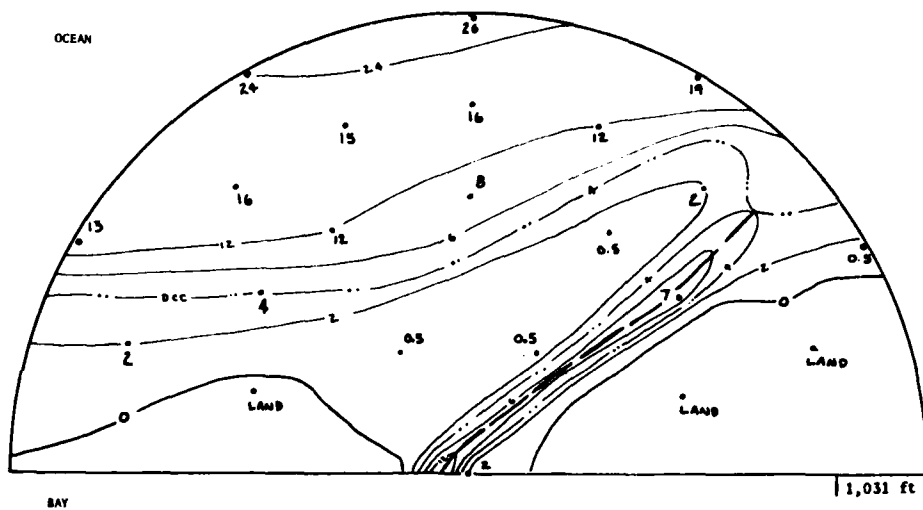


LOCKWOODS FOLLY 1924 CGS4450

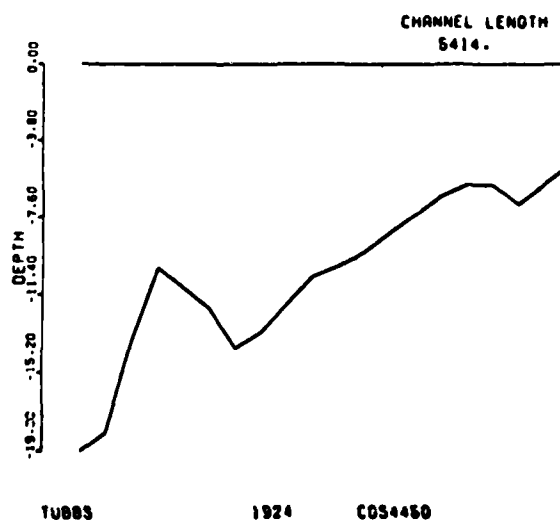
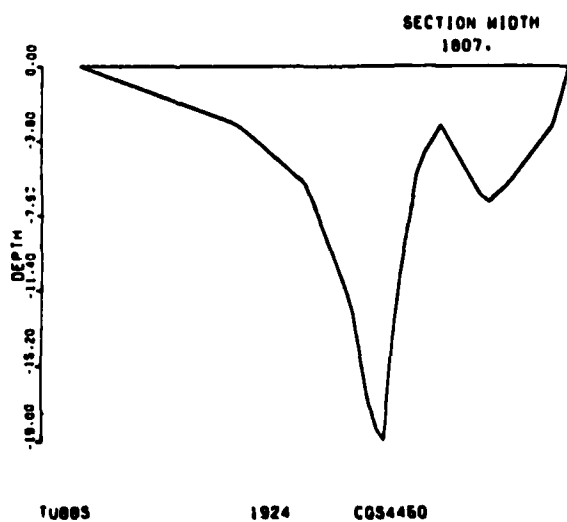
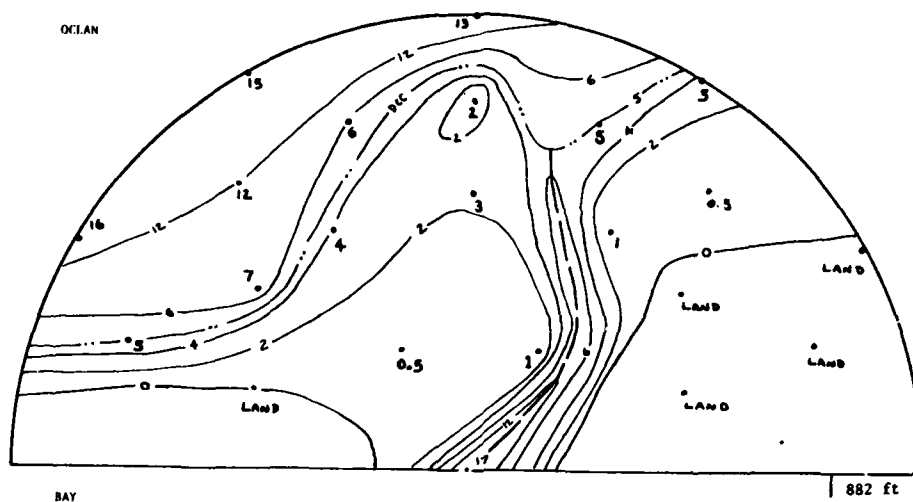


LOCKWOODS FOLLY 1924 CGS4450

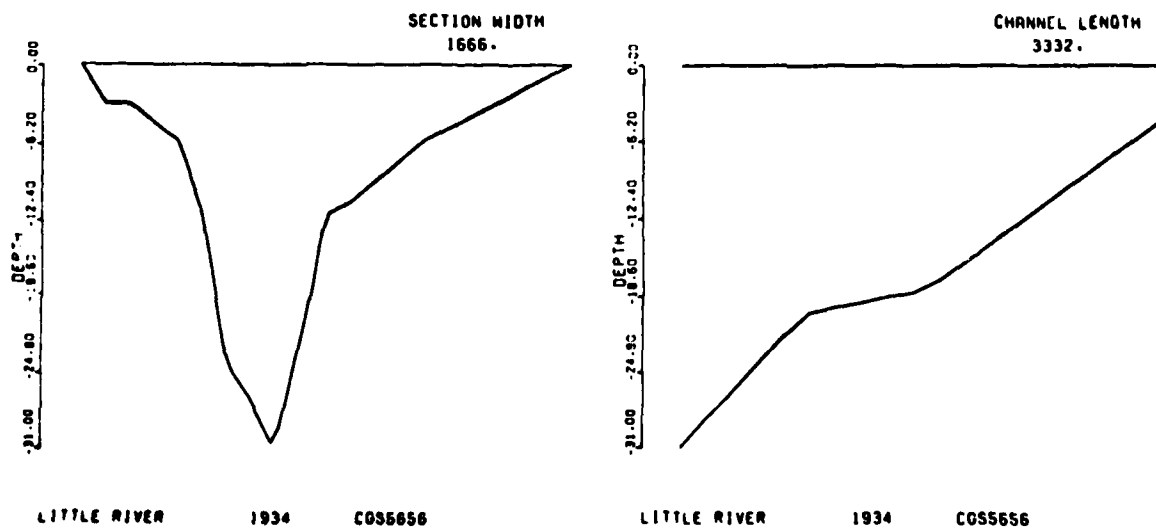
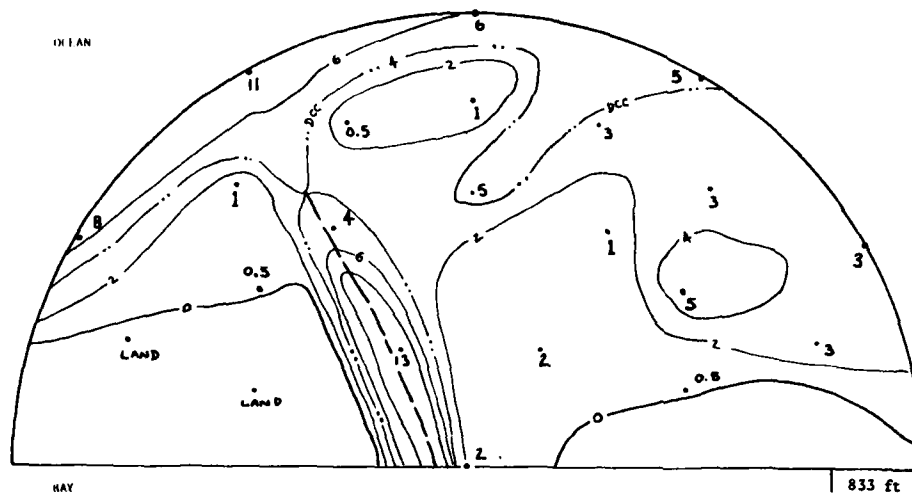
Lockwoods Folly Inlet, N.C. 1924



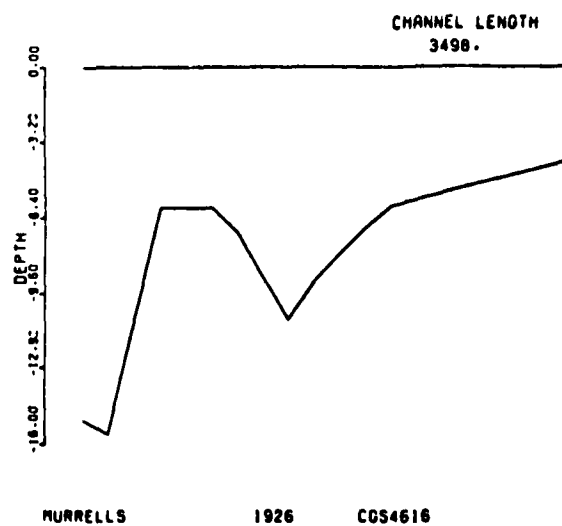
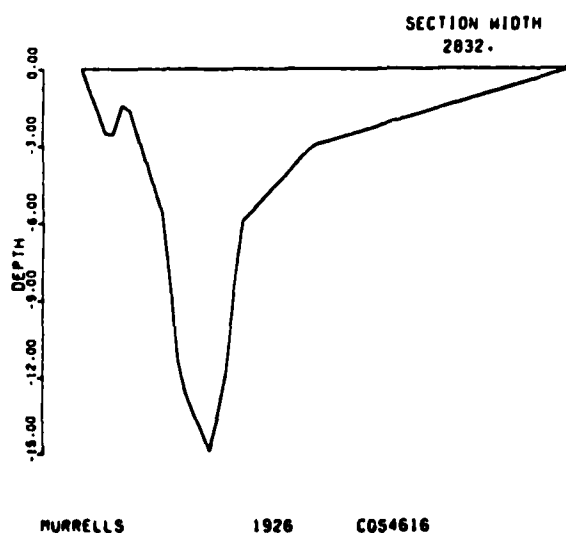
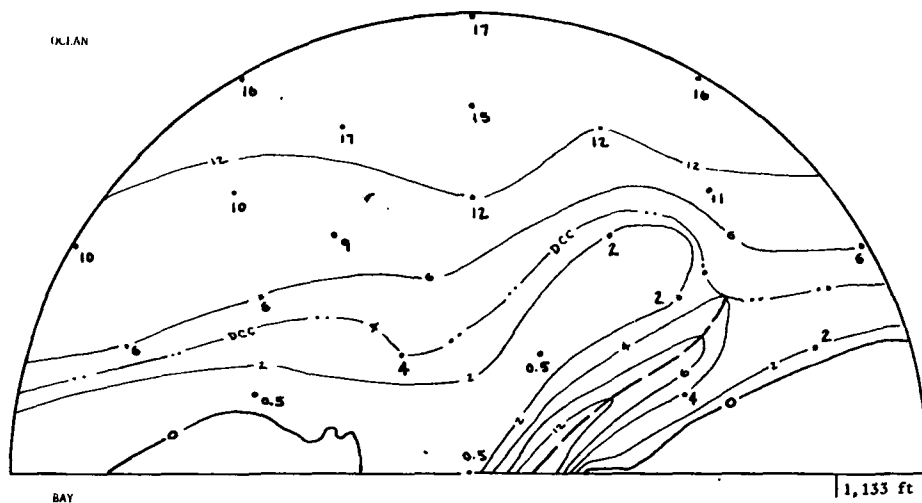
Shallotte Inlet, N.C. 1934



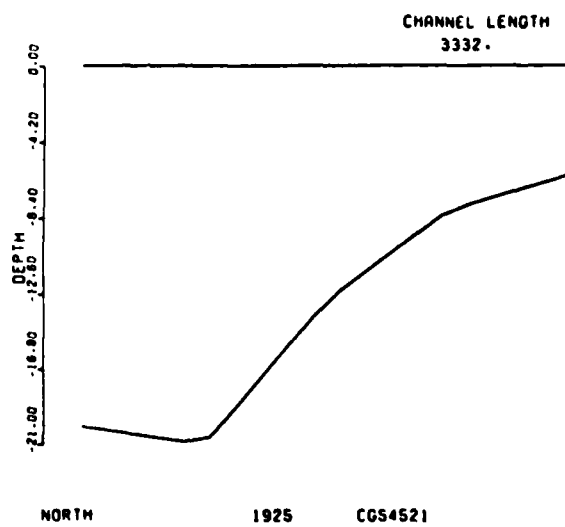
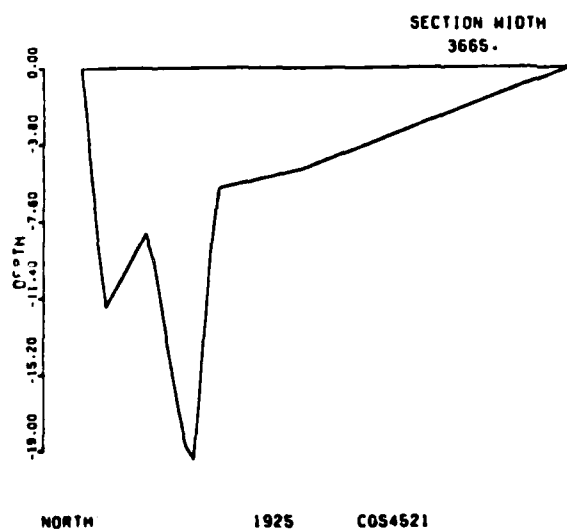
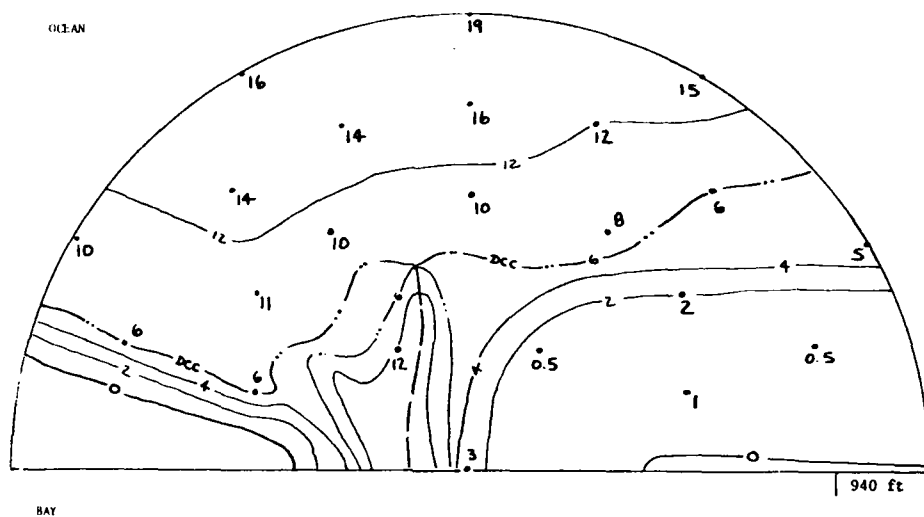
Tubbs Inlet, N.C. 1924



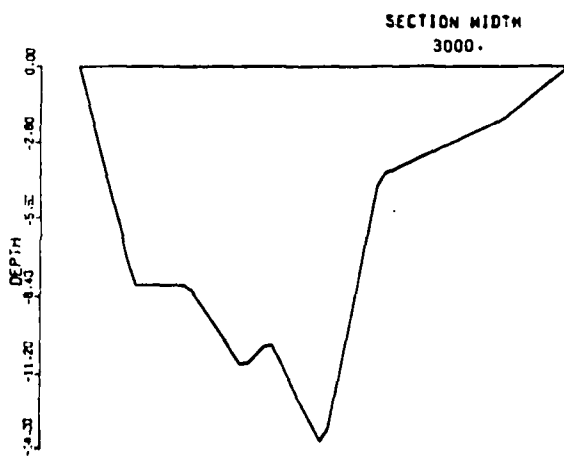
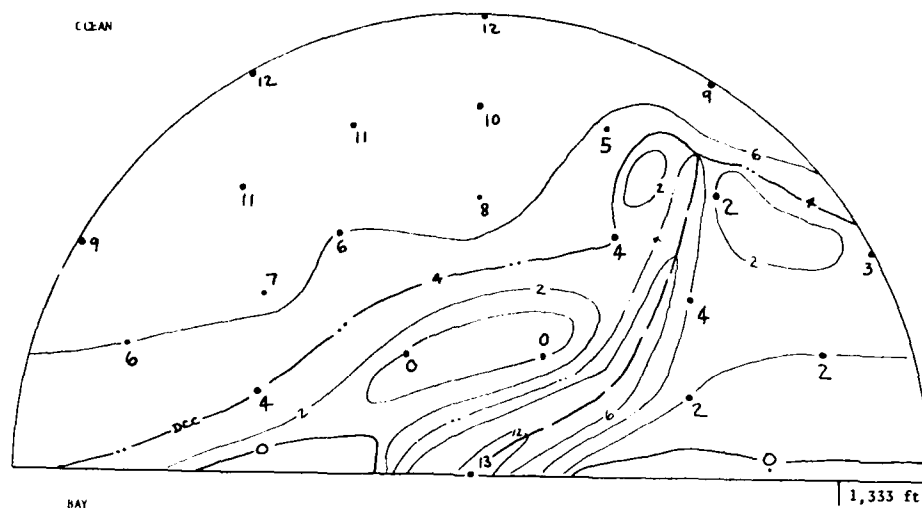
Little River Inlet, S.C. 1934



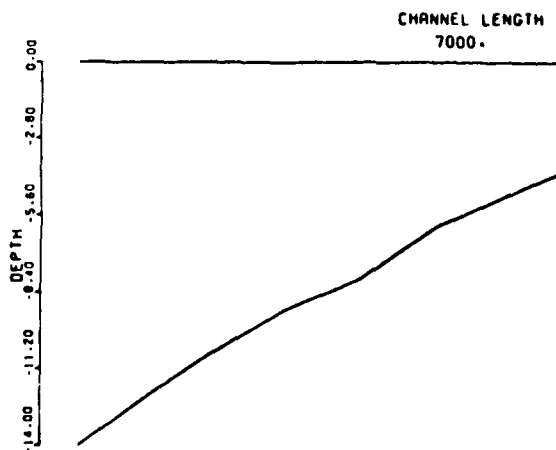
Murrells Inlet, S.C. 1974



North Inlet, S.C. 1925

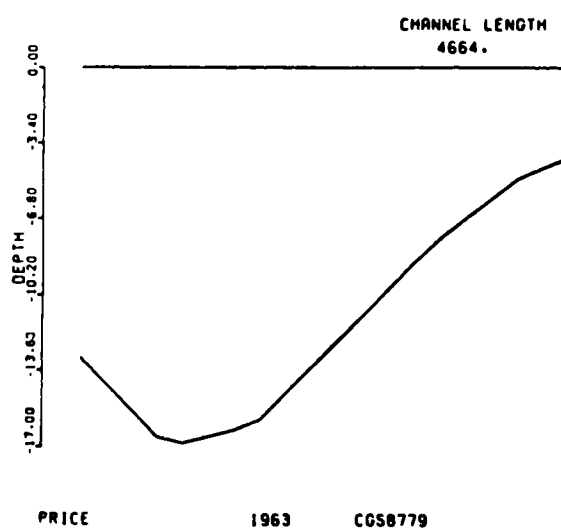
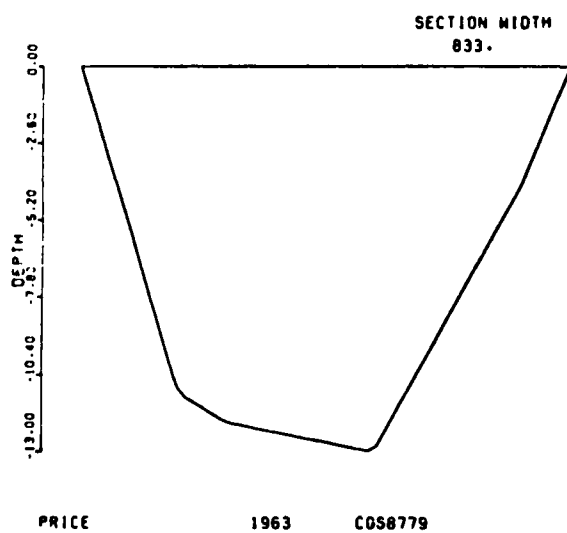
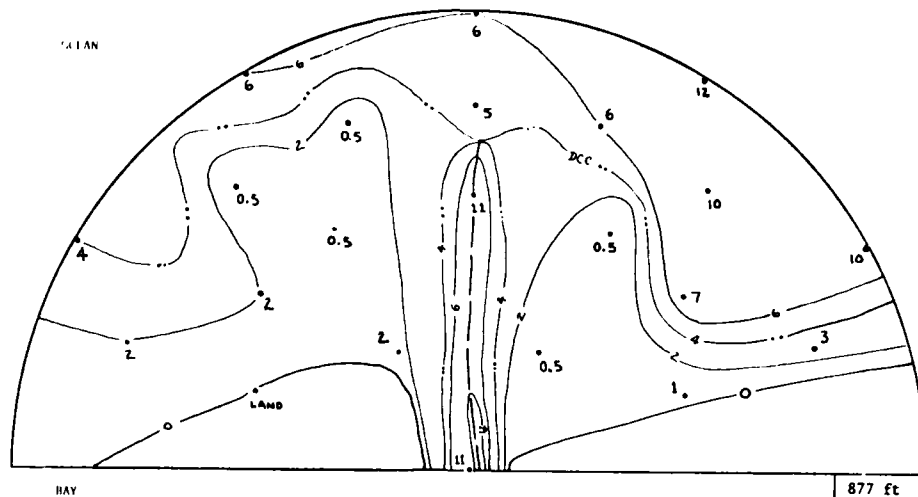


SOUTH SANTEE 1925 COS4522

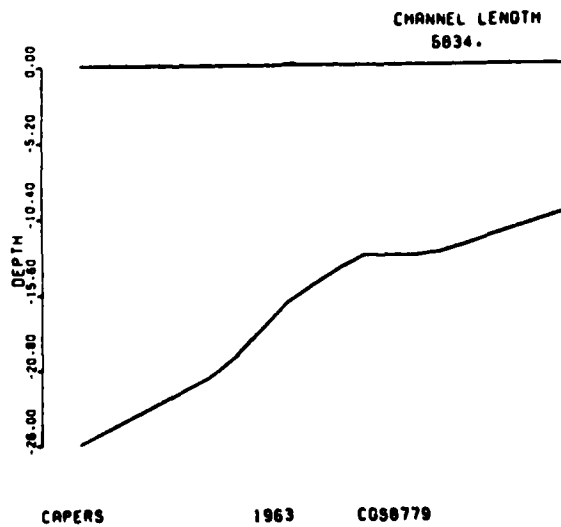
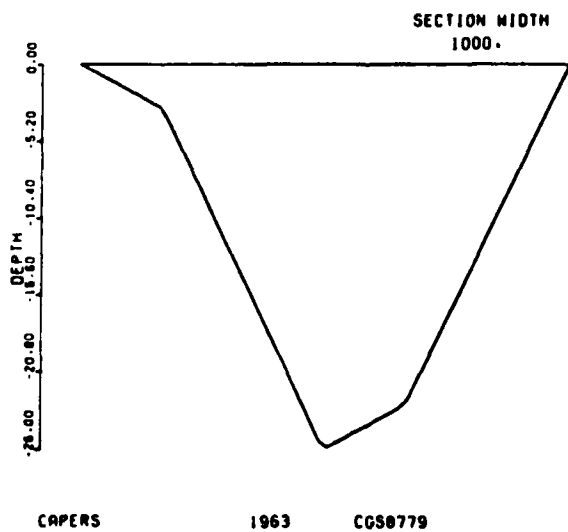
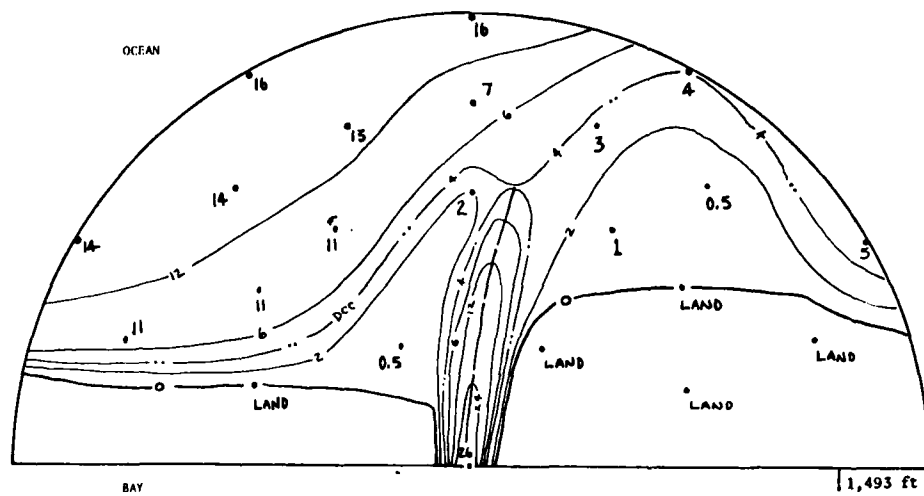


SOUTH SANTEE 1926 COS4622

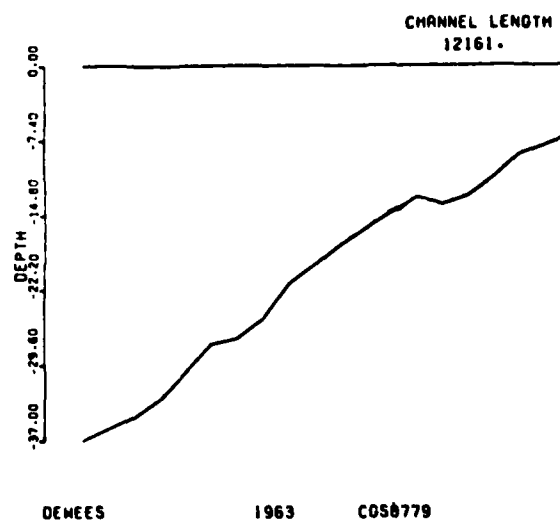
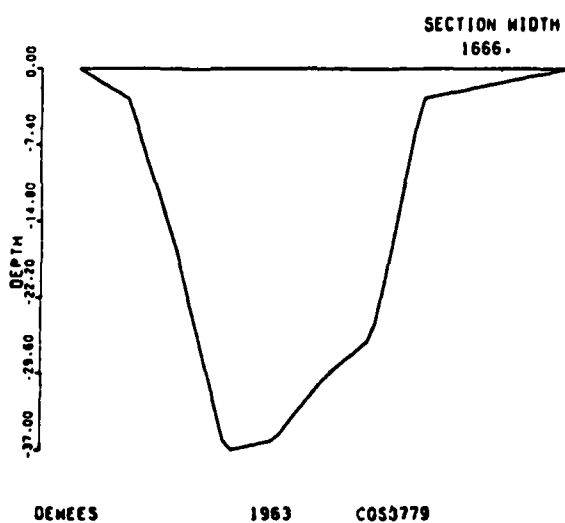
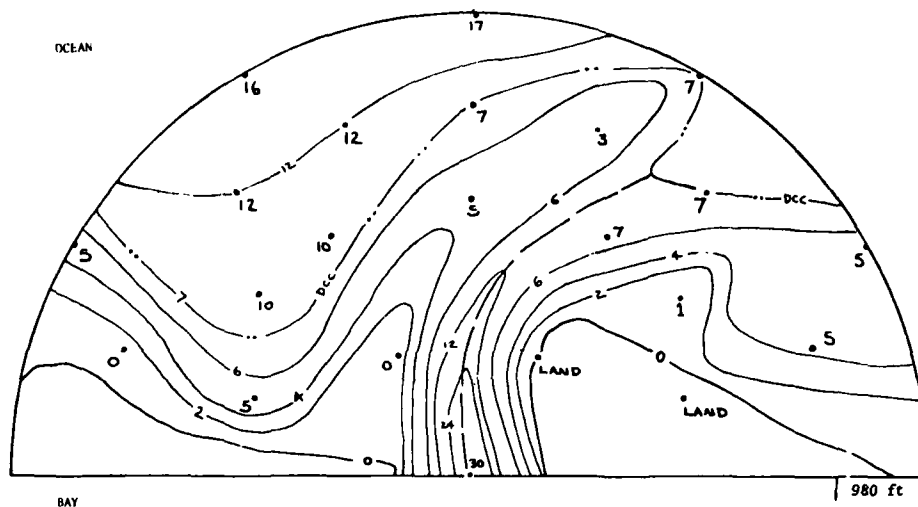
South Santee River Inlet, S.C. 1924



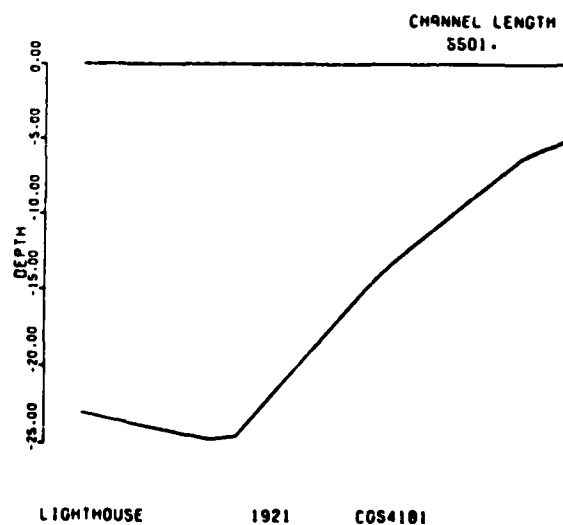
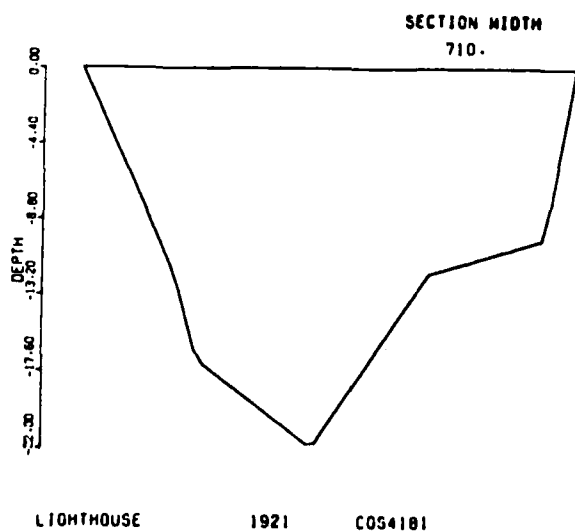
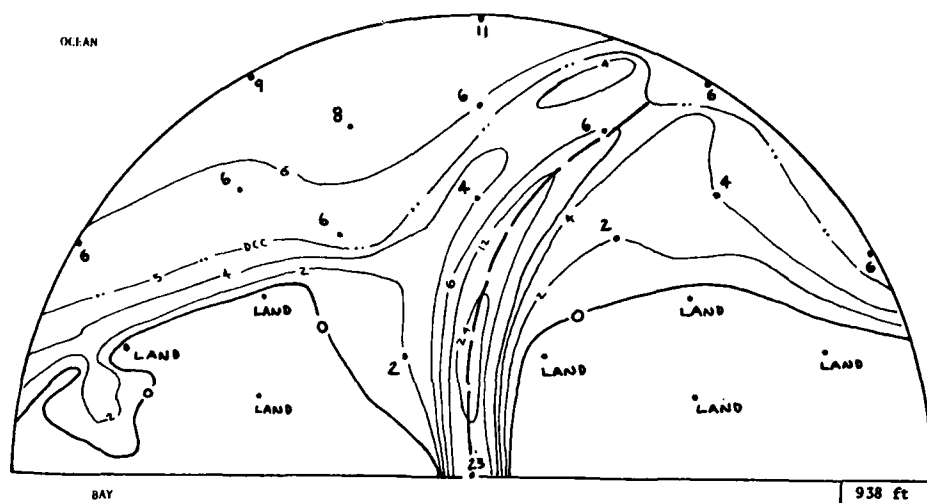
Price Inlet, S.C. 1963



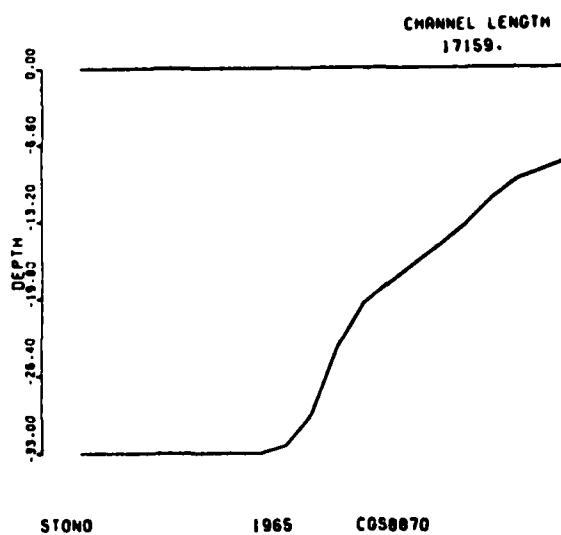
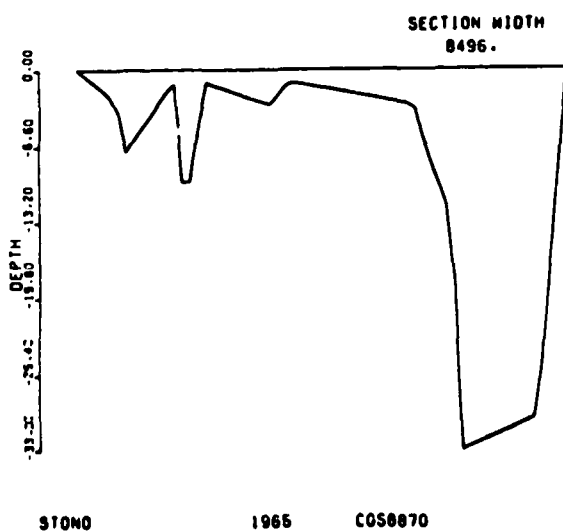
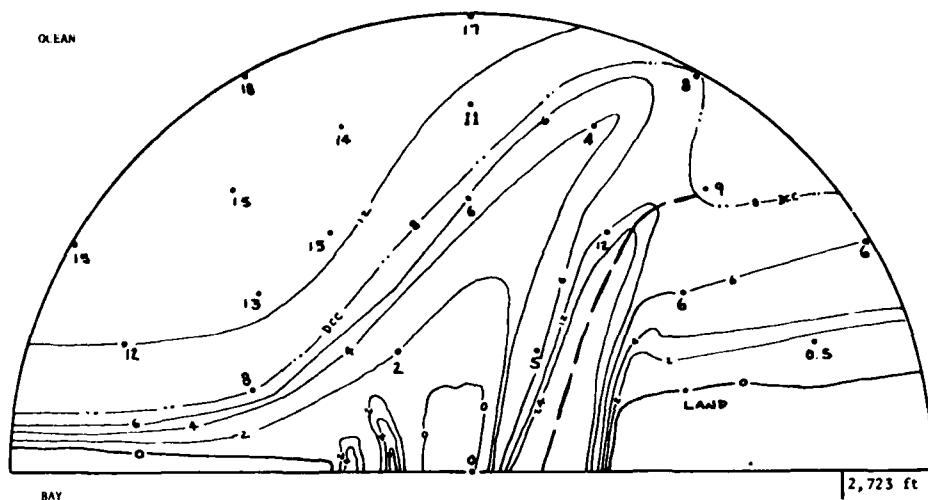
Capers Inlet, S.C. 1963



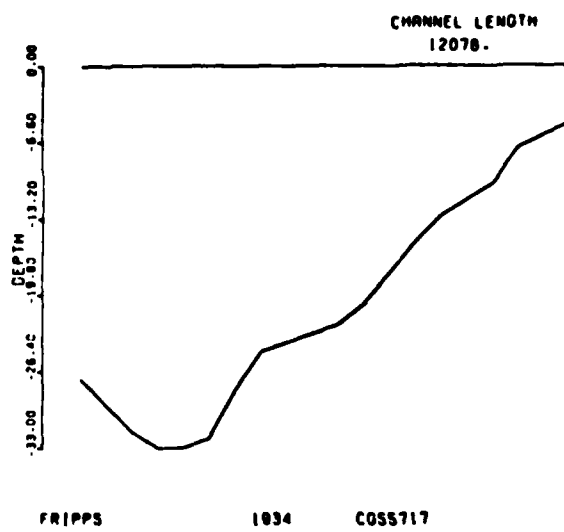
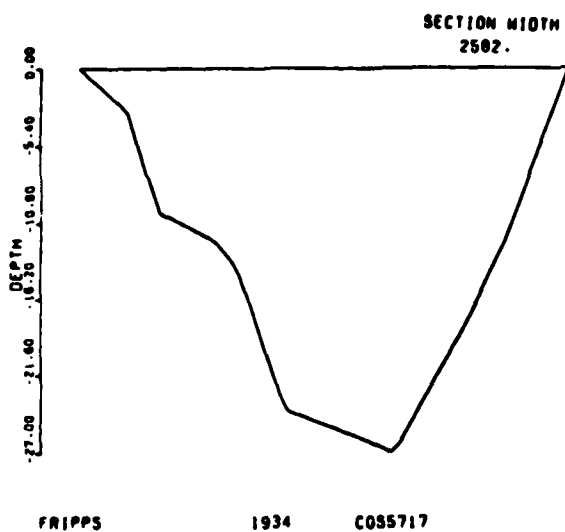
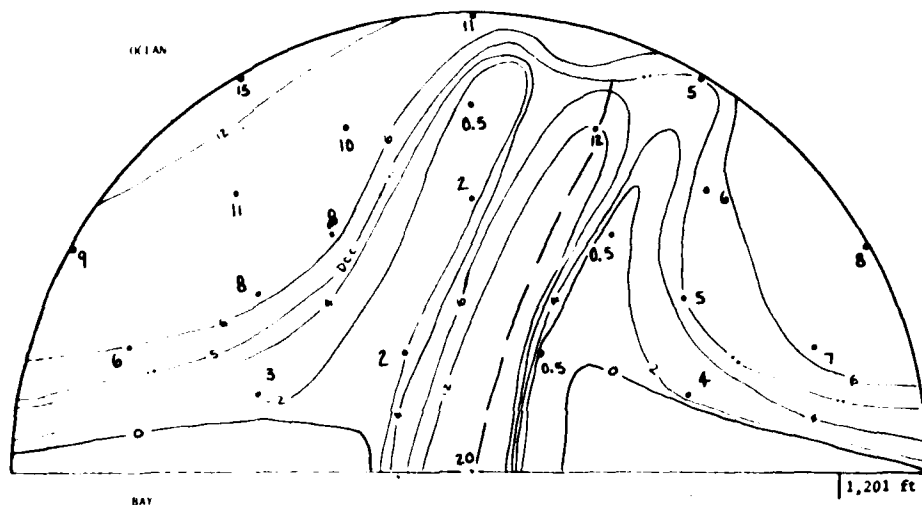
Dewees Inlet, S.C. 1963



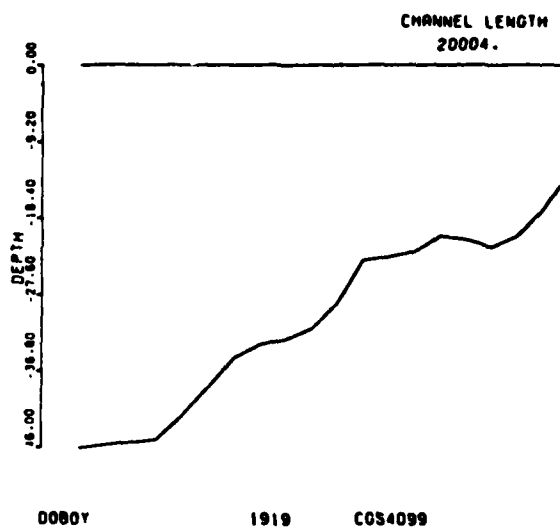
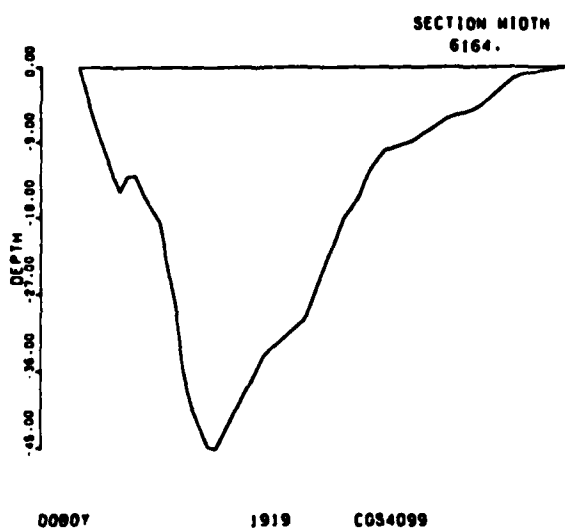
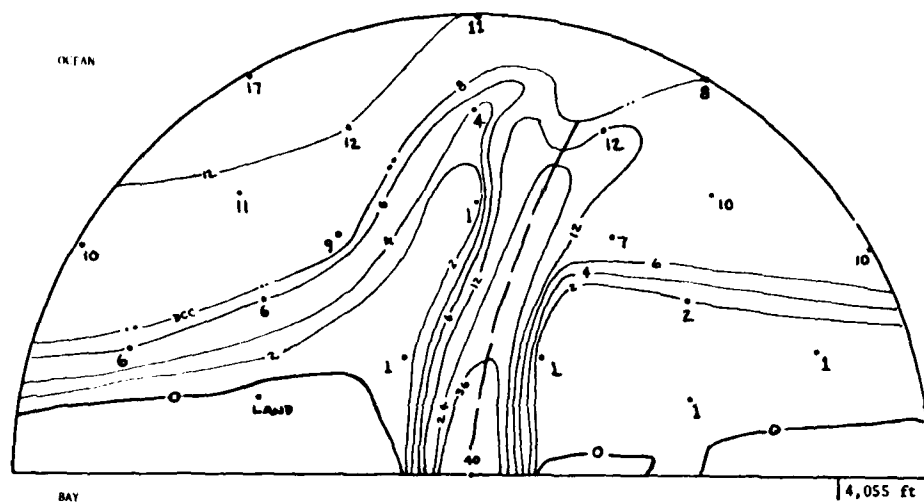
Lighthouse Inlet, S.C. 1921



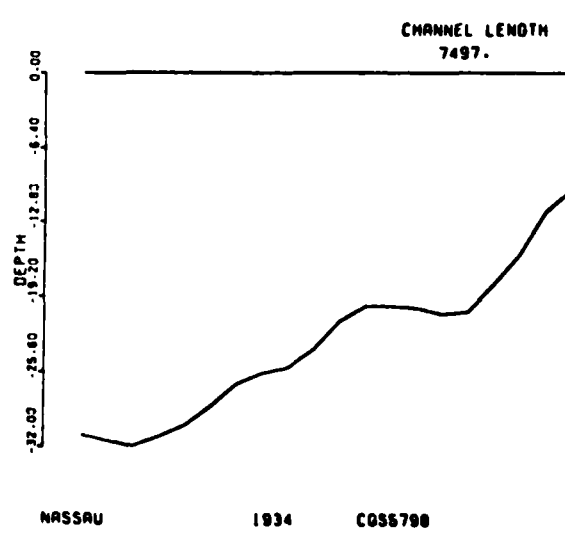
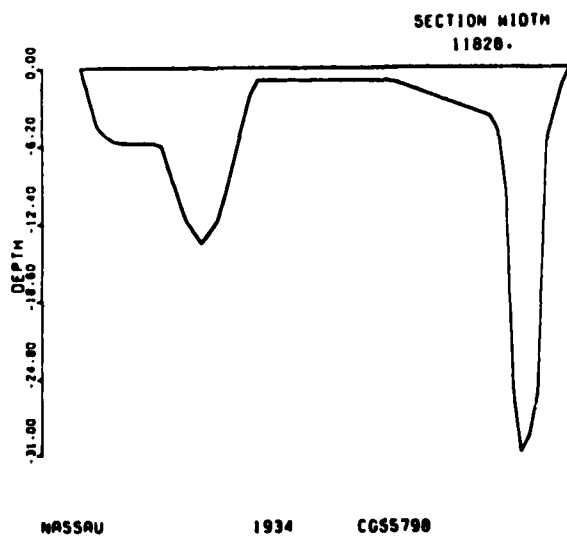
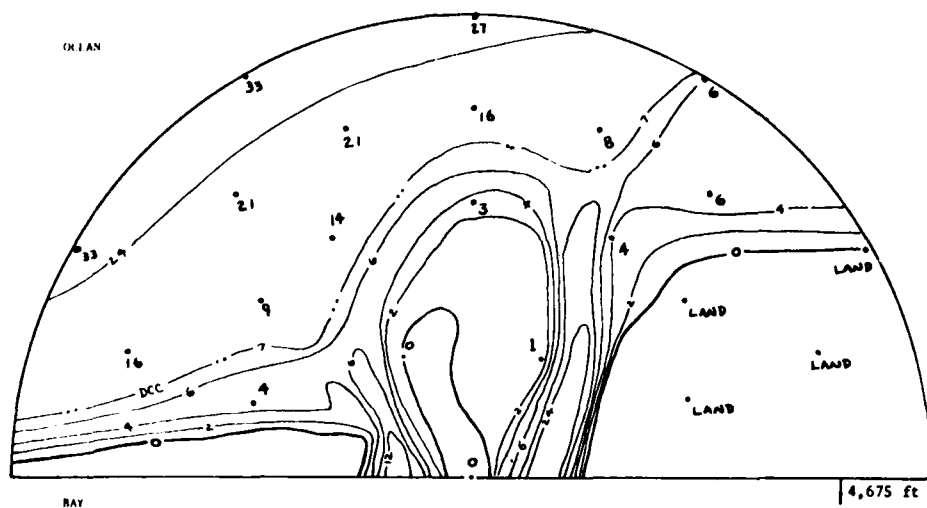
Stono Inlet, S.C. 1965



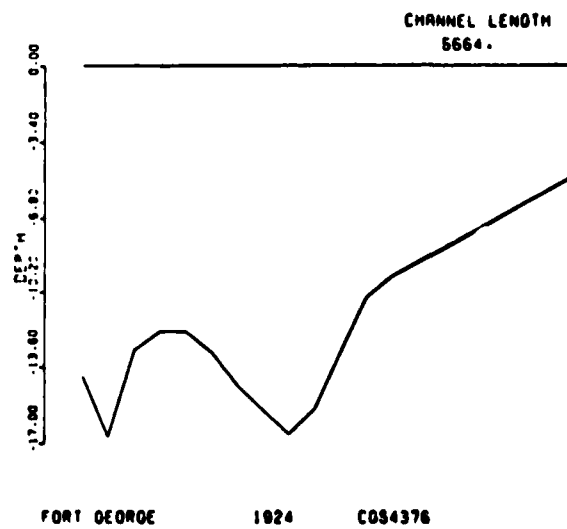
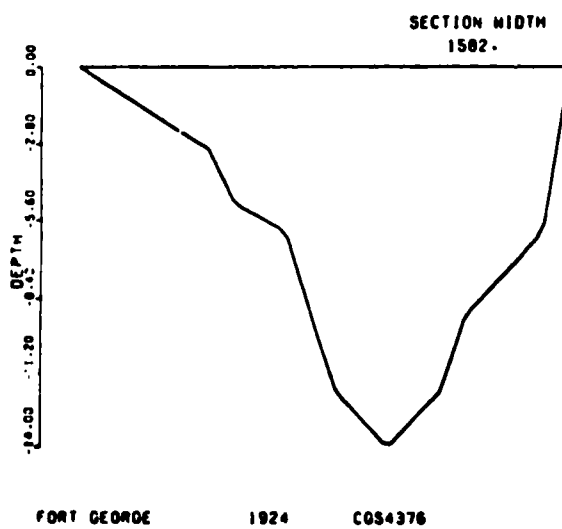
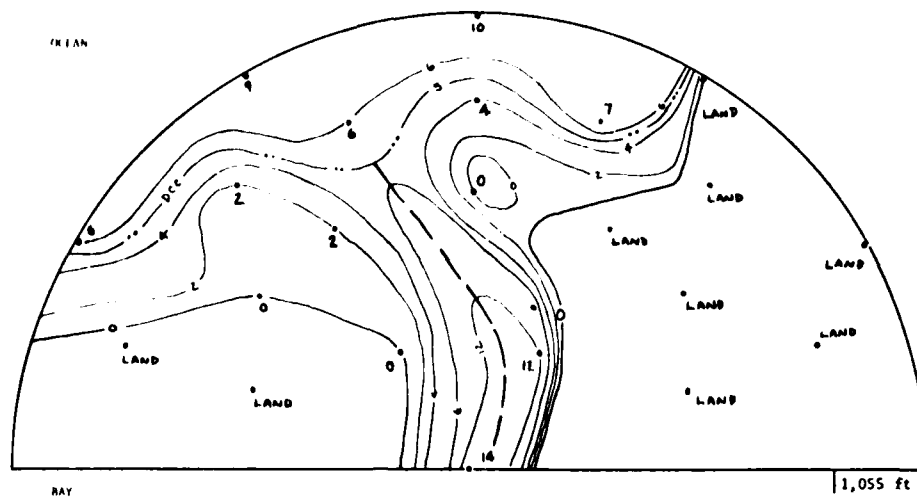
Fripps Inlet, S.C. 1972



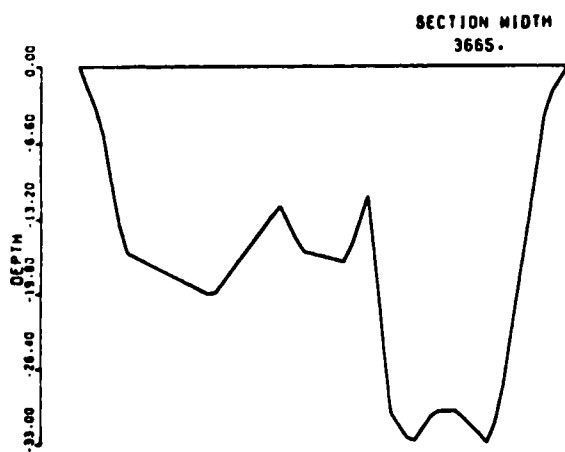
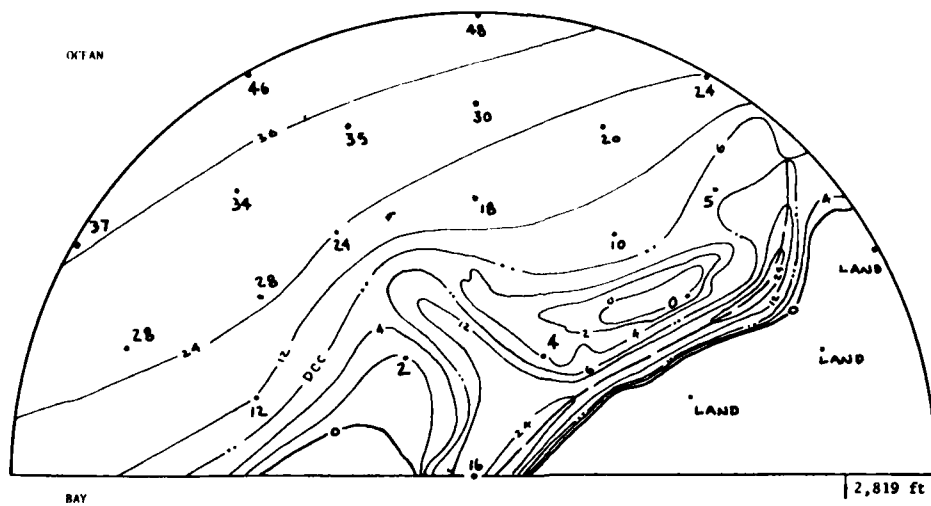
Doboy Inlet, Ga. 1972



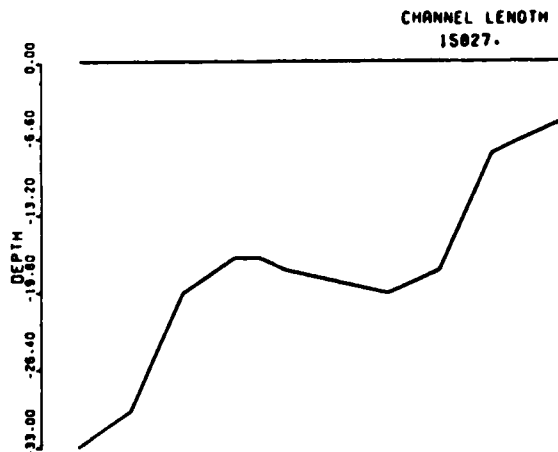
Nassau Sound, Fla. (E) 1871



Fort George Inlet, Fla. (E) 1924

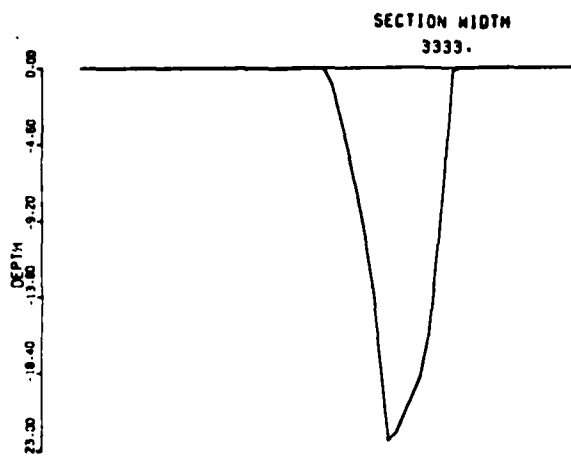
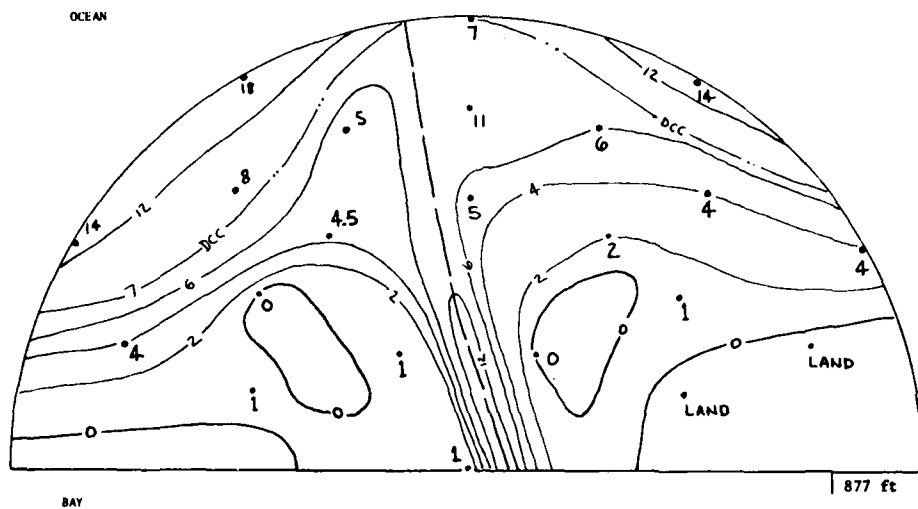


ST. AUGUSTINE 1924 COS4435

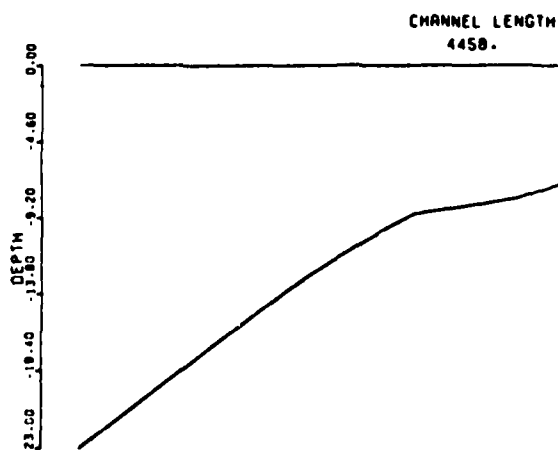


ST. AUGUSTINE 1924 COS4435

St. Augustine Inlet, Fla. (E) 1924

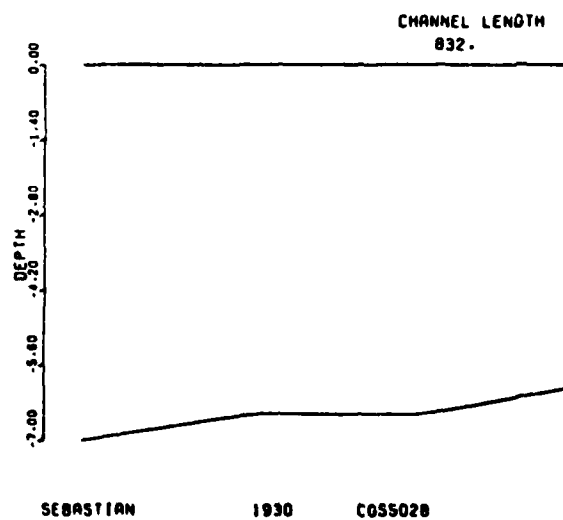
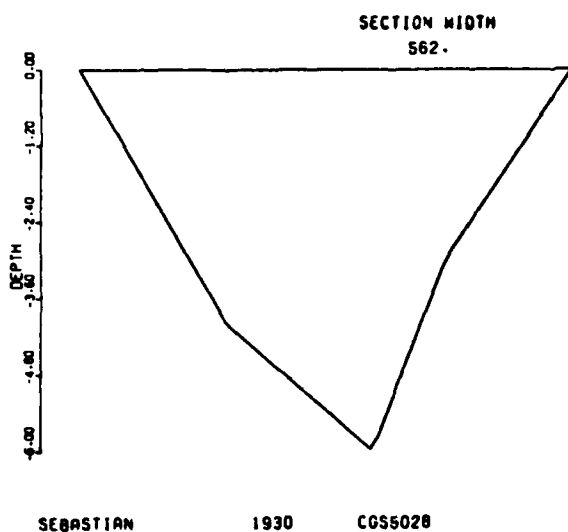
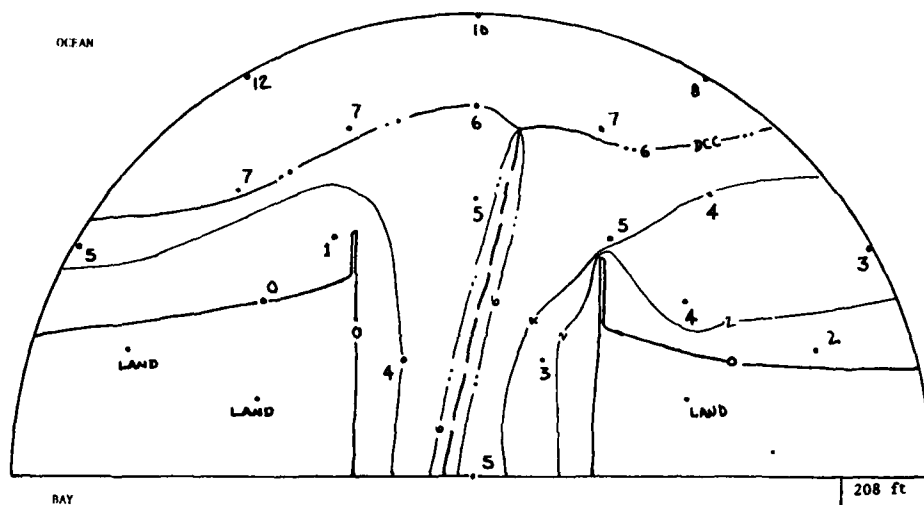


PONCE DE LEON 1926 C054478

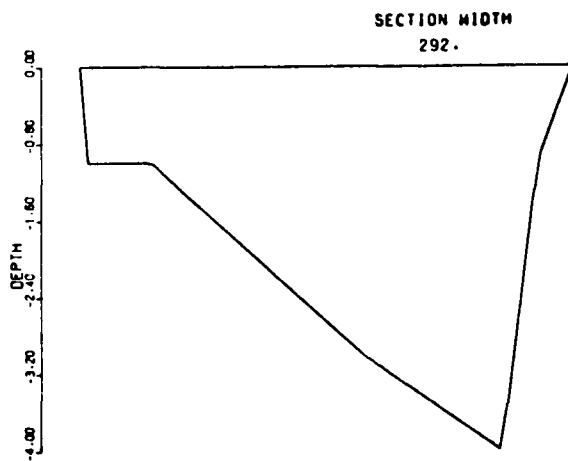
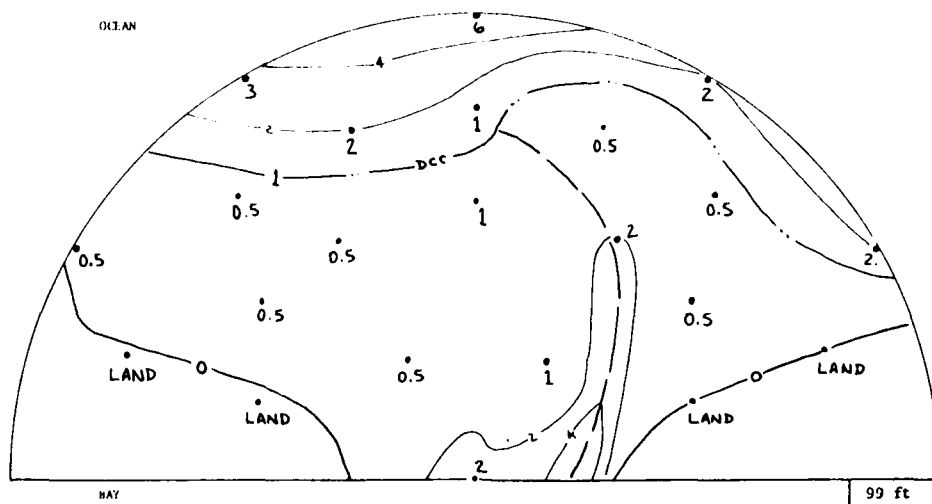


PONCE DE LEON 1925 C054478

Ponce de Leon Inlet, Fla. (E) 1925



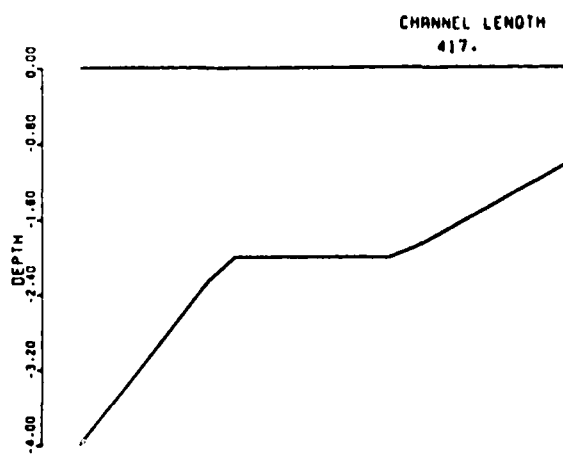
Sebastian Inlet, Fla. (E) 1930



BOCA RATON

1929

CG55015

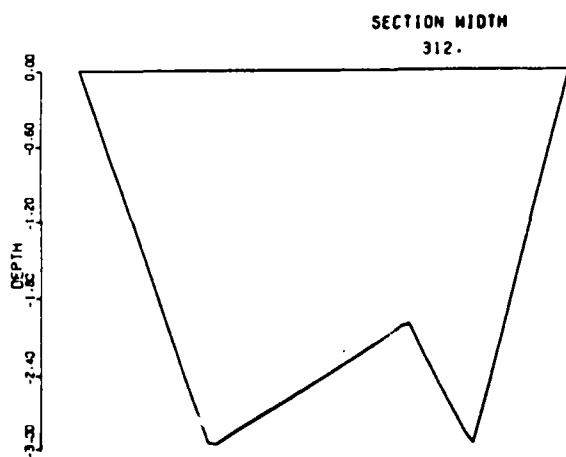
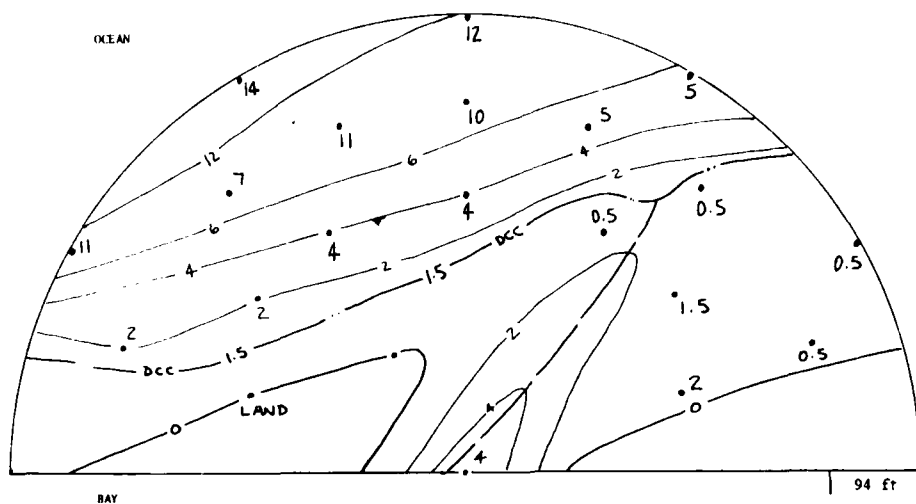


BOCA RATON

1929

CG55015

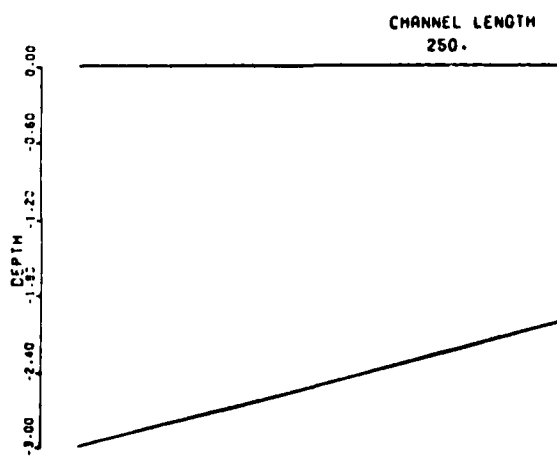
Boca Raton Inlet, Fla. (E) 1929



HILLSBORO

1929

CG55015

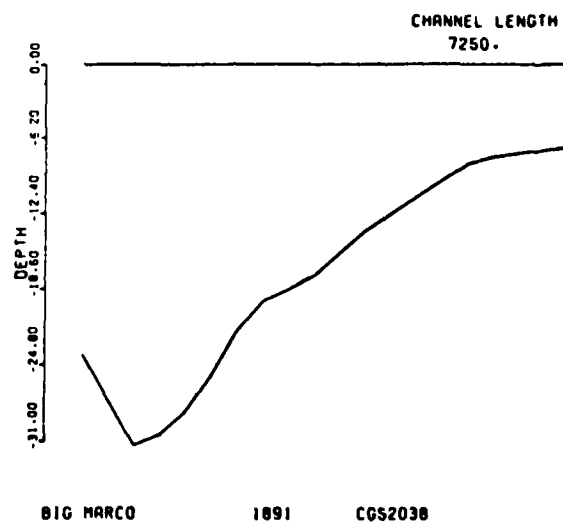
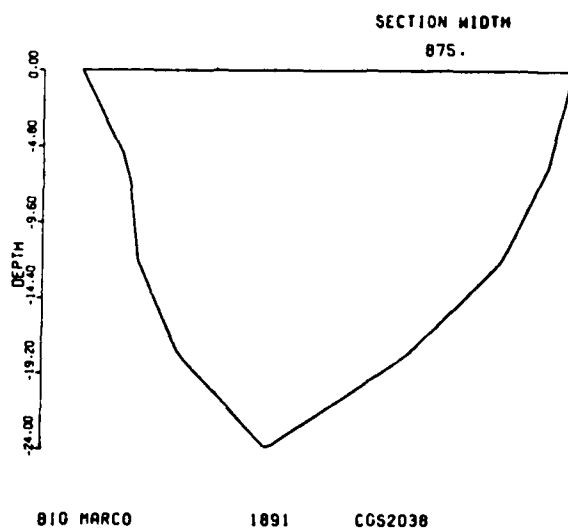
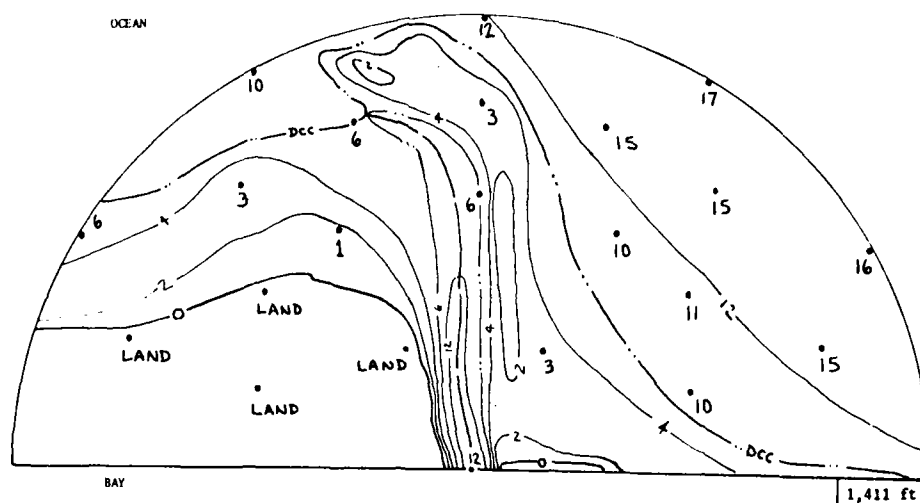


HILLSBORO

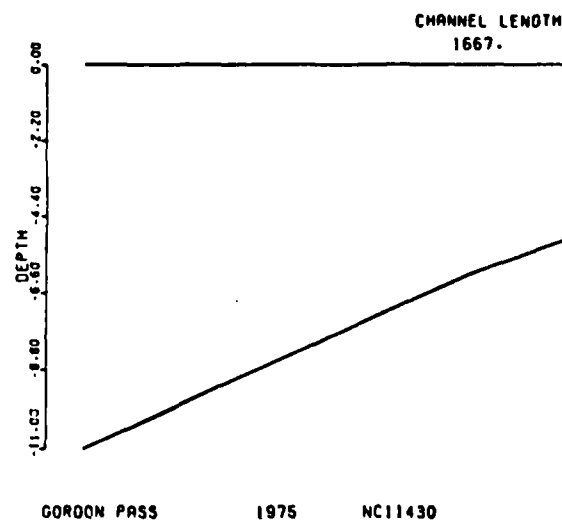
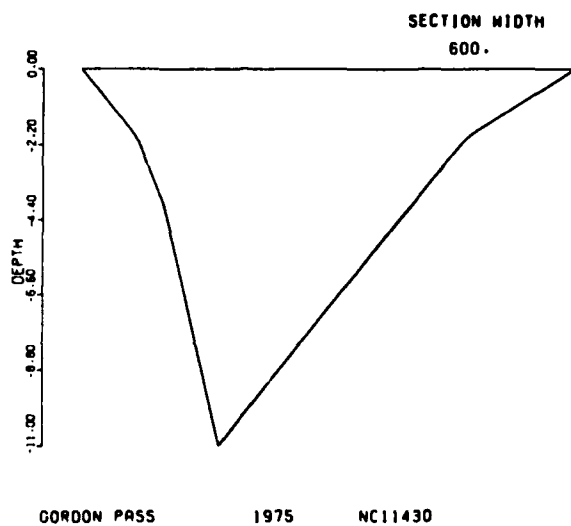
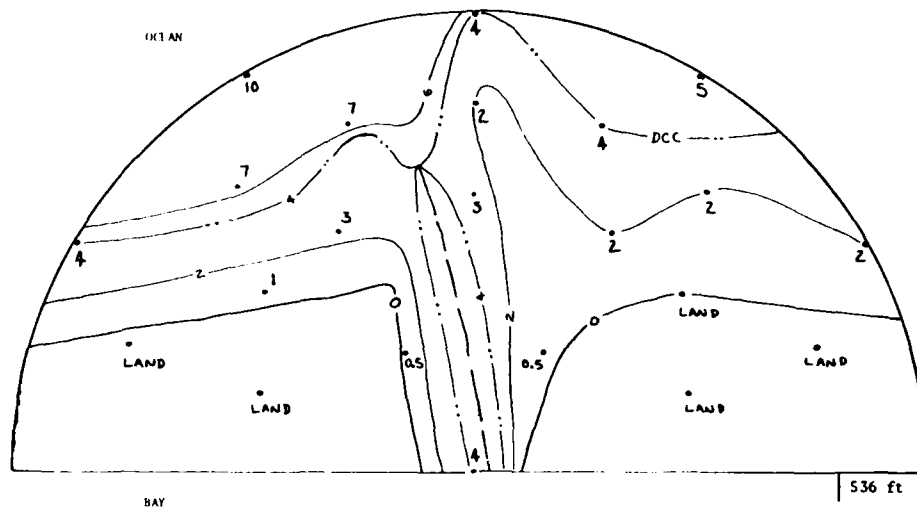
1929

CG55015

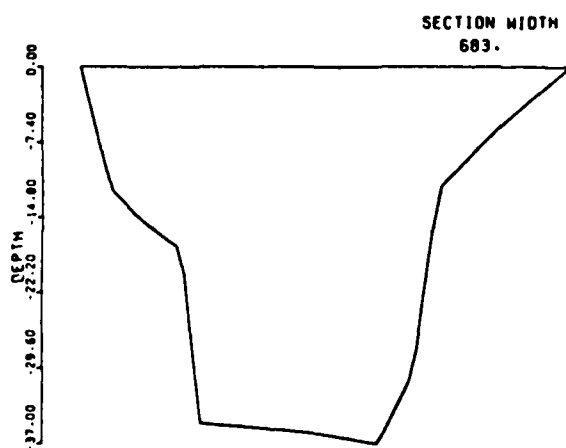
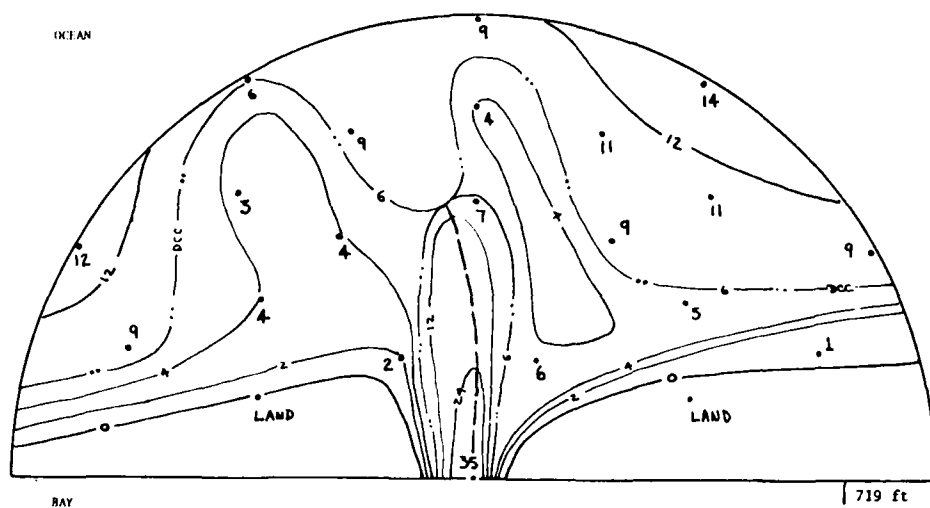
Hillsboro Inlet, Fla. (E) 1929



Big Marco Pass, Fla. (W) 1970

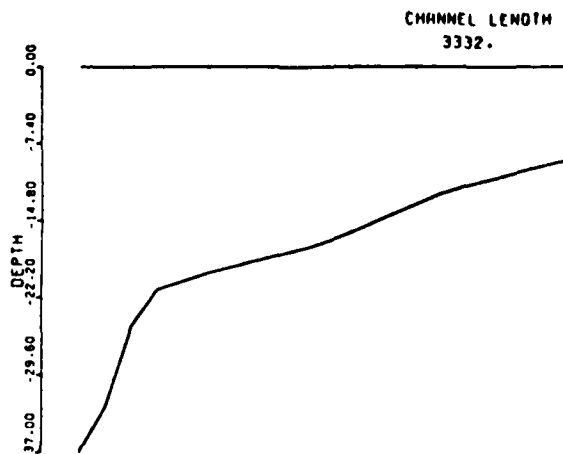


Gordon Pass, Fla. (W) 1970



REDFISH

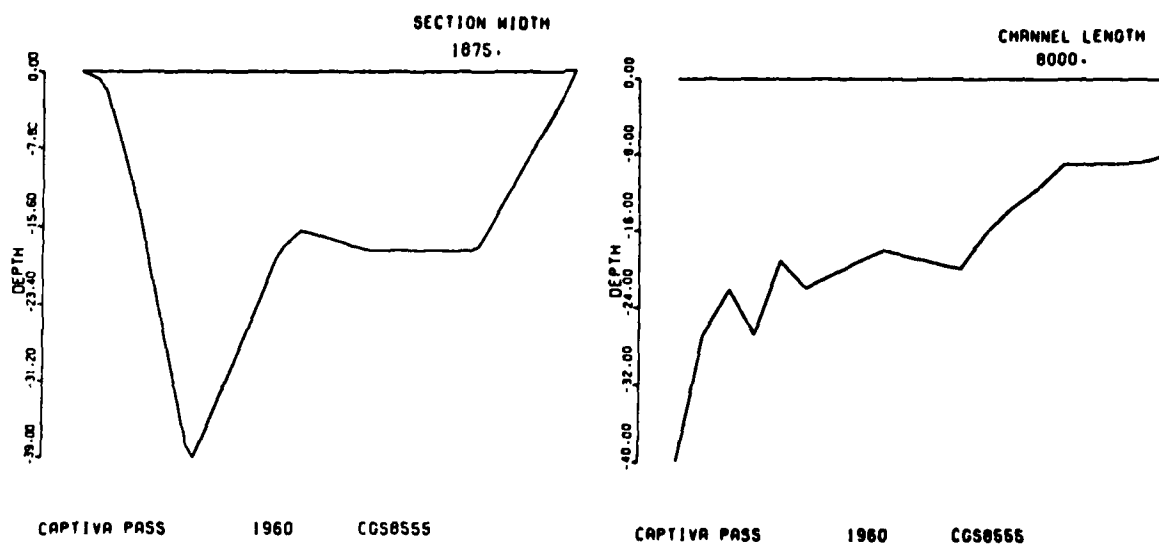
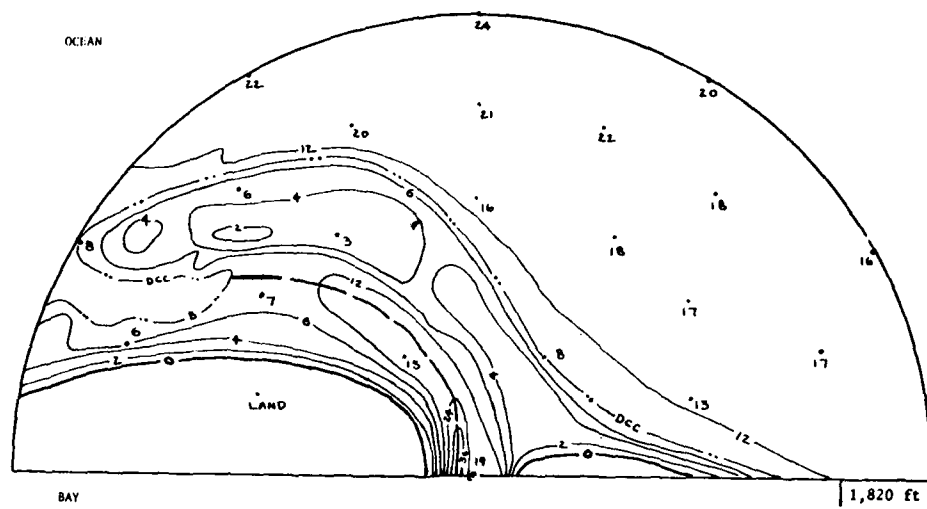
1960-1961 C050590



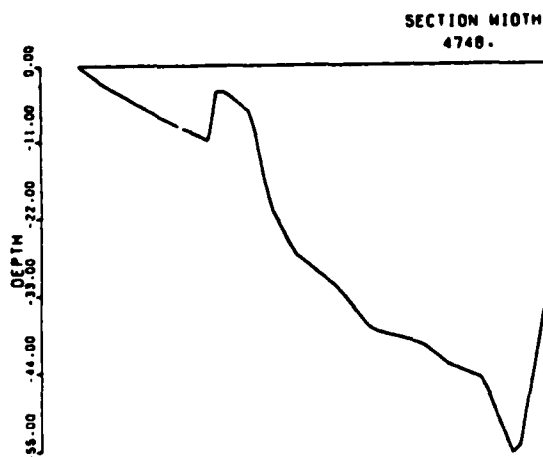
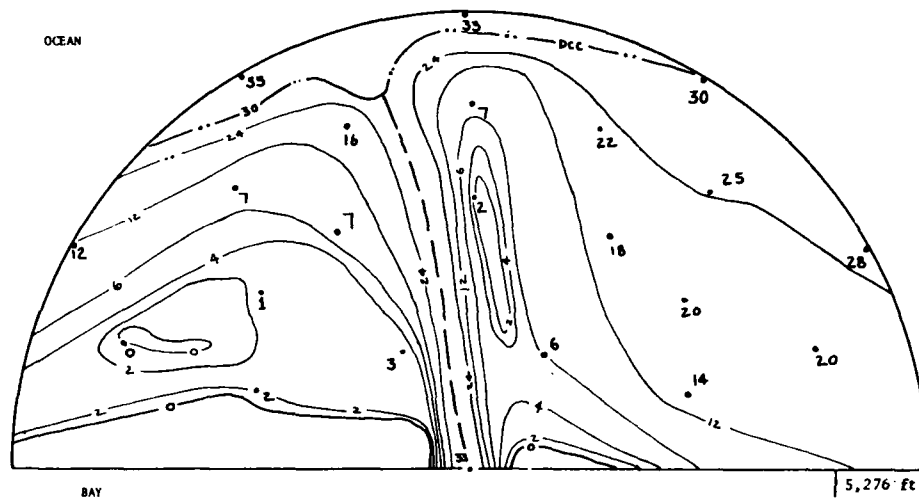
REDFISH

1960-1961 C050590

Redfish Pass, Fla. (W) 1960-61

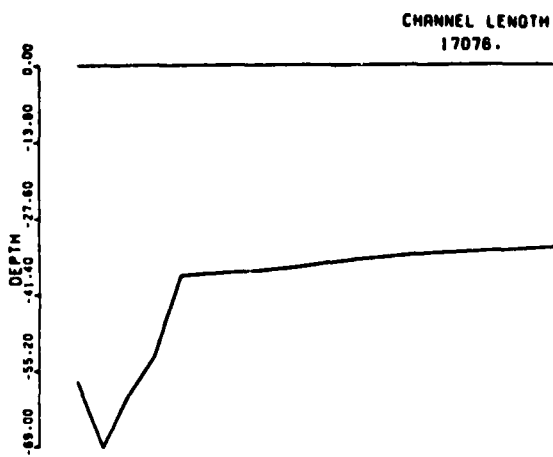


Captiva Pass, Fla. (W) 1960



BOCA GRANDE

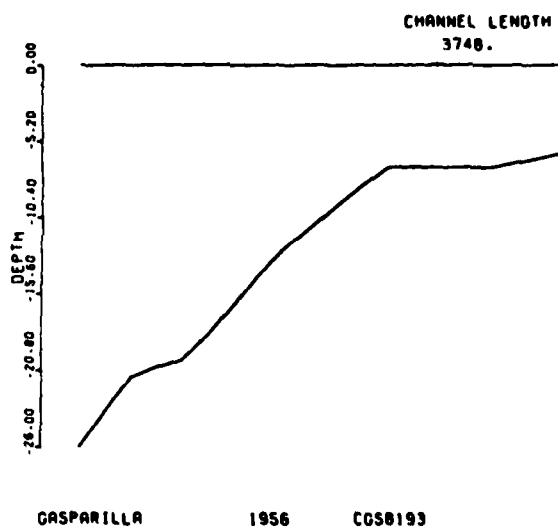
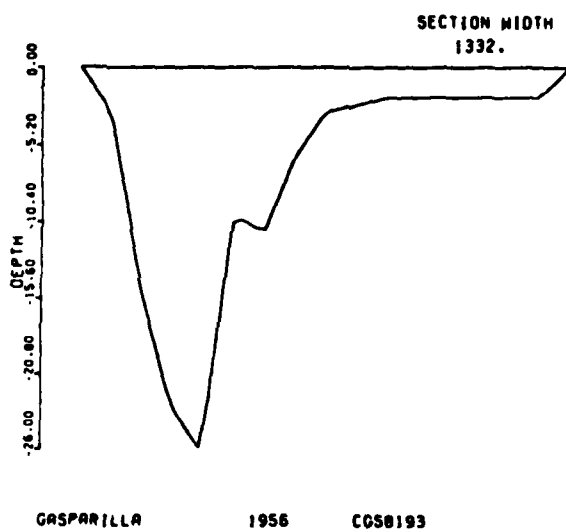
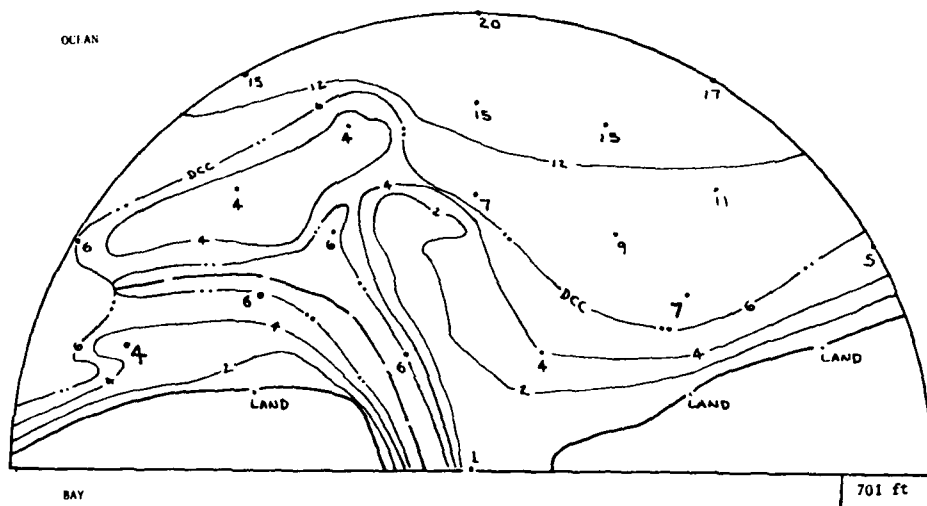
1956-1957 CGS0350



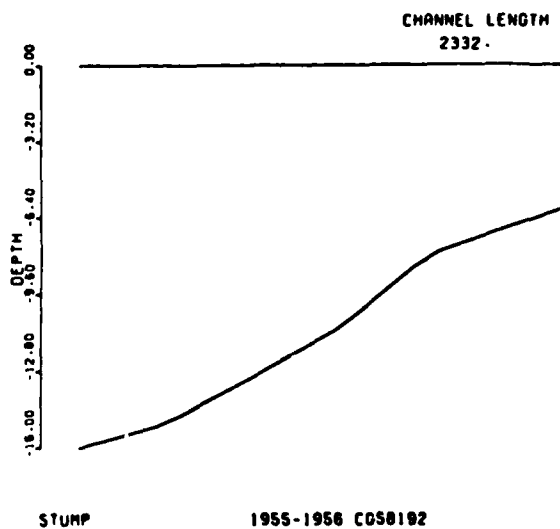
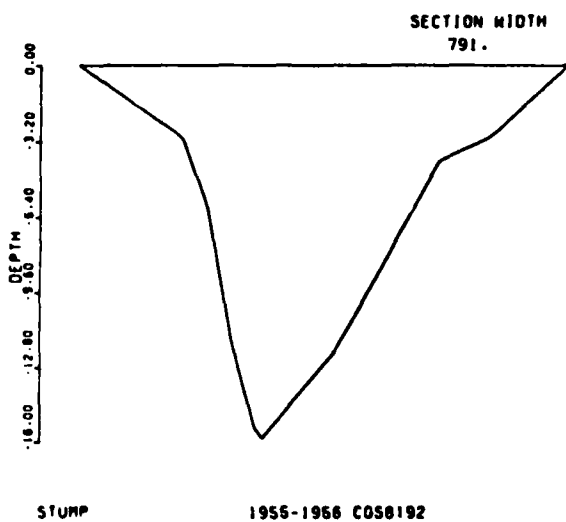
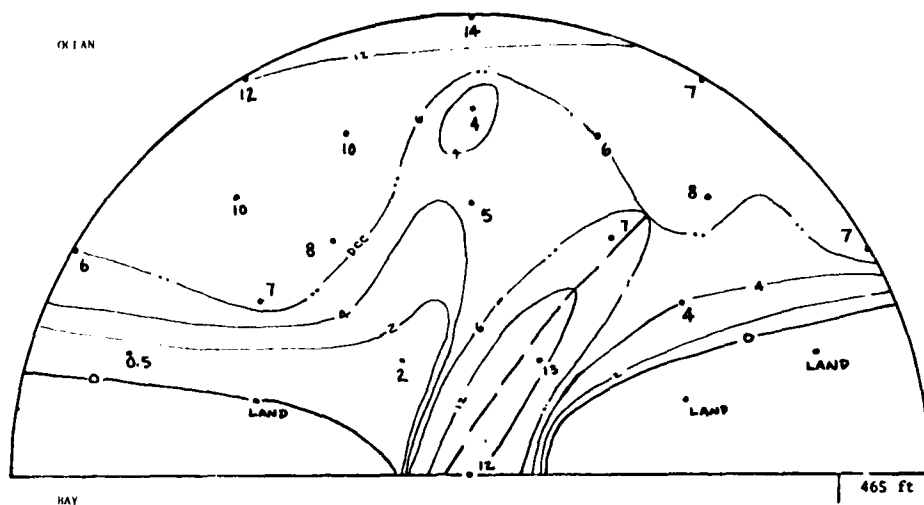
BOCA GRANDE

1956-1957 CGS0350

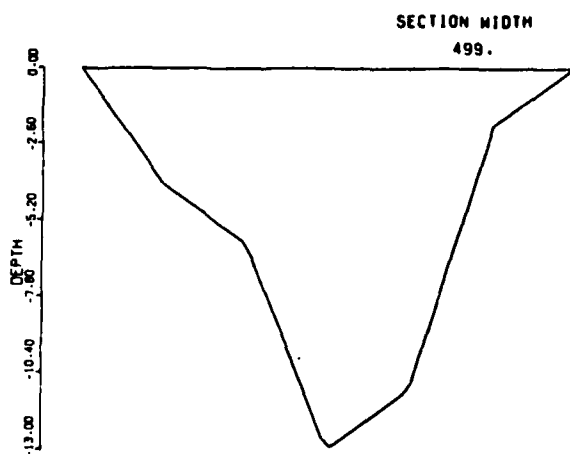
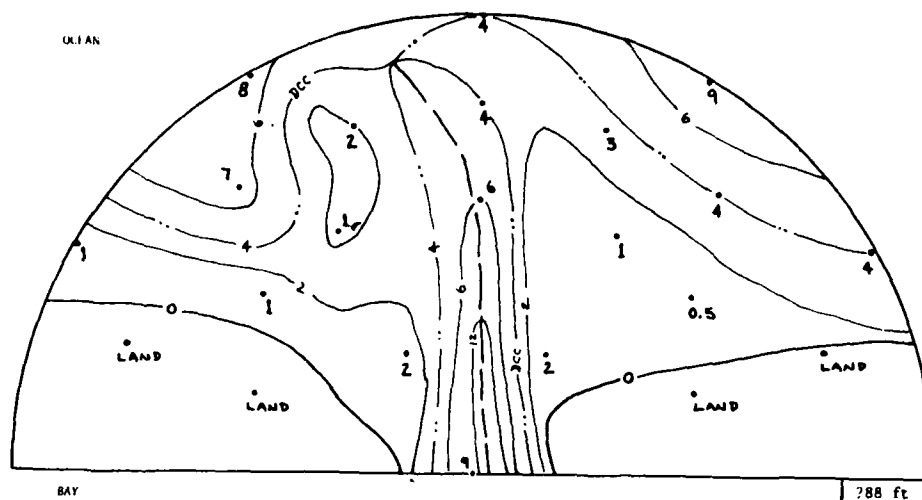
Boca Grande Pass, Fla. (W) 1970



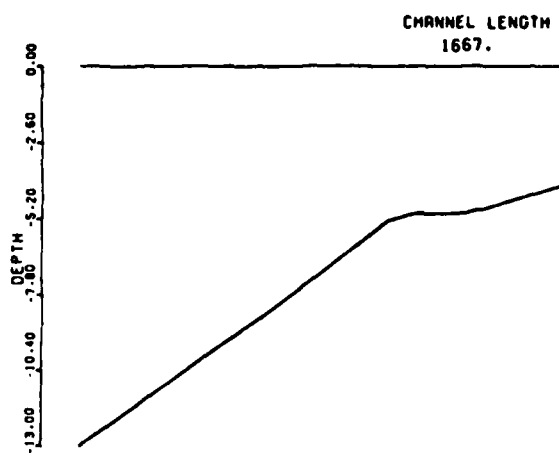
Gasparilla Pass, Fla. (W) 1956-59



Stump Pass, Fla. (W) 1955-56

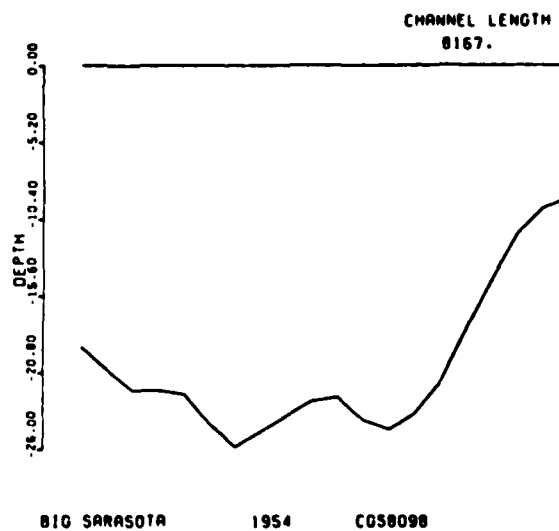
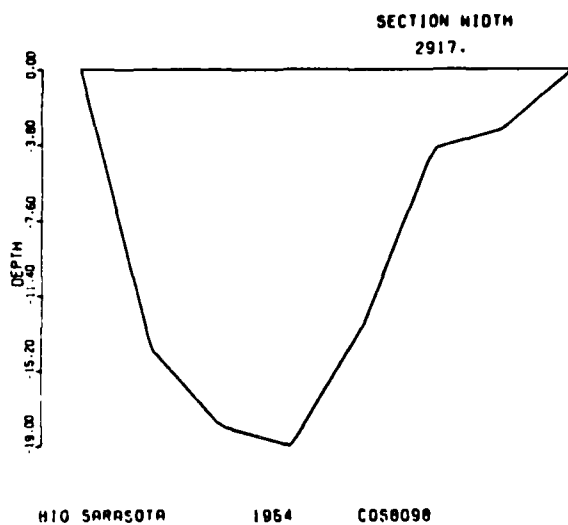
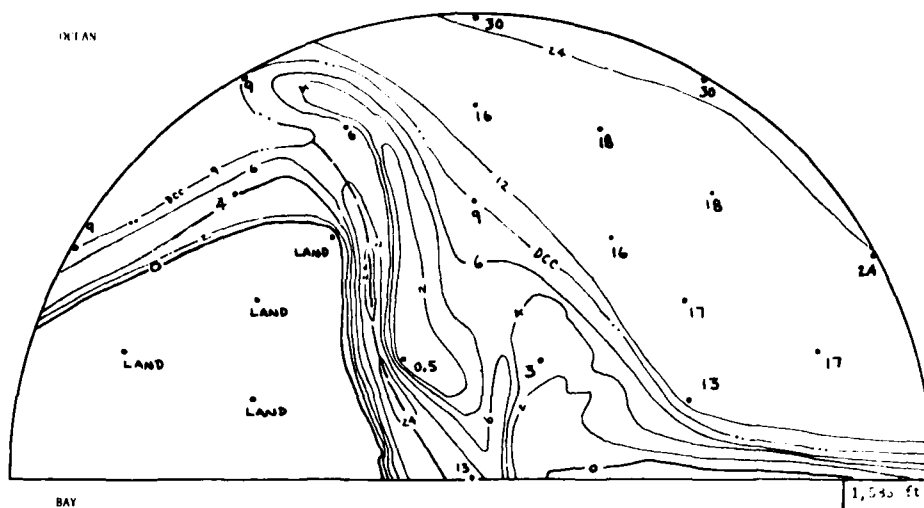


MIDNIGHT PASS 1955 CCS0154

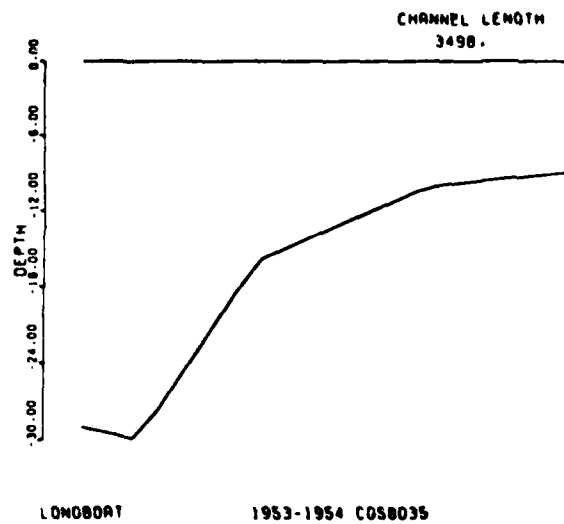
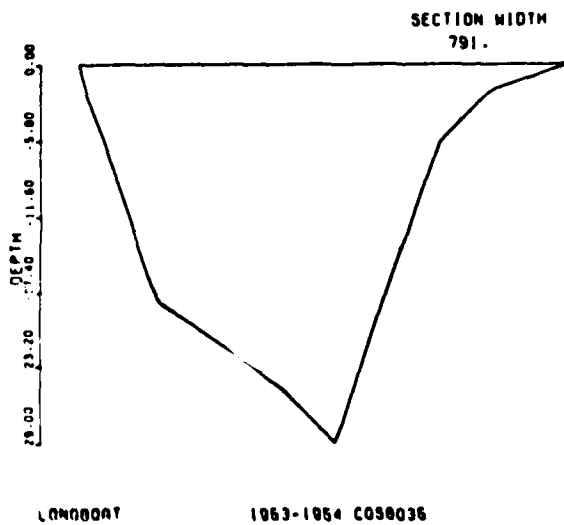
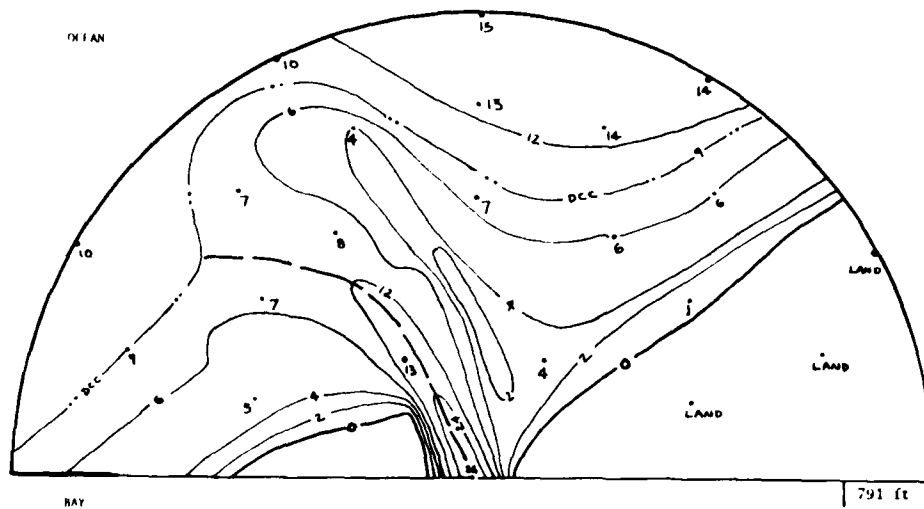


MIDNIGHT PASS 1955 COS0154

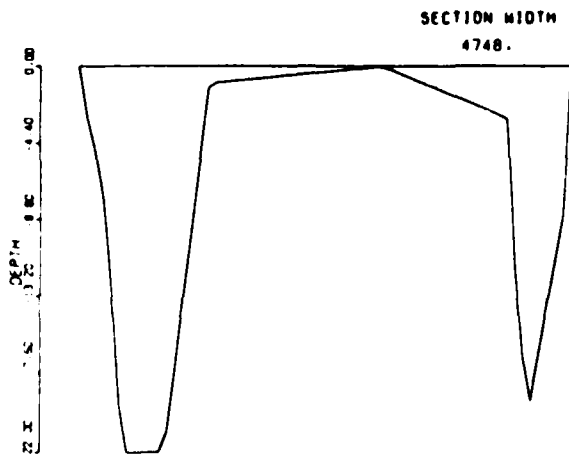
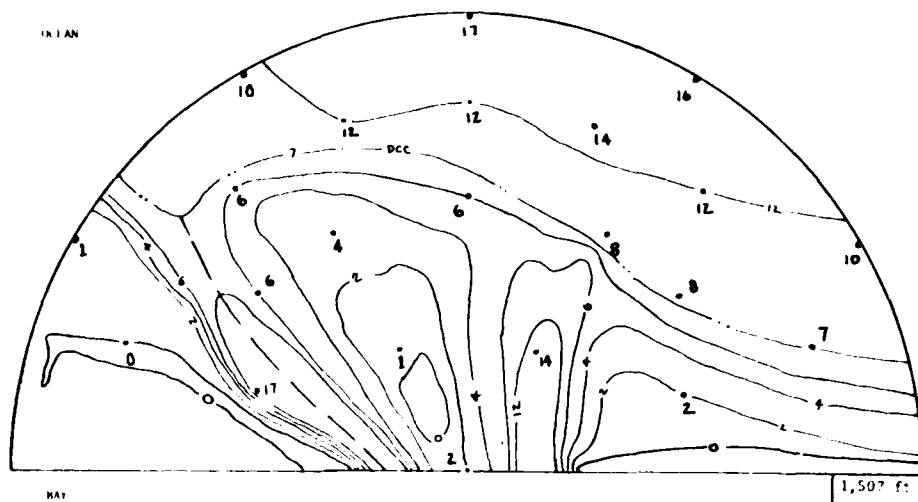
Midnight Pass, Fla. (W) 1955



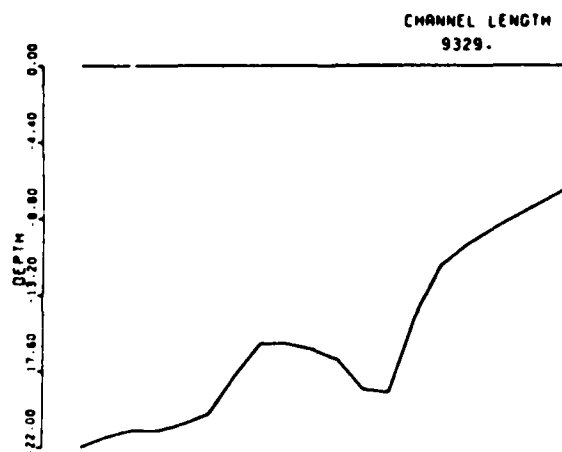
Big Sarasota Pass, Fla. (W) 1954



Longboat Pass, Fla. (W) 1953-54

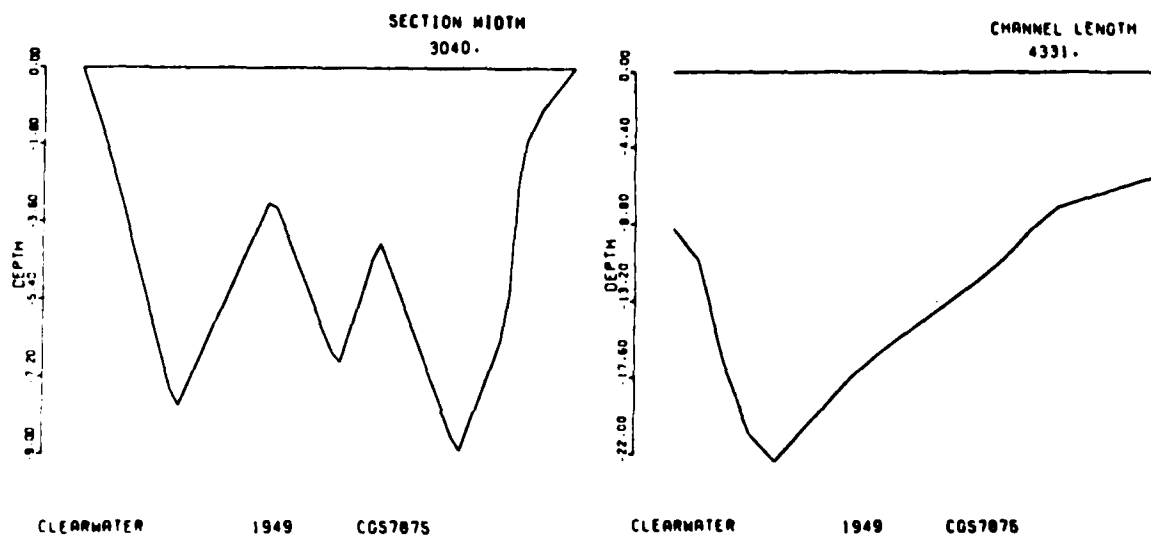
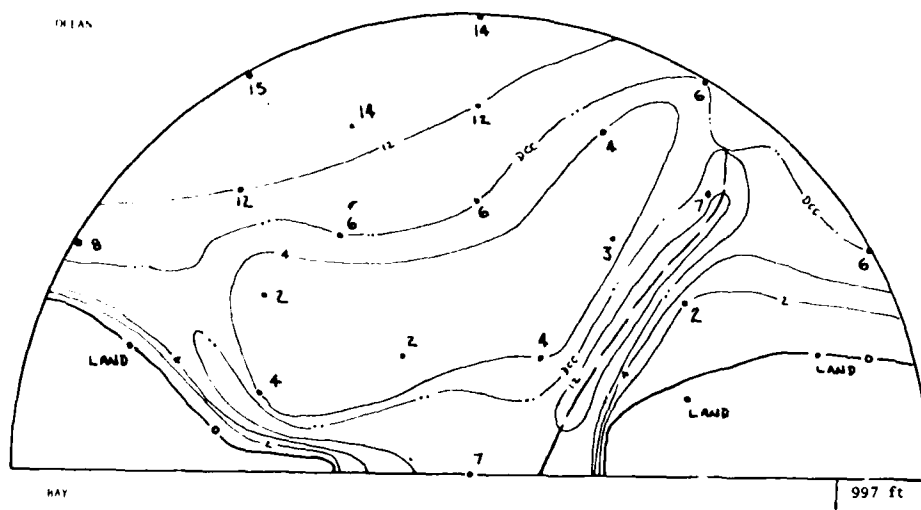


PASS-A-GRIFFE 1926 C094569

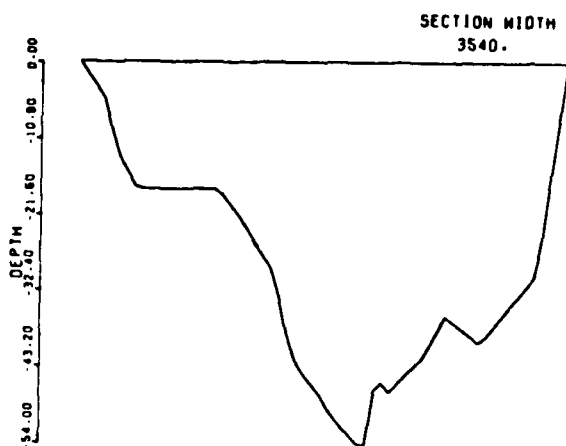
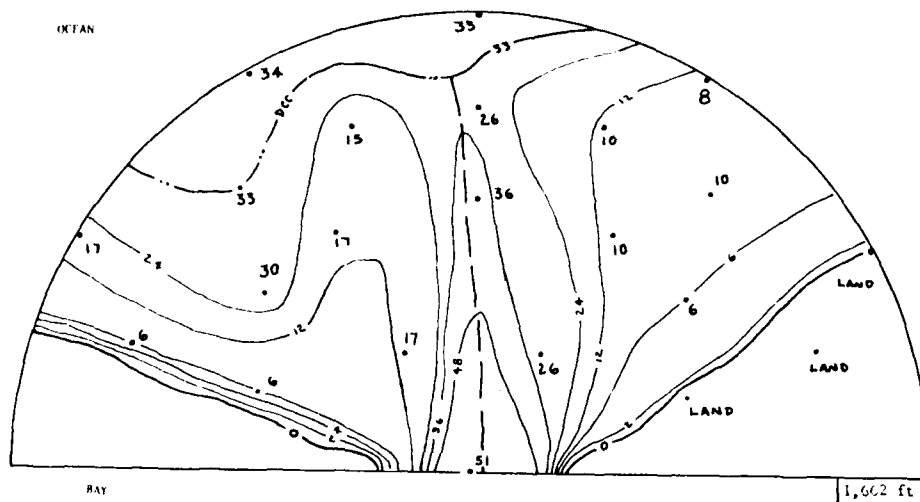


PASS-A-GRIFFE 1926 C094569

Pass A Grille, Fla. (W) 1926

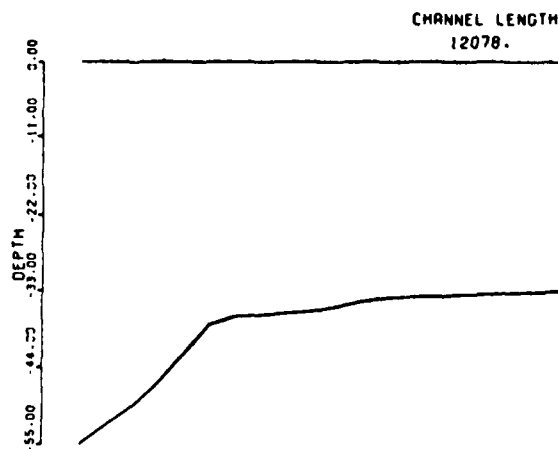


Clearwater Pass, Fla. (W) 1949-50



PENSACOLA

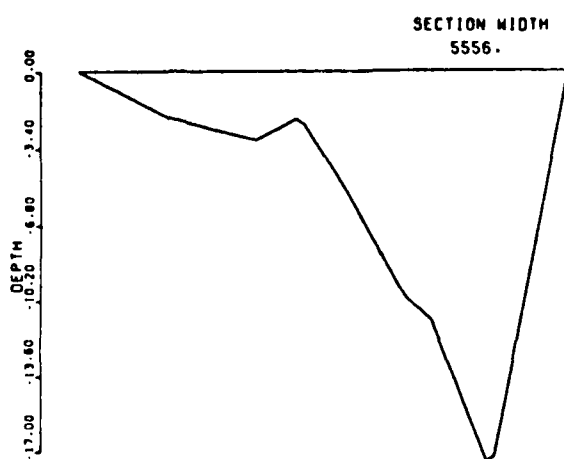
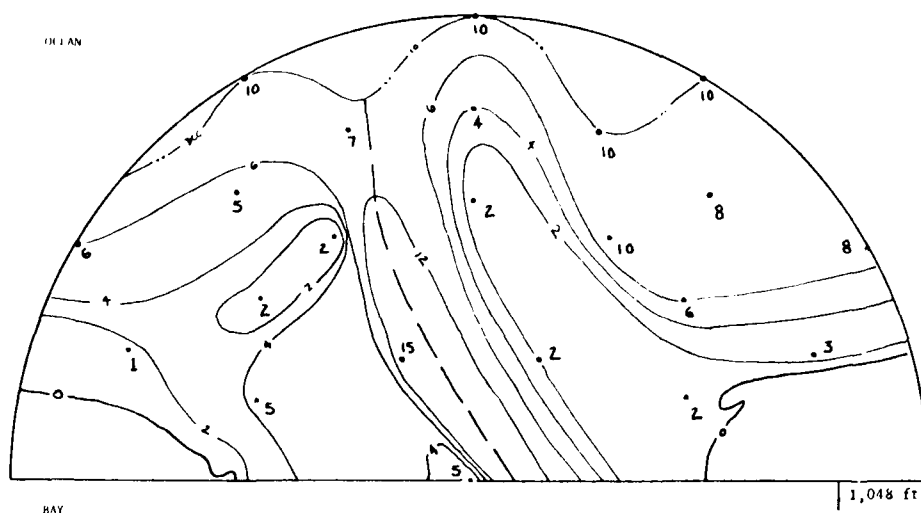
1919-1920 CGS4103



PENSACOLA

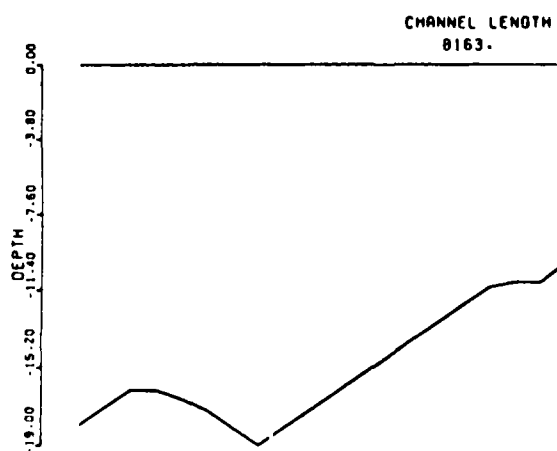
1919-1920 CGS4103

Pensacola Inlet, Fla. (W) 1919-20



SAN LUIS

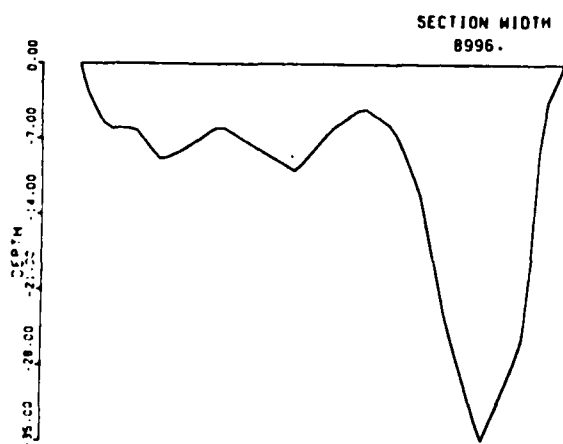
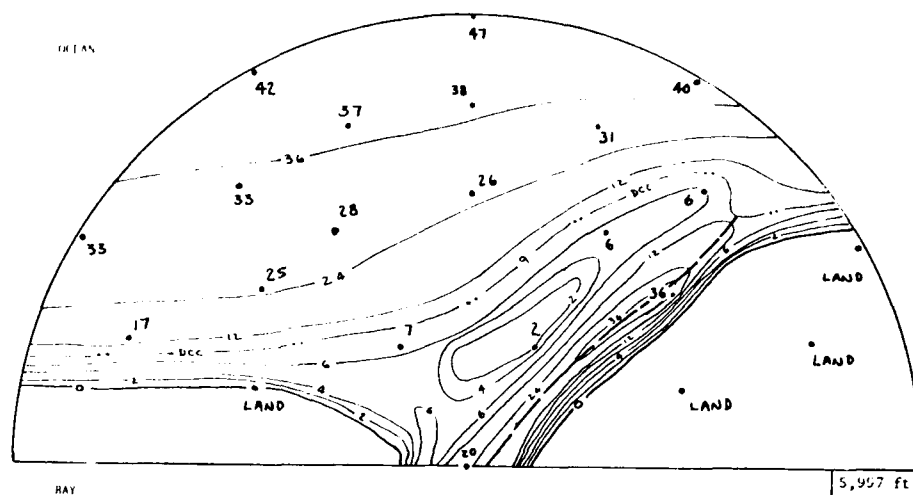
1933-1934 C055400



SAN LUIS

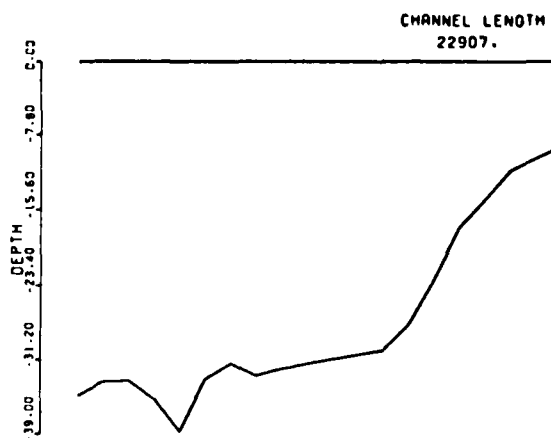
1933-1934 C055400

San Luis Pass, Fla. (W) 1933-34



PASS CAVALLO

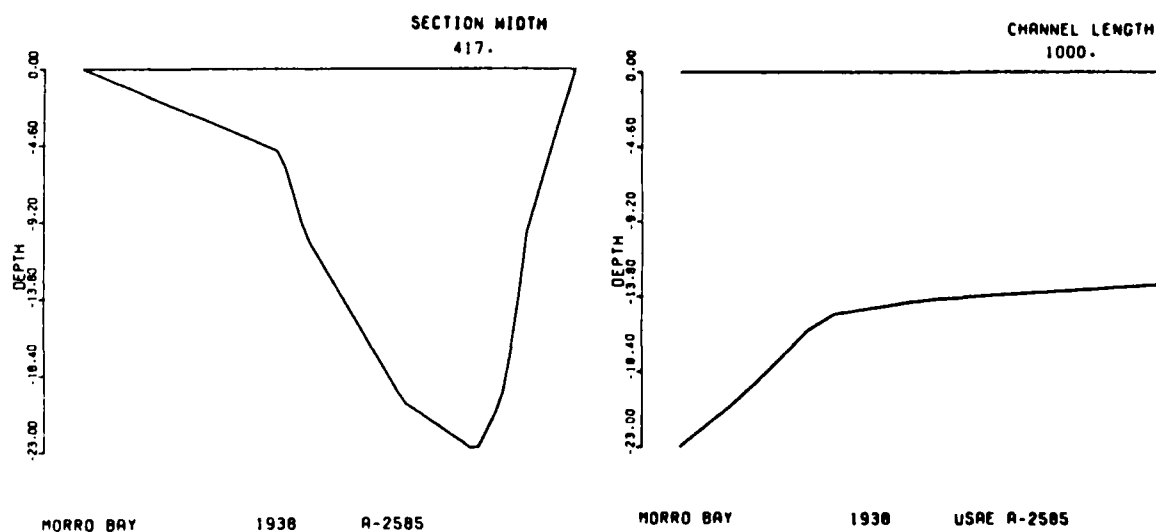
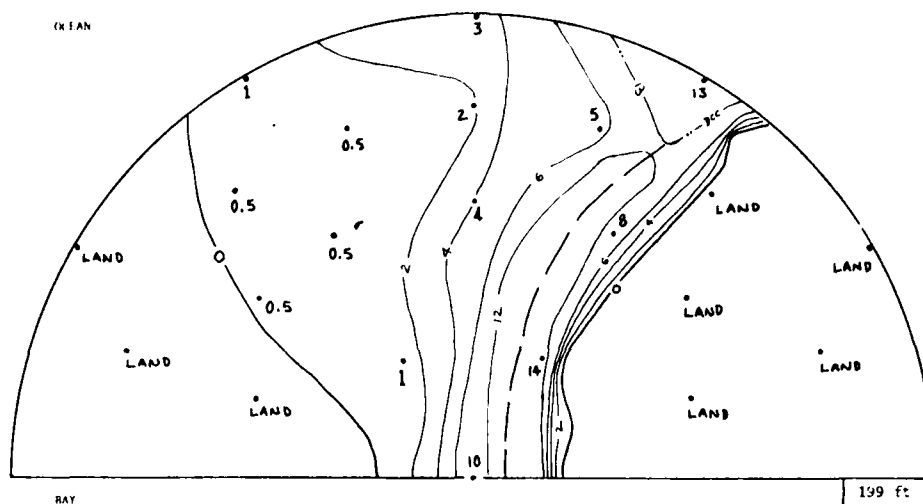
1934-1935 CGS5864



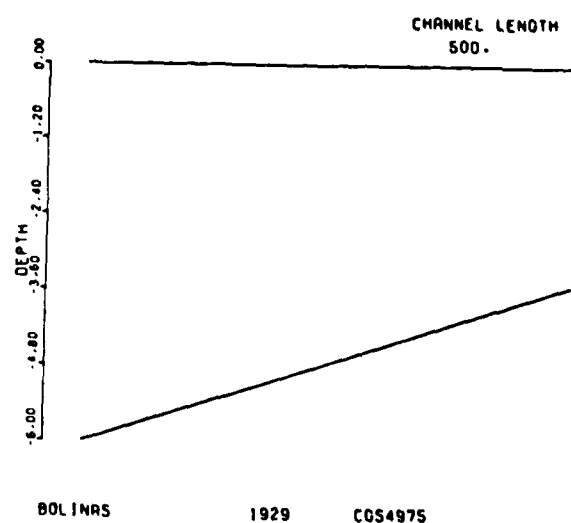
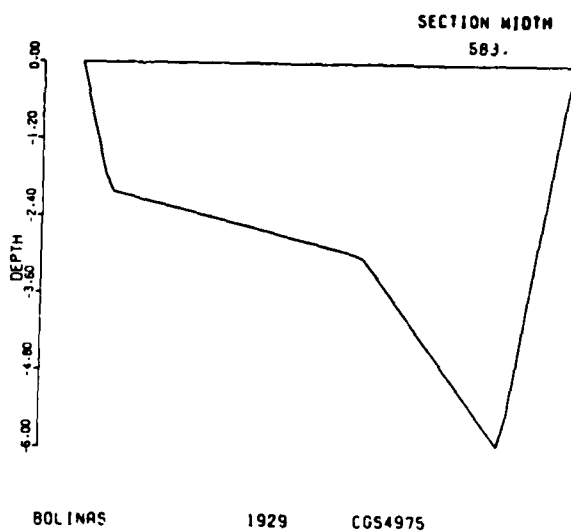
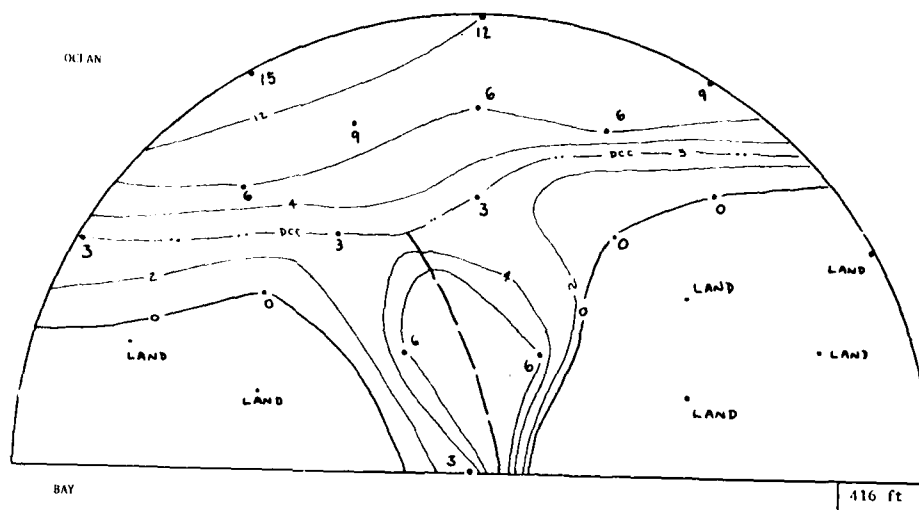
PASS CAVALLO

1934-1935 CGS5864

Pass Cavallo, Tex. 1934-35



Morro Bay Inlet, Calif. 1938



BOLINAS

1929

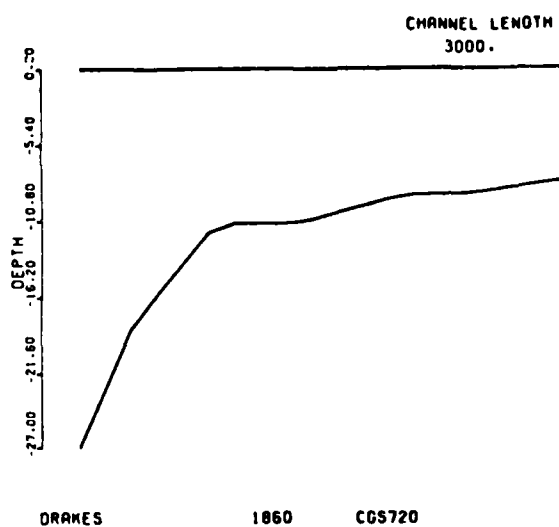
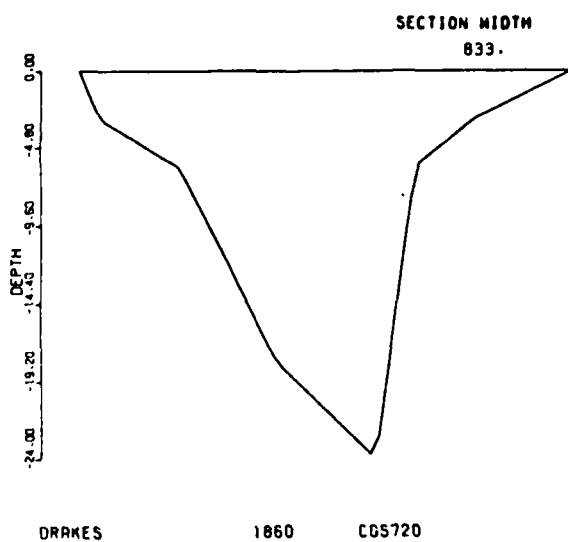
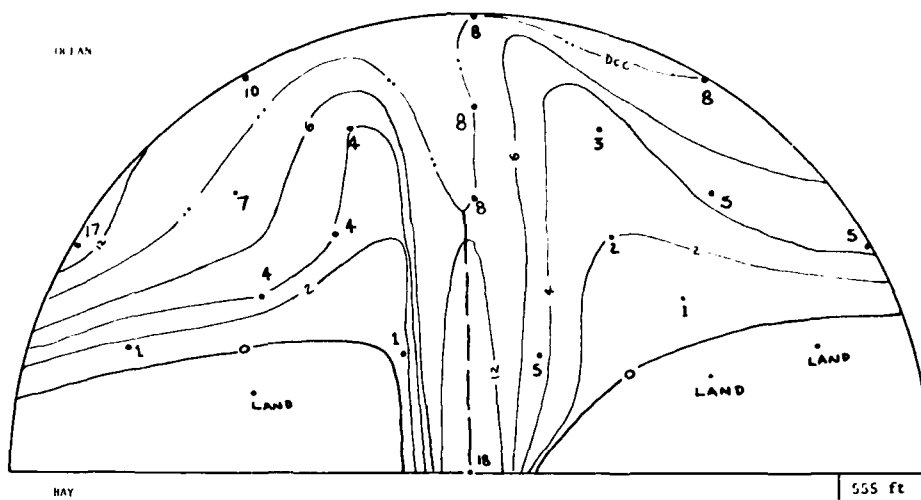
CGS4975

BOLINAS

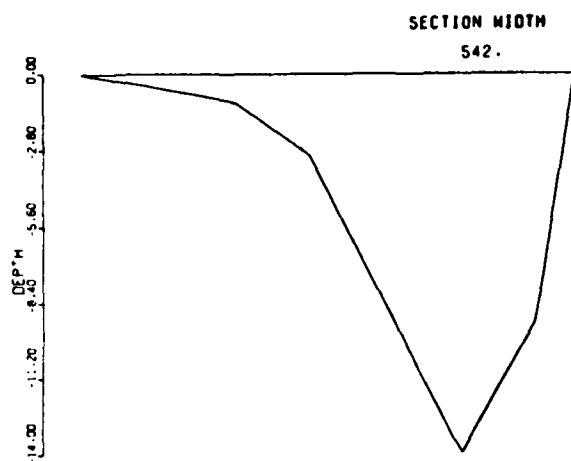
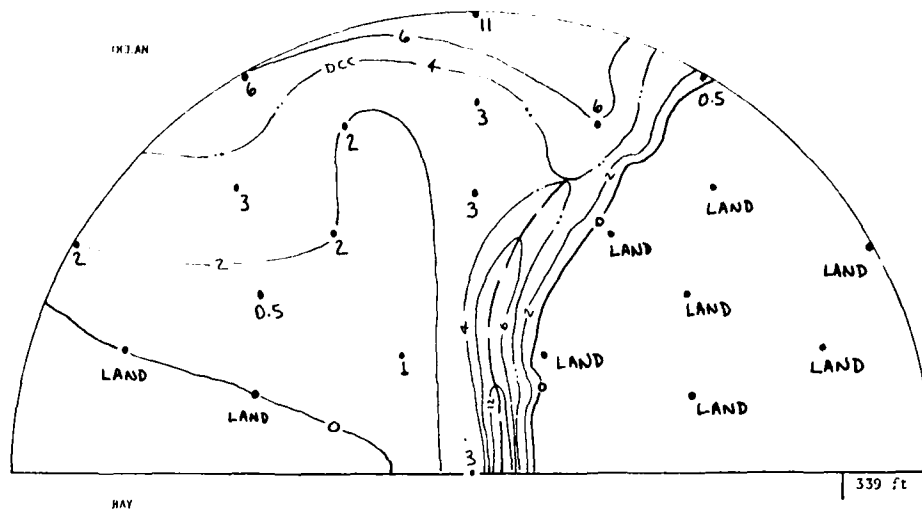
1929

CGS4975

Bolinas Inlet, Calif. 1929



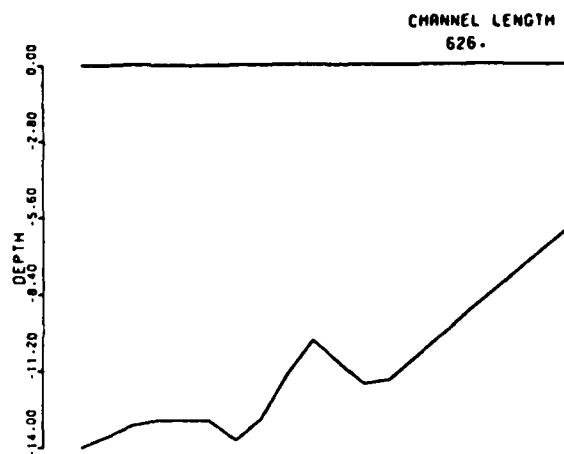
Drakes Inlet, Calif. 1860



BODEGA BAY

1931

CGSS162

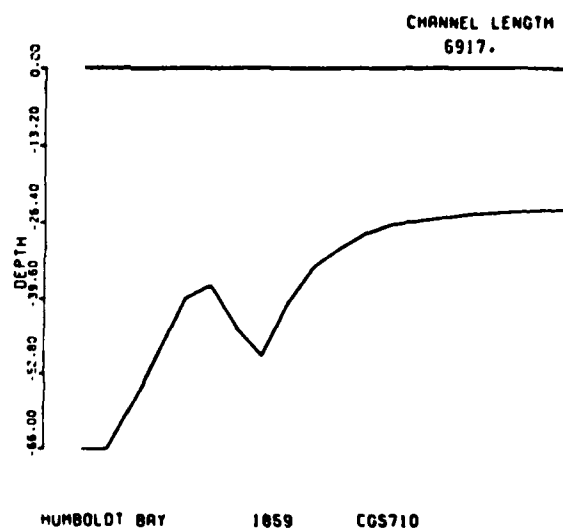
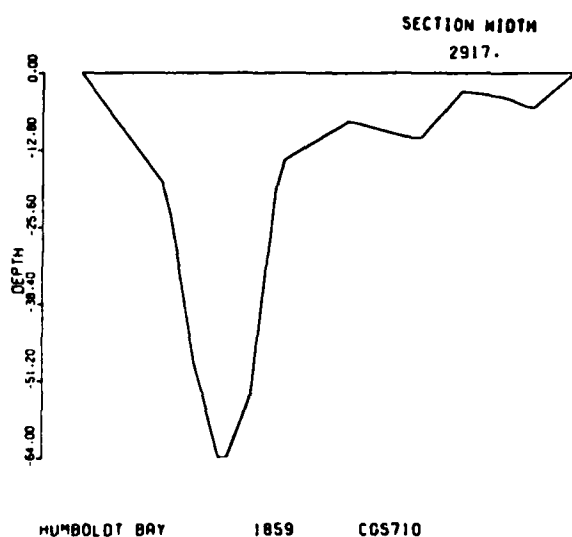
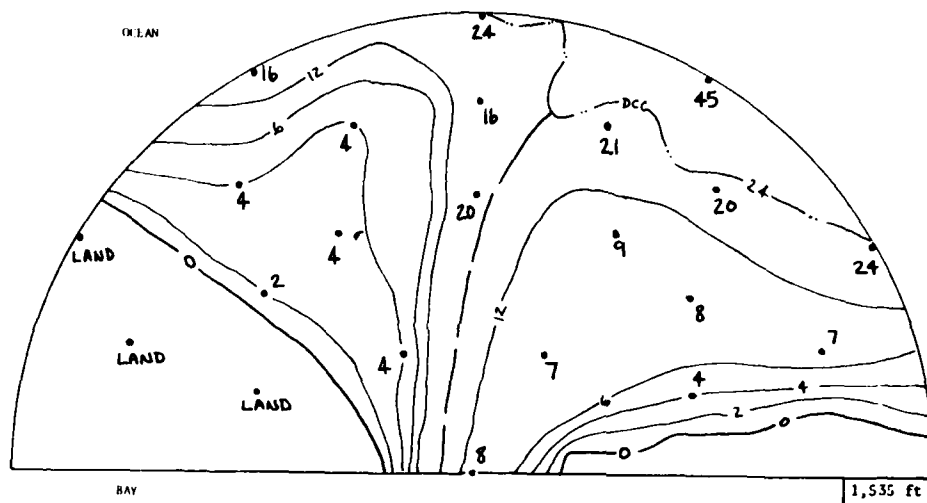


BODEGA BAY

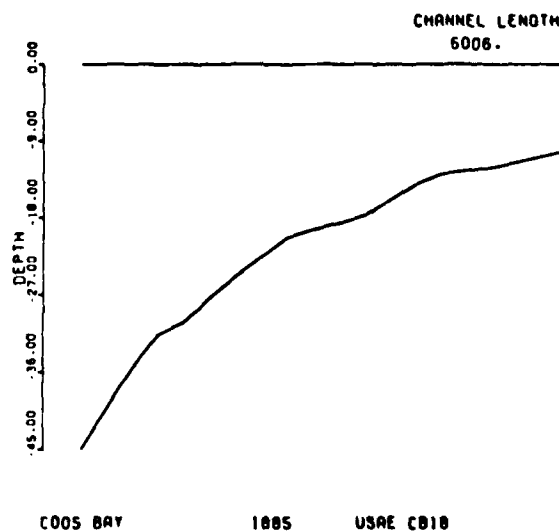
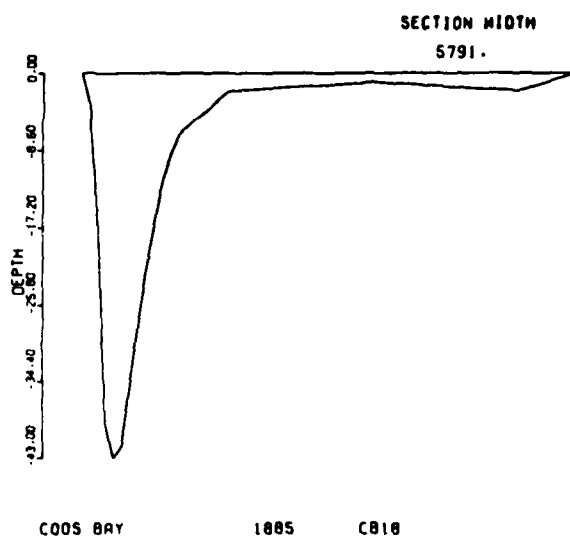
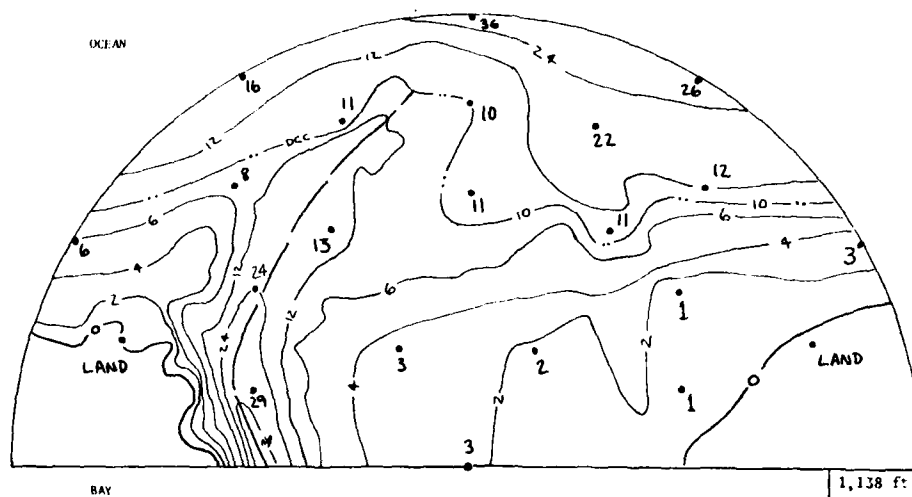
1931

CGSS162

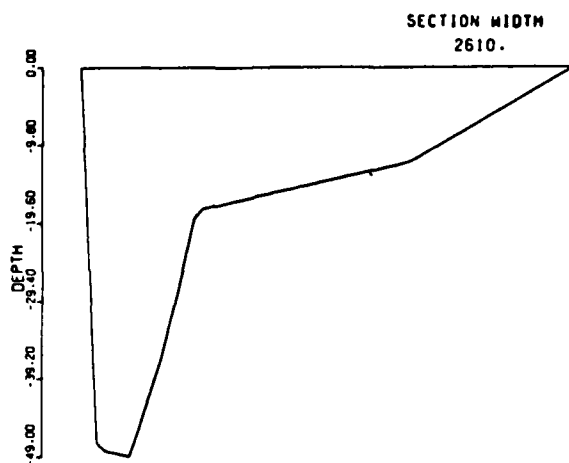
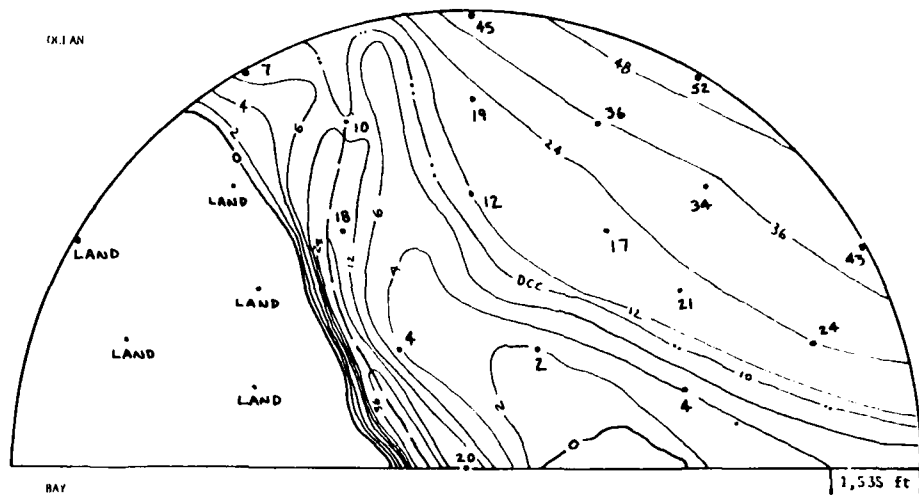
Bodega Bay Inlet, Calif. 1931



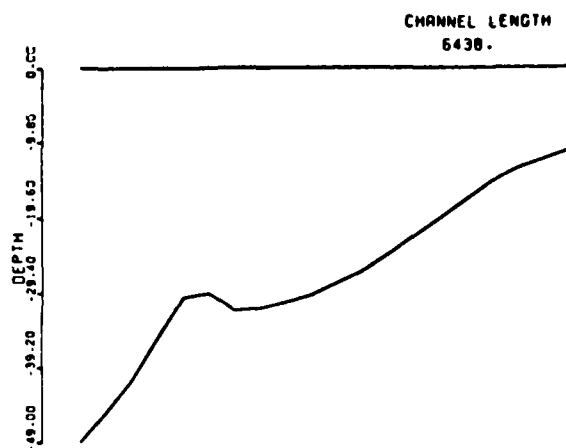
Humboldt Bay Inlet, Calif. 1859



Coos Bay Inlet, Oreg. 1885

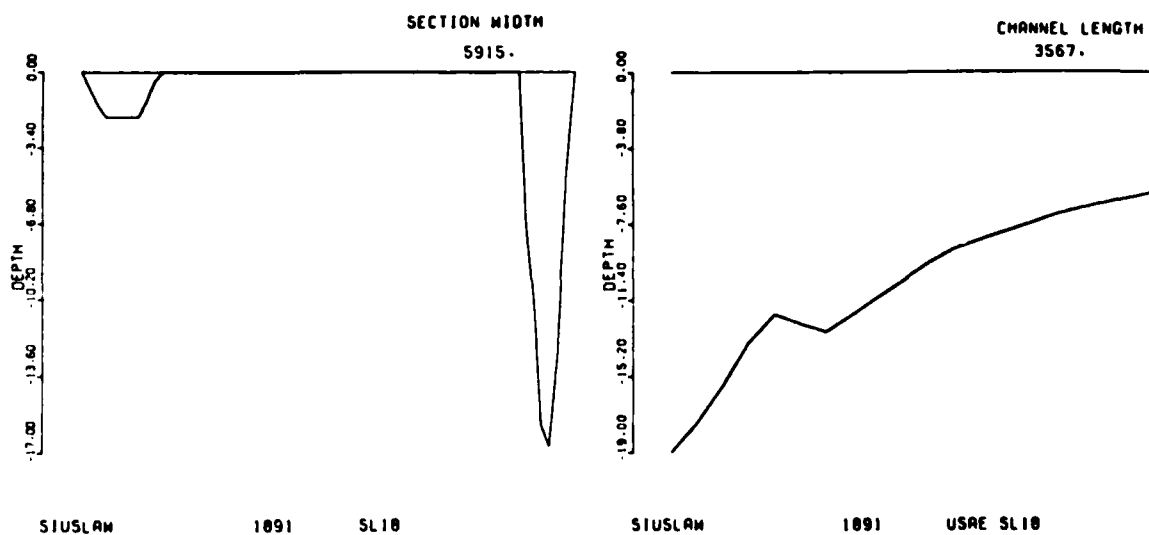
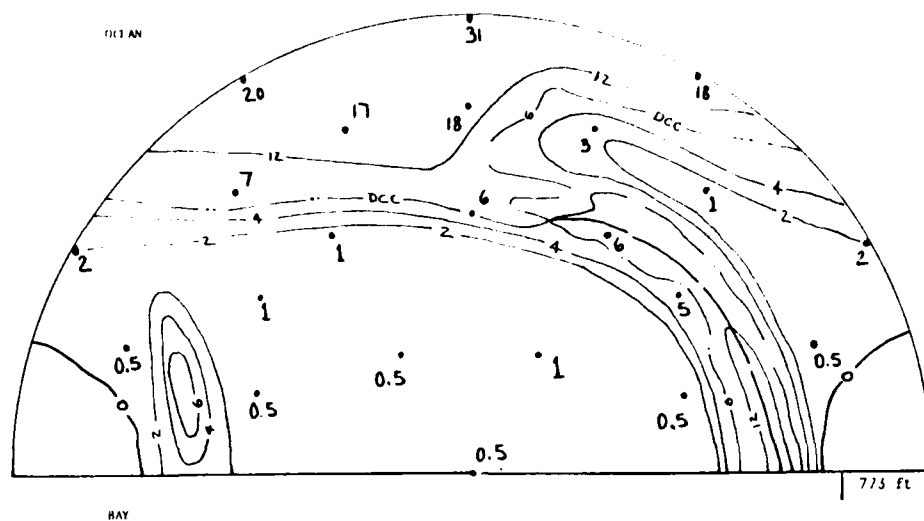


UMPQUA RIVER 1903 UM111

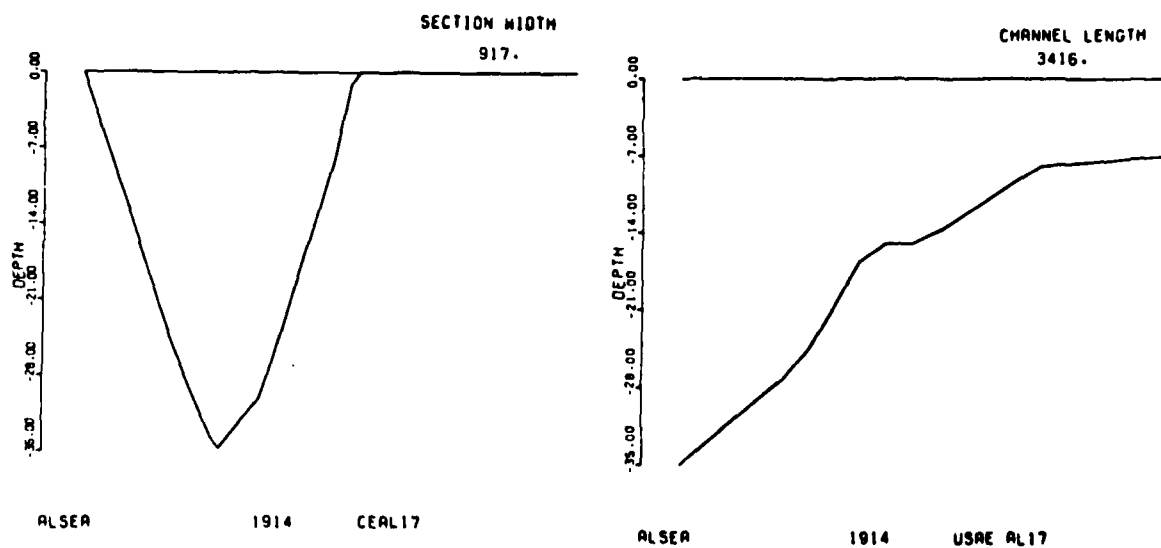
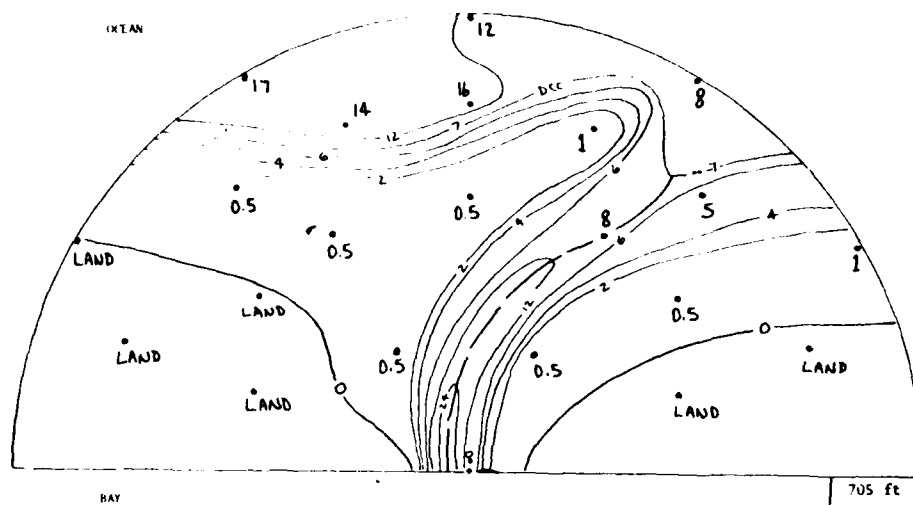


UMPQUA RIVER 1903 UM111

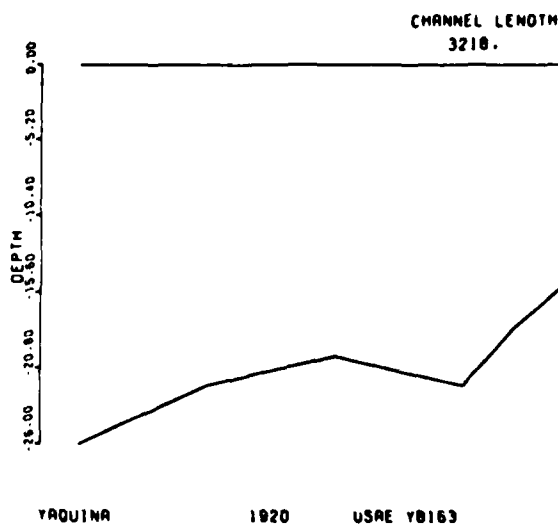
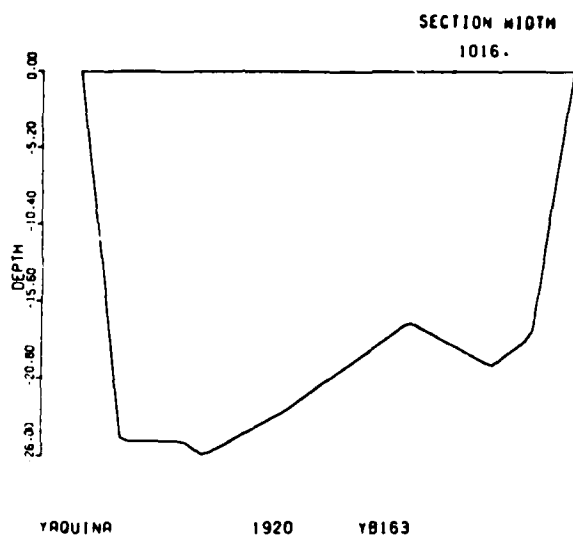
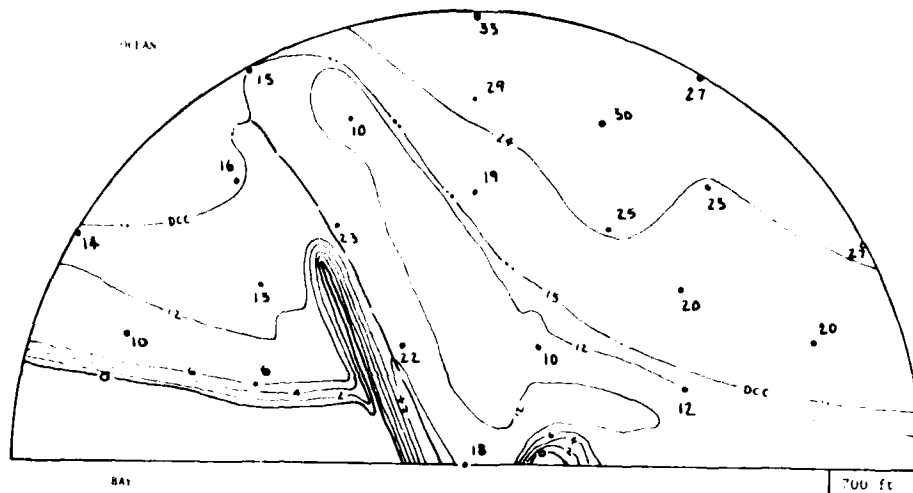
Umpqua River Inlet, Oreg. 1903



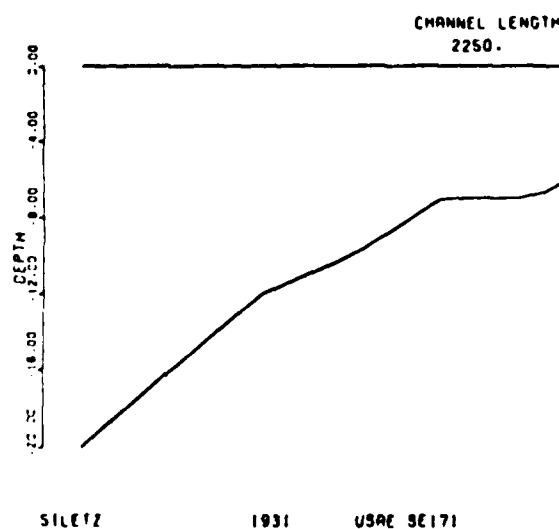
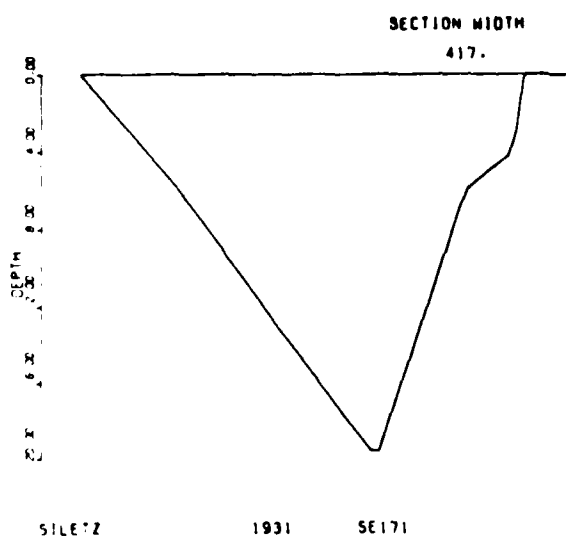
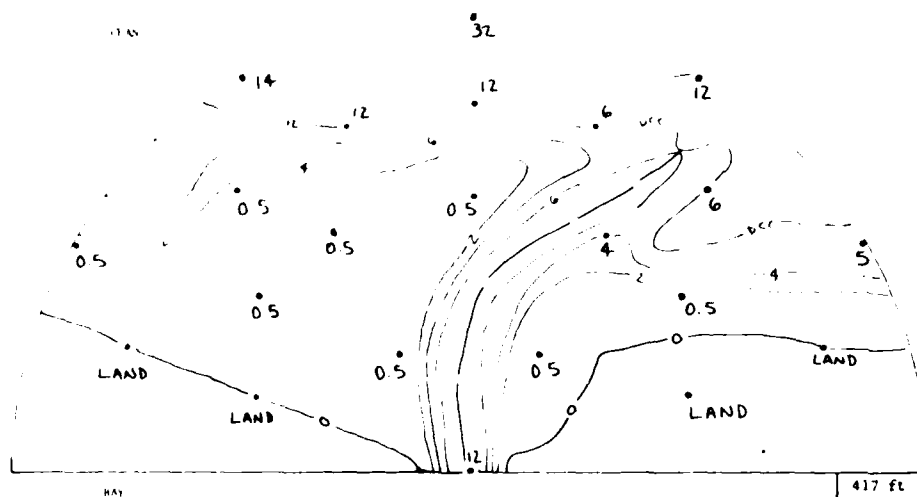
Siuslaw River Inlet, Oreg. 1891



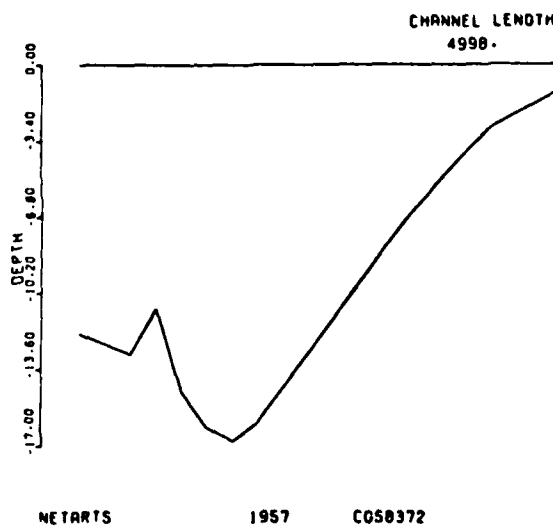
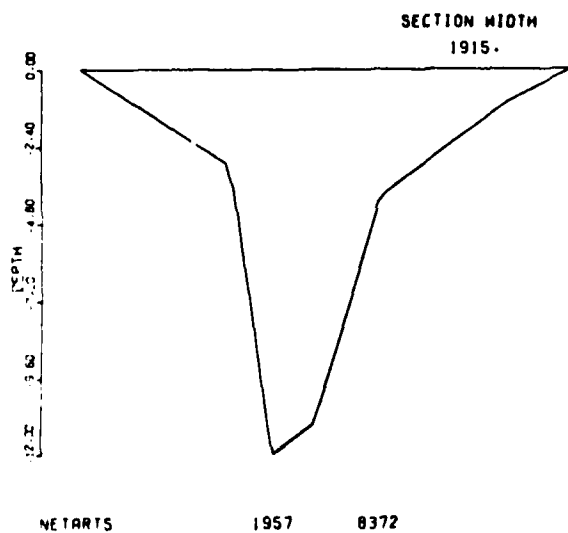
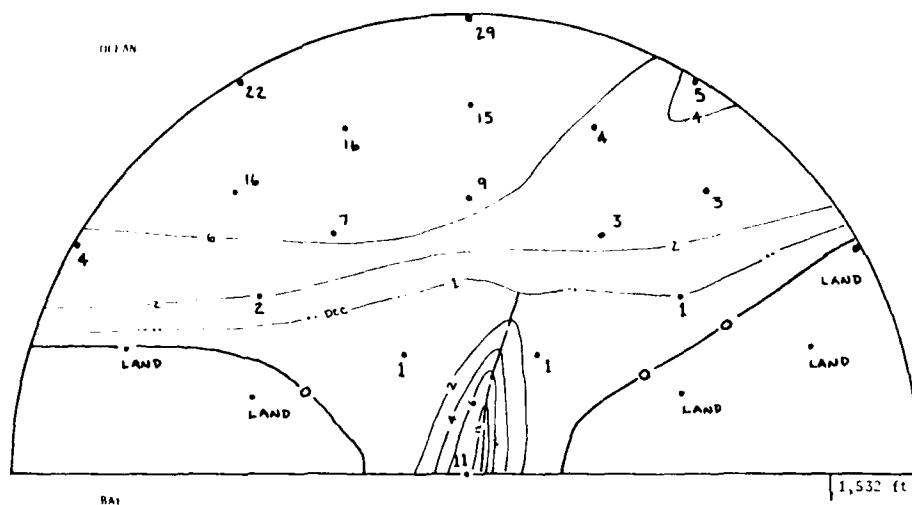
Alsea Bay Inlet, Oreg. 1914



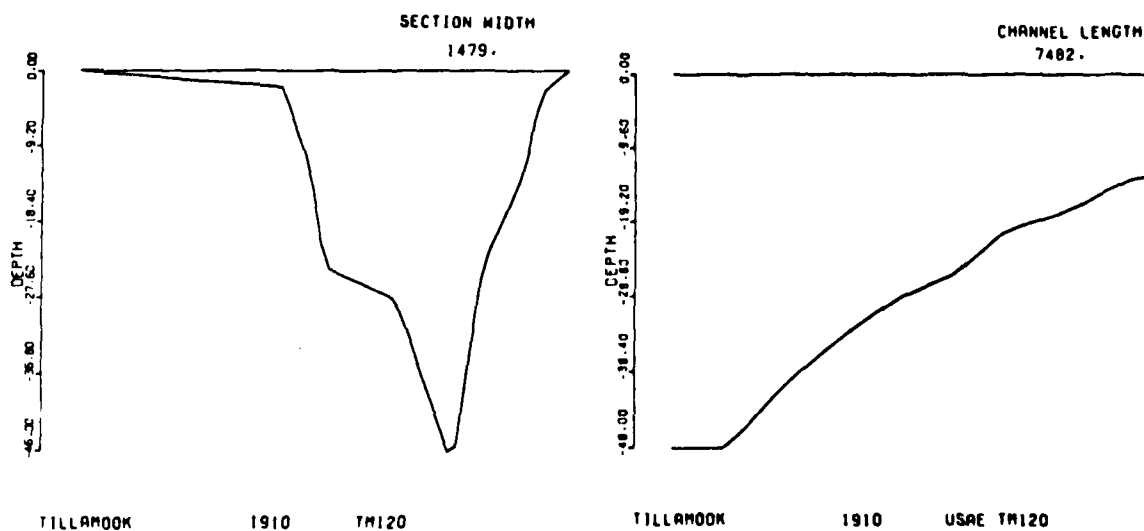
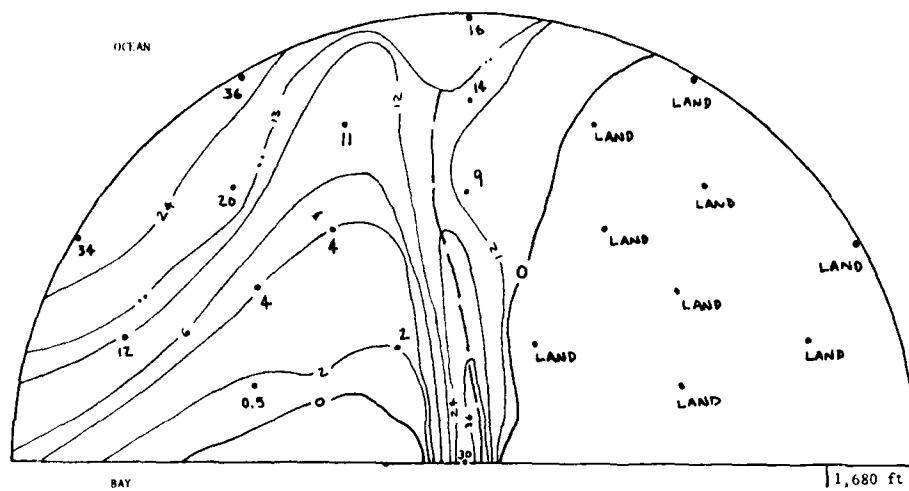
Yaquina Bay Inlet, Oreg. 1920



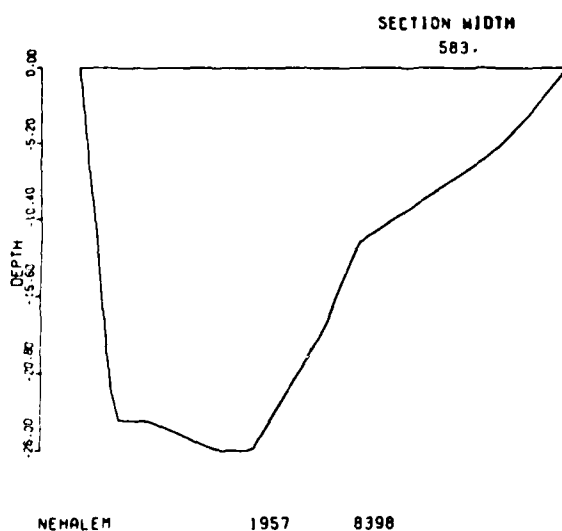
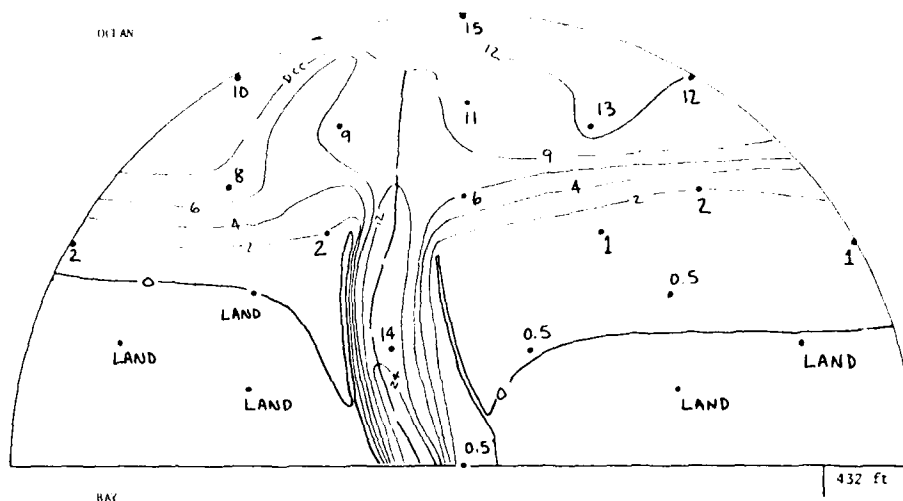
Siletz River Inlet, Oreg. 1931



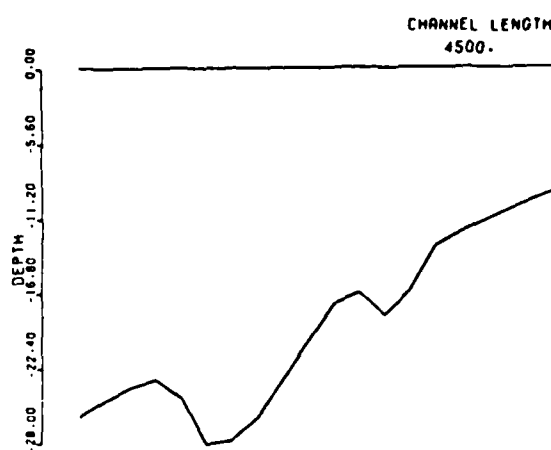
Netarts Bay Inlet, Oreg. 1957



Tillamook Bay Inlet, Oreg. 1910

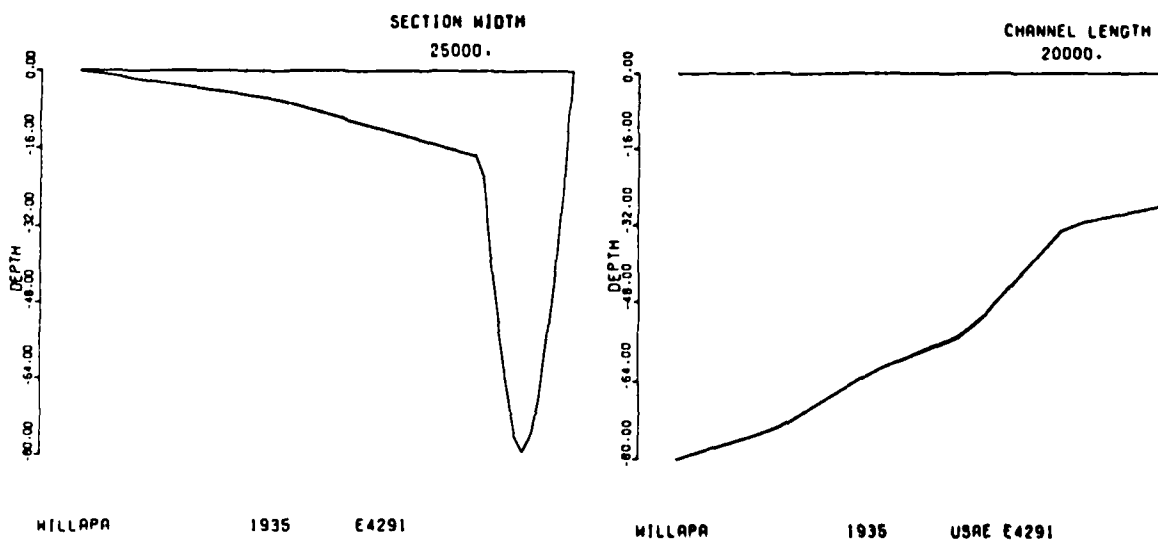
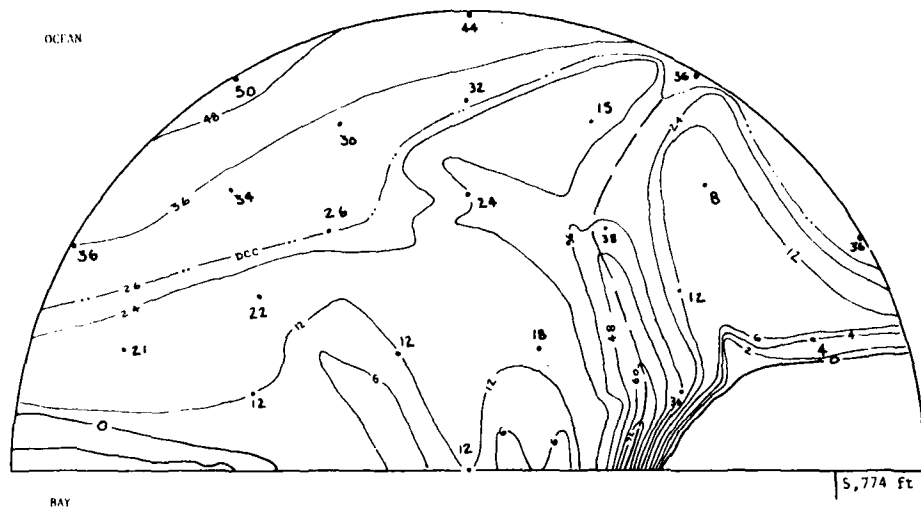


NEHALEM 1957 8398



NEHALEM 1957 COS8398

Nehalem Inlet, Oreg. 1957



WILLAPA

1935

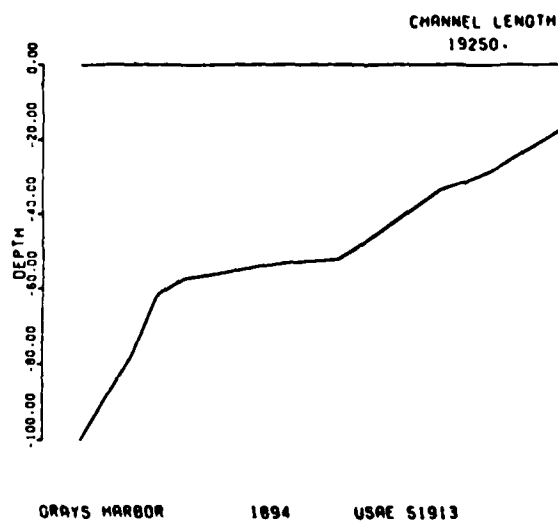
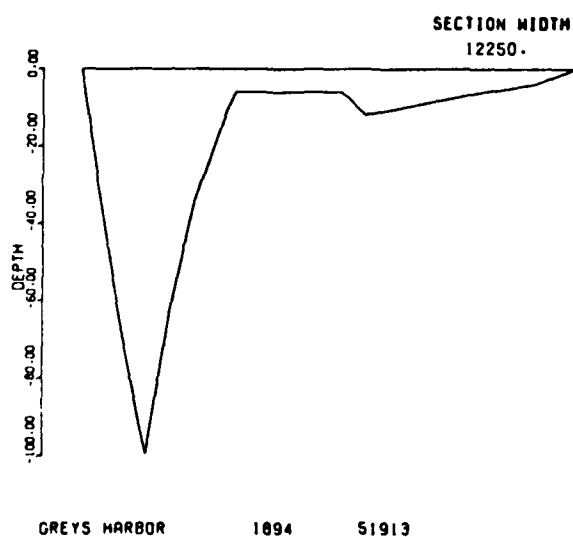
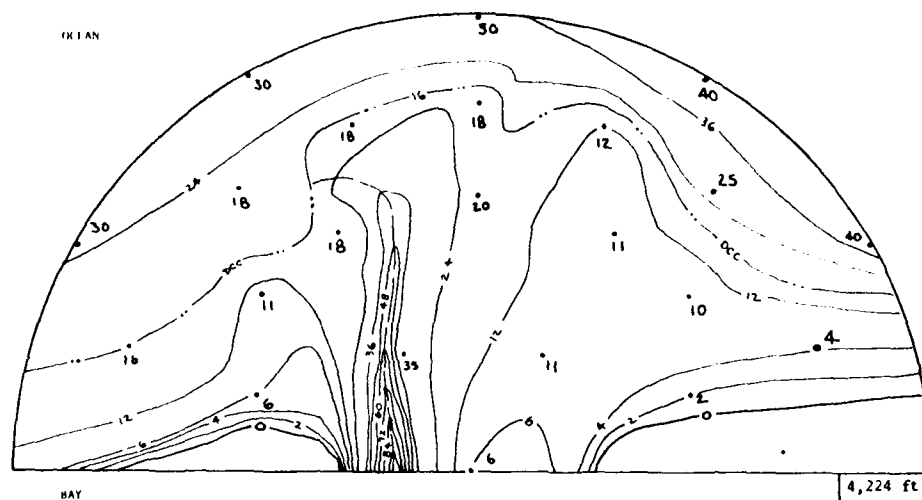
E4291

WILLAPA

1935

USRE E4291

Willapa Bay Inlet, Wash. 1935



Grays Harbor Inlet, Wash. 1894

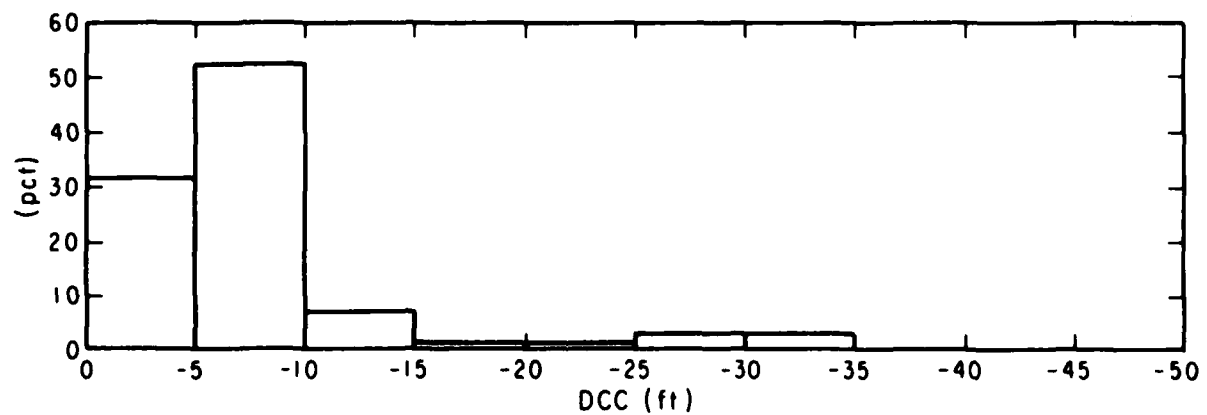
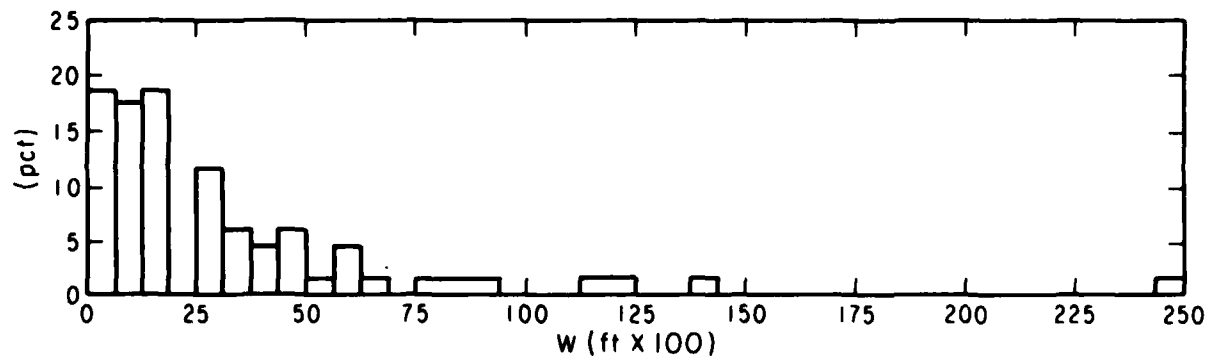
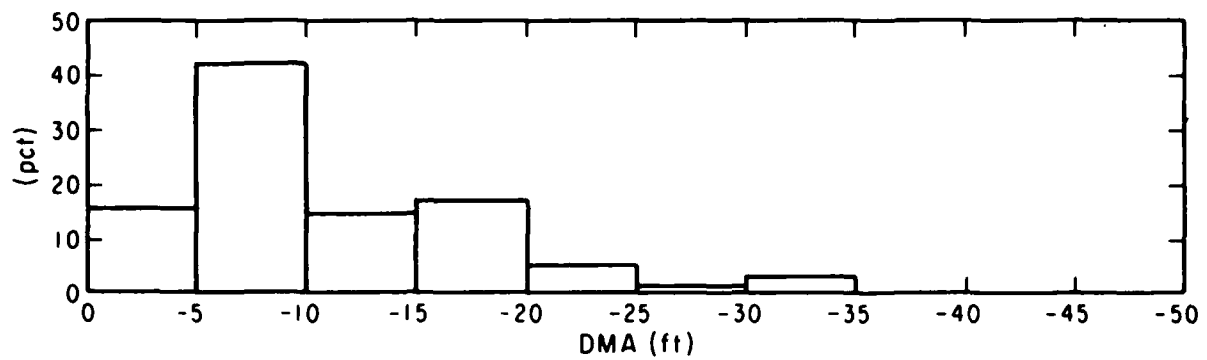
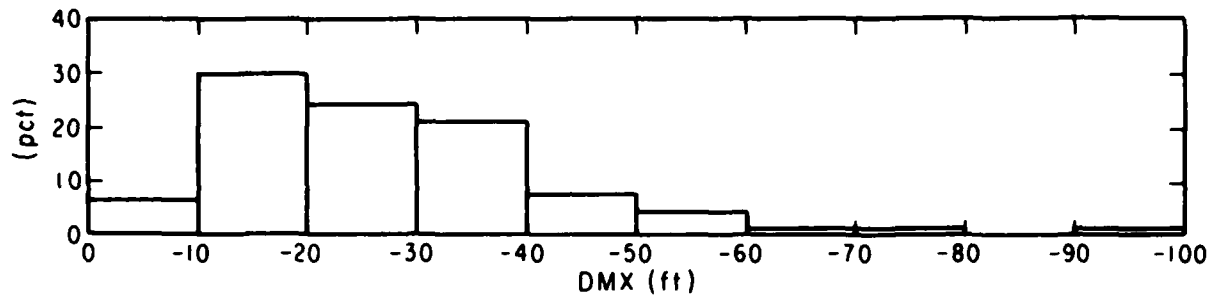
APPENDIX B

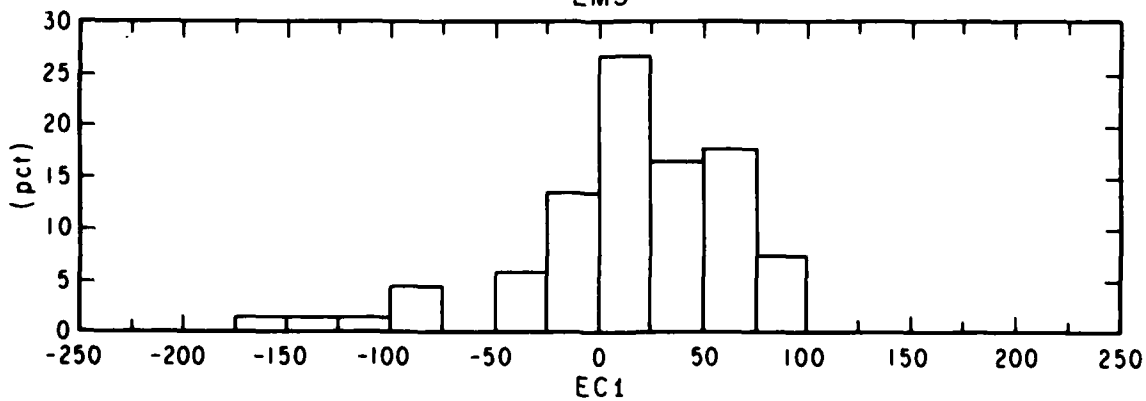
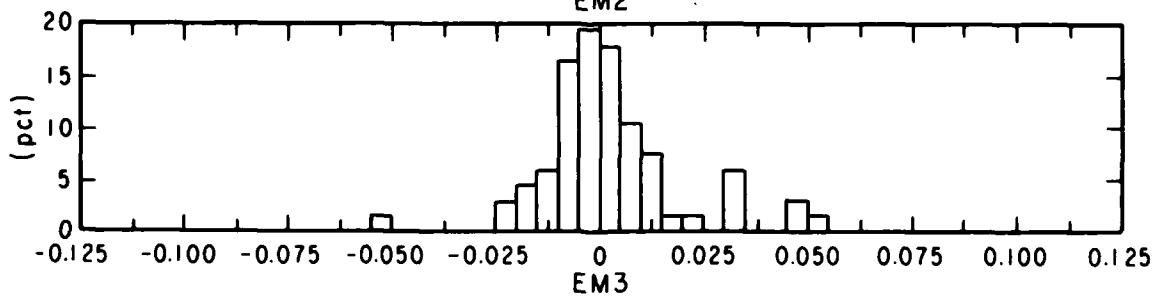
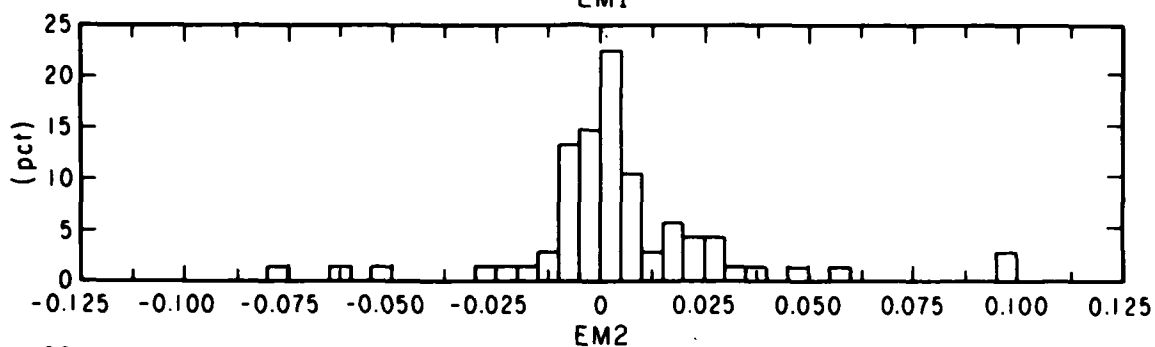
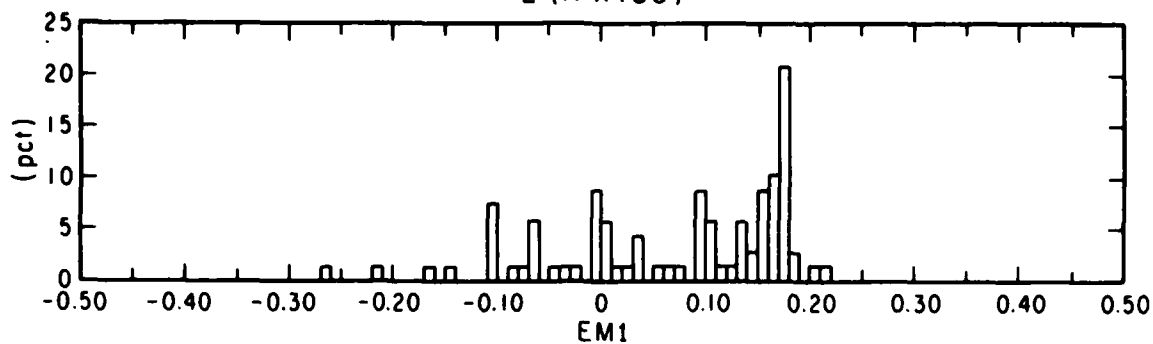
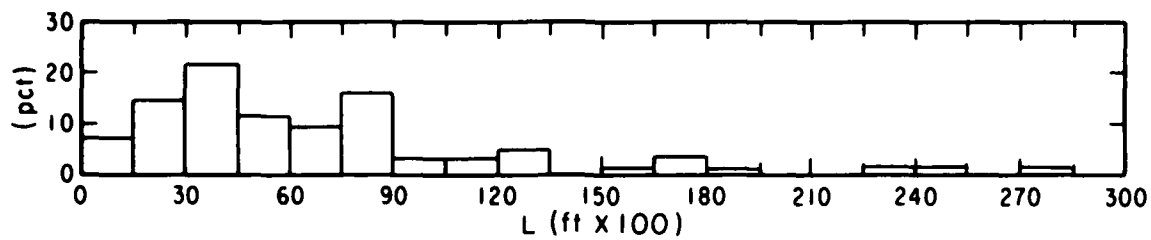
VALUES OF THE 13 INLET GEOMETRIC PARAMETERS BY INLET

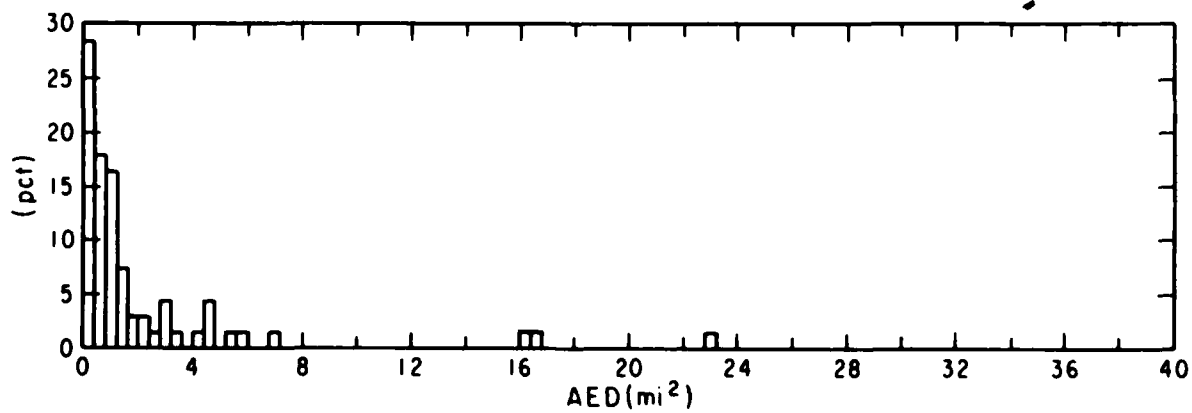
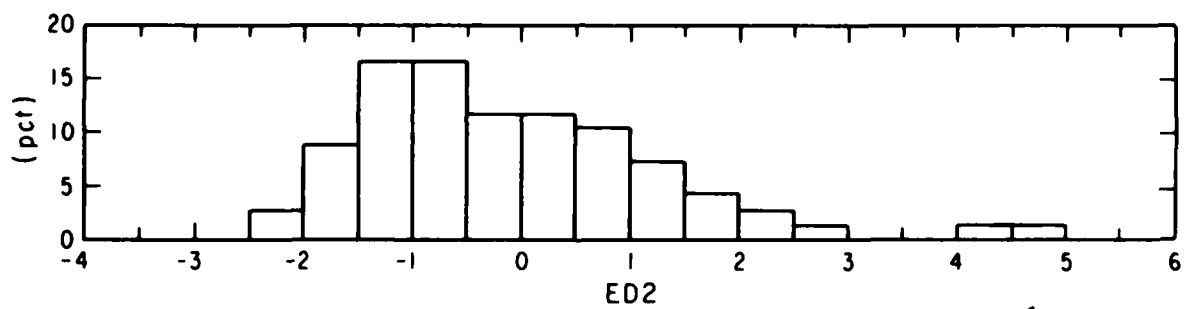
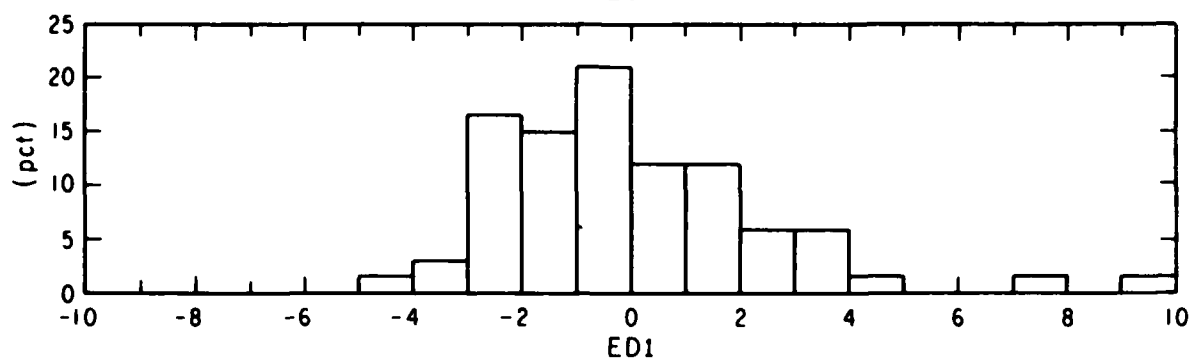
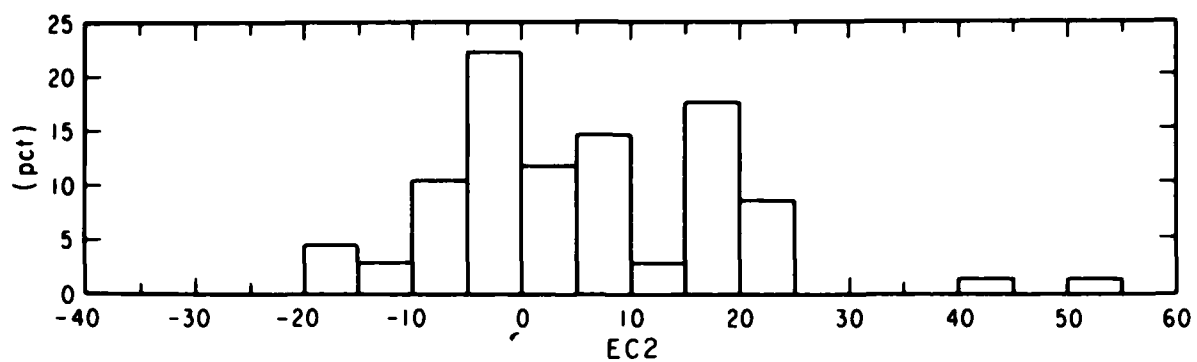
INLET	DMX 1	DMA 2	W 3	DCC 4	L 5	EM1 6	EM2 7	EM3 8	EC1 9	EC2 10	ED1 11	ED2 12	AED 13
MORICHES	-17.0	-6.0	1416.0	-4.0	1833.0	0.0470	0.0020	0.0120	34.0	-0.5	-0.5	-0.01	0.20
FIRE ISLAND	-24.0	-8.0	4831.0	-14.0	3748.0	0.0670	0.0150	0.0030	-5.4	16.6	4.0	0.9	1.21
BEACH HAVEN	-25.0	-8.0	13994.0	-8.0	9829.0	0.0730	0.0010	0.0010	-16.9	17.9	0.9	-0.6	4.77
BRIGANTINE	-40.0	-8.0	5000.0	-7.0	7833.0	0.0740	0.0091	0.0012	5.8	15.3	-0.6	1.1	1.54
GRFAT EGG	-39.0	-10.0	4414.0	-14.0	7080.0	0.0590	0.0110	0.0060	-19.8	24.1	-0.6	-0.5	2.60
CORSON	-25.0	-5.0	1566.0	-6.0	3250.0	0.0677	0.0200	0.0214	26.1	9.4	-0.7	-0.6	0.80
TOWNSEND	-40.0	-10.0	791.0	-5.0	7913.0	0.1140	0.0510	0.0360	19.9	6.6	-2.2	-0.2	0.66
HEREFORD	-27.0	-11.0	2873.0	-8.0	8246.0	0.0530	0.0020	0.0070	31.9	17.5	-2.2	-0.4	1.57
CHINCOTEAGUE	-33.0	-7.0	6830.0	-9.0	8330.0	0.0770	0.0020	0.0030	16.1	4.1	1.0	-1.3	0.79
METOMKIN	-40.0	-17.0	1032.0	-8.0	6664.0	0.0860	0.0670	0.0420	3.8	16.2	-2.5	-0.6	1.09
WACHAPREAGUE	-33.0	-20.0	1332.0	-8.0	11495.0	0.1470	0.0830	0.0430	-28.4	30.3	-2.3	0.9	3.08
OREGON	-32.0	-11.0	4040.0	-7.0	7913.0	0.0622	0.0020	0.0090	13.6	15.7	-0.7	0.5	0.69
WATTERAS	-26.0	-12.0	4165.0	-8.0	5747.0	0.0620	0.0020	0.0120	3.7	-2.3	-1.2	-1.0	3.16
BEAUFORT	-46.0	-10.0	8019.0	-28.0	11867.0	0.0710	0.0060	0.0090	-81.8	-64.9	0.3	-1.8	4.67
CAROLINA BEACH	-19.0	-7.0	500.0	-3.0	3375.0	0.1157	0.0474	0.0072	32.4	0.1	-1.3	2.2	0.19
LOCKHOODS FOLLY	-16.0	-8.0	983.0	-4.0	2500.0	0.1690	0.0790	0.0880	50.1	11.4	-3.1	0.9	0.21
SHALLOTE	-13.0	-6.0	1474.0	-4.0	5497.0	0.0590	0.0080	0.0100	58.4	-4.4	4.2	1.7	0.41
TUBBS	-19.0	-9.0	1807.0	-5.0	5414.0	0.0120	0.0290	0.0120	73.6	-4.6	-1.4	0.5	0.40
LITTLE RIVER	-31.0	-16.0	1666.0	-4.0	3332.0	0.0490	0.0080	0.0350	20.6	-0.6	-3.7	-1.5	0.52
MURRELLS	-15.0	-4.0	2832.0	-4.0	3498.0	0.0760	0.0090	0.0080	77.8	-18.3	7.1	-2.9	0.46
NORTH	-20.0	-6.0	3665.0	-6.0	3332.0	0.0790	0.0020	0.0050	33.5	-4.8	3.3	-1.3	0.95
SOUTH SANTEE	-14.0	-7.0	3000.0	-4.0	7000.0	0.0647	0.0060	0.0043	61.2	1.0	0.4	-1.2	1.18
PRICE	-13.0	-6.0	833.0	-4.0	4664.0	0.0010	0.0010	0.0070	50.8	-5.5	-0.2	-0.4	0.65
CAPERS	-26.0	-9.0	1000.0	-4.0	8829.0	0.0690	0.0050	0.0200	36.4	8.3	-0.5	0.3	1.20
DEWEES	-37.0	-16.0	1666.0	-7.0	12161.0	0.0670	0.0270	0.0130	-3.1	19.8	-2.1	-1.0	2.25
LIGHTHOUSE	-23.0	-15.0	750.0	-5.0	5501.0	0.0739	0.0190	0.0015	19.6	6.6	-2.8	-0.2	0.58
STENO	-33.0	-12.0	8496.0	-8.0	17159.0	0.0780	0.0090	0.0030	-3.2	16.4	-0.5	-1.6	6.29
FRIPR	-27.0	-16.0	2582.0	-5.0	12078.0	0.0090	0.0040	0.0780	3.7	0.6	-2.2	-1.5	3.66
DORRIS	-46.0	-19.0	6164.0	-8.0	24157.0	0.0530	0.0130	0.0050	-25.9	15.1	-2.3	-0.9	16.85
NASSAU	-31.0	-6.0	11828.0	-7.0	8330.0	0.0640	0.0030	0.0100	-23.4	-17.2	1.6	0.3	9.49
FORT GEORGE	-14.0	-7.0	1582.0	-5.0	5664.0	0.0010	0.0060	0.0090	52.8	-6.5	-2.7	1.6	0.60
ST. AUGUSTINE	-33.0	-21.0	3665.0	-6.0	15827.0	0.0060	0.0010	0.0180	-4.6	3.5	0.8	0.5	4.79
PONCE DE LEON	-23.0	-5.0	3333.0	-7.0	4458.0	0.0718	0.0074	0.0095	38.9	7.6	1.6	0.4	0.49

INLET	DMX 1	DMA 2	M 3	DCC 4	L 5	EM1 6	EM2 7	EM3 8	EC1 9	EC2 10	ED1 11	ED2 12	AED 13
SEBASTIAN	-6.0	-3.0	562.0	-6.0	832.0	0.0324	0.0030	0.0110	79.1	-9.4	3.0	2.0	0.33
BOCA RATON	-4.0	-2.0	292.0	-1.0	417.0	0.0194	0.0189	0.0029	91.1	-1.7	-1.5	4.5	0.01
HILLSBORD	-3.0	-1.5	312.0	-1.5	540.0	0.0284	0.0010	0.0057	91.4	-3.7	13.6	4.2	0.01
BIG MARCO	-24.0	-18.0	875.0	-7.0	7250.0	0.0658	0.0195	0.0047	18.5	16.6	-1.7	-1.3	1.59
GORDON PASS	-11.0	-5.0	600.0	-4.0	2100.0	0.0158	0.0274	0.0038	65.8	-2.5	0.1	1.2	0.13
REDFISH	-37.0	-18.0	683.0	-6.0	4414.0	0.2620	0.0040	0.0330	24.4	17.5	-1.9	-1.0	0.30
CAPTIVA	-40.0	-16.0	1875.0	-8.0	8000.0	0.0070	0.0180	0.0180	15.4	8.9	-0.6	-1.0	1.06
BOCA GRANDE	-57.0	-28.0	4748.0	-33.0	17076.0	0.0320	0.0180	0.0010	-101.5	-5.3	-1.1	-1.3	16.58
GASPARILLA	-26.0	-8.0	1332.0	-6.0	3748.0	0.0630	0.0170	0.0160	39.7	12.3	1.2	0.1	0.37
STUMR	-16.0	-6.0	791.0	-6.0	2332.0	0.0080	0.0060	0.0240	52.8	-0.7	0.9	0.4	0.10
MIDNIGHT	-13.0	-6.0	499.0	-4.0	1667.0	0.0284	0.0031	0.0310	62.9	1.5	-1.4	1.3	0.06
BIG SARASOTA	-19.0	-9.0	2917.0	-9.0	8167.0	0.0531	0.0125	0.0029	6.6	-16.8	2.1	0.4	1.17
LONGBOAT	-29.0	-14.0	791.0	-9.0	3498.0	0.0380	0.0380	0.0100	25.8	9.9	-1.9	-0.7	0.41
PASS A GRILLE	-22.0	-7.0	4748.0	-7.0	9329.0	0.0761	0.0009	0.0067	21.9	-6.1	1.4	-1.9	2.23
CLEARWATER	-9.0	-5.0	3040.0	-6.0	4331.0	0.0687	0.0022	0.0010	40.5	-0.8	1.8	0.7	2.57
PENSACOLA	-55.0	-27.0	3540.0	-33.0	12078.0	0.0060	0.0250	0.0010	476.7	-10.3	-1.8	-0.4	2.86
SAN LUIS	-18.0	-7.0	5556.0	-10.0	8163.0	0.0710	0.0100	0.0010	34.0	-6.6	-0.8	-1.3	1.59
PASS CAVALLO	-35.0	-12.0	8996.0	-9.0	22907.0	0.0720	0.0040	0.0040	-31.7	-8.5	9.0	0.9	7.00
MORRO BAY	-23.0	-10.0	417.0	-13.0	1000.0	0.1239	0.0000	0.0062	23.8	-3.4	-1.3	1.1	0.07
BOLINAS	-6.0	-3.0	583.0	-3.0	2000.0	0.0410	0.0137	0.0084	81.0	-3.7	2.0	5.6	0.10
DRAKES	-27.0	-18.0	833.0	-8.0	3000.0	0.0218	0.0220	0.0369	38.6	6.7	0.2	0.9	0.40
BODEGA	-14.0	-7.0	542.0	-4.0	1000.0	0.0036	0.0628	0.0128	51.2	-4.3	-3.0	1.1	0.04
HUMBOLDT	-66.0	-22.0	2917.0	-24.0	6917.0	0.0373	0.0323	0.0126	-83.7	18.8	-1.4	-0.4	2.36
COOS BAY	-45.0	-14.0	5971.0	-10.0	6006.0	0.0773	0.0031	0.0031	-1.2	21.7	-0.3	-1.6	1.37
UMPUA	-49.0	-22.0	2610.0	-10.0	8526.0	0.0399	0.0236	0.0208	-18.3	20.8	0.2	0.6	1.69
SIUSLAN	-19.0	-7.0	5915.0	-6.0	3567.0	0.0811	0.0030	0.0029	52.0	3.1	1.5	0.1	0.87
ALSEA	-35.0	-18.0	917.0	-7.0	3416.0	0.0072	0.0948	0.0352	19.7	23.6	-2.3	0.5	0.43
YAQUINA	-26.0	-28.0	1016.0	-15.0	3218.0	0.0650	0.0230	0.0439	6.8	-12.0	0.3	-2.4	0.23
SILETZ	-20.0	-8.0	417.0	-6.0	2250.0	0.1160	0.0084	0.0510	48.8	9.7	0.5	2.2	0.16
NETABTS	-12.0	-5.0	1915.0	-1.0	4998.0	0.0632	0.0028	0.0111	55.8	4.3	3.2	2.9	0.49
YILLAMOOK	-48.0	-19.0	1479.0	-13.0	7482.0	0.0017	0.0981	0.0072	-38.3	22.8	-2.0	-0.01	1.85
NEHALEM	-26.0	-16.0	583.0	-9.0	4500.0	0.1145	0.1065	0.0325	-12.8	3.8	-2.1	-0.8	4.00
WILLAPA	-80.0	-38.0	25000.0	-26.0	28000.0	0.0777	0.0061	0.0013	-155.9	23.8	-0.6	-2.0	23.40
GRAYS HARBOR	100.0	-32.0	12250.0	-16.0	19250.0	0.0726	0.0063	0.0067	-132.3	40.2	-1.3	-1.8	16.10

APPENDIX C
HISTOGRAMS OF THE 13 VALUES







APPENDIX D

MEAN AND STANDARD DEVIATION VECTORS REQUIRED IN EIGENVECTOR ANALYSIS

a. Normalized cross section

	Mean	Std. dev.		Mean	Std. dev.
1	-0.0012	0.0015	31	-0.0135	0.0154
2	-0.0024	0.0028	32	-0.0136	0.0155
3	-0.0034	0.0041	33	-0.0135	0.0156
4	-0.0043	0.0053	34	-0.0135	0.0157
5	-0.0051	0.0061	35	-0.0135	0.0157
6	-0.0058	0.0068	36	-0.0135	0.0157
7	-0.0065	0.0075	37	-0.0134	0.0156
8	-0.0071	0.0081	38	-0.0133	0.0155
9	-0.0071	0.0088	39	-0.0132	0.0154
10	-0.0082	0.0094	40	-0.0130	0.0152
11	-0.0086	0.0100	41	-0.0129	0.0150
12	-0.0091	0.0104	42	-0.0126	0.0148
13	-0.0095	0.0108	43	-0.0124	0.0145
14	-0.0099	0.0113	44	-0.0121	0.0142
15	-0.0102	0.0117	45	-0.0118	0.0139
16	-0.0106	0.0121	46	-0.0114	0.0135
17	-0.0109	0.0124	47	-0.0110	0.0131
18	-0.0112	0.0127	48	-0.0106	0.0126
19	-0.0115	0.0129	49	-0.0101	0.0121
20	-0.0117	0.0132	50	-0.0095	0.0116
21	-0.0119	0.0134	51	-0.0090	0.0111
22	-0.0121	0.0136	52	-0.0085	0.0105
23	-0.0123	0.0139	53	-0.0078	0.0100
24	-0.0125	0.0141	54	-0.0071	0.0092
25	-0.0127	0.0144	55	-0.0063	0.0084
26	-0.0129	0.0146	56	-0.0055	0.0076
27	-0.0131	0.0148	57	-0.0046	0.0067
28	-0.0132	0.0150	58	-0.0037	0.0054
29	-0.0133	0.0152	59	-0.0026	0.0038
30	-0.0135	0.0153	60	-0.0013	0.0020

b. Channel profile

c. Normalized ebb delta

Mean	Std. dev.	Mean	Std. dev.
-30.0	16.5	1.22	0.93
-29.0	15.9	-0.44	0.95
-28.0	15.5	0.31	0.69
-28.0	15.3	0.46	0.77
-27.0	15.3	-0.37	0.75
-26.0	14.9	0.13	0.79
-25.0	14.3	0.37	0.68
-24.0	13.9	0.79	0.72
-23.0	13.6	0.87	0.61
-22.0	13.1	0.60	0.62
-21.0	12.5	0.23	0.89
-20.0	12.2	1.24	0.92
-19.0	11.8	1.38	1.12
-18.0	11.4	1.26	1.15
-17.0	10.9	0.94	0.91
-16.0	10.5	0.48	0.64
-15.0	10.1	-0.37	0.75
-14.0	9.8	0.32	0.79
-13.0	9.5	1.21	1.12
-12.0	9.2	1.88	1.53
		2.00	1.41
		1.25	1.11

EIGENVECTORS FOR THE MINIMUM INLET CROSS SECTION,
CHANNEL PROFILE, AND EBB DELTA GEOMETRY ANALYSES

EM1			EM2			EM3		
1	0.0083	31 0.1731	1	-0.0211	31 -0.0245	1	0.0346	31 -0.1540
2	0.0175	32 0.1740	2	-0.0429	32 -0.0089	2	0.0697	32 -0.1572
3	0.0275	33 0.1750	3	-0.0677	33 0.0057	3	0.1017	33 -0.1581
4	0.0373	34 0.1759	4	-0.0856	34 0.0205	4	0.1374	34 -0.1554
5	0.0462	35 0.1761	5	-0.1012	35 0.0347	5	0.1595	35 -0.1503
6	0.0549	36 0.1753	6	-0.1119	36 0.0484	6	0.1706	36 -0.1398
7	0.0639	37 0.1743	7	-0.1234	37 0.0619	7	0.1794	37 -0.1276
8	0.0719	38 0.1731	8	-0.1320	38 0.0760	8	0.1868	38 -0.1127
9	0.0799	39 0.1715	9	-0.1405	39 0.0901	9	0.1916	39 -0.0964
10	0.0878	40 0.1694	10	-0.1496	40 0.1046	10	0.1938	40 -0.0792
11	0.0948	41 0.1669	11	-0.1550	41 0.1171	11	0.1921	41 -0.0592
12	0.1009	42 0.1635	12	-0.1585	42 0.1295	12	0.1843	42 -0.0354
13	0.1065	43 0.1599	13	-0.1620	43 0.1412	13	0.1734	43 -0.0114
14	0.1120	44 0.1561	14	-0.1658	44 0.1513	14	0.1577	44 0.0127
15	0.1174	45 0.1512	15	-0.1685	45 0.1608	15	0.1392	45 0.0405
16	0.1232	46 0.1455	16	-0.1689	46 0.1691	16	0.1148	46 0.0691
17	0.1283	47 0.1391	17	-0.1677	47 0.1770	17	0.0891	47 0.0962
18	0.1331	48 0.1323	18	-0.1650	48 0.1845	18	0.3636	48 0.1178
19	0.1373	49 0.1246	19	-0.1606	49 0.1890	19	0.0397	49 0.1358
20	0.1414	50 0.1164	20	-0.1544	50 0.1905	20	0.0176	50 0.1514
21	0.1449	51 0.1084	21	-0.1474	51 0.1899	21	-0.0042	51 0.1620
22	0.1485	52 0.1001	22	-0.1390	52 0.1861	22	-0.0294	52 0.1727
23	0.1520	53 0.0916	23	-0.1293	53 0.1809	23	-0.0535	53 0.1803
24	0.1556	54 0.0821	24	-0.1187	54 0.1737	24	-0.0759	54 0.1781
25	0.1590	55 0.0723	25	-0.1066	55 0.1609	25	-0.0959	55 0.1747
26	0.1618	56 0.0629	26	-0.0933	56 0.1486	26	-0.1120	56 0.1671
27	0.1648	57 0.0526	27	-0.0808	57 0.1315	27	-0.1264	57 0.1508
28	0.1676	58 0.0405	28	-0.0675	58 0.1053	28	-0.1377	58 0.1241
29	0.1698	59 0.0275	29	-0.0543	59 0.0734	29	-0.1440	59 0.0866
30	0.1717	60 0.0138	30	-0.0398	60 0.0388	30	-0.1493	60 0.0454

EC1	EC2	ED1	ED2	ED3
0.2709	-0.3390	0.0057	0.1562	-0.3068
0.2698	-0.3248	-0.0475	-0.4063	0.0290
0.2697	-0.2945	-0.0829	0.0002	0.4224
0.2688	-0.2546	0.0463	0.0239	0.0588
0.2684	-0.2050	0.0413	-0.3839	-0.2539
0.2678	-0.1511	0.1896	-0.2432	0.0643
0.2543	-0.0796	0.1202	-0.2592	0.2238
0.2476	-0.0143	0.2504	-0.0147	0.0574
0.2422	0.0565	0.2642	0.0622	0.0001
0.2326	0.1143	0.2126	-0.1933	-0.0729
0.2205	0.1571	0.1292	-0.3008	-0.3174
0.2133	0.1816	0.3129	0.0274	-0.1276
0.2043	0.2174	0.3201	0.0874	-0.0999
0.1952	0.2355	0.3300	0.0850	0.0267
0.1822	0.2545	0.2798	0.0109	0.2227
0.1743	0.2543	0.1748	-0.1870	0.3902
0.1646	0.2579	0.0302	-0.4300	-0.1713
0.1574	0.2483	0.0969	-0.3019	0.1555
0.1475	0.2480	0.2569	0.0612	0.2851
0.1354	0.2465	0.2962	0.1681	0.0666
		0.3003	0.1952	-0.1055
		0.2637	0.0841	-0.3400

APPENDIX F

COMPUTER PROGRAM FOR THE CALCULATION OF THE PROBABILITY THAT AN INLET BELONGS TO AN INLET GROUP

This appendix contains a simple computer program that incorporates the discriminant functions of Table 7(a) and can be used to calculate the posterior probability that an inlet belongs to a group. The program is written in time-sharing FORTRAN for a Honeywell 637 computer. Input and output are free field. A person with modest programming capabilities should be able to make the program run on any FORTRAN system.

The following input to the program is for one inlet:

- (a) DMX, DMA, W
- (b) DCC, L
- (c) EM1, EM2, EM3
- (d) EC1, EC2
- (e) ED1, ED2, AED

EM2 must be input as an absolute value.

The output is the values of the discriminant function, the prior probability, and the posterior probability as a triplet for each inlet group.

```

00010      MARCH 1978
00020 DIMENSION P(6),POTAP(6),X(13),S(6)
00030 DATA P/31.,6.,4.,4.,12.,5./
00040 DIMENSION CM(6,14)
00050      PROGRAM TO COMPUTE DISCRIMINANT VALUES
00060      BASED ON EMD EQUATION:
00070      PROGRAMMER VINCENT AT MES
00080 DATA ((CM(I,J),J=1,14),I=1,6)/-1.36836,-1.24218,0.00293,-2.20527,
00090 0.00061,-7.11257,9.94051,-185.17853,0.86302,-0.19929,0.96681,
00100 1.65025,1.07974,-48.95216,
00110 -1.76092,-2.05815,0.00211,-2.31869,0.00071,-21.88881,-50.70179,
00120 -330.82570,0.93846,-0.41634,2.51213,0.96279,1.39159,-74.75916,
00130 -1.33679,-0.83469,0.00329,-1.81093,0.00026,-34.11697,239.22370,
00140 -246.29120,0.86239,-0.16273,0.12991,4.61465,1.87022,-57.24019,
00150 -1.42992,-0.47482,0.00376,-2.40258,0.00014,-101.60954,718,
00160 -413.10246,0.96286,-0.00902,0.77541,3.16339,2.78669,-98.38555,
00170 -1.38346,-1.37509,0.00247,-1.80977,0.00073,-73.07272,85.99466,
00180 -70.30244,0.82931,-0.15155,1.13826,1.08608,1.23236,-52.82636,
00190 -1.92433,-1.64856,0.00156,-4.24295,0.00038,-34.87828,-135.51790,
00200 -369.25665,0.92330,-0.57072,1.98759,1.59529,1.67421,-102.44255
00210
00220
00230      DATA COEFFICIENTS ARE TAKEN FROM TABLE 7A OF REPORT
00240      DATA ORDER IS 13 COEFFICIENTS THEN CONSTANT FOR EACH
00250      FUNCTION
00260      READ THE THIRTEEN VARIABLES IN THE ORDER
00270      DMC,DMA,M - DCC,L - EM1,EM2,EM3 - EC1,EC2 - ED1,ED2,RED
00280
00290 DO 10 I=1,6
00300   DO 10 J=1,14
00310     READ,X(1),X(2),X(3)
00320     READ,X(4),X(5)
00330     READ,X(6),X(7),X(8)
00340     READ,X(9),X(10)
00350     READ,X(11),X(12),X(13)
00360     COMPUTE THE 6 FUNCTIONS
00370     DO 100 I=1,6
00380       SED=CM(I,14)
00390       DO 100 J=1,13
00400         SED=SED+CM(I,J)*X(J)
00410         IF(J.EQ.13) SED=SED
00420       100 CONTINUE
00430
00440      CALCULATE THE PROBABILITY BASED ON A PRIORI AND
00450      DISCRIMINANT FUNCTIONS
00460      SP=0.
00470      DO 155 I=1,6
00480       SP=SP+P(I)*EXP(SED(I))
00490      DO 160 I=1,6
00500       POTAP(I)=P(I)*EXP(SED(I))/SP
00510      DO 200 I=1,6
00520       PRINT,11,I,P(I),POTAP(I)
00530      STOP
00540      END

```

Vincent, Charles L.

The geometry of selected U.S. tidal inlets / by Charles L. Vincent and William D. Corson. - Fort Belvoir, Va. : U.S. Coastal Engineering Research Center ; Springfield, Va. : available from National Technical Information Service, 1980.

[163] p. : ill. : 27 cm. - (GITI report ; 20)

"General Investigation of Tidal Inlets - a program of research conducted jointly by U.S. Army Coastal Engineering Research Center, Fort Belvoir, Virginia, U.S. Army Engineer Waterways Experiment Station, Vicksburg, Mississippi."

Includes bibliographical references.

Appendixes.

The geometry of the throat and ebb delta of 67 U.S. tidal inlets is investigated. Thirteen parameters indicative of the tidal inlet geometry are defined and measured with correlations developed.

1. Tidal inlets. 2. Tidal hydraulics. 3. Movable beds. 4. Tidal models. I. Title. II. Corson, William D. III. Series: U.S. Army Corps of Engineers. GITI report ; 20.

GB454 .15 .U581r

no. 20

551.4

Vincent, Charles L.

The geometry of selected U.S. tidal inlets / by Charles L. Vincent and William D. Corson. - Fort Belvoir, Va. : U.S. Coastal Engineering Research Center ; Springfield, Va. : available from National Technical Information Service, 1980.

[163] p. : ill. : 27 cm. - (GITI report ; 20)

"General Investigation of Tidal Inlets - a program of research conducted jointly by U.S. Army Coastal Engineering Research Center, Fort Belvoir, Virginia, U.S. Army Engineer Waterways Experiment Station, Vicksburg, Mississippi."

Includes bibliographical references.

Appendixes.

The geometry of the throat and ebb delta of 67 U.S. tidal inlets is investigated. Thirteen parameters indicative of the tidal inlet geometry are defined and measured with correlations developed.

1. Tidal inlets. 2. Tidal hydraulics. 3. Movable beds. 4. Tidal models. I. Title. II. Corson, William D. III. Series: U.S. Army Corps of Engineers. GITI report ; 20.

GB454 .15 .U581r

no. 20

551.4

Vincent, Charles L.

The geometry of selected U.S. tidal inlets / by Charles L. Vincent and William D. Corson. - Fort Belvoir, Va. : U.S. Coastal Engineering Research Center ; Springfield, Va. : available from National Technical Information Service, 1980.

[163] p. : ill. : 27 cm. - (GITI report ; 20)

"General Investigation of Tidal Inlets - a program of research conducted jointly by U.S. Army Coastal Engineering Research Center, Fort Belvoir, Virginia, U.S. Army Engineer Waterways Experiment Station, Vicksburg, Mississippi."

Includes bibliographical references.

Appendixes.

The geometry of the throat and ebb delta of 67 U.S. tidal inlets is investigated. Thirteen parameters indicative of the tidal inlet geometry are defined and measured with correlations developed.

1. Tidal inlets. 2. Tidal hydraulics. 3. Movable beds. 4. Tidal models. I. Title. II. Corson, William D. III. Series: U.S. Army Corps of Engineers. GITI report ; 20.

GB454 .15 .U581r

no. 20

551.4

Vincent, Charles L.

The geometry of selected U.S. tidal inlets / by Charles L. Vincent and William D. Corson. - Fort Belvoir, Va. : U.S. Coastal Engineering Research Center ; Springfield, Va. : available from National Technical Information Service, 1980.

[163] p. : ill. : 27 cm. - (GITI report ; 20)

"General Investigation of Tidal Inlets - a program of research conducted jointly by U.S. Army Coastal Engineering Research Center, Fort Belvoir, Virginia, U.S. Army Engineer Waterways Experiment Station, Vicksburg, Mississippi."

Includes bibliographical references.

Appendixes.

The geometry of the throat and ebb delta of 67 U.S. tidal inlets is investigated. Thirteen parameters indicative of the tidal inlet geometry are defined and measured with correlations developed.

1. Tidal inlets. 2. Tidal hydraulics. 3. Movable beds. 4. Tidal models. I. Title. II. Corson, William D. III. Series: U.S. Army Corps of Engineers. GITI report ; 20.

GB454 .15 .U581r

no. 20

551.4